Molecular Analysis of DNA Double Strand Break Repair Systems after Proton versus Photon Irradiation

Dissertation

zur

Erlangung der naturwissenschaftlichen Doktorwürde

(Dr. sc. nat.)

vorgelegt der

Mathematisch-naturwissenschaftlichen Fakultät

der

Universität Zürich

von

Nicole Grosse

aus

Deutschland

Promotionskomitee

Prof. Dr. Martin Pruschy (Leitung der Dissertation und Vorsitz)

Prof. Dr. Eugen B. Hug

Prof. Dr. Josef Jiricny

Prof. Dr. Alessandro A. Sartori

Prof. Dr. Ekkehard Dikomey

Zürich, 2011

Abstract

Currently, the most common form of radiotherapy is using high energy linear accelerators to generate an external photon beam directed towards the tumour mass. Other forms of radiation used in radiotherapy include charged particles such as electron beams, neutrons, pi-mesons, protons, and heavier charged ions such as ^{12}C. Of these, proton radiotherapy has gained, and is gaining, much attention worldwide. Protons display special physical characteristics that provide a more localized delivery of radiation to the tumour site than can be achieved with photon-based radiotherapy. Many leading cancer centres worldwide have established new proton therapy facilities or will become operational within the next few years. With this expansion, it will be possible to treat more patients, and therefore new clinical indications are planned to be treated with protons. However, the conclusion that it is safe to expand this technology without additional knowledge based on scientific and radiobiological data cannot be directly drawn. *Preclinical* experiments reveal an enhanced efficacy for proton versus photon irradiation. But the cause for the increased efficacy of protons on the molecular level is not clear. Proton irradiation-induced DNA damage might be quantitatively or qualitatively different compared to photon irradiation-induced DNA damage, and only few studies have been done to elucidate this question.

In this PhD thesis, I have investigated several molecular and cellular end points in response to photon and proton irradiation using genetically defined biological cell systems. A special focus has been placed on the involvement of DNA double strand break (DNA DSB) repair after proton vs. photon irradiation. A panel of different cell lines was used to reveal a possible differential sensitivity to proton radiation depending on the repair capacity due to the genetic background of the cell. All tested cell lines were more sensitive to proton irradiation in comparison to photon irradiation on the level of clonogenic cell survival. For both wild type cells used in the study (AA8 and CHO9), irradiation with protons decreased cell survival by 1.1 ± 0.1 and 1.8 ± 0.2 fold at 2 and 5 Gy, respectively, when compared to photon irradiated cells. A cell line mutated in the nucleotide excision repair pathway was used as a control and showed the same sensitivity as the corresponding wild type cell line. As expected, mutant cells in homologous recombination (HR) and non-homologous end joining (NHEJ) were in general much more sensitive towards irradiation than wild type cells. But interestingly, exponentially growing cells deficient in HR were significantly more sensitive to proton irradiation than cells with intact HR (relative biological effectiveness, RBE_{10} wild type=1.24±0.03, HR-deficient=1.44±0.06). When these cells were irradiated in plateau (growth arrested) phase, there was no longer a difference in the RBE of the two cell lines (RBE_{10} wild type=1.29±0.03, HR-deficient=1.27±0.03), indicating a more critical role of HR after proton vs. photon irradiation, as HR is only active in S/G2 phase. On the other hand,

exponentially growing NHEJ-deficient cells did not show a specifically enhanced sensitivity to proton irradiation (RBE_{10} wild type=1.2±0.05, NHEJ-deficient=1.09±0.10). However, after irradiation in plateau phase, these cells became highly radiosensitive and significantly more sensitive to proton radiation. Cells lacking NHEJ possess only minor backup repair pathways in plateau phase, which possibly can deal with some photon-induced DNA damages but not with proton-induced ones. These data point to a differential DNA damage complexity or amount of DNA damage after proton vs. photon irradiation. In an attempt to explore these findings further on a molecular level, we determined initial DNA DSBs, repair kinetics, cell cycle distributions, and chromosomal aberrations. No quantitative differences in initially induced γH2AX and 53BP1 foci could be determined in response to the two types of radiation. The repair kinetics of DNA damage in wild type cells were the same after both types of radiation (γH2AX, Rad51, and 53BP1 foci), even though proton irradiation resulted in more residual chromosomal DNA fragments and lethal chromosome aberrations. Interestingly, the repair kinetics in HR-deficient cells were significantly delayed after proton irradiation, leading to an elevated amount of residual γH2AX-foci 24 h after irradiation (45 % vs. 27 % γH2AX foci after protons vs. photons, respectively). Thus, these data show the same amount of initial DNA DSBs after both types of radiation and rather point to a differential damage pattern. As all previous experiments have been performed with Chinese hamster ovary (CHO) cells we used additionally U2OS cells to validate the importance of HR for the repair of proton irradiation-induced DNA damages in a human system. However, human U2OS cells, which are proficient in p53, did not show an increased proton radiosensitivity when HR was depleted. This was in contrast to the previously mentioned data obtained using p53-mutated CHO cells. To test another human cell type, we used a pancreas adenocarcinoma cell line with a non-functional, truncated BRCA2 protein, as BRCA2 is an important mediator for HR and often mutated in certain cancer types. These cells were more sensitive towards proton vs. photon radiation at higher dose levels, validating our finding in a human cell system.

This work demonstrates for the first time that the genetic background of cells can strongly influence their response to proton radiation. When HR was missing in highly proliferative, p53-deficient cells, the proton radiosensitivity was significantly increased compared to wild type cells, indicating that HR is essential for the proper repair of a certain percentage of proton-induced DNA damages. Therefore, aggressively proliferating tumour cells lacking HR and cell cycle check points would be best treated with proton radiotherapy. Other mutations should be tested with regard to the differential sensitivity towards proton and photon irradiation. Furthermore, these data indicate a differential quality of DNA damage induced by proton vs. photon irradiation, which might become relevant for clinical stratification of patients carrying mutations in the DNA damage repair and response pathways.

Zusammenfassung

Die gängigste Methode der Strahlentherapie ist heutzutage die Erzeugung eines Photonenstrahls mit hochenergetischen Linearbeschleunigern, der gegen das Tumorgewebe gerichtet wird. Weitere Bestrahlungsarten, die in der Strahlentherapie verwendet werden sind mit Partikeln erzeugte Strahlen wie Elektronen, Neutronen, Pi-Mesonen, Protonen und schwere, geladene Ionen wie Carbon-ionen. Von diesen ist die Protonentherapie die bekannteste Form und erlangt immer mehr an Beachtung. Protonen haben spezielle physikalische Eigenschaften, welche eine exaktere Bestrahlung des Tumors möglich machen als dies mit Photonen-basierter Strahlentherapie möglich ist. Viele führende Krebszentren weltweit besitzen mittlerweile eine funktionelle Protonentherapieanlage oder werden diese in den nächsten Jahren in Betrieb nehmen. Durch diese Expandierung wird es möglich mehr Patienten und somit mehr neue klinische Indikationen mit Protonen zu behandeln. Jedoch kann nicht einfach vorausgesetzt werden, dass es sicher ist, ohne weitere radiobiologische Grundlagenforschung, diese Technologie einfach für andere Indikation zu übernehmen. Präklinische Experimente zeigen eine stärkere Effektivität von Protonen im Vergleich zu Photonenstrahlung. Aber der Grund für diese besserer Effektivität ist auf molekularer Ebene noch nicht geklärt. Protonen-induzierte DNA Schäden sind möglicherweise quantitativ oder qualitativ verschieden verglichen mit Photon-iniduzierten DNA Schäden. Bis jetzt wurden nur wenige Studien durchgeführt, um diese Frage zu beantworten.

In dieser Doktorarbeit habe ich die molekulare und zelluläre Reaktion von Zellen nach Photonen und Protonenbestrahlung auf mehreren Ebenen untersucht. Dafür wurden genetisch definierte Zellsysteme verwendet. Der Fokus lag auf der zellulären Beteiligung von DNS Doppelstrangbruch (DSB) Reparatur Systemen nach Photonen vs. Protonenbestrahlung. Verschiedenen Zelllinien (Wildtypen/Mutanten) wurden verwendet, um mögliche Unterschiede in der Strahlensensitivität nach Protonenbestrahlung in Abhängigkeit von der Reparaturfähigkeit und dem genetischen Hintergrund der Zelle aufzudecken. Alle getesteten Zelllinien waren, gemessen auf der Ebene des klonogenen Überlebens, sensitiver gegenüber Protonen als gegenüber Photonbestrahlung. Protonenbestrahlung verringerte das Zellüberleben in beiden Wildtypzellen (AA8 und CHO9) verglichen mit Photonenbestrahlung um 1.1 ± 0.1 und 1.8 ± 0.2 fach nach 2 und 5 Gy, respektive. Eine mutierte Zelllinie im Nukleotidexzisionsreparaturweg wurde als Kontrolle verwendet und zeigte dieselbe Sensitivität wie die dazugehörige Wildtypezelllinie. Wie erwartet, waren die Mutanten der Homologen Rekombination (HR) und des Nicht-Homologen End Joining (NHEJ) generell viel sensitiver gegenüber Bestrahlung als die Wildtypzellen. Hochinteressanterweise, waren exponentiell wachsende HR-defiziente Zellen signifikant sensitiver gegenüber

Protonenbestrahlung als Zellen mit intakter HR (relative biologische Effektivität, RBE_{10} Wildtyp=1.24±0.03, HR-defizient=1.44±0.06). Wurden diese Zellen in der Plateauphase (wachstumsarretiert) bestrahlt, war der Unterschied im RBE zwischen den beiden Zelllinien nicht mehr vorhanden (RBE_{10} Wildtyp=1.29±0.03, HR-defizient=1.27±0.03). Dies zeigt eine wichtigere Rolle von HR nach Protonen als nach Photonenbestrahlung an, da HR nur in der S/G2 Phase aktiv ist. Auf der anderen Seite waren exponentiell wachsende NHEJ-defiziente Zellen nicht sensitiver gegenüber Protonenbestrahlung (RBE_{10} Wildtyp=1.2±0.05, NHEJ-defizient=1.09±0.10). Dieselben Zellen waren nach Bestrahlung in der Plateauphase viel radiosensitiver und signifikant sensitiver gegenüber Protonenbestrahlung als der Wildtyp. Zellen ohne NHEJ Reparatur besitzen nur wenige Ersatzreparaturmechanismen in der Plateauphase. Ersatzreparaturwege können möglicherweise einige Photonen-induzierte DNA Schäden reparieren, jedoch womöglich keine Protonen-induzierten. Diese Daten deuten auf unterschiedlich komplexe DNA Schäden oder unterschiedlich viele DNA Schäden nach Protonen vs. Photonenbestrahlung hin. Weiterhin wurden diese Erkenntnisse auch auf molekularer Ebene untersucht: hierfür wurde die initiale Anzahl an DSB, Reparaturkinetiken, Zellzyklusverteilungen und chromosomale Aberrationen bestimmt. Es wurden keine Unterschiede in der Anzahl von initialen γH2AX und 53BP1 Foci nach Bestrahlung mit einer der beiden Strahlentypen festgestellt. Die DNA Reparaturkinetiken waren in den Wildtypzellen gleich (γH2AX, Rad51, and 53BP1 Foci), obwohl die Protonenbestrahlung mehr übrige Chromosomenfragmente und letale Chromosomenaberrationen nach sich zog. Interessanterweise war die Reparaturkinetik in HR-defizienten Zellen nach Protonenbestrahlung signifikant langsamer, was 24 Stunden nach Bestrahlung zu einer erhöhten Anzahl an nicht aufgelösten γH2AX Foci führte (45 % vs. 27 % γH2AX Foci nach Protonen vs. Photonen, respektive). Folglich zeigen die Daten gleich viele DNS DSB nach beiden Bestrahlungsarten und deuten eher auf eine unterschiedliche Struktur des Schadens hin. Da alle Experimente bis hierher mit Chinesischen Hamster Ovarial (CHO) Zellen durchgeführt worden sind, wurden zusätzlich U2OS Zellen verwendet, um die Wichtigkeit der HR für die Reparatur von Protonen-induzierten Schäden in einem humanen Zellsystem zu zeigen. Jedoch zeigten die humanen U2OS Zellen, welche p53 positiv sind, keine erhöhte Sensitivität gegenüber Protonenbestrahlung wenn HR nicht vorhanden war. Diese Daten waren widersprüchlich zu den vorher erwähnten Daten, in welchen p53-defiziente CHO Zellen verwendet wurden. Eine humane Pankreasadenokarzinom Zelllinie mit nicht-funktionalem, kürzerem BRCA2 Protein, wurde als weiteres humanes Testsystem verwendet. BRCA2 ist ein wichtiger Vermittler für die HR Reparatur und oft in bestimmten Krebsarten mutiert. Diese Zellen waren nach Bestrahlung mit höheren Dosen vermehrt sensitiver gegenüber Protonen vs. Photonen, was unsere Entdeckung in einem humanen Zellsystem bestätigen konnte.

In dieser Arbeit wird zum ersten Mal gezeigt, dass der genetische Hintergrund der Zellen die Zellantwort gegenüber Protonenbestrahlung stark beeinflussen kann. Wenn HR in schnell proliferierenden, p53-defizienten Zellen fehlte, war deren Sensitivität gegenüber Protonenbestrahlung im Vergleich zu Wildtypzellen signifikant erhöht. Dies zeigt, dass HR für die richtige Reparatur eines bestimmten Anteils von Protonen-induzierten DNA Schäden essentiell ist. Diese Daten weisen darauf hin, dass aggressive, schnell wachsende Tumoren, denen HR und Zellzykluskontrollmechanismen fehlen, am besten mit Protonentherapie behandelt werden. Weitere Mutationen sollten im Hinblick auf die unterschiedliche Sensitivität nach Protonen und Photonenbestrahlung getestet werden. Weiterhin weisen die Daten auf einen qualitativ unterschiedlichen, induzierten DNA Schaden nach Protonen vs. Photonenbestrahlung hin. Dies könnte für die klinische Stratifizierung von Patienten mit Mutationen in DNA Reparaturwegen und in der Stressantwort auf DNA Schäden genutzt werden.

Content

List of Abbreviations

2DXRT	2 dimensional x-ray therapy
3D	3 dimensional
4D CRT	4 dimensional conformal radiation therapy
53BP1	p53 binding protein 1
Ab	Antibody
ADP	Adenosine diphosphate
AP	Abasic site
APE1	AP endonuclease 1
ATM	Ataxia telangiectasia mutated
ATP	Adenosine triphosphate
ATR	ATM and Rad3-related
ATRIP	ATR interacting protein
Bax	Bcl-2-associated X protein
BER	Base excision repair
BLM	Bloom syndrome mutated protein
B-NHEJ	Backup non-homologous end joining
BRCA1/2	Breast cancer gene 1/2
BrDU	Bromodeoxyuridine
BSA	Bovine serum albumin
C. griseus	Cricetulus griseus
CD-1	Cluster of differentiation-1
Cdc25A/C	Cell division cycle 25 homolog A/C
CDK1/2	Cyclin dependent kinase 1/2
CDKI	Cyclin depenent kinase inhibitor
Chk1/2	Checkpoint homologue kinase 1/2
CHO	Chinese hamster ovary
CtIP	C-terminal binding protein interacting protein
CTV	Clinical target volume
Dapi	4′,6-Diamidin-2-phenylindol
DDR	DNA damage response
DNA	Deoxyribnucleic acid
DNA-PK	DNA-dependent protein kinase
DNA-PKcs	DNA-dependent protein kinase catalytic subunit
DMSO	Dimethyl sulfoxide
dRP	Deoxyribosephosphate

DSB(s)	Double strand break(s)
ECR	Electron cyclotron resonance
EGF	Epidermal growth factor
EGFR	Epidermal growth factor receptor
Epx	Eosinophil protein X
ERCC1/2	Excision repair cross-complementing rodent repair deficiency
ERK1/2	Extracellular-regulated kinase 1/2
FA	Fanconia
Facs	Fluorescence activated cell sorter
Fanc	Fanconi anemia, complementation group
FCS	Fetal calf serum
FDA	Food and drug administration
FEN1	Flap endonuclease 1
GADD45	Growth arrest and DNA damage gene 45
GeV	Giga electron volt
GGR	Global genome repair
GSI	Helmholtzgesellschaft für Schwerionenforschung
GTV	Gross tumour volume
Gy	Gray
h	Hour
H2AX	Histone variant 2AX
HAT	Histone acetyltransferase
H&E	Hematoxylin and eosin
HeLa	Henrietta Lachs
HR(R)	Homologous recombination (repair)
HRP	Horseradish peroxidase
HSP70B	Heat shock protein 70B
ICL	Interstrand crosslink
IL-19	Interleukin 19
IMPT	Intensity modulated proton therapy
IMRT	Intensity modulated radiotherapy
IR	Ionizing radiation
IRIF	Ionizing radiation induced foci
JNK1/2	c-Jun N-terminal kinase 1/2
keV	Kilo electron volt
LD	Lethal dose
LET	Linear energy transfer

Lig	Ligase
LOH	Loss of heterzygocity
LP	Long patch
Luc	Luciferase
MAPK	Mitogen activated protein kinase
Mdm2	Mouse double minutes 2-protein
MEF	Mouse embryonic fibroblast
MeV	Mega electron volt
MFIR	Mean fluorescence intensity ratio
mm	Millimeter
MMEJ	Microhomology mediated end joining
MPP4	Membrance protein, palmitoylated 4
MRN	Mre11, Rad50, and Nbs1
mRNA	Messenger ribonucleic acid
MRT	Magnet resonance tomography
ms	Milliseconds
mTOR	Mammalian target of rapamycin
MTRA	Medical technical radiology assistant
MTT	3-(4,5-dimethylthiazol-2)-2, 5 diphenyltetrazolium bromide
NBS1	Nijmegen breakage syndrome 1
NER	Nucleotide excision repair
NHEJ	Non-homologous end joining
NTH1	Endonuclease III-like protein 1
OER	Oxygen enhancement ratio
OGG	Oxyguanine glycolyase
p16/21/53	protein 16/21/53
PAR	Poly ADP-ribose
Parp-1	Poly (ADP-ribose) polymerase 1
PBS	Phosphate buffered saline
PCC	Premature chromosome condensation
PCNA	Proliferating cell nuclear antigen
PE	Plating efficiency
PET	Positron emission tomography
PhD	Philosophiae doctor
PI3K	Phosphoinosite-3 kinase
PLD(R)	Potentially lethal damage (repair)
Plk1/3	Polo-like kinase 1/3

PML	Promyelocytic leukemia protein
PNK	Polynucleotide kinase
PNKP	Polynucleotide phosphatase/kinase
Pol	Polymerase
PPTases	Protein phosphatases
PSI	Paul Scherrer Institute
PTCOG	Particle therapy co-operative group
RB	Retinoblastom
RBE	Relative biological effectiveness
RDS	Radioresistant DNA synthesis
RIPA	Radio-Immunoprecipitation assay
RNA	Ribonucleic acid
RNF8	Ring finger protein 8
RNS	Reactive nitrogen species
RPA	Replication protein A
RT	Room temperature
SAC	Spindle assembly checkpoint
SCC	Sister chromatid cohesion
SD	Standard deviation
SDSA	Synthesis dependent strand annealing
SDS-PAGE	Sodium dodecyl sulfate- polyacrylamid-gelelektrophoresis
SEM	Standard error of mean
SF	Surviving fraction
siRNA	small interfering RNA
SLD(R)	Sublethal damage (repair)
SMC1	Structural maintenance of chromosome 1
SOBP	Spread out bragg peak
SP	Short patch
SSA	Single strand annealing
SSB(R)	Single strand break (repair)
ssDNA	Single stranded DNA
SWS1	SWIM domain containing Srs2 interacting protein 1
TBS	Tris buffered saline
TCR	Transcription coupled repair
TGFα	Tumour growth factor α
Tip60	TAT interacting proteins 60
TLS	Translesion DNA synthesis

TNM	Tumour, lymph node, metastasis
USZ	University hospital Zurich
UV	Ultraviolet
vs.	versus
WHO	World health organization
WRN	Werner syndrome, RecQ helicase-like
WT	Wild type
XPA/B/D/F	Xeroderma pigmentosum, complementation group A/B/D/F
XRCC1/3/4	X-ray complementing defective repair in Chinese hamster cells 1/3/4

1 Introduction

1.1 Cancer and cancer treatment

Cancer is a malignant disease, which is characterized by uncontrolled growth of a cell mass (tumour), its invasion into normal tissue, and often times its spread throughout the body. The name arises from early reports where swollen blood vessels of a huge tumour under the skin gave a picture of a crab (in astrology: cancer). Today we know about 100 different kinds of cancer. Cells from almost every tissue of the body can give rise to cancer. Classification of the different types is due to the site of origin: carcinoma – cancer of epithelial origin, sarcoma – originate from mesenchymal tissue, leukaemia – result from haematopoietic cell lineages (*1*). To rank the severity of the disease, an international TNM classification is used. T0-T4 indicate the expansion of the primary tumour, N0 – N3 display how many lymph nodes are infiltrated by tumour cells, and M0 – M1 stand for absence or presence of metastases.

According to the World Health Organization, cancer causes 20 % of deaths in the Europe. With more than 3 million new cases and 1.7 million deaths per year cancer remains the most important cause of death and morbidity in Europe after cardiovascular diseases. Lung, stomach, liver, colorectal, oesophagus and prostate cancers are the most frequent types among men whereas breast, lung, stomach, colorectal and cervical cancers are the most frequent ones among women (Fig. 1.1, 1.2). European trends in incidence are favourable in the more prosperous countries from Northern and Western Europe, except for obesity related cancers and tobacco-related cancers, in the case of women (*2*).

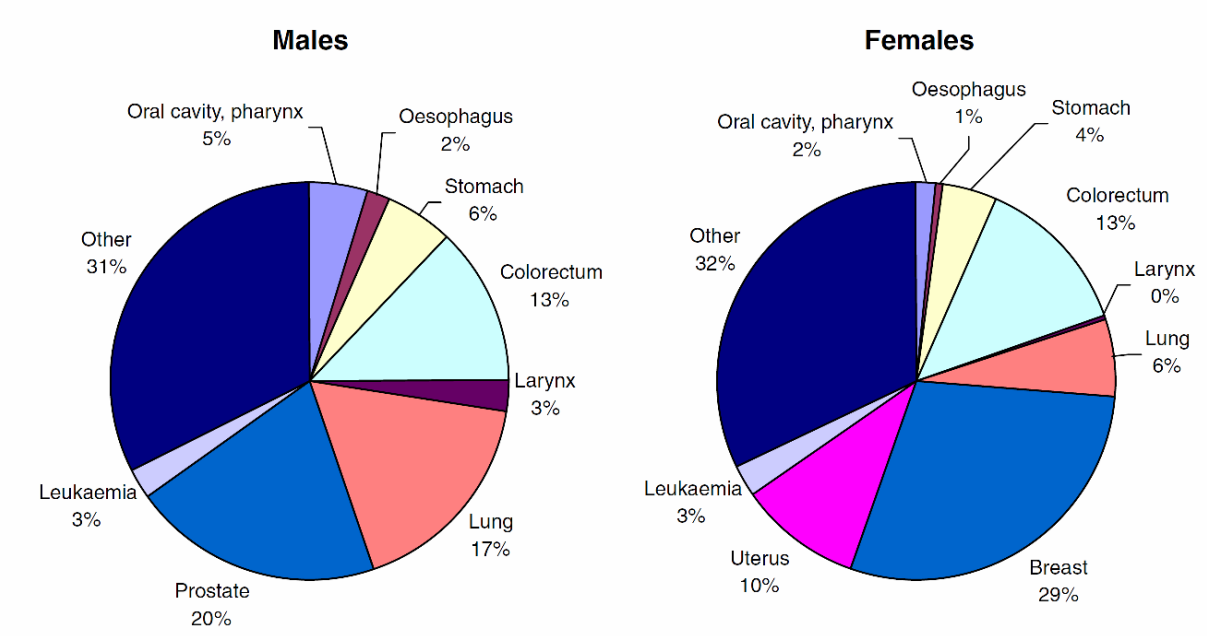

Figure 1.1 Cancer incidences by gender in Europe in 2006 (*2*)

Early malignant cells gain certain mutations in important control genes, which result in a growth advantage. Normally those cells get cleared by the immune system. But they further evade several control mechanisms and cell death pathways, which are normally activated in cells to prevent them from becoming “uncontrolled”. When the tumour is growing, new blood vessels have to be formed, which is promoted by the secretion of angiogenic factors. If the cells gain the ability to move and invade into the blood stream or lymph system and build a new cell colony at a distant site in the body, this process is called metastasis, which is the most severe problem. 90% of cancer deaths result from metastatic disease. Compromise of normal organ functions can lead to morbidity and mortality. Therefore it is very important to detect the primary tumour at an early stage. Huge screening programs and prevention campaigns resulted in a decrease of cancer mortality in Europe Union. Mortality rates decreased by 9% in men and 8% in women from 1990 to 1994 and 2000 to 2004 (*3*), which shows a favourable trend that is similar to the US and which has also been found in Japan. On the other hand, worldwide prognosis is not that good. According to WHO estimations (from 2004) deaths from cancer worldwide will rise to an estimated 12 million in 2030. This trend is mainly attributed to low-income countries, which have no adequate programs for cancer prevention and treatment.

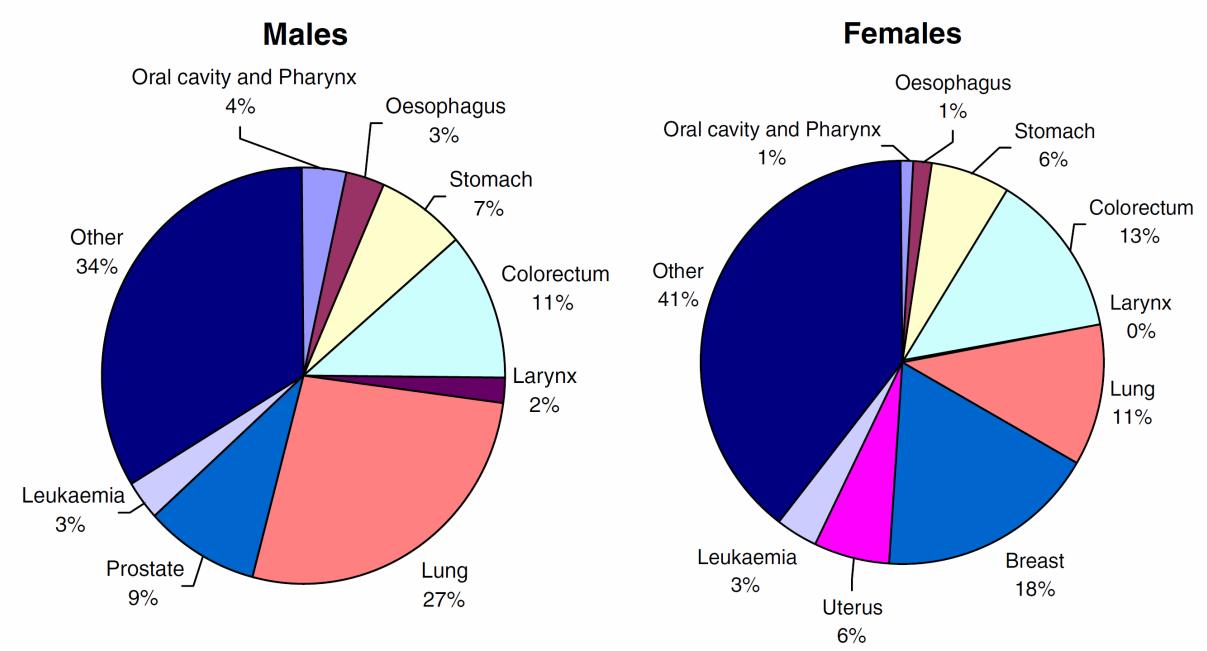

Figure 1.2 Distribution of cancer deaths by gender in Europe in 2006 (*2*)

Cancer prevention is possible with a healthy lifestyle and early diagnosis. Some of the most common tumour types, like breast, colorectal and cervical cancer, can be cured if detected early enough. Screening programs with annual cervical pap tests or mammography and colonscopy every 5 years detect very early stages of those cancer types.

Three main treatment options are available, namely surgery, radiotherapy, and chemotherapy. Surgery is the oldest treatment form and leads to good therapeutic results in early non-metastatic tumours. It is often followed by concomitant radiation therapy or chemotherapy to ensure that all malignant cells, including metastatic cells, have been removed. The latter two treatment modalities take advantage of the fact that tumour cells are different from normal cells. Due to the loss of control mechanisms, they are much more sensitive to genotoxic stress. Radiotherapy gives good results for long-term control of many tumours of the head and neck, lung, cervix, bladder, prostate, and others. It is actually often used if a tumour cannot be excised because it is situated close to or within a critical organ (e.g. brain, lung). In addition, many patients receive chemotherapy at some point in their treatment schedule. Symptom relief and arrest of the disease are often obtained with these drugs, but very few cancers (among them lymphomas) can be cured by chemotherapy alone (*4*).

1.2 Role and rationale for radiotherapy in management of cancer

X-rays were first produced in 1895 and have been used for cancer treatment since, but several decades passed before it became a standard treatment option. After Wold War II with the usage of nuclear weapons the interest in the effect of radiation on humans and cells grew. 1951 the first clinical cobalt-60 unit was implemented in London, Ontario, Canada (*5*). Already in 1956 the first patient was treated with a medical linear accelerator in Stanford. Since then over 40 million of patients have been treated primarily with the help of a medical linear accelerator. Radiotherapy is a good example of a multidisciplinary field. Physicians, physicists, and biologists came together to make the use of X-rays a major treatment option today. More than 50 % of all cancer patients receive radiotherapy at some point during their illness (*6, 7*).

All treatment options follow the goal to cure the disease with as few side effects as possible, leading to a high therapeutic index. However, administration of some radiation to healthy tissue and organs is unavoidable. A too high single dose delivered to a critical organ like lung or rectum leads often to severe side effects or even mortality. Therefore the total dose is fractionated over the treatment time. Conventional treatment protocols use 30 fractions with each 2 Gy over 6 weeks. This is done due to several important reasons which led to the 4 R’s of radiobiology.

1.2.1 Four R´s of Radiotherapy

The four R´s determine the final response of tumour and normal tissue after irradiation. Due to these four main biological response mechanisms to radiation, normal-tissue toxicity can be minimized and tumour control can be maximized.

Recovery (Repair) of the normal tissue from sublethal and potentially lethal damage after exposure to radiation can occur in between the fractions. Radiotherapy counts on the fact that repair and control mechanisms are functional in normal tissue and less efficient in tumour cells. Therefore normal tissue can repair damages more accurately in between the fractions. For convenience, fractions are given in 24 hour intervals. The intervals could also be shortened, as most DNA damage is repaired 6 hours after irradiation.
The term sublethal damage (SLD) repair was first described by Elkind *et al.* who showed *in vitro* that splitting a high total dose into two equal fractions separated by a time interval (30 min – 8 hours) would increase the survival of the cells (*8*). Under these conditions sublethal radiation damage is repaired. However, if the entire dose is given without a break, the damages have a higher chance to interact and to form a non-repairable lethal damage. In a second case when the dose is administered slowly over a longer time period, sublethal damage repair occurs during the time of exposure. This is called the *dose-rate effect*. Dose rates below 1 Gy/min can lead to a better survival of cells as they start to repair during the time of radiation exposure. For higher dose rates this can be excluded (*9*).
A potentially lethal damage (PLD) is lethal under normal circumstances, but under certain conditions this damage can be repaired and is not lethal. If cells are kept in a density-inhibited state for 6-12 hours after irradiation before plating them for clonogenic survival assays, they show an enhanced survival (*10*). This was also demonstrated *in vivo* where tumour cells were removed only 2-8 hours after irradiation and assayed for their reproductive capacity (*11*). In general, PLD is repaired if cells are situated in suboptimal growth conditions, where they do not attempt the complex processes leading to mitosis and cell division. Under these conditions they have time to repair damages. Whether PLD repair is clinically relevant is a matter of debate. However, radioresistant tumours seem to be able to repair PLD (*5*). Hypoxic tumour cells are within suboptimal growth conditions and might also profit from PLD repair.

Repopulation is the proliferation of cells to fill the gap left by cells that died. Normal cells harbour a very stringent regulation of “when it has to die”. A percentage of normal cells will receive lethal damages or will not repair the damage properly. Those cells die via programmed cell death pathways. Other healthy cells start to divide and to fill the gap. This will help to keep the tissue intact even though it is not the same as non-irradiated one. But

repopulation does also occur in the tumour. Rapid repopulation is an important factor leading to bad outcomes. Especially for head and neck cancers, it was proposed that treatment be completed as soon as possible after initiation (*12*). In general it is believed that any unnecessary treatment breaks should be avoided to prevent tumour regrowth.

Redistribution of cells within the cell cycle is the return toward a more even cell cycle distribution, after the selective killing of cells in radiosensitive phases of the cell cycle (M/G1/early S phase cells). Surviving cells, which were predominantly in a resistant phase at the time point of irradiation (late S/early G2 phase), move together to a more radiosensitive phase and might be more efficiently killed with the next fraction. Also normal cells, which arrested in late G2 phase, are more radiosensitive. This might be another advantage, because normal cells with non repaired damage should not survive (*5*).

Reoxygenation of the tumour mass will sensitize the tumour cells for the next fraction. In 1968 it was shown by van Putten that the percentage of hypoxic cells in the tumour did not change after 4 fractions compared to the untreated tumour (*13*). This phenomenon indicated that hypoxic cells can become oxygenated in the course of the treatment, which was called reoxygenation. Hypoxic tumour cells are more radioresistant. Normally oxygen takes part in the radical reactions and leads to better damage fixation and more efficient cell killing. This is called the oxygen enhancement ratio (OER). Oxygenation of the tumour cells makes them again more susceptible to radiation. Therefore long treatment breaks (such as over weekends) are helpful with regards to reoxygenation.

1.2.2 Molecular stress responses after ionizing radiation exposure

1.2.2.1 Radical formation and scavengers

Ionizing radiation (IR) can be either of electromagnetic (X-ray and γ-ray) or particulate (carbon, neutron, proton ions) origin. As the word ionizing radiation implies, radiation is used to ionize atoms in the cell, this can happen directly or indirectly (Fig. 1.3). Particles (also called hadrons) act dominantly through direct ionizations, meaning they damage DNA or other molecules through direct particle interactions. However, the percentage of direct actions depends on the particle mass and speed. When a particle becomes slowed down (through interaction with matter) the direct interaction probability increases. As part of this thesis, proton ions will be explained later on. Photons from high frequency electromagnetic radiation are mainly indirectly ionizing. As they pass through the cell, they interact with loosely bound planetary electrons of atoms and give up part of their energy to the electron as

kinetic energy. This so-called secondary electron is a fast-moving charged particle. The photon itself becomes deflected, proceeds with reduced energy, and if energetic enough may

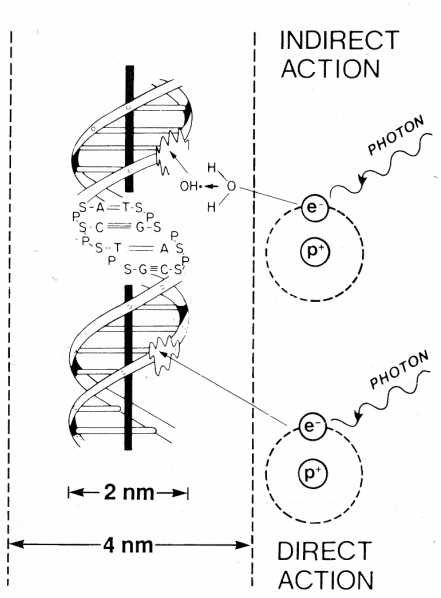

Figure 1.3 Direct and indirect actions of radiation. A secondary electron generated by the absorption of an X-ray photon interacts directly with DNA (direct action). If a secondary electron interacts with water molecules, hydroxyl radicals ($OH^{\cdot}$) can be produced, which in turn might generate damage to DNA (indirect action) (adapted from (*5*)).

energize another electron. Many of those fast secondary electrons can directly or indirectly ionize other atoms. The predominant interaction takes place with water molecules, which compose the most abundant medium in the cell. An ion radical and a free electron are generated. The highly reactive ion radical will react with water molecules forming highly reactive hydroxyl radicals ($OH^{\cdot}$). These can diffuse and account for most of the damage produced in the cell. In the presence of oxygen even more reactive oxygen species (ROS) can be formed. Radical reactions lead to a cascade and take place until the restoration of electronic charge equilibrium is reached. Chemical modifications may damage almost any component of the cell, including proteins, lipids, DNA, etc., with DNA damage being the most toxic one (*5, 14, 15*). In contrast to the very fast events during radiation exposure, the actual cell death takes time, as do secondary cancers, evolving over years after radiation treatment (*16*).

To protect themselves from radical-mediated damage, cells have developed several scavenging mechanisms or take up antioxidant molecules e.g. glutathione, peroxiredoxin I and II, SOD, ascorbic acid (*17, 18*). These systems can cope with the daily environmental levels of radicals, but not with the huge amount produced after exposure to clinically relevant doses of radiation. Hence it was shown that administration of antioxidants like DMSO to cells could minimize the effect of radiation (*19*).

From experiments with cytosolic microbeam irradiation it became obvious that radicals propagate throughout the cell and thereby harm the cell at more distant sites, which includes the nucleus (*20, 21*). Furthermore the generation of mitochondria-dependent reactive oxygen/nitrogen after irradiation might play a role (*22, 23*). Damaged mitochondria may produce ROS and this stress signal is forwarded via adjacent mitochondria through Ca^{2+}-dependent mitochondrial permeability. It was reported that ROS persist in normal diploid fibroblasts with functional p53 for up to two weeks after X-ray exposure. In cells with depleted p53, ROS levels were decreased in magnitude and duration (*24*). Late responses to radiation, like the abundance of ROS for up to 2 weeks, might be important for the proper reaction of the cell.

1.2.2.2 Signal transduction

Ionizing radiation can activate nuclear and membrane-cytoplasmic signal transduction pathways. On the nuclear level, generation of DNA damage activates the PI3K-like kinases ATM, ATR, and DNA-PKcs, which in turn can regulate cytoplasmic signalling pathways. ATM was found to negatively regulate the anti-survival JNK1/2 signalling pathway and positively regulate signalling through ERK1/2 (*25, 26*). Whereas in the other direction, cytoplasmic to nuclear signalling, MEK1/2-ERK1/2 positively affect ATM, as inhibition of the former reduced homologous recombination and completely abrogated autophosporylation of ATM at S1981 (*27*). If DNA double strand breaks affect the ERK1/2 pathway in a positive way depends on the extent of DNA damage, namely the dose (*28*).

An example of membrane to nucleus signalling is the translocation of the EGF receptor (EGFR) into the nucleus together with Ku70/80 and protein phosphatase 1, which leads to an increase of DNA-PKcs activity and therefore to an increased DNA repair activity (*29*). When tumour cells over-express EGFR or express certain EGFR isoforms, radioresistance occurs due to promotion of DSB repair via activated DNA-PKcs (*30*). EGF receptors become initially activated up to 10 min after exposure and reactivated ~ 60 – 180 min later. The initial activation of EGFR1 leads to the cleavage, release and activation of presynthesized paracrine ligands (e.g. pro-transforming growth factor α, TGFα), which in turn promotes growth and survival of irradiated and distant non-irradiated tumour cells often having the receptor over-expressed (*31*).

Another effect on the membrane level is the activation of acidic sphingomyelinase after exposure to radiation, which increases the concentration of ceramide in the cell and facilitates the clustering of receptors, promoting their activation (*32*).

Not only phosphorylation modulates cellular signalling after radiation exposure. Protein phosphatases (PPTases) are very sensitive to oxidation or nitrosylation. The huge amount of

ROS/RNS produced after radiation exposure decreases their activity and therefore increases the activity of certain rapidly phosphorylated receptors after irradiation (*33*).

Cytosolic signal transduction pathways are induced within minutes after radiation exposure, such as MAPK and PI3K pathways. The different pathways can lead to the expression of pro-/anti-apoptotic genes as well as genes needed for proliferation. All these pathways interact to determine the final outcome like cell death, survival, or sensitization/resistance to the next fraction of radiation (*33*).

Irradiation can also regulate the level of protein synthesis. Rapid activation of the MAP kinase ERK1/2 resulted in an early transient increase in cap-dependent mRNA translation over mTOR. Translation of mRNAs, encoding proteins involved in DNA repair and cell survival, leads to radioprotection in normal cells. In contrast this increase in translation has not been found in transformed cells, which have often up-regulated basal ERK activity and constitutively active mTOR signalling (*34*).

A complex interplay of all these pathways and modifications determines the response of the irradiated cell. Here, the genetic status of the cells and the extent of the damage will influence the outcome. Accordingly, tumour cells and normal tissue cells must respond differently.

1.2.2.3 Cell death mechanisms

Different types of cell death occur after exposure to ionizing radiation e.g. apoptosis, autophagy, necrosis, senescence, and mitotic catastrophe. Which type will occur depends on the cell type. Fast apoptotic response takes place within hours after irradiation and is limited to thymocytes, lymphocytes, and other cells in rapidly proliferating tissues as in hair follicles, small intestine, and developing embryos (*35*). Endothelial cells can also activate a fast apoptotic response but only after high doses (above 15 Gy) (*36*). Autophagy is another type of programmed cell death, which is characterized by the formation of autophagic vesicles in the cytoplasm. Senescence is a state where cells lose their ability to proliferate but stay metabolically active. Necrosis is not a form of programmed cell death, as cells die without any signalling to the environment and will not be removed by immune cells. Necrotic areas were reported after radiotherapy (*37, 38*).

Solid tumours and most normal cells die at a relatively long time after exposure to radiation, often attempting mitosis one or several times (*39*). Cell death, which occurs after few attempts of mitosis, can be executed by apoptotic or autophagic proteins but is called mitotic catastrophe. Cells with several aberrant nuclei and micronuclei cannot proceed any more through mitosis and will die. An irradiated cell can still divide itself for several cycles, but eventually always one daughter cell dies and the surviving daughter cells will die at the next attempt to divide. In this case the cell is not called a survivor in radiobiological terms, as a

surviving cell has to form a colony of at least 50 cells before it is called a survivor. Because of this the clonogenic survival assays are important for determining the ultimate response of individually irradiated cells.

1.3 Conventional Radiotherapy

In the early days of radiotherapy, treatment planning was based on a two-dimensional X-ray image, and calculations were performed by hand. Uncertainties about the actual tumour margin, the tumour volume, and the true radiation dosage delivered to cancerous and healthy tissue were common. The big improvements in radiotherapy and also for other disciplines came with the fast progress in imaging modalities (computer tomography, MRI, and PET). Today's treatment planning has access to three-dimensional X-ray based images of the tumour and applies increasingly complex computer algorithms to formulate a treatment plan specifically for the 3D image (3D conformal radiation therapy). Now a radiation oncologist can no longer work without high performance computers.

Historically, radiotherapy is divided into three fields, sealed source radiotherapy (brachytherapy), unsealed source radiotherapy (systemic radioisotope therapy), and external beam radiotherapy, which is the main field.

During *brachytherapy* the radiation source is placed inside or next to the treatable site. It is used as an effective treatment for cervical, prostate, breast and skin cancer. The main advantage is that irradiation only affects a narrow localized area. High doses of localised irradiation can be used while the dose to the surrounding healthy tissue is often low.

During *systemic radioisotope therapy* soluble radioactive substrates are given to the patient orally or intravenously. These substances have similar properties as their non-radioactive physiological forms. In common use is radioactive iodine-131 to treat thyroid cancer. Due to its physiological function it will concentrate in the thyroid and produce beta and gamma radiation directly at the site of interest. But the patient will excrete radioactive substance over a period of time and has to be monitored.

External beam radiotherapy is the most prominent form of radiotherapy using mainly X-rays. State of the art devices today are medical linear accelerators producing high energetic X-rays. In general electrons are extracted from an electron "gun" usually made of tungsten and the electrons become accelerated within a high voltage linear accelerator tube. A limiting factor for the beam energy is the voltage of this tube. The high energy electrons become abruptly stopped by a metal target usually made of tungsten or other high Z materials. At this moment a big part of the kinetic energy of the electrons is converted to X-rays, which can be further shaped and selected for target coverage.

In conventional external beam radiotherapy (2DXRT) radiation is delivered to the patient from several directions: often front or back and from several sides (Fig. 1.4). Radiation fields resemble “boxes” which cannot spare critical tissues lying within this box (Fig. 1.4A).

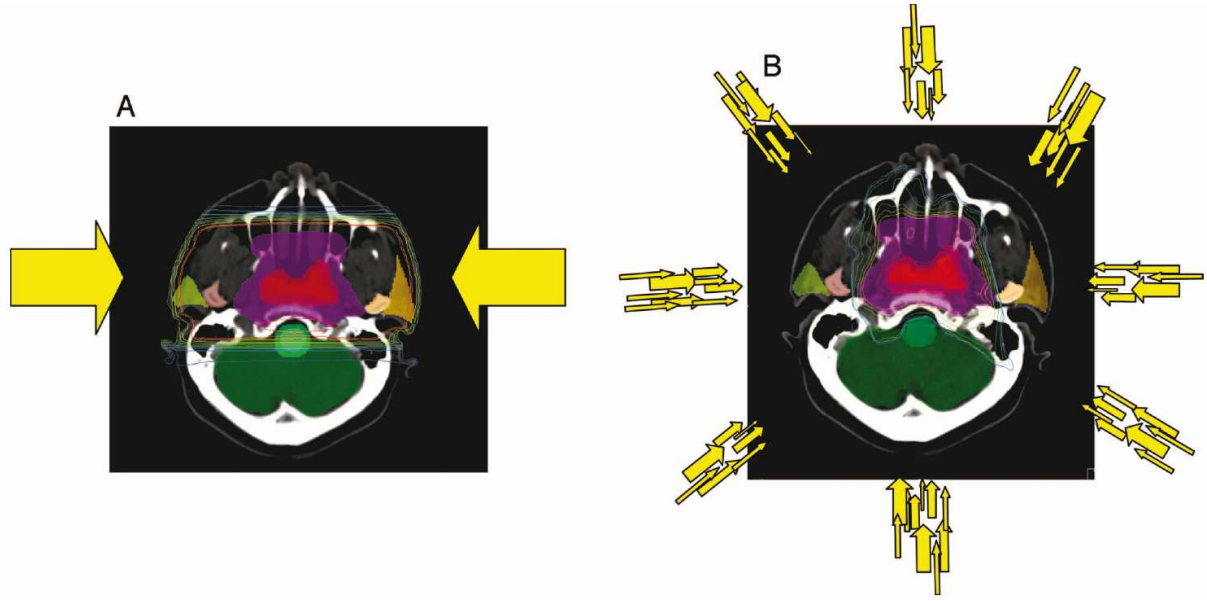

Figure 1.4 Two exemplified treatment plans for conventional radiotherapy (A) and IMRT (B) of a nasopharynx tumour (red = GTV; purple = CTV), isodose lines are plotted reaching from red to blue. (A) Two opposing beams of uniform intensities (yellow arrows). (B) Schematic view of multiple beams with different intensities from any number of angles (here 8 angles) to generate a highly conformal dose distribution with relative sparing of the brain, brainstem, and parotid glands (*40*).

This box shape is due to the depth-dose distribution of X-rays, which deposit most of its energy just under the skin and some residual dose to the tissue behind the tumour (Fig. 1.5, grey line).

3D planning allowed for accurate dose calculations to irregular shapes and critical organs, e.g. in the head and neck region, but corrections in dose delivery could not be made. Therefore intensity-modulated radiation therapy (IMRT) was developed, which allows modulation of the intensity of each radiation beam. Each field can have many areas of high intensity radiation along with lower intensity areas, thus allowing an adapted dose distribution to the irregular shape of the tumour or the critical organs (Fig. 1.4B). With the possibility to spare critical organs, IMRT is used now for prostate cancer where the rectum and the bulb of the penis can be spared, for head and neck cancer where xerostomia (dry mouth due to loss of salivary glands) can be reduced, and for breast cancer where the dose delivered to lung and heart can be decreased (*40*).

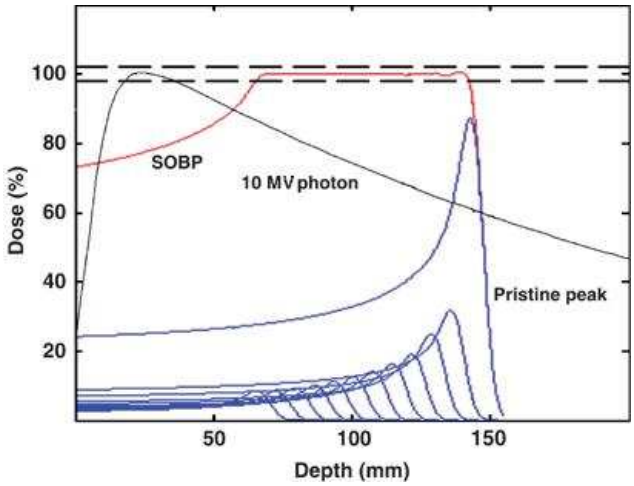

Figure 1.5 Depth dose distribution in tissue of a 10 MV X-ray beam (grey line), of several single proton beams with a pristine Bragg peaks (blue lines), and of a proton spread-out Bragg peak (red line) (Wikipedia, proton therapy).

Some concerns exist about the longer overall treatment time per fraction (15 – 30 min) during IMRT, which might give tumour cells the time for more efficient repair leading to decreased cell killing (*41*). But *in vivo* data showed that the lower cell killing was compensated by rapid reoxygenation (*42*). Another approach tries to decrease overall treatment time and the repair time in between fractions by hypofractionation schemes (16 fractions over 3 weeks vs. 25-28 fractions over 5-6 weeks). These are especially used for palliative care of fast growing, incurable head and neck tumours and increasingly as accelerated scheme for early-stage breast cancer patients (*43-45*).

However, more accurately delivered radiotherapy together with more accurate tumour volumes bears the danger of underdosing or even missing parts of the area of interest during treatment due to minor errors in positioning (*46*). As a control mechanism, the treatment is virtually simulated on the patient before the actual treatment start. Markers on the skin will help to position the patient. Some accelerators even have an integrated X-ray imaging system making the accurate positioning of critical organs directly on the patient table possible. This is called image guided radiotherapy (IGRT).

Furthermore, some target volumes are naturally moving during treatment, such as the lung during breathing. Four-dimensional conformal radiation therapy (4D CRT) measures the motion of tumours and includes this in the treatment formula configurations. This ensures that the tumour is targeted during motion and as much as possible healthy tissue is spared.

All these technical improvements can diminish side effects and increase the actual dose to the cancerous tissue, which is the ultimate goal of a radiation therapist. Highly trained staff is needed, and the consumption of time per patient is rather high, which makes radiotherapy expensive. But new technologies have never been cheap. In the next century radiotherapy will become increasingly multidisciplinary. Together with new advances in personalized medicine and concurrent treatment regimens the patients will further benefit.

1.4 Proton Radiotherapy

1.4.1 History and rationale for proton radiotherapy

Robert Wilson proposed in 1946 the use of light particles like protons and helium ions in cancer therapy, as they result in excellent dose distributions (*47*). In contrast to photons, protons penetrate the tissue only to a certain depth (range) depending on their initial energy. Along their path the tissue absorbs a relatively low dose from the protons. At the end of their range they stop and deposit most of their energy at the so-called Bragg peak, and no further dose reaches the distal tissue (Figure 1.5, blue lines). This makes protons an ideal irradiation source to solely cover the tumour volume but little of the normal tissue. Physicians saw the superior advantage for treatment of neoplasias of the brain, close to the brain stem, etc., and only ten years later the first cancer patients were treated with protons (*48*).

Protons are 1836 times heavier than electrons. When they move through tissue they interact with orbiting electrons through Coulomb forces. Because of their positive charge they attract electrons, resulting in ionization of atoms and formation of loose secondary electrons. Overall they lose relatively little energy during each ionization process and are minimally deflected due to their large mass. If a proton passes close to a positively charged nucleus of an atom it can get slightly deflected (Coulomb interaction with atomic nuclei). However, if the proton strikes a nucleus, it can lead to breakage while the proton loses a huge fraction of its energy and is significantly deflected (non-elastic collisions). During this process secondary proton and neutron irradiation is produced, which has to be kept in mind. In an elastic collision the nucleus stays intact but the proton loses as well a big fraction of its energy. The rate of energy loss is about proportional to the inverse of the square of the proton's mean speed. A proton with a higher energy can travel farther because it is not interacting very strongly with matter. Only at a certain velocity a proton does experience stronger interactions until it is so slow that it finally deposits all of its energy due to maximal interactions with electrons at the Bragg peak, named after Sir William Henry Bragg (*49*).

With regard to the next chapters some definitions have to be introduced. The **linear energy transfer** (LET) is a measure of the energy, which is transferred to a material/tissue per µm (keV/µm) when ionizing radiation passes through it. For low LET radiation (< 10 keV/µm) secondary electron effects are very important. In the case of high LET radiation (> 10 keV/µm) the relative contribution of secondary electrons to the yield of complex lesions is only about 10% compared to direct effects (*50*). The LET range of protons can be from 0.5 – 30 keV/um (1000 – 1 MeV protons).

To measure the impact of the dose deposited in a biological system (cells, tissues, whole body) the **relative biological effectiveness** (RBE) is determined. It is the ratio of the dose of

photons (250 keV x-rays) divided by the dose of protons which is needed to result in the same biological effect. A RBE > 1 shows that this type of radiation is biologically more effective because a lower dose is needed to result in the same biological effect.

The **oxygen enhancement ratio** (OER) describes the enhanced radiosensitivity of aerated cells in contrast to hypoxic cells (factor 3), which disappears if cells are irradiated with high-LET radiation (*51*). Radiation forms radicals, which produce highly toxic peroxides in the presence of oxygen. Oxygen is needed to fix the damage when indirectly ionizing radiation is used. This is also the case for low LET protons (*52, 53*).

As a sole Bragg peak will never cover the usual size of a tumour, a **spread out Bragg peak** (SOBP) is usually formed (Fig. 1.5, blue vs. red line). Several mono-energetic beams of different energies are overlaid to result in the SOBP. With the SOBP the realization of the dream of unique tumour irradiation is prevented, as the proximal dose to the skin tissue is increased compared to conventional photon therapy (Figure 1.5, red line). The broader the SOBP, the bigger is the entrance dose at the plateau region (Fig.1.4 very left area of red line before it crosses the grey line), and unfortunately this is a major draw back to high energy photons, as skin can get injured severely by protons, which enter the tissue. To prevent this site effect several beams are used from multiple sides to cover the tumour volume (*54*).

Before the first patients were irradiated with protons, several studies were performed by laboratories in Berkeley and Harvard. After whole-body irradiation experiments with mice the end point of LD_{50} (dose where 50% of the mice died 30 days after exposure) resulted in an RBE of 0.8 - 1.0 (*55*), but when LD_{50} within 6 days was analyzed an RBE ~ 1.2 was observed (*56*). These data went along with earlier primate experiments and indicated a higher sensitivity of gastrointestinal tissues to protons compared to conventional radiation (*57*). Ten years later, after Withers and Elkind developed the mouse jejunal crypt assay, the first fractionation experiments with protons displayed an RBE of 1.23 (±0.02), which was independent of fraction size (*58, 59*). In the same period two important studies showed for fractionation and single-dose proton exposure an RBE = 1.15 for acute mouse skin reactions (*58, 60*). Before the initiation of clinical trials in Boston, the group determined RBEs for various normal murine tissues, which ranged from 1.09 – 1.32 (lens to tail vertebra respectively) (*61*). Even RBE-values for a spontaneous mouse mammary carcinoma were determined (*62*). All of these studies resulted in important *in vivo* data, which led to the implementation of the RBE of 1.1 into the clinic.

In terms of specific indications for protons, they were proposed early on as a neurosurgical tool (*63*). Experiments with rabbit and goat brains revealed a discrete lesion after 200 Gy proton irradiation exposure (*64, 65*). Damage was restricted to a small area deep in the brain,

sparing surrounding brain tissue. Later on pituitary neoplasias of human patients were and are still treated using protons.

The second very specific indication was the treatment of uveal melanomas, a cancer of the eye (*66*). Interest in proton therapy grew due to the successful therapy of these special melanomas. But all of those early patients and even patients today were treated in a physics institute, which owned an accelerator to produce a pure high energy proton beam to accomplish proton therapy. At the hospital of the Loma Linda University the first hospital based proton therapy facility was implemented in 1990. Today a hand full of hospital based facilities are in operation and several more are under construction. This comes 54 years after the first patient was treated with proton therapy, and in this time different technical advances have been developed and will be explained in the next chapter.

1.4.2 Equipment and technical advances

Protons are the positively charged nuclei of hydrogen atoms, which are surrounded by a negatively charged shell electron. The source for protons is hydrogen gas. At the Paul Scherrer Institute an internal “cold cathode” ion source is used to extract the protons (Varian/Accel), but the most frequently used cyclotrons contain an external ion source (electron cyclotron resonance (ECR) ion source from IBA), which is a so-called hot-plasma ion source. In general electrons are accelerated and ionize the plasma. Special extraction geometry of the source helps to extract the positively charged protons, which normally tend to follow the electrons to keep the plasma in a neutral charge. After extraction protons need to be accelerated to clinically relevant desired energies of 70 - 250 MeV. For this two different types of accelerators exist, cyclotrons and synchrotrons.

A *cyclotron* uses dipole magnets in order to generate a region of uniform magnetic field, and has an electric field. Protons will be injected perpendicular to the magnetic field region and travel on a semicircular path. When reaching the gap with a high-frequency alternating voltage, they will be accelerated. Now the protons have gained energy, which results in a higher velocity. In order to reach the gap in the same time interval again, they travel now on a larger radius than before. They become accelerated like this for several rounds until they reach the desired energy, which is achieved in milliseconds (ms).

Synchrotrons are circular accelerator rings with electromagnetic resonant cavities at specific intervals around the ring, which accelerate protons while they are circulating. Here the particles follow the same radius, and therefore the strength of the magnetic field must be increased and synchronized with the proton energy, which increases with each turn. It delivers its protons in pulses (seconds). Variation of the proton energy is achieved by extracting protons with the desired energy providing a flexible solution with excellent beam

qualities. In contrast, cyclotrons have a fixed energy, and if protons of lower energies are needed they have to be degraded downstream of the accelerator. This leads to a reduction in beam quality, which minimizes the efficiency of the system. However, synchrotrons are much bigger (~ 30 m radius vs. ~ 12 m) and more expensive than cyclotrons, though costs for an accelerator cover a small portion of the costs of a facility.

After extraction of the beam it has to be transported to the treatment room using huge bending magnets, which steer and focus the beam. For real time assurance of the beam quality, ionizing chambers check deviations of the beam position, the total beam current, and the beam size, and uniformity.

In order to cover the whole tumour volume two different delivery systems exist. As the pure beam has a diameter of about 1 cm it is not able to cover larger tumour volumes. With the *passive scattering technique* a larger field size can be achieved by scattering of the beam. Sometimes a single scattering foil made of lead is sufficient to broaden the beam to the desired size. For larger fields the reduction in beam quality is too huge and therefore a double-scattering technique is applied (*49*). A second Gaussian-shaped scatterer, contoured with two different materials which help to minimize the energy loss and production of secondary radiation, is used. The SOBP is formed with a range modulator consisting of absorbers with variable thickness. Furthermore the shape of the specific tumour is mirrored by custom milled molds or compensators. Due to all these interfering steps, efficiency with the double scattering technique can be down to 10% for typical treatment fields (*67*).

With the *spot scanning technique* a “pencil beam” is magnetically scanned over the target volume. This technique requires not necessarily compensators nor collimators, as the target is scanned and the beam energy can be varied through selected extraction of proton energies from a synchrotron allowing adaptation for each spot. Though, at the Paul Scherrer Institute (PSI) in Villigen, Switzerland, the beam of each spot is still degraded by range shifters. Physicists at the PSI have pioneered the proton *spot scanning technique* for a very compact gantry. The first veterinary patients were treated in 1994 and in 1996 the first human patient could be treated (*68*). During *discrete spot scanning* the beam is switched of while the magnet settings are changed and the next spot can be applied. Covering of the target volume is reached by simply scanning it. The scan follows in x-y direction whereas the orthogonal direction is changed by table positioning. If the scan starts at the most distal layer, the proximal layers accumulate already a certain dose, and therefore intensity modulation of the beam is needed for more proximal layers to reach a uniform target dose. With scanning it is possible to construct dose distributions with complex shapes and accurate conformation of the dose, which provides additional dose sparing of the healthy tissues compared to scattering. Secondly, no scatterers are needed, which reduces nuclear interactions outside the patient leading to a smaller neutron ion contamination. Spot scanning gives a high

flexibility, which makes it possible to generate intensity modulated proton therapy (IMPT) plans, which means that non-uniform dose distributions are delivered from several treatment fields. A steeper dose gradient with high dose conformality, a further reduction in integral dose, and a lower sensitivity to several uncertainties would be reached (*69*). Furthermore the dimensions of the gantry are reduced by a factor of 3. Difficulties like the complex technical set up to generate a very narrow pencil beam are only problematic in the beginning. But spot scanning is problematic with regard to organ motion. If one spot is delivered to the wrong position it can have quite a huge impact. This problem is solved by rescanning the volume a second time, with each scan delivering half of the dose. When IMPT is used, it would be also possible to track organ motion (*69*).

Another more sophisticated issue is the patient positioning and immobilization, which is similar to IMRT. However, the range of the proton beam is also affected by bony structures moving in the path of the beam. Therefore the positioning of the target volume and of the surrounding structures is important and has to be verified with an X-ray image before every treatment session (*67*).

Beam scanning was pioneered at Berkeley and the PSI in Switzerland developed the first compact spot scanning Gantry. Now the MD Anderson Cancer Centre in Houston and the Rinecker Proton Therapy Centre in Munich have commissioned hospital based spot scanning gantries. All future facilities or the ones under construction will also implement the spot scanning technique, as it seems superior to scattering (statement by MD.Anderson staff). The whole construction and implementation costs of such a facility are about 100 million USD and can reach 150 million (*70*)

A development, which possibly would make proton therapy more widely available, is the laser-based generation of proton beams (*71*). So far these lasers can generate 23 MeV protons, which were already tested for biological efficiency. Protons are delivered in pulses and not continuously and therefore more biological studies are needed to verify the biological effectiveness (*72, 73*). High frequency lasers are still under construction. They could produce clinical relevant proton energies but would still need a gantry for guidance of the beam and extensive shielding for the scattered and secondary radiation.

1.4.3 Experience in the clinics and the need for randomized trials

Until 2010 about 67 000 patients were treated with protons worldwide (March 2010 by Martin Jermann, PTCOG Secretary). The niche for uveal melanomas and pituitary adenomas promoted proton therapy during the last 50 years. Soon other indications, which are obviously profiting from the excellent dose distribution were irradiated with protons: paediatric intracranial tumours, chordomas and chondrosarcomas. Once hospital-based proton facilities

started being built in the 1990s more patients were able to be treated with protons, other indications were included like prostate cancer, non-small lung cancer, hepatocellular cancer and today also breast cancer.

Two different types of treatment goals exist. As first, disease sites, which favour higher doses for cure (local control), are treated with bigger doses per fraction (dose escalation in the tumour volume). This can be either achieved by hypofractionation (fewer fractions with higher doses, if the surrounding tissue is not extremely radiosensitive) or by keeping the fraction size as in conventional radiotherapy and increasing the dose per fraction slightly. Examples are uveal melanoma, skull base, paraspinal tumours (chondrosarcoma and chordoma), and unresectable sarcomas (*74-76*). The second option is to use the increased precision for minimizing unwanted side effects. Here the actual dose targeting the tumour is the same as in conventional radiotherapy, but the dose to the healthy tissue is reduced. This treatment option is very common for paediatric neoplasms (e.g. medulloblastoma with sparing of healthy brain tissue) and prostate cancer (to spare the rectum) (*77, 78*). In both cases the *therapeutic ratio* is thought to be increased.

On the basis of the biological studies in the 1980s the RBE of 1.1 was implemented into the clinics. The photon equivalent dose is 0.9 Gy of protons for 1 Gy of photons which is applied everywhere in the treatment volume. In the actual proton therapy the dose to healthy tissue is diminished due to the superior dose distribution but the biological effective dose at sites irradiated with protons is thought to be equivalent to conventional photon radiation therapy due to the RBE factor used. Therefore the effectiveness of protons regarding tumour cell killing is equal compared to conventional therapy. With this approach it is only possible to reduce adverse side effects.

Many studies deal with treatment planning and dose painting, which show the superiority of protons (Figure 1.6). However, clear evidence from clinical trials is still missing. There was increasing demand from the medical society to show that morbidity is really reduced or an improved local tumour control is reached with proton radiotherapy. Normally the better effectiveness of a new treatment regimen has to be approved by randomized clinical trials. But in the field of radiation oncology many improvements were implemented due to its logical advantage (e.g. Cobalt machine → Linac → IMRT) (*79*). Reasons for the few clinical proton therapy trials in the past were limited beam energies, as not all centres had access to megavoltage beams, limited technology, and limited beam availability. Furthermore ethical discrepancies exist. Protons deliver less dose to critical structures and for that reason one cannot randomize a child to a treatment that gives higher dose to healthy tissue like with photon irradiation. As third point, it is difficult to gather comparable patient populations as most of them have encountered gross tumour resection and/or chemotherapy in advance.

In 2007 only 4 randomized trials studying proton therapy with 700 patients were available. From a combination of trials and case studies, only few have clearly demonstrated a better clinical efficacy of protons (*79, 80*).

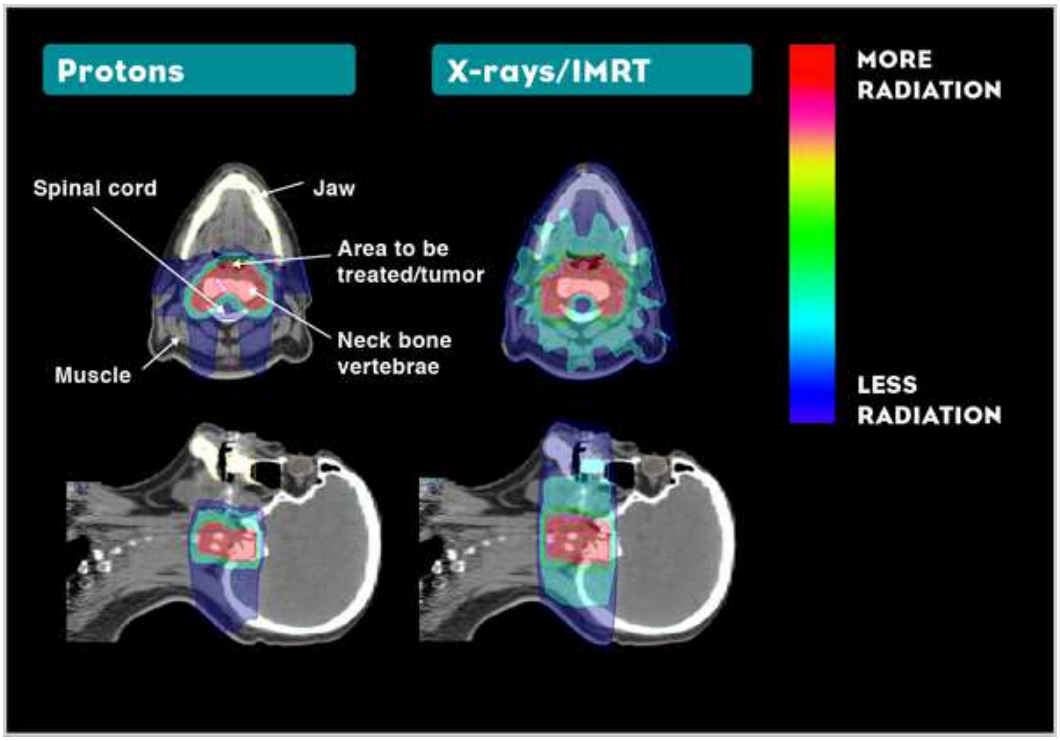

Figure 1.6 Examplary treatment plans for a tumour of the skull base comparing a proton therapy and a IMRT plan. Isodose regions indicate the dose delivered to the tissue ranging from high dose (red) to low dose (blue) (copied from procure training center page). http://www.procure.com/ProtonTherapy/TumorsTreated/Other.aspx

For example many case studies exist for paediatric intracranial tumours, which are not comparable and therefore the evidence level of clinical efficacy is low. Whereas in the case of prostate cancer, at least for some studies a reduction in long term rectal and genito-urinary damage could be detected. Others revealed a small difference. The advantage of precise dose delivery by protons may be reduced in those studies due to errors in patient set-up and internal organ movement during treatment. Especially errors in patient set-up destroy the better therapeutic ratio gained with the increased precision. The errors are in the 2 – 5 mm range but can affect drastically the outcome. (*79, 81*). For two other indications, ocular tumours and chordomas of skull base, protons resulted in a superior efficacy (*80*).

With more custom built proton facilities, consisting of several treatment rooms, many more patients will be treated. Collaboration of these therapy centres world wide will increase the number of good quality randomized clinical trials. This has to be done within an acceptable time frame so that decisions can be made before more centres are constructed. On the other hand reduction of late side effects and secondary malignancies would only be possible to validate within a ~ 10 - 20 year patient follow-up study. It is problematic to prove that saving more healthy tissue during treatment is beneficial for the patient. Only in the case of

paediatric patients it becomes evident as their still dividing tissues (even brain) can propagate mutations and lead to secondary cancers at later time points.

Studies on dose escalation and not only on the reduction of side effects would validate the second type of treatment goals for proton therapy. If the dose constraints to organs at risk could be kept the same, a study like this might be possible.

Finally the advantage of protons might be just too small to be detectable by tumour control or normal tissue complication analysis for certain tumour sites.

1.4.4 Molecular stress responses after proton beam exposure

Money should be as well invested in basic research due to uncertainties about the RBE. According to the tissue, cell line, end point, or physical beam characteristics investigated, it can vary heavily. Furthermore the applicability of chemotherapy regimens together with proton therapy has not been validated yet.

All studies determining the RBE were summarized in 2002 by Paganetti (*82*), showing little variation *in vivo* (mean RBE 1.1) and rather huge variation *in vitro* (mean RBE 1.2) (Fig. 1.7).

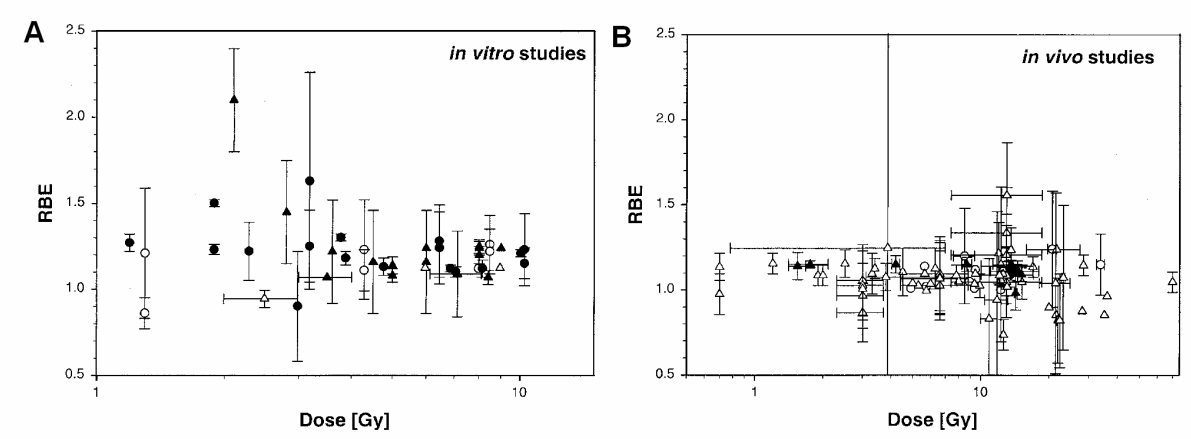

Figure 1.7 Experimental proton RBE values (relative to ^{60}Co) over dose/fraction for (A) cell inactivation *in vitro* and (B) measured *in vivo* in the centre of a SOBP. In (A) closed symbols show data points for Chinese Hamster cell inactivation and open symbols stand for other cell lines. In (B) closed symbols show RBE values for jejunal crypt cells and open symbols stand for RBEs of all other tissues. Circles represent RBEs for < 100 MeV beams and triangles for > 100 MeV beams (by Paganetti (*82*)).

The huge variation of the RBE of *in vitro* studies might be due to the different genetic background of the cells. Immortalized cell lines rather resemble cancer cells with their various mutations, and it would be interesting to see if and how these mutations affect the RBE of protons. On the other hand, *in vivo* healthy tissues without mutations, which were used in the mouse studies, responded in a similar range indicating the response of healthy tissue with less genetic variations. Furthermore huge variations can also be generated due to the use of protons with different energies. Many studies have been performed with energies

below 30 MeV (range of below 1 cm; LET=20 keV/um) showing significantly larger and different biological effects than high energy protons. For example low energy protons induce significantly more apoptosis (*83-85*). Biological data regarding low-energy protons (below 70 MeV) will not be discussed further, as the work in this dissertation is dealing with treatment relevant high-energy protons. Clearly a SOBP consists of a mixture of Bragg peaks and some percent of the damage is produced in the high-LET region (> 100 keV/µm) but is estimated to be ~ 2% (*86*).

Despite the assumption of many physicists and others that the cellular responses induced by protons and photons are rather equal some molecular studies of the recent years showed differences between low-LET proton and photon irradiation. Almost all of these studies were performed at the Loma Linda proton beam facility. With 250 MeV protons a more immediate apoptosis induction was reported for irradiated thyroid follicular cells, which must have encountered more severe damage (*86*). Treatment of 2 different pancreatic tumour cell lines with 10 Gy protons caused a significant number of cells to become polyploid which indicates severe problems of these cells during cell division (*87*). Unfortunately this finding was not compared to photons. Two studies reported a faster ROS production in neural precursor cells and a more effective peroxidation of low-density lipoproteins by protons *in vitro*, though irradiation was conducted with Bragg peak protons or very high doses (*88, 89*). Irradiation of mouse brains with 2 Gy and expression analysis revealed altered expression patterns of oxidative stress and antioxidant-associated genes. IL-19, MPP4 and Epx were up-regulated and Mb was down-regulated after exposure. Yet this was not compared to photons, which also induce severe oxidative stress (*90*). A Japanese group revealed that particle irradiation (carbons and protons) suppresses the metastatic potential of HT1080 cells in contrast to photons which promote cell migration and invasive capabilities already at low dose levels. This finding provides the rationale that proton irradiation might be superior due to a lack of radiation induced tumour cell migration and metastasis formation (*91*).

Beside molecular studies, which address therapy related and basic research questions, space research is also interested in the effects of proton exposure. In space the most prominent particles are protons (*92*). Bandstra analyzed the effect on trabecular bone volume fraction and mineral density after long-term incubation (4 months) of mice following an acute 2 Gy whole body proton irradiation. With 0.5 Gy no difference could be detected versus the control whereas with 1 Gy a reduction in those parameters was visible which became significant with 2 Gy. However acute whole body irradiation in space with 2 Gy of monoenergetic protons is not realistic. But with regard to clinical doses to bone structures this study indicates that bone-forming and bone-resorbing cells might respond differently to proton irradiation, which is important with respect to paediatric patients.

These few studies point to a differential molecular response of cells after proton irradiation compared to photons. Even if treatment plans account for an RBE of 1.1, it is not known if the response of each single tumour on the molecular level is the same. Different unknown parameters could influence the RBE. Therefore it is also risky to combine proton radiotherapy with chemotherapeutics.
So far we leaped the topic of DNA damage induction and repair after proton irradiation, which will be introduced and discussed at the end of the last chapter.

1.5 The DNA damage response

Cells have to suffer from DNA damage every second due to metabolic stresses, naturally occurring radiation like UV-light, or just because of collapsed replication forks. Several treatment approaches for cancer intend to induce DNA damage like chemotherapeutics or ionizing radiation. To deal with these toxic lesions cells have evolved mechanisms to detect them (sensors), signal their presence (transducers) and promote their repair (effectors), which is called the DNA damage response (DDR) (*93, 94*). This multifaceted response includes activation of cell cycle checkpoints and transcriptional induction and posttranslational modifications of various proteins involved in DNA repair, apoptosis, etc. (*94*). Activation of this program enhances the ability of the cell to repair and survive the encountered DNA damage. However, if residual damage is left, a chronic DDR activation triggers cell death by apoptosis or cellular senescence (*95*). Out of this complex response the sensing of DNA damage, checkpoint activation and DNA repair mechanisms will be presented.

1.5.1 Sensing of the DNA double strand breaks

It is well established that the following three kinases PI3 like kinases: ataxia telangiectasia mutated (ATM), ATM and Rad3-related (ATR), and catalytic subunit of DNA-dependent protein kinase (DNA-PKcs), are the conductors of the DSB damage/checkpoint orchestra with ATM as the main player (*96*). The kinases phosphorylate H2AX, a histone variant that makes up about 10 – 15 per cent of total cellular histone H2A, at sites of DSBs (*97*). All three of these proteins are not able to detect the DSB by themselves. Recruitment of ATM to the break requires the MRN protein complex. It contains three proteins, Mre11, Rad50 and NBS1 where Rad50 binds directly to DNA breaks and the adaptor protein NBS1 recruits ATM to the break. MRN assembles at DSB sites faster than any other protein and does not depend on any other protein to induce repair foci formation (*98*). When ATM reaches the DSB it undergoes autophosphorylation (S1981) and changes from an inactive dimer to an active

monomer (*99*) leading to H2AX phosphorylation of relatively large chromatin regions (megabases) and to alterations in the chromatin structure. Mre11 is involved at a later step when its exonuclease activity digests the ends of the break, which may not be compatible for repair. DNA-PKcs can also phosphorylate H2AX, but only ATM promotes γH2AX formation to maximal distance and maintains γH2AX densities at DSBs (*100*). However, DNA-PKcs seems to be more important than generally assumed because its absence results in the down-regulation of ATM (*101*). Ku70-Ku80 complex senses DSBs, binds directly to them, and recruits DNA-PKcs (both together are called the DNA-PK complex). The third protein complex capable of phosphorylating H2AX is ATR-ATRIP. ATRIP (ATR interacting protein) recruits ATR to damage sites. However, ATR is not important for the initial response to DSBs produced by IR, instead it phosphorylates H2AX at single-stranded DNA and at stalled or broken replication forks. Therefore, when DSBs become processed for homologous recombination, the ssDNA stretches will activate ATR (*96*). This activation down-stream of ATM is needed to fully activate all components of the DDR effector pathways as ATM and ATR phosphorylate not only H2AX but a distinct set of proteins that participate in the DDR (*102*). An important function is the activation of cell-cycle checkpoints. The pause of cells in G1, S and G2 phase of the cell cycle provides more time to repair DNA damages. All movements through the cell cycle are driven by cyclin-dependent kinases (CDKs). CDK activity is affected by the binding of its specific cyclins, which are differentially expressed during the cell cycle, by its phosphorylation status, and through special CDK inhibitors (CDKIs). In the following the three most important checkpoints induced after irradiation will be described.

1.5.2 G1 checkpoint

Depending on the stage of the cell cycle where the DNA damage arose, different signalling pathways are triggered. When exposed to IR, most of the untransformed eukaryotic cells arrest at the G1 checkpoint, as this is the phase containing the highest percentage of cells. The aim is to avoid transition of the cell with damaged DNA into S phase to prevent replication of damaged templates, which would consequently lead to the creation of more DSB in the sister chromatids. In general the transition from G1 to S phase is a critical point as it is the ultimate decision of the cell to divide a further round. Once the chromosomes have been duplicated the cell has to divide at one point. The block is achieved by two different mechanisms activated at the same time while the first mechanism is implemented faster than the second one.

For the fast stop, the cell division control protein 25A (Cdc25A), a phosphatase leading normally to the activation of CDK2, is phosphorylated through ATM dependent activation of Chk2 and primed for proteasomal degradation. Therefore CDK2 cannot be activated.
Secondly, modulation of the inhibitory p53 interaction with Mdm2 results in a fast activation of p53 followed by a longer time period until its target genes are transcribed. Hereby Chk2 phosphorylates p53, which leads to its stabilization and dissociation from Mdm2. On the other site, ATM phosphorylates Mdm2 and p53, preventing the nuclear export of p53. Accumulation of p53 in the nucleus is followed by the transcription of its target genes. One of these is the CDK inhibitor p21.
The combination of these two levels of regulation results in a fast and long-standing cell cycle arrest (*96*). However, many tumour cells lack p53 and often a proper G1 checkpoint, which results in a different response towards radiation induced damage (*103, 104*).

1.5.3 Intra-S phase checkpoint

In the S phase three checkpoints exist, the replication checkpoint is initiated when the progression of replication forks becomes stalled, the S-M checkpoint makes sure that the entire genome is duplicated before progression to mitosis continues, and the third one is initiated in response to DSBs that are generated outside the active replication loci – called intra-S phase checkpoint (*105*). Normal cells, which were irradiated react with a fast but reversible decrease in DNA synthesis by reducing the rate of origin firing and strand elongation. However, there are cell mutations leading to the lack of this checkpoint and to so-called radioresistant DNA synthesis (RDS). Target is again the CDK2 kinase, which is dephosphorylated by Cdc25A and Cdc25C. When Chk1 and Chk2 become activated by ATM and ATR they phosphorylate Cdc25A/C leading to their inactivation. An increase in phosphorylated CDK2 slows the progression through S phase. In this phase single stranded DNA can be abundant and therefore ATR is also involved in the early response. But also another pathway including BRCA1 and NBS1 exists as NBS1 can restore Chk2 deficiency. Phosphorylation of NBS1 by ATM is required for the phosphorylation of structural maintenance of chromosome 1 (SMC1), which is necessary for sister chromatid cohesion (SCC). SCC is essential for proper repair, as the homologous chromatids stay close together and facilitate the search for homology. This ATM-NBS1-SMC1 pathway is a separate one to the ATM/ATR-Chk2/Chk1-Cdc25A/C-axis.
A slowing down of the replication fork progression and elongation minimizes the chances of encountering a damage site before it is repaired. However, all cells from G1 and S phase have still the possibility to be arrested in G2 (*96*).

1.5.4 G2/M checkpoint

There are two additional checkpoints in G2. The early checkpoint meets cells that are irradiated while in G2 involving also ATM-Chk2-Cdc25A/C. It is blocking the cell cycle progression at the end of G2 by inhibiting the mitotic cyclinB-CDK1 complex. Dephosphorylation of CDK1 is prevented by degradation of Cdc25A and C. The pathway blocks the movement of the cells into mitosis with a fast but short drop in the mitotic cell number (*4, 96*). A counteracting kinase is Akt whose activation suppresses DNA damage processing and checkpoint activation of cells that stayed in late G2 at the time point of irradiation exposure. Cells form γH2AX foci but fail to recruit repair factors, which can be reversed if Akt is inhibited (*106*). Akt is often over-activated in tumours and can lead to this behaviour. In that case tumour cells accumulate chromosome aberrations. This has often been seen in advanced cancers (*107*).

The later checkpoint leads to a long G2 delay including cells that have been previously irradiated while in G1 or S phase. After their transient blocks with attempts of repair, cells progress to G2 phase where they reach hours later and may experience a second delay. This stop can last many hours depending on the applied dose. Importantly, this late G2 checkpoint is independent of ATM and relies on many other regulatory branches. Until that point DNA damages have already been processed and are able to activate ATR/ATRIP. ATR activates Chk1, which in turn leads to the degradation of Cdc25A/Cdc25C. Further regulators have been described. BRCA1 has been reported to activate Chk1 and contribute to the G2 arrest. Polo-like kinases target Cdc25C independent of ATM and ATR. Plk3 negatively regulates the phosphatase whereas Plk1 is an activator. This checkpoint is also regulated on the level of cyclin B, which is sequestered in the cytoplasm. Also a decline in the mRNA levels of cyclin B has been reported. For a prolonged arrest, p53 dependent activation of p21, GADD45, and 14-3-3 proteins was shown. But the arrest can also occur in p53-mutated cells. These multiple mechanisms make sure that a cell which still harbours DNA damage is arrested. A long duration of this arrest implies problems of the cell to repair all DNA damages. Pausing too long in G2 may lead to the activation of cell death or senescence pathways.

If cells have been irradiated in mitosis the spindle assembly checkpoint (SAC) is triggered and leads to a delayed progression of mitosis. This is the only time point, which is not controlled by ATM/ATR pathways. Cells in the M phase are generally the most radiosensitive ones (*96, 108*).

1.6 DNA damage repair mechanisms

Depending on the phase of the cell cycle and the nature of the induced DNA damage, different DNA-repair mechanisms are activated. Non-homologous end joining (NHEJ), single

strand break repair (SSBR), base excision repair (BER) and nucleotide excision repair (NER) are active throughout the cell cycle. Whereas homologous recombination (HR) is only able to work when the sister chromatid DNA strands are available, which is the case in late S and G2 phase. If the damage persists after several attempts of repair, it can be transferred to the next cell cycle phase where another pathway might be successful. However, not all DNA damages are of a certain category. Damages can be very close thus forming a clustered DNA damage site. At such sites it is difficult for certain proteins to recognize the damage or to dock for repair. Even the repair of simple base damages might take hours when situated in such a damage cluster. If those were generated in S phase the probability increases that a replication fork runs into the damage and generates a double strand break. Or single strand breaks can have base damages in their near vicinity. During base excision repair single strand breaks are temporarily formed. If this nick is opposite of the original SSB a DSB is formed. Especially these clustered damages and the DNA double strand breaks lead to the severity of ionizing radiation induced cell toxicity. All of those aspects and the exact repair mechanisms will be explained in the following chapters.

1.6.1 DNA single strand break and base/nucleotide excision repair

A DNA double strand break is the most severe damage when not repaired because it causes loss of complete chromosomal regions. However, after radiation exposure DNA single strand breaks and base damages are up to 50 times more frequent than DSBs. Proteins of the base excision repair pathway repair these numerous lesions efficiently (*109*).

Due to metabolic stresses or UV-light exposure proteins of the ***single strand break repair*** (SSBR) and ***base excision repair*** (BER) pathways encounter such lesions every day and help to maintain genome integrity. But a single strand break generated by IR is often a “dirty” break, which blocks the access for polymerases (pol). End-processing is achieved by AP endonucleases, and polynucleotide kinase-phosphatase (PNKP), or tyrosyl DNA phosphodiesterase (Tdp1) (*110*). For proper resynthesis and end ligation a 3’ hydroxyl end and a phosphate 5’ end is needed and these enzymes prepare the ends. When the nick is clean, poly(ADP-ribosyl)ation by poly (ADP-ribose) polymerase (PARP) is thought to aid the sequestration of other DNA repair proteins, like XRCC1 and ligase III. As the following steps of SSBR use the same proteins like BER it is often mentioned as a part of it.

In the case of base damages, almost every special type is detected and removed by specialized proteins called glycosylases. There are several of such enzymes, which are specific for a particular class of base damage. Mainly they hydrolyze the N-glycosidic bonds to generate abasic sites (APs). A specialized enzyme called 5’ AP endonuclease 1 (APE1) cuts the DNA backbone leaving a 3’ hydroxyl adjacent to a 5’ deoxyribosephosphate (dRP),

which generates a SSB. Other DNA glycosylases/AP lyases such as endonuclease III (NTH1) and 8-oxoguanine DNA glycosylase (OGG1) conduct both steps, base excision and DNA cleavage. However, APE1 still has to generate a 3' OH and PNKP can add a phosphate to the free 5' end if it is missing.

From now on repair is equal between SSBR and BER. A decision between short patch (SP) and long patch (LP) repair has to be made. *Short patch repair* replaces only the damaged base, which is carried out by DNA polymerase β (pol β). The genetic information is copied from the existing non-damaged strand, which can be also carried out by polymerase λ (*111*). These enzymes have also a lyase domain that removes the 5' dRP left behind by APE1. Finally, ligase III along with its cofactor XRCC1 connects the ends.

For *long patch repair* 2 - 10 nucleotides are cut out and replaced. Here DNA synthesis occurs by DNA polymerases δ and ε together with the processivity factor PCNA, which are the normal replication polymerases. However, also polymerase β can perform long patch repair (*112*). The polymerases perform a displacing synthesis leaving a free 2-10 nucelotides long 5' DNA end. These 5´ flaps are removed by FEN1, the flap endonuclease. Finally the two DNA ends are connected by ligase I.

Which of the two pathways is chosen can be influenced by various factors like type of the lesion, cell cycle stage, and whether the cell is terminally differentiated or actively dividing. However, it is not at all known for all lesion types and many studies were solely performed *in vitro* (*113*). Furthermore the relative concentration of each repair factor is expected to impact sub-pathway selection and efficiency. *In vivo* studies showed a more relevant contribution of the PCNA-dependent LP-repair for oxidative DNA damage and SSBs. Parp-1 and XRCC1 play an important role. XRCC1 accumulation at the irradiation-induced SSBs is promoted by PAR formation. Only then PCNA and other factors could be efficiently recruited (*113, 114*).

XRCC1 has a crucial role in coordinating BER and SSBR. It shows no catalytic activity but is a scaffold protein stabilising and modifying the activity of other proteins. Interaction partners are DNA ligase IIIα, APE1, Pol β, PNK, PCNA, and PARP1 and 2 (*115, 116*). When XRCC1 levels of normal prostate tissue cultures were compared to malignant ones, increased levels were accompanied by higher polymerase β and δ levels (*117*). Rare XRCC1 variants were found in radiotherapy treated cancer patients, which showed acute normal tissue cytotoxicities (*118, 119*).

In summary, BER and SSBR are two important pathways to repair radiation induced breaks and base damages. However, if they are deregulated or mutated they are involved in cancer development and adverse therapy responses.

A third repair pathway ***nucleotide excision repair*** (NER) has to be mentioned. It deals with distorting base damages for example induced by UV-light (T-T dimmers). It is divided into

global genome repair (GGR), which removes damages in non transcribed regions and transcription coupled repair (TCR), which deals with damages induced in transcriptionally active regions of the genome. They differ with regard to the damage recognition step. XPA and RPA serve for further damage detection and dictate the helicases XPB and XPD (ERCC2 homolog in hamster cells) to the lesion. A 30 base pair oligonucleotide is removed and resynthesized by polymerase β together with other factors. Ligation is carried out by DNA ligase I (*120*). But NER is in general involved in the repair of UV-light induced DNA damage and not in the repair of ionizing radiation induced damages (*121*). However, irradiation of hypoxic cells causes distorting crosslinks where a purine is attached by two covalent bonds to the sugar-phosphate backbone. Those lesions can be exclusively removed by NER (*122*).

1.6.2 DNA double strand break repair

DNA double strand breaks (DSBs) are generated by different means, maybe accidentally, or during DNA replication if the fork meets a DNA break, or indirectly by camptothecin and other drugs, or through direct exposure to ionizing radiation. Already one unrepaired DSB can lead to cell death. However, after exposure to 1 Gy of IR ~ 20 DSBs are generated. Those can be located in heterochromatic or euchromatic regions of the genome, they can be complex or simple, and they occur in different phases of the cell cycle leading to differential responses. After DNA damage response proteins have marked the breaks and maybe led to chromatin relaxation, the two main repair pathways, homologous recombination and non-homologous end joining try to fix the damage. Both pathways are completely different from each other regarding the set of proteins/enzymes they use, the speed, the accuracy, and activity pattern during the cell cycle. Furthermore backup pathways exist, which can jump in if a main pathway is lacking. However, they are not as efficient. If cells lack NHEJ or HR they become radiosensitive demonstrating their importance (*123*).

1.6.2.1 Homologous recombination

When cells progress through S phase replication produces a second copy of the genome in form of a sister chromatid. It provides a template for accurate repair by homologous recombination (HR). As explained earlier the MRN complex and ATM mark the DNA breaks (Fig. 1.8). MRN is also thought to tether the broken DNA ends together. Furthermore the cohesion proteins SMC5/6 might be important in keeping the homologous sister chromatids in proximity (*124*). Now, the first and most critical step during homologous recombination is the nucleolytic degradation of the 5’-ended DNA strand in order to have a single strand, which searches for homology in the sister chromatid (*125*). Although the processes leading

to resection have not been understood completely, important known players are Mre11 and CtIP. Mre11 exhibits only a 3'-5' exonuclease activity, which is the wrong polarity and also CtIP does not perform the 5'-ended strand resection. But both exonucleases are important for efficient end resection, because they are required at DSBs with modified ends (Pardo, 2009). After initiation by Mre11 and/or CtIP the processive single-strand exonuclease Exo1 carries out extensive 5'-3' resection (*125, 126*). During the 3'- single stranded DNA is formed it is immediately stabilized and protected by binding of the single strand binding protein replication protein A (RPA). As next Rad51 proteins have to be loaded onto the single strand. Since RPA binds more avidly to ssDNA than Rad51, additional help is needed for efficient loading of Rad51 onto RPA-coated ssDNA to form the presynaptic Rad51 filaments. In

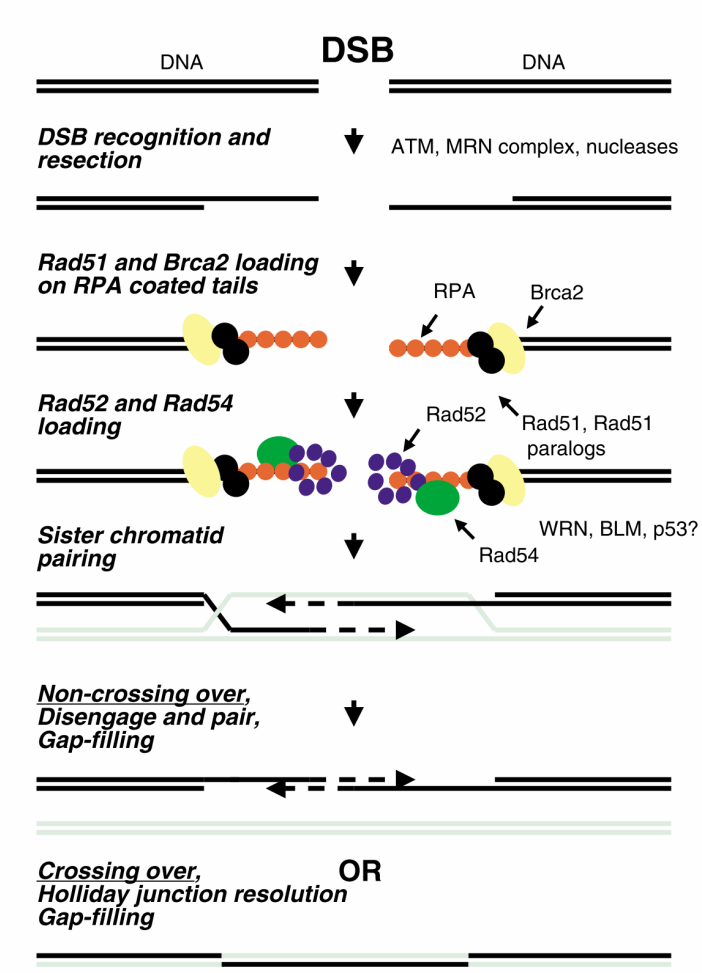

Figure 1.8 Model of homologous recombination (HR) repair. After DSB recognition by ATM and the MRN complex the DNA ends get resected in 5' → 3' direction. Here Mre11 and CtIP most probably have an end cleaning role and Exo1 does the long resection step. RPA binds immediately to the ssDNA and becomes replaced by Rad51 with the help of BRCA2 and other Rad51 paralogs. In turn Rad52 and Rad54 are attracted. The BLM and WRN helicases interact with Holliday junctions and assist also the loading of other proteins. After sister chromatid pairing two possible ways for finishing HR exist: (1) Non-crossing-over where after a first synthesis step the strands become disengaged and finish then the gap filling reaction, or (2) Crossing-over resulting from complete gap filling while the chromatids are still engaged and final resolution of the Holliday junction. Some DNA polymerases are described but their exact involvement has not been understood, yet. Ligation occurs with the help of ligase I (*130*).

mammalian cells the crucial mediator is BRCA2 and potentially Rad52. BRCA2 can directly interact with several Rad51 molecules and bring them to ssDNA (Fig. 1.8) (*127*). Formation of the Rad51 nucleoprotein filament initiates the search for homology in the sister chromatid. The search for homology is random by testing segments of the dsDNA in an iterative fashion until homology is found (*128*). Now the chromatin remodeler Rad54 stimulates strand invasion in an ATP dependent manner (*125, 129*). Further helpers during homology search and strand invasion include Rad51B, Rad51C, Rad51D, XRCC2 and XRCC3. Pairing of the two strands occurs with the help of Rad52. From this stage several HR pathways can complete the repair. In synthesis dependent strand annealing (SDSA) the information is copied from the intact strand and afterwards the newly synthesized strand reverts to its original position. Having replaced the missing information repair can be completed. Alternatively the two sister chromatids can exchange strands and built a so-called Holliday junction. Here the sequence is copied during branch migration. This step might involve the Rad51 paralogs Rad51B, Rad51C and Rad51D. Due to gross sterical forces the helicases BLM, WRN and the topoisomerase TopIIIa are also localized at the junction helping to untangle the DNA (Fig. 1.8).

For resolution of the Holliday junction a nuclease is needed, which is most likely the Slx1-Slx4 nuclease complex. Further proteins involved in the resolving step are Rad51C and XRCC3. Now two possibilities to cut the strands generate either a chromatid exchange or not (Fig. 1.8). In each case the genetic information is accurately restored. The exact identity and involvement of the DNA polymerases is still uncertain but *in vitro* studies revealed polymerases δ, ε and η to promote repair synthesis (*131, 132*). Finally, gaps are sealed with the help of ligase I. As many specific steps have to be completed in an ordered fashion, homology directed repair can take up to 6 hours or more but is very accurate.

In the case of a double strand break lying in between two repeated sequences oriented in the same direction another repair process called ***single strand annealing*** (SSA) can occur (*131*). In this case the two 3’ overhangs are simply aligned and annealed within the region of the repeated sequences. Overhanging single stranded DNA will be digested, and gaps will be filled plus sealed. This process is Rad51-independent but involves common HR proteins including RPA, Rad52 and Rad50. Mismatch repair proteins deal with the 3’ tails. Evidently sequences lying between the repetitive repeats are often lost, which can lead to large genomic deletions. SSA does play a role in DSB repair. However, the repeats in the human genome exhibit high sequence diversity and mismatches suppress SSA drastically. In normal cells it might play a fairly limited role for DSB repair but in Rad51 disrupted cells SSA is increased appearing to be a backup mechanism (*131, 133*).

Compared to oxic conditions, irradiation under hypoxia produces a greater number of DNA crosslinks, which are lethal for a cell (*134*). In this case a third repair mechanism becomes important, ***interstrand cross link (ICL) repair.*** ICL in mammals uses different sets of proteins from other repair pathways including ERCC1 and XPF from NER, Rad51 and Rad52 from HRR, and proteins of the FANC group, which play a critical role for ICL repair. In eukaryotes the primary mode creates a DSB as intermediates, which is preferentially repaired via HR with the help of a complex orchestra of FANC proteins (*135*).

1.6.2.1.1 The DNA repair protein Rad51

The mammalian Rad51 protein is structurally, biochemically, and genetically identical to the bacterial RecA and the yeast Rad51 recombination proteins. Rad51 plays a pivotal role in the process of gene conversion and its regulation (*136*). Its inactivation results in embryonic lethality of mice and chicken DT40 lymphoma B-cells (*137, 138*). The maintenance of genetic stability relies mainly on the high fidelity HR repair. Cells harbouring mutations in Rad51 or other HR genes (e.g. BRCA1, BRCA2, Rad54, XRCC3) exhibit high levels of genetic instability (*139*). On the other site HR contributes to genetic instability if the pathway is over-activated in a non-physiological way. Inappropriate recombination reactions, like between repeat sequences or mutant alleles, result in deletions, translocations, duplications, or loss of heterozygocity (LOH) (*140, 141*). In ATM-defective cells Rad51 foci formation is markedly increased, which is in agreement with the high levels of HR between direct repeat sequences in ATM-/- cells (*142, 143*). Up-regulation of spontaneous HR has been also described in p53-defective cells (*144-147*). Alterations of the p53 protein stimulate HR repair of γ-ray-induced damages independently of its role in the G1/S checkpoint (*148*). Over-activated HR may lead to chemo- and radiotherapy resistance (*136, 149*). For this reason HR repair has to be tightly regulated in order to prevent inaccurate repair leading to genetic instability and tumour formation. For this purpose the expression level and activity of the essential HR protein Rad51 is regulated carefully. Binding of p53 to the Rad51 promoter leads to a suppression of Rad51 mRNA transcription and to reduced Rad51 protein levels (*144, 150*). Additionally, p53 can impair nuclear Rad51 foci formation at generated DSBs through direct interaction (*151, 152*). Mutations of p53 influence the protein-protein interaction with Rad51 and abolish its regulatory functions (*147*). Beside the regulation by tumour suppressors Rad51 is also up-regulated by oncogenes like the Bcr/Abl fusion kinase (*153*). Furthermore Rad51 expression is regulated during the course of the cell cycle where it is induced in S phase, rising until G2 and decreasing in G0/G1 cells (*154, 155*). HR events in G1 might lead to gross chromosomal aberrations and are therefore prevented.

In summary, a basal level of Rad51 activity seems to be essential for the processing of spontaneous and S phase generated DNA lesions. If expression control is lost the fine

balance between different components of the DNA repair systems gets destroyed. Many tumour tissues reveal a significant increase of *Rad51* mRNA contents (e.g. breast, uterus, small intestine, lung, stomach) when compared to normal tissue (*156*). Since high Rad51 protein levels are restricted to tumour cells, Rad51 is used as a tumour specific antigen (*157*). Further it is an independent predictor for tumour recurrence as well as tumour progression, which makes Rad51 expression a clinical relevant prognostic marker (*158*). Down-regulation of Rad51 by anti-sense techniques sensitizes cells to DNA-damaging agents and radiotherapy, making it a target for future therapy approaches (*159, 160*).

1.6.2.1.2 The DNA repair protein XRCC3

XRCC3 and some other genes were identified by their ability to complement mutated rodent cell lines for their hypersensitivity to ionizing radiation meaning “X-ray repair cross-complementing” (*161, 162*). XRCC3 is one of the Rad51 paralogs, which evolved through gene duplication of Rad51 and further diversification. Therefore and because of the mutant’s hypersensitivity to DNA cross-linking drugs it was believed to take part in HR repair. Soon it was reported that XRCC3-complementation in Irs1sf cells (XRCC3-/-) could highly elevate the frequencies of HR repair in this cell line (*163*). Furthermore XRCC3 influences Rad51 focus formation without affecting Rad51 protein level. Therefore it is required for the assembly or stabilization of the Rad51 filament (*164*). Unresolved DNA damage in XRCC3 mutants leads to centrosome fragmentation and increased chromosome mis-segregation, which points to a potential role as a tumour-suppressor gene (*165*). Rad51c, another Rad51 paralog, forms a complex together with XRCC3 (*166*). This complex functions as resolvase at Holliday junctions and modulates together with Rad51 the progression of the replication forks at DNA damages (*167, 168*). Stabilisation of XRCC3 seems to be dependent on the interaction with Rad51c. Depletion of Rad51c results in a sharp reduction of the XRCC3 protein level. Mutating the ATPase domain in XRCC3 also leads to a destabilisation of the complex. Dissociation and formation of Rad51C-XRCC3 complexes seem to underlie a fine balance and to depend on ATP binding plus hydrolysis by XRCC3 (*169, 170*). Beside its resolving function XRCC3 may prevent long-tract gene conversions by facilitating an earlier termination of gene conversion (*171, 172*). However, XRCC3 has also been described to be involved in earlier steps of HR. XRCC3 can form distinct foci at the sites of DNA damage within 10 minutes after exposure to radiation independently of Rad51, which might facilitate formation of Rad51 nucleofilaments. Association of XRCC3 with RPA indicates also an early association at the breaks (*173, 174*).

During the whole process of HR XRCC3 is an important protein influencing initiation of the Rad51 nucleofilament and the proper processing of HR intermediates. Deficient cells have

elevated levels of chromosome aberrations and the variability of the HR genes *XRCC3* and *Rad51D* may play a role in breast cancer risk (*175*).

1.6.2.1.3 The breast cancer susceptibility protein BRCA2

Inheritance of one defective copy of the breast cancer susceptibility gene, BRCA2, predisposes those individuals to breast and ovarian cancer. This applies to about 10-30% of genetically predisposed individuals. BRCA2 mutations show a high penetrance, with a 50% risk of developing cancer before the age of 50 and 80% risk before the age of 70 (*176*). The BRCA2 protein is a large protein with a molecular weight of approximately 385 kDa (*127*). In 1995 the gene was cloned and it was characterized by a very large exon 11, which encodes essential peptide motifs for the interaction with Rad51 (*177, 178*). Rad51 and BRCA2 were shown to co-localize in nuclear foci in somatic cells after treatment with IR (*179*). In BRCA2-deficient cells the formation of Rad51 foci was impaired leading to the suggestion that BRCA2 is required for the recruitment of Rad51 to sites of DSBs (*180*). Accumulation of spontaneous chromosomal aberrations during cell division in cell culture implicate that BRCA2 is involved in the maintenance of genome stability (*181*). Disruption of the interaction between BRCA2 and Rad51 leads to radiation and chemosensitivity and a reported defect in the G2/M transition (*127, 177*). In BRCA2-deficient Chinese hamster cells a defective S phase checkpoint was described (*182*). Over the years BRCA2 was acknowledged to be an important facilitator for HR, which plays a direct role. The protein was not found to be involved in NHEJ as deficient cells display normal levels of end joining (*183*). Further support for the important role in HR is the ease how BRCA2 and Rad51 can be co-immunoprecipitated from cell-free extracts (*184*). The generally conserved BRC motifs in the *BRCA2* gene are likely to interact with a unique motif or region in Rad51, which appears to be the Rad51 core domain together with BRC3 and BRC4 (*176, 184*). Several *in vivo* studies revealed the biological function of the various domains of BRCA2. Capan-1 cells have only one remaining BRCA2 allele, which is solely coding for the first six BRC motifs without the ssDNA-binding domain. This indicates that BRCA2 needs to bind as well ssDNA to fulfill its helper function. BRCA2 loaded with Rad51 binds to ssDNA and by displacing RPA it helps to form the Rad51 filament (*127, 180*). Before Rad51 proteins can form nucleofilaments they have to translocate into the nucleus, which appears to be as well regulated by BRCA2 in response to genotoxic stress (*185*). Even an influence on both BER pathways was reported where the final ligation of BER intermediates was impaired in Capan-1 cells (*186*).

The role of BRCA2 in facilitating orderly homologous recombination is highly important to maintain genomic integrity. In the absence, replication errors produce a mutation prone phenotype that is a key factor for carcinogenesis.

1.6.2.2 Non-homologous end joining

The fastest and most straight forward way to repair a DSB is simply to rejoin the broken ends. This process is called non-homologous end joining (NHEJ). Blunt ended breaks or breaks with complementary overhangs are sealed efficiently with relatively high fidelity (*187*). However, DNA ends are altered after treatment with ionizing radiation, which leads to their procession before ligation and then NHEJ is often mutagenic. Even if this repair process is error-prone, it appears to be very powerful because of the potential to ligate any kind of DSBs without the need for homologous sequences within a reasonable time (*124, 125*).

Binding of the Ku heterodimer (Ku70/80) to the free DNA ends occurs within seconds after break formation. The high abundance of this complex and its high affinity make this possible (*188, 189*). The DNA end is threaded through the Ku complex's central fissure structure (Fig. 1.9) (*190*). Ku70/80 serves for at least two main goals, which are tethering of the different broken DNA ends and serving as a recruitment platform for additional NHEJ factors (*191*). A conformational change induced by the binding to DNA ends promotes the recruitment of the large DNA-dependent protein kinase catalytic subunit (DNA-PKcs), which can bind to DNA and Ku70/80 (*192*). The association with Ku bound to DNA activates its serine/threonine kinase activity, which leads to extensive autophosphorylation and phosphorylation of H2AX and other target proteins. How essential this phosphorylation capacity of DNA-PKcs is for certain steps in NHEJ is unclear. However, the protein itself is important to promote later steps and to recruit other factors (*124*). MRN is also recruited to the ends but beside a possible support during DNA end tethering by Rad50 no other function is known. The nuclease activity of Mre11 is not needed for NHEJ (*124*).

After treatment with IR most of the DNA ends are not compatible for ligation. For this reason different proteins are very versatile in processing the various modifications. The endonuclease Artemis interacts with DNA-PKcs, which is required for its activity. It cleaves 3'-overhangs, 5'-overhangs, hairpins, flaps, and gaps (*193*). In Artemis-deficient fibroblasts, which were arrested in G0/G1 about 10% of radiation induced DSBs remain unrepaired (*194*). Another enzyme, the mammalian polynucleotide kinase (PNK), is recruited through its interaction with XRCC4. With the 5'-kinase and 3'-phosphatase activities it generates ligatable ends. A third enzyme, Aprataxin, does remove adenylate groups from 5´phosphates and also interacts with XRCC4 (*125*).

Ku70/80 recruits two polymerases (pol λ and pol μ), which are able to fill single-stranded gaps after pairing of partially complementary overhangs or after nucleotide processing. It has to be mentioned that both polymerases can work template independent (*195*).

Once DNA ends have been made compatible, they are ligated by the DNA ligase IV-XRCC4-XLF complex. DNA ligase IV is very versatile and can ligate a wide variety of DNA ends. In

the absence of XRCC4 it is still capable of ligating compatible 4 nucleotide overhangs but the presence of XRCC4, XLF and Ku70/80 improves its efficiency and versatility. XRCC4 has no biochemical activity it serves as an adapter and stabilizing partner for several proteins involved in NHEJ. XRCC4-like factor (XLF) has a similar structure as XRCC4 and is needed for efficient ligation of incompatible DNA ends (*191*).

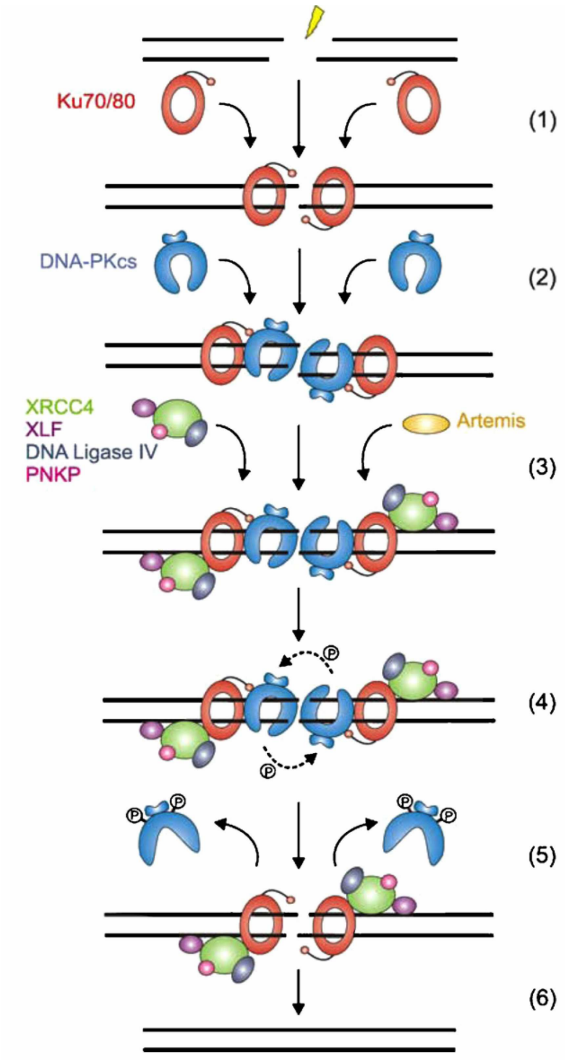

Figure 1.9 Model for non-homologous end joining. (1) After generation of a DSB with overhangs by IR it is detected and bound by the Ku70/80 heterodimer (red). (2) The flexible CTR of Ku80 recruits DNA-PKcs (blue), which leads to inward translocation of Ku and positions itself at the ends. (3) DNA end processing by several possible enzymes like Artemis, and PNKP (pink). (4) Autophosphorylation of DNA-PKcs, which might also happen at an earlier time point. (5) Resulting in the release of DNA-PKcs from DNA. (6) Finally, the XRCC4/DNA ligase IV complex (green/grey) ligates the ends with the help of XLF (purple) (*196*).

NHEJ is evolutionary conserved and because of its speed and abundance throughout the cell cycle it is the predominant DSB repair pathway in mammalian cells. Patients with mutations in ligase IV or XLF are highly sensitive to IR, immunodeficient, and show microcephaly (*197*). Whereas ligase IV knock out mice dye early during embryogenesis, mice lacking Ku and DNA-PKcs are viable showing that low levels of end joining can still

occur in these mice (*197, 198*). However, all mutants in NHEJ show a highly sensitive phenotype towards IR exposure.

1.6.2.2.1 The role of DNA-Pkcs in double strand break repair

The DNA-dependent protein kinase catalytic subunit (DNA-PKcs) is with about 470 kDa the largest protein kinase known in biology and plays an essential role in non-homologous end joining (*199, 200*). By the Ku-complex DNA-PKcs is recruited to the free DNA ends and both built the DNA-PK complex. Ku70 and Ku80 form an asymmetrical ring, which allows the complex to bind in the major groove closest to the DSB and the minor groove distal to the break. A flexible arm at the C-terminal region of Ku80 was shown to recruit DNA-PKcs to the break site (Fig. 1.9, step 2). The arm is thought to position a DNA-PKcs molecule next to itself and may also stabilize adjacent DNA-PKcs at the opposite side of the DSB, which leads to the so-called “synapsis of the ends” (*190, 201*). This alignment of the ends was shown to be more efficient when Ku and DNA-PKcs worked together (*202*). The whole DNA-PK complex is acting as activator and scaffold for the following NHEJ steps.

DNA bound DNA-PKcs is forming a channel where the DNA fits in and differs from the conformation of unbound DNA-PKcs (*203*). Its interaction with the second DNA-PK complex in *trans*-position at the other break end is needed for kinase activation (*201*). DNA-PKcs autophosphorylates itself at the known ABCDE, and/or PQE autophosphorylation clusters, and at one site in the activation loop of the kinase (*196*). Furthermore the kinase was shown to phosphorylate several proteins *in vitro*, but little evidence exists for *in vivo* functional relevance (*204-206*). Its major target seems to be itself (*196, 207*).

In the case of a kinase dead protein version the DNA-PK complex inhibits repair by blocking accessibility to the ends (*208*). This let to a significant observation where cells expressing threonine to alanine mutations in the ABCDE cluster are more radiation sensitive than cells lacking DNA-PKcs completely (*209*). DNA-PKcs presence is protecting the ends from most DNA-modifying enzymes and is blocking other repair pathways. Consequently, activation of the kinase is essential for complete NHEJ. Another conformational change of DNA-PKcs seems to orchestrate the end processing by Artemis, pol μ, PNK and more. Later it directs as well XRCC4/ligase IV to the break for the final sealing procedure (*201*). Further autophosphorylation of DNA-PK induces complex dissociation. Co-immunoprecipitation of purified DNA-PK proteins in the absence of ATP was possible but not if ATP was administered showing that DNA-PKcs will finally be released (*202*). Cellular phosphatases influence the DNA-PK phosphorylation status *in vivo* (*210*). In general it is thought that they allow for complex recycling (*196*). However, not everything has been clarified yet, like the significance of DNA-PKcs being able to phosphorylate many other target proteins.

It was shown that the absence of Ku80 or XRCC4 in CHO cell extracts leads to strongly reduced NHEJ efficiency and fidelity in the ligation of special substrates whereas DNA-PKcs-deficiency leads to a milder effect (*211*). Therefore a non-essential but facilitating role of DNA-PKcs in NHEJ was proposed. However, recently the first human mutation in the DNA-PKcs gene has been identified leading to a radiosensitive T-B-SCID patient. In contrast, spontaneous mutations were identified in dogs, mouse, and horse models before. This hypomorphic missense mutation (L3062R) in a human did not change expression level or autophosphorylation status of the protein whereas the same mutation in an animal model let to complete loss of kinase activity. Therefore some functions of DNA-PKcs might be unique to humans (*207*). However, human colon cancer HCT116 cells lacking DNA-PKcs are viable, although showing defective proliferation and genomic instability (*212*). DNA-PKcs might not be essential for repair of metabolically induced DSB but appears to be highly important for the repair of IR induced DSB. In response to IR it is not only involved in repair but also in signal transduction of the complex responses to IR (*213*).

1.6.2.2.2 The role of p53-binding protein 1

p53-binding protein 1 (53BP1) was identified to be a p53 binding partner that could promote the transcriptional activity of p53 (*214, 215*). Nowadays it has been classified as a mediator and adaptor of the DNA-damage response. It is a huge protein with a molecular weight of 450 kDa, has no characterized enzymatic activity, and serves instead as a recruitment platform for other DDR proteins (*216*). The protein contains two BRCA1 carboxy terminal (BRCT) domains and a tandem Tudor domain. Tudor domains recognize methylated histones and methylated lysine 79 of H3 and can target 53BP1 to DSBs (*217, 218*).

53BP1 was described to be involved in checkpoint activation. Abrogation results in a decent defect in G2/M cell cycle arrest and in a partial intra-S phase checkpoint defect (*219-221*). This was observed at low doses of IR and others have reported the opposite (*222, 223*). 53BP1 was found to act in some cell lines upstream of ATM where it is required for efficient ATM Ser^{1981} autophosphorylation (*224, 225*). Like MDC1 and BRCA1 it mediates Chk2 phosphorylation following IR (*225*).

Secondly, 53BP1 is involved in direct DSB repair. After cells encountered genotoxic stress 53BP1 rapidly translocates from a diffuse nuclear distribution towards IR induced foci (IRIFs) (*224, 226*). Because of this localization to DSBs and the induction of genome instability in deficient cells, 53BP1 was believed to play a role in DSB repair. For the repair of DSBs, which are located in heterochromatin, it colocalizes along with γH2AX, NBS1 and Mre11 to promote ATM-dependent NHEJ (*194, 227*). However, the formation of foci is not in general dependent on ATM, NBS, DNA-PKcs or wild type p53 as foci form in the respective deficient mutant cells (*224*). Rad9, the yeast homolog, is necessary for efficient NHEJ and 53BP1

Tudor domains have been reported to enhance the activity of the DNA ligase IV/XRCC4 complex *in vitro* (*228, 229*). Furthermore 53BP1 foci formation is not induced by agents that block DNA replication (*224*). Additionally, 53BP1 is involved in the choice between HR and NHEJ in S-phase BRCA1-deficient mouse cells where it promotes erroneous NHEJ repair (*230*). These findings indicate that 53BP1 is involved in efficient NHEJ but not necessarily in the classical NHEJ pathway (*222*).

For efficient recruitment of 53BP1 to the breaks ubiquitylation of Lys^{119} of H2AX by RNF8 and the direct interaction with MDC1 is required whereas phosphorylated H2AX is needed for the sustained retention at IRIFs (*231-233*). The acetylation of histone residues by the Tip60 HAT was also shown to be crucial for foci formation, which forms a more open and mobile chromatin structure (*234*). With regard to chromatin 53BP1 influences its mobility in the surrounding of a DNA damage focus, which might increase the likelihood that two ends meet for repair. Modulating chromatin mobility may be facilitated by the interaction of 53BP1 with dynein motor proteins (*235, 236*). In summary 53BP1 is an important DNA damage response protein, which helps in checkpoint activation, in the choice of DSB repair pathways, and facilitates non classical NHEJ. Disruption leads to growth retardation, immune deficiency, radiation sensitivity, and susceptibility to cancer (*233*). However, the exact mechanisms have still to be elucidated.

1.6.2.2.3 The scaffold protein XRCC4 in NHEJ

The XRCC4 protein has no known enzymatic function. It is rather a scaffold protein that promotes the efficiency of DNA ligase IV to join ends with low homology by stabilizing intermediates of the process (*199, 237*). Structural studies revealed a globular head domain and a coiled coil C-terminus of which two proteins form a dimer (*238*). Its complex with DNA ligase IV consists of 1 ligase and 2 XRCC4 molecules and it interacts as well with Ku serving as a flexible tether between Ku and the ligase (*239, 240*). During this process XRCC4 is phosphorylated by DNA-PKcs. However, this modification is not essential for break ligation but may be supportive (*241, 242*). The DNA-binding ability of XRCC4:DNA ligase IV is not strong and appears to be mediated by DNA-PK (*243*). As mentioned earlier, XRCC4-deficiency is embryonic lethal and it appears to be more important for the repair of enzyme induced breaks than for radiation-induced DSBs (*244*). However, a mutation in the *xrcc4* gene in hamster cells let to the stimulation of Rad51 foci assembly after γ-ray exposure. Therefore HR can overtake repair at the break even at late NHEJ steps in a sequential manner (*245*). Depletion of XRCC4 in G1 checkpoint-defective cells let as well to an over-stimulation of HR. DSB produced in G1 could be transferred to S/G2 phase and processed by HR (*246*). Ectopically expressed XRCC4 fragments compete in a dominant-negative fashion with full-length XRCC4 for binding to ligase IV, which leads to a sensitization of MDA-

MB-231 breast tumour cells to ionizing radiation (*247*). This finding indicates that a sterical blocking of the ligase inhibits further processing of the break by other repair pathways.
Overall XRCC4 is an important repair protein for fast and efficient repair of DSBs. The classical NHEJ pathway is the preferred choice for repair. Lack or mutations of XRCC4 is leading to a switch to HR or alternative end joining and can promote carcinogenesis (*240*).

1.6.2.2.4 Alternative non-homologous end joining

In the absence of core NHEJ-factors like ligase IV, XRCC4, and DNA-PKcs end joining can still take place but with slower speed. In the last decade this form of end joining was given several names: alternative NHEJ (alt EJ), back-up NHEJ, and microhomology-mediated NHEJ (MMEJ). However, little is known about the exact enzymes involved and if there are different branches (*191*). In general it was reported that alternative pathways are at least about 10-fold slower than NHEJ (*199, 248*). Yet, the repair time might also depend on the complexity of the damage.
MMEJ seems to be used on a normal basis when too much DNA damage is saturating the Ku-pathway or when the Ku protein is unable to bind the DNA ends in the case of polypeptides cross-linked to the DNA ends (*124, 249*). The pathway uses imperfect microhomologies of about 5 - 20 nucleotides. Therefore, it requires resection of the ends, which is normally a prerequisite for HR repair. Components of NHEJ and HR (MRN, Ku, Lig4, CtIP, Rad52) are involved and seem to be used when the two classical pathways, NHEJ and HR, have failed to repair the damage. Factors of the DDR response regulate the uncontrolled use of mutagenic MMEJ. ATM partly suppresses DNA end degradation by Mre11 but over-expression of Mre11 increases alternative end joining in an ATM-independent manner (*250, 251*). Lack of 53BP1 results in an ATM-dependent increase in DNA end resection and to increased MMEJ repair (*252*). This pathway is more error-prone than classical NHEJ but seems to be used when the amount of damage is too huge. As it uses the resection enzymes, which are also involved in SSA it can also be termed “micro SSA” (*125, 199*).
Other people impaired classical NHEJ in HR-defective cells, which excludes an involvement of HR for still occurring repair but rather proposed also the existence of an alternative NHEJ pathway with backup functions (B-NHEJ) (*253*). In assays using HeLa cell extracts it was shown that the majority of DNA end joining activity derived from ligase III (*254*). But also DNA ligase I and DNA ligase IV showed a significant contribution to the end joining activity. Ligase III is also involved in BER and SSBR therefore it is difficult to study its specific involvement in B-NHEJ. In higher eukaryotes knockout of *LIG3* is lethal (*255*). Using an end joining reporter assay in DNA ligase IV-deficient MEFs additionally silenced for DNA ligase III reduced DNA end joining to further 80% (*256*). Other identified factors are Parp-1, XRCC1 and histone H1. The first two are well known BER and SSBR factors. Parp-1 binds to free

DSB ends in direct competition with Ku and non-DSB lesions (*257*). *In vitro* assays showed that the abundance of histone H1 around the break site significantly increased the activity of ligase III compared to ligase IV and it enhanced the function of Parp-1 (*258*).
In vivo and *in vitro* end joining assays validated a more enhanced activation of B-NHEJ in G2 phase than in G1 phase (*240*). Furthermore by letting cells grow to plateau phase (growth inhibited state) they show a significant reduction in end joining activity that could be corrected by recombinant ligase IIIα. This is pointing to a connection between growth signalling and B-NHEJ (*254, 259*). Therefore terminally differentiated cells like neurons (in G0 phase) might not be able to use this backup pathway and rely on classical NHEJ or SSA.
Interestingly, a high fidelity NHEJ pathway was described for human embryonic stem cells, which are using the canonical NHEJ pathway but without DNA-PKcs. When these cells differentiated, a progressive decrease in the accuracy of NHEJ was observed (*260*).
In summary the relevance, regulation, and separation of these alternative NHEJ pathways is not clear. Proteins of pathways like HR and BER/SSBR seem to act very versatile and can work in alternative end joining mechanisms.

1.6.2.3 Choice and hierarchy of double strand break repair pathways

As indicated before the availability of the repair pathways is differentially regulated throughout the cell cycle (HR or alt-NHEJ). However, more parameters can impact the balance between DSB repair pathways like the cell type, status of the chromatin compaction, complexity of the DNA damage, and the degree of DNA damage burden (*261*).
Immediately after exposure to IR several proteins will compete for DNA ends. This passive competition between Ku, MRN, and Parp-1 may already partially determine the choice of the pathway (*257, 262*). Ku exhibits the higher affinity for free DNA ends therefore it dominates DSB repair in the first place. Parp-1 is sequestered as well by other forms of DNA lesions, which limits its contribution to DSB repair (*257*). Ku regulates the choice between different NHEJ pathways (classical versus backup-NHEJ) (*263*). Actively proliferating cells need to repair their damage as fast as possible. NHEJ between compatible ends is twice as efficient as NHEJ between incompatible ends whereas HR is additionally 3 times less efficient. With NHEJ being the fastest DSB repair pathway it might be the first choice for repair and only after failure other pathways can continue (*264, 265*). However, in the late S phase and early G2 phase both, HR and NHEJ, contribute significantly to ionizing radiation-induced DSB repair (*266*). The increased cell survival of S phase cells after exposure to IR, called S phase radioresistance, was shown to depend on active HR (*267*). HR is tightly regulated to prevent deleterious genomic rearrangements in M and G1 phase. But later on in S/G2 phase sister chromatids ensure accurate repair. Replication induced DSBs are exclusively repaired by HR. These breaks harbour one free DSB end and a SSB end and would be erroneously repaired

via NHEJ. Radiation induced SSBs and non-DSB damages are converted to such lesions when they encounter a replication fork (*268*).

The active regulation is done by CDKs, which influence expression levels, activation status, and interaction status of certain HR proteins. Rad51, Rad52, and CtIP expressions increase during S phase (*154, 269, 270*). Phosphorylation of BRCA2 in M and early G1 phase at serine 3291 blocks its interaction with Rad51 and therefore HR. However, immediately after irradiation this phosphorylation was rapidly decreased to promote HR (*271*). On the other hand phosphorylation of critical threonine residues (T2609, T3950) in DNA-PKcs is reduced in irradiated S phase cells, which is consistent with decreased DNA-PK activity in S phase HeLa cells (*272, 273*). The point of no return for HR repair is reached at the DNA resection step and therefore this step is tightly regulated. CtIP proteins are phosphorylated at several sites by CDK, which lead to up-regulated DNA end-resection and an increase of HR repair in S phase (*269*). Due to the serine^{327} phosphorylation CtIP can interact with BRCA1 and BRCA1 might therefore also regulate end-resection (*270*). Two other studies suggest a regulation of resection by 53BP1 and BRCA1, with BRCA1 being a positive regulator and 53BP1 being a negative regulator (*90, 230, 274*).

Several lines of evidence propose DNA-PKcs to be an active regulator in the choice between HR and NHEJ. Depletion of the whole protein increased HR but chemical inhibitors let to a decrease of HR activity (*275-277*). Another laboratory identified a splice variant lacking the kinase domain, which is expressed along full length DNA-PKcs solely in quiescent cells. By this means HR is limited in differentiated cells (*278*). It is believed that kinase inactive DNA-PKcs cannot dissociate from the DNA ends any more and thereby block it for HR. Surprisingly, another kinase inactive mutant harbouring a single lysine to arginine change close to the kinase active site resulted in HR stimulation (*261*). All kinase inactive mutants can still be recruited to the repair focus but influence HR differently. Here ATM plays a role. ATM levels are lower in cells lacking DNA-PKcs, but could be restored in the K3752R mutant (*261, 279*). ATM can also phosphorylate threonine^{2609}, but serine^{2056} is solely autophosphorylated by DNA-PKcs itself. Phosphorylation of both sites regulate the accessibility of repair factors to DSBs, and therefore HR might be increased above wild type level as only one site is phosphorylated by ATM (*261*). However, the clear role of ATM in pathway choice is still not known, but it appears to be a positive regulator of HR (*25, 280*).

This picture of all the interaction partners and modifications shows the complexity and fine balance involved in this delicate process. Both pathways share some repair proteins, which might all be involved in the choice like BRCA1, H2AX, Parp-1, Rad18, DNA-PKcs, and ATM (*261*). Even if NHEJ factors are recruited more rapidly to DSBs than HR factors, both seem to stay a period of time at the same DSB site (*281*). Therefore the interplay of multiple

proteins regulates the choice directly at the break. However, this precisely balanced choice is often deregulated in tumour cells.

In many studies the hierarchy of NHEJ and HR was analyzed looking for the repair of simple endonuclease induced DSB (*264, 282*). These are very efficiently rejoined by classical NHEJ. However, about 30% of the ionizing radiation induced DSBs reside within lesion clusters (*283*). A clustered lesion is a lesion containing 2 or more breaks/modifications within 2 helical turns of the DNA. Much more non-DSB clusters do exist after irradiation, which can be converted to DSBs (*284, 285*). For example two opposing tetrahydrofurans (stable AP site analogs) are cleaved to form a DSB by AP endonucleases and these are partially inaccurately repaired by NHEJ (*286*). Or repair intermediates produced by a defective fanconi anaemia (FA) repair pathway (repair of crosslinks) will be overtaken by NHEJ, which is not able to act properly. In this case inappropriate usage of NHEJ leads to cellular toxicity (*287*). In contrast, other groups showed that repair proficient cells did not generate additional DSBs post-irradiation (*288*). Gulston *et al.* quantified that a fraction of 10% of clustered damage is finally converted to DSBs (*289*). The composition of all induced DNA damages can differ as well with regards to the quality of radiation. 1 GeV low-LET protons induced relatively more DSBs compared to abasic and oxybase clusters than ionizing photons (*290*). These differences in the complexity of the DNA damage might influence pathway choice.

In recent publications the importance of HR and SSA after exposure to ionizing radiation was demonstrated. When HeLa cells were exposed to equipotent doses of Bleomycin or X-rays with regard to DSB production, Rad51-foci could only be observed in irradiated cells indicating the use of HR after X-ray exposure (*265*). Another hint for the involvement of HR is the radiosensitivity of HR-deficient cells exposed in G1 phase meaning that NHEJ alone is not efficient in repairing certain DSBs (*291*). Furthermore after HR complementation by human XRCC3 cDNA cells showed a greater radioresistance than parental cells but resistance to mitomycin C was only partially restored. This suggests as well an important role for HR in the repair of complex DSBs (*291*). Even SSA is more important for the repair of complex DSBs than NHEJ in hamster S phase cells. For human fibroblasts it was shown that about 15% of X-ray induced DSBs are repaired via HR in G2 (*292*). DSBs, which were induced in G2 after irradiation and were processed by HR required Artemis and ATM. Artemis endonuclease is required for efficient DSB repair and seems to promote end processing in heterochromatic DNA regions (*292*).

These studies clearly show the action of HR after production of DNA DSBs by ionizing radiation. However, the influence seems to depend on the cell system with its genetic background. In earlier studies with high doses of radiation (> 20 Gy) the detection of HR involvement was prohibited as HR appears to be saturated at high radiation doses. Therefore

future studies should use physiologically relevant radiation doses to be able to measure the contribution of HR (*266*).

1.6.3 Chromosomal aberrations

Mis-repair or no repair of DNA damages can lead to chromosomal aberrations, which do not necessarily result in cell death but mutations. Less severe mutagenic events are accepted in order to prevent severe deletions at a later time point. For example translesion DNA synthesis (TLS) across an abasic site located at a break will lead to the expense of a point mutation but can prevent severe deletions by NHEJ (*293*).

Ionizing radiation is very efficient in inducing chromosomal aberrations. In general survival correlates with incomplete or improper repair and progression of these cells into mitosis. Dicentric- and micronucleus-formation induce mitotic catastrophes after exposure to IR (*294*). But cells with reciprocal translocations often survive because they encounter no problems during mitosis (*4*).

If sticky DSBs are formed after irradiation they may restitute to their original configuration, or they fail to join and a deletion will be visible at the next mitosis, or broken ends from different sites may rejoin and give rise to grossly distorted chromosomes (*5*). The later possibility will lead mainly to mitotic catastrophe but a cell might survive with a deletion if the genetic information was not essential.

Metaphase spreads are usually prepared at the first metaphase after X-ray exposure and then aberrations can be separated into two classes: chromosome aberrations and chromatid aberrations. ***Chromosome aberrations*** result from early interphase irradiation, before the chromosomes have been duplicated. The break is generated in a single chromatin strand and the aberration will be duplicated during the next replication round. If breaks of two different chromosomes are ligated, dicentrics are formed after replication. If two breaks in the two different arms of a chromosome are ligated, a ring will be formed. In both cases the aberrations are always accompanied by two identical acentric fragments (Fig. 1.10). In contrast if the cell nucleus is irradiated when the cell has duplicated its DNA the break occurs only in one of the chromatid arms and leaves the opposite arm undamaged leading to gaps and breaks. These breaks occurring on a single chromatid arm are called ***chromatid aberrations***. An exception here is the isochromatid deletion. Though little chance exists that breaks are generated in both chromatid arms those can be incorrectly joined to a sister union and a fragment (Fig. 1.10). At the next mitosis this aberration will be lethal. However, not only DSBs induced in S phase but also single-strand breaks induced in early interphase can be converted to one-sided DSBs during replication and look like a chromatid aberration. As mentioned before symmetric translocations and small interstitial deletions can be nonlethal

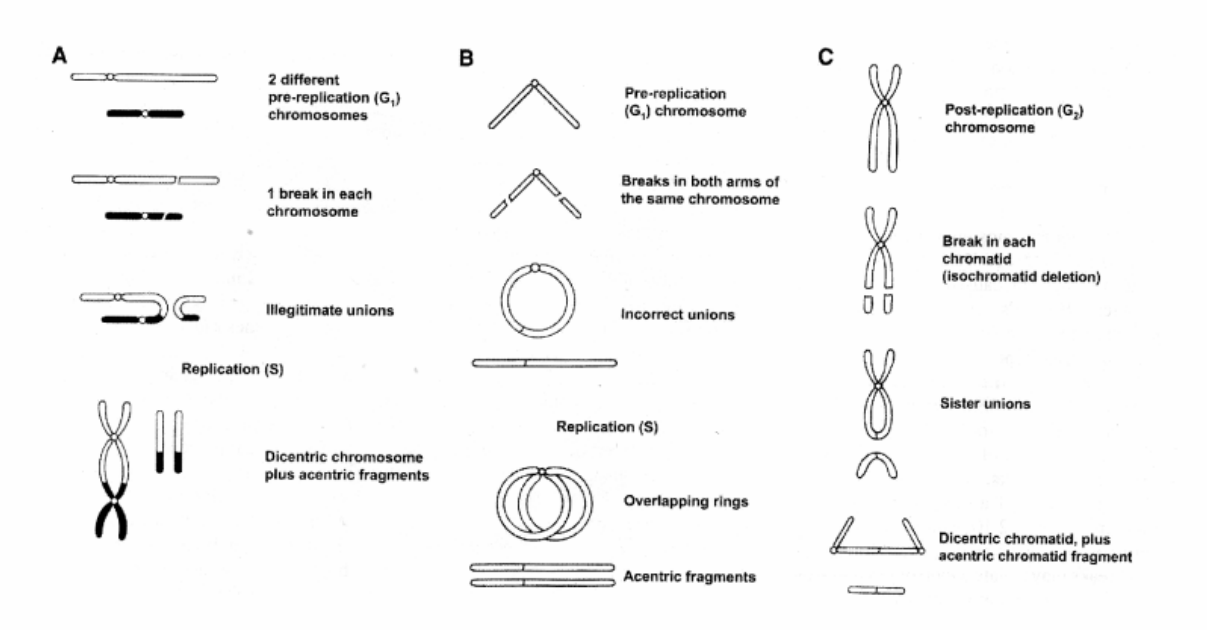

Figure 1.10 Exemplary formation of three major aberrations types induced after irradiation. (A) DSBs are induced in 2 different G1 phase chromosomes. The ends can be joined incorrectly leading to an interchange between the two chromosomes. The Chromosome with two centromeres is called **dicentric**. (B) Two DSBs are generated in the two different arms of a chromosome. Incorrect joining leads to a **ring** formation. In (A) and (B) acentric fragments will be duplicated. (C) DSBs are induced in a postreplication (G2 phase) chromosome. Both sister chromatids are effected and incorrect joining can lead to the formation of a **sister union** and a fragment (from (*5*)).

chromosomal changes. But if a tumour suppressor gene may be lost this is associated with tumorigenesis (*5*). With the classical Giemsa-staining technique for chromosomes these inter-/and intrachanges cannot be visualized and quantified.

An unexpected and dangerous finding (e.g. for astronauts) is that targeted cytoplasmic irradiation with alpha particles induces mutations in mammalian cells (*21*). This is dangerous as the cytoplasmic traversal is almost not followed by cell death of the target cells but more likely by transformation.

Many studies were performed in rodent cells as the 22 chromosome sets can be easily analyzed. It was demonstrated that impairment of NHEJ causes aberrations in all cell cycle phases implicating its importance for DSB repair. HR seems not to be error free and B-NHEJ, which is highly error prone, seems as well to contribute to the huge aberration burden in DNA-PK-deficient CHO cells. However, also in HR-deficient mutants the frequency of chromosome exchanges is increased compared to the parental cells but less than in NHEJ-deficient cells. Both pathways are important for correct repair in G2 and S phase irradiated cells (*108, 295*).

Ionizing radiation-induced chromosomal aberrations correlate with cell killing in p53-defective CHO cells (*108*). Also human p53-defective cells might propagate aberrations more efficiently to the next mitosis, which leads thereafter to mitotic cell death.

1.6.4 DNA damage after proton beam exposure

Some molecular studies were looking for the amount of DNA damages, chromosomal aberrations, and changes in DNA damage gene expression after exposure to proton irradiation *in vivo* (mice), and *in vitro* (cell systems), or *in silico* (modelling studies). Unfortunately only few directly compared their results to photon radiation exposure.

A study, which irradiated genomic T7 DNA with different types of radiations, found that radiation types with similar LETs (X-rays, γ-rays, protons) do not produce similar spectra of initial complex damages. Protons produced the highest ratio of DSBs to non DSBs clusters indicating a differential DNA damage induction (*290*). A Japanese group quantified a bigger amount of initial γH2AX foci 30 minutes after proton compared to photon radiation exposure in two different cell lines. However, 30 minutes after exposure to low doses of 0.5, 1, and 2 Gy the amount of foci do not necessarily represent the initial amount of DSBs. A big part of the photon induced DNA damage could have been already repaired. Anyways 12 hours after exposure to IR DSB repair was finished following both types of radiation, which correlates with the minor RBE they found (*296*). In thyroid follicular cells 20% fewer free 3' DNA ends were quantified 1h post-irradiation with photons in contrast to protons. This late time point is rather indicating the amount of less repairable damage after proton exposure and not the initial amount of breaks (*86*). The DNA damage induced by low-LET protons seems to be more severe in comparison to photon irradiation. Consequently this would lead to another composition or amount of chromosomal aberrations. Green *et al*. found an RBE of 1.7 for micronuclei induction and overall larger micronuclei were detected after proton versus photon radiation exposure, which indicated quantitatively more unrepaired DNA damages and more severe classes of damages (*86*). Exposure of heparinized blood to different doses of 60 MeV protons showed a similar dose-response relationship to that of ^{60}Co γ-rays with regard to dicentric and ring formation. But irradiation at greater depths within the spread-out Bragg peak induced a higher aberration frequency at low proton doses than in γ-ray samples (*297*). A more efficient transmission of a significant fraction of complex-type exchanges to third-generation lymphocytes was found after proton irradiation in comparison to carbon ion irradiation (*298*). Irradiated peripheral blood cells are normally cleared from the organism after a certain time period depending on the dose. However, *in vivo* studies indicated that the mutant frequency in the lacZ gene of mouse brains was significantly increased only 8 weeks after exposure and stayed high until 16 weeks thereafter (*299*). Mutation analysis in lymphocytes does not reflect the response of late responding tissues. Unfortunately these results have not been compared to photon irradiation. Overall protons seem to induce more severe chromosome aberrations.

Modelling studies are very helpful to get an idea of the lesion complexity. At high-LET radiation exposure the contribution of secondary electron tracks to the induction of clustered

lesions is almost negligible, though they seem to dominate at low-LET radiation types, below ~ 10 keV/µm. Ottolenghi *et al*. proposed that the larger biological efficiency of protons is related to the larger energy density within a small radius around the primary track (*50*).

Expression profile analysis of DNA damage signalling genes in mouse brains, which have been exposed to 2 Gy of protons displayed a down-regulation of Chk1, Parp, and Rad52 and an up-regulation of Rad51/1, and Brca1. Even without the photon control arm, this indicates an interesting modulation of the DNA damage response with regard to proton exposure (*300*). Until today studies have indicated that protons induce more severe and complex DNA damages, which might be even differentially processed. Therefore, in this work and future work this topic has to be addressed in more detail.

1.7 Aim of the study

There is presently a widening gap between the rapid introduction of proton therapy in clinical practice worldwide and the apparent lack of solid radiobiological evidence and data to support the expansion of new clinical indications, particularly when combined with other treatment modalities.

Radiobiologic experiments conducted several decades ago revealed an approximately 10% higher biologic effectiveness of protons (RBE) compared to photons. Many *in vitro* and *in vivo* experimental approaches have been performed to better define the observed RBE (*82, 301, 302*). These studies confirmed that the continued employment of a generic RBE value of 1.1 is reasonable, even though the RBE can vary heavily according to tissue, cell line, or the end point investigated. However, the cause for this increased RBE on the physical-chemical and molecular-cellular level is far from clear. Many researchers assumed no big differences on the molecular level, as the oxygen enhancement ratio of protons and photons appeared to be equal (*52, 53*). Yet, several studies showed a bigger efficiency in cell killing, in ROS production, or in micronuclei generation after proton versus photon radiation exposure (*86, 88, 89*). Unfortunately, all of these studies have been done in different centres with a small number of cell lines and cannot be generalized toward a common conclusion. Differences have been demonstrated with regard to DNA repair kinetics, and chromosomal aberration induction (*86, 296, 297, 299*). Modelling studies proposed a larger amount of small DNA fragments after proton irradiation (*50, 303*).

DNA is known to be the most important target for radiation-induced effects, and some studies indicate a differential DNA damage induction after proton radiation exposure. Therefore, the goal of the present study was to investigate *in vitro* whether the DNA damage induced by proton radiation exposure differs or equals the damage after photon radiation exposure. Our questions were:

1) Does proton radiation induce a bigger amount of DNA damage than photon radiation?
2) Is the DNA damage after proton exposure more complex than after photon exposure?
3) Is the hierarchy of different repair machineries changed after proton compared to photon radiation exposure?
4) Is the DNA damage generated by proton as compared to photon irradiation more often mis-repaired or even not repaired?

We addressed these questions by using 1) an indirect approach screening several DNA repair mutants for their survival after proton compared to photon irradiation, 2) quantification of the initial DNA damage and of the repair kinetics of different repair proteins after both types of radiation, and assessment of 3) chromosomal aberrations to detect eventually mis-repaired DNA damage.

2 Materials and Methods

2.1 Cell lines and cell culture

All cell lines used during this thesis were cultured in 5% CO_2 atmosphere at 37℃. Hamster cells (listed in Table 2.1) were kept in Ham's F-10 nutrient mixture supplemented with 10% FCS and penicillin-streptomycin (100U/ml-100µg/ml).

Tabelle 2.1 Hamster cell lines

Cell line	Deficiency	Mother cell line	Origin	Kindly provided by	Ref.
AA8			Ovary	M. Zdzienicka, Leiden, NL and M. Löbrich, Darmstadt, GER	(*304*)
UV-5	ERCC2-/-	AA8	Ovary	M. Zdzienicka, Leiden, NL	(*304*)
Irs1sf	XRCC3-/-	AA8	Ovary	M. Zdzienicka, Leiden, NL and L. Thompson, Livermore, CA, USA	(*305*)
1SFK8	XRCC3 complemented	Irs1sf	Ovary	L. Thompson, Livermore, CA, USA	(*170*)
CHO9			Ovary	M. Zdzienicka, Leiden, NL	(*306*)
XR-C1	DNA-PKcs-/-	CHO9	Ovary	M. Zdzienicka, Leiden, NL	(*211, 306*)
Em-c11	XRCC1-/- (C389Y substitution leading to protein instability)	CHO9	Ovary	M. Zdzienicka, Leiden, NL	(*307*)
V79			Lung	M. Zdzienicka, Leiden, NL	(*308*)
V-C8	BRCA2 truncation (biallelic nonsense mutations)	V79	Lung	M. Zdzienicka, Leiden, NL	(*308*)
V79B			Lung	M. Zdzienicka, Leiden, NL	(*309*)

CL-V4B	Rad51c-/-; deletion of ATP-binding site	V79B	Lung	M. Zdzienicka, Leiden, NL	(*309*)

Human osteosarcoma U2OS cells (see Table 2) were kept in DMEM supplemented with 10% FCS, glutamine (2 mM), sodium pyruvate (1 mM) and penicillin-streptomycin (100U/ml-100µg/ml). Human pancreatic adenocarcinoma cells BxPC-3 and Capan-1 (listed in Table 2) were kept in RPMI 1640 supplemented with 10% or 15% FCS respectively, glutamine (2 mM) and penicillin-streptomycin (100U/ml-100µg/ml).

Tabelle 2.2 Human cell lines

Cell line	Deficiency	Origin	p53-status	Kindly provided by	Ref.
U2OS		Bone (osteosarcoma)	+/+	A. Sartori, Zurich, CH	(*310*)
Capan-1	BRCA2-/-; LOH at BRCA2 locus+truncation mutation in the 2nd allele	Pancreas (from metastatic site: liver)	mutated	Purchased from Cell Line Service (CLS), Eppelheim, GER	(*186, 275*)
BxPC-3	BRCA2-/+; LOH in one BRCA2 allele	Pancreas	mutated	H. Friess, Munich, GER	(*186*)

All cells were cultured in TPP plastic flasks or in 10 cm Petri dishes (Falcon) for clonogenic assays.

Every 2 month cells were tested for mycoplasma infection with the MycoAlert® Assay (Lonza, Rockland, USA). This assay can detect mycoplasma in the supernatant of cell cultures by measuring the abundance of mycoplasma specific enzymes. Together with a special substrate these enzymes produce ATP. This ATP is converted in a second Luciferin based reaction to light and oxiluciferin what can be easily measured in a fluorescence reader. Hamster cells, Capan-1 and BxPC-3 cells were never tested mycoplasma positive. U2OS cells were treated for two weeks with 25 µg/ml Plasmocin (Invitrogen, Basel, CH). After another two weeks the cells were mycoplasma free and only then used for experiments.

2.2 Reagents and Antibodies

Tabelle 2.3 Reagents

Reagents	**Manufacturer**
Alamar Blue	Biosource Int.
All cell culture media and supplements	Gibco, Invitrogen
MycoAlert® Assay	LONZA
Plasmocin	Invitrogen
OPTIMEM	Gibco, Invitrogen
Lipofectamine™ 2000	Invitrogen
Lipofectamine® RNAiMAX Reagent	Invitrogen
RNAse A	Quiagen
Demecolcemide	Sigma
Giemsa	Sigma
Entellan	Merck
Dako Fluorescence Mounting Medium	Dako
All other chemical reagents were of highest purity grade	Sigma-Aldrich®, Merck

Tabelle 2.4 Antibodies

Antibodies	**Manufacturer**	**Ref. number**
Anti-ß-actin ab (clone AC-15), mouse monoclonal	Sigma	A5441
Anti-Rad51 ab, mouse monoclonal	Abcam	Ab213
Anti-p-DNA-PKcs (Ser2056) ab, rabbit polyclonal	Abcam	Ab18192
Anti-XRCC4 ab, rabbit polyclonal	Abcam	Ab145

Anti-XRCC1 ab, rabbit polyclonal	Cell Signaling Technology®	#2735
Anti-XRCC3 ab, rabbit polyclonal	Abcam	Ab6494
Anti-53BP1 ab, rabbit polyclonal	Cell Signaling Technology®	#4937
Anti-γH2A.X (Ser139) ab (clone JBW301), mouse monoclonal monoclonal	Millipore	#05-636
Anti-Chk2 ab (clone 7), mouse monoclonal	Millipore	05-649
Anti-p-ATM (Ser1981) ab, rabbit polyclonal	Abcam	Ab79891
Anti-pH2A.X (Ser139) ab (Alexa Fluor® 488 conjugate), rabbit monoclonal	Cell Signaling Technology®	#9719
Rabbit (DA1E) IgG Isotype Control (Alexa Fluor® 488 conjugate), rabbit monoclonal	Cell Signaling Technology®	#2975
Secondary sheep anti-mouse ab, HRP-linked	GE Healthcare	NA931V
Secondary donkey anti-rabbit ab, HRP-linked	GE Healthcare	NA9340V
Secondary goat anti-mouse ab, Alexa-Fluor®488-linked	Molecular Probes®, Invitrogen	A-11001
Secondary goat anti-rabbit ab, Alexa-Fluor®546-linked	Molecular Probes®, Invitrogen	A11071
Secondary goat anti-mouse ab, Alexa-Fluor®546-linked	Molecular Probes®, Invitrogen	A-11018
Secondary goat anti-rabbit ab, Alexa-Fluor®488-linked	Molecular Probes®, Invitrogen	A-11070

2.3 Irradiation procedures

2.3.1 Transport of the cells

Cell culture and all experiments were performed in the Laboratory for Molecular Radiobiology of the University Hospital Zurich (USZ). The centre for proton therapy at the Paul Scherrer Institute (PSI; Villigen, Switzerland) is located in 1 h distance from the hospital by public transport. In order to irradiate the cells with protons, they had to be transported. Cells were seeded into 25 cm^2 TPP-Vent-flasks. For transport the lids of the flasks were completely sealed so that no increase in O_2 pressure would occur and the gas atmosphere in the flask stayed the same as in the incubator. This could be checked by the colour of the culture medium. Phenol red turns bright pink (pH > 8.2) if it has contact to normal air. Flasks were placed into a styrofoam box buffered with 37°C temp erature water containers. Carrying of the box was accomplished with big caution. Cells were either transported or “pseudotransported” in the case of photon irradiation. Afterwards they were placed into a CO_2 incubator for ~1h before irradiation took place. After irradiation cells were reincubated over night for ~12 hours prior to retransport or “pseudotransport”.

2.3.2 Photon irradiation

Photon irradiation was performed using a Pantak Therapax, 300 keV at 0.7 Gy/min or a Gulmay 200 keV X-ray unit at 1 Gy/min at room temperature. Vigilant-Dosimeter was used for quality assurance. The flasks or slides were placed in a field of 20 x 20 cm, which was covered by the tubus.

2.3.3 Proton irradiation

All proton irradiations were delivered using the spot scanning approach performed at the PSI, centre for proton therapy (*311*) with the cells being placed in the centre of a Spread-Out-Bragg-Peak (SOBP) with a length of 5 cm and maximum proton energy of 138 MeV. The field size orthogonal to the beam was adjusted to the number of cell culture flasks. During beam delivery the field size was scanned, which could fit 1, 2, or 4 cell culture flasks or microscopy slides (6 x 8; 11 x 8; 11 x 15 cm, respectively). The duration of the whole scan was determined by the field size and the dose. Irradiation was performed at room temperature and took never longer than 8 minutes, on average 5 minutes. One spot during scanning is relatively large, ~7 mm (*311, 312*). Therefore a cell is almost always covered by one spot. Dosimetry of the fields was performed using both small diameter cylindrical ionisation chambers (active volume 0.3cm^3) and a Farmer NE2571 ionisation chamber using the IAEA TRS-398 protocol.

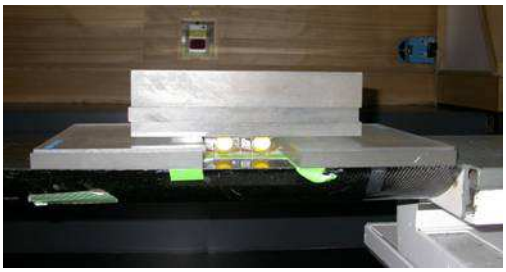

Figure 2.1 Photograph of the flask arrangement on the gantry table.

2.4 Proliferation assay

Cell proliferation was assessed with the colorimetric AlamarBlue® assay that is based on the detection of metabolic activity. It is a REDOX indicator correlating with metabolic cellular activity. The blue resazurin is converted to pink resorufin via the reduction reactions of metabolically active cells. In contrast to MTT (3-(4,5-dimethylthiazol-2)-2, 5 diphenyltetrazolium bromide), AlamarBlue® can be reduced by Cytochromes due to its bigger oxidation reduction potential, and therefore it cannot lead to shut down of the respiratory chain and cell cytotoxicity (Manual, Invitrogen). Measurements were performed 4 h after incubation with AlamarBlue® reagent. Absorption at 570/670 nm was measured using an EL 808 Ultra Microplate Reader (BIO-TEK INSTRUMENTS, INC., Switzerland). The percentage of the reduced agent was calculated for each well and the blank value was subtracted.

Measurements could only start 44 hours after irradiation. Cells were processed ~20 hours after irradiation following recovery and transport. 500 cells were plated per well into 96-well plates. Measurements were performed the next day, ~ 44h after irradiation, and the following ones at 68h, 92h and 116 h after irradiation. All measurements were carried out in triplicate in at least 3 independent experiments.

2.5 Clonogenic survival assay

Clonogenic survival was determined by the ability of single cells to form colonies *in vitro*. 20 hours following irradiation of exponentially growing or plateau phase cells, cells were trypsinised, and single cell suspensions were plated on Petri dishes (Falcon, 10cm^2). The number of plated cells was adjusted to obtain ~ 50-300 colonies per cell culture dish with a given treatment. In order to prevent unwanted cell density effects, equal amount of cells was plated for similar doses of photon and proton irradiated samples. The dishes were maintained at 37℃ in 5% CO_2 and allowed to form colonies for different time periods depending on the cell system (see Table 2.5).

Tabelle 2.5 Clonogenic survival assay conditions

Cell line	**Number of cells/flask (25 cm^2)**	**Time from plating to irradiation**	**Time of clonogenic assay until fixation**
Hamster cells in logarithmic growth phase	300 000	24 h	7 – 10 days
Hamster cells in plateau phase (G0/G1)	1 000 000	50 h	7 – 10 days
U2OS cells	300 000	24 h	14 days
Capan-1 cells	1 000 000	48 h	21 days
BxPC-3	300 000	48 h	17 days

For fixation of the colonies Carnoy's fixative (methanol/acetic acid; 3:1) or 70% ice cold ethanol was used. Staining was performed with a 0.5% crystal violet solution. Colonies with > 50 cells/colony were counted manually with a GALLENKAMP Colony counter. The survival fraction (SF) with a given treatment was determined in the following way: SF = (amount of counted colonies)/(amount of seeded cells x PE), where PE is the plating efficiency of untreated cells: PE = (amount of counted colonies)/(amount of seeded cells). The survival data represent the means and standard deviations of at least three independent experiments performed in triplicates.

In order to calculate RBE values, α- and ß-values for each survival curve had to be determined. Survival data were fitted by a weighted, stratified, linear regression according to the linear–quadratic formula $S(D)/S(0) = \exp(\alpha D+ßD^2)$ (Franken, 2006). An SPSS-file was created for each survival curve with following variables: dose, number of plated cells, number of surviving colonies and PE of that experiment. Furthermore for the quadratic term "D2" = dose*dose, for survival "S"= ln(colonies/cells) – ln(PE) and for the weight of the colonies found "W"=colonies*cells/(cells – colonies). A linear regression was performed in SPSS (Version 17) as described in Franken *et al*. (*313*) and the coefficients provide linear (α) and quadratic (ß) parameters. Those were entered into an Excel-file were the formula of Staab *et al*. was used to calculate RBE values at 50, 37, 10 and 1 % survival level (*314*).

2.6 Flow cytometry

Flow cytometry allows the simultaneous multiparametric analysis of physical and biochemical characteristics of up to thousands of cells per second. Volume and granularity of the cell is automatically recorded. If certain molecules, e.g. DNA with a specific dye or proteins with

specific antibodies, are fluorescently labelled, they can be quantified over the intensity of the signal (events/signal intensity). Laser light of a specific wavelength is directed onto the single cell and scattered, which is collected by a detector. In the case of fluorescently labelled molecules, they are excited and emit light with a certain wavelength, which is detected by one or more special fluorescent detectors. In this way the amount of DNA molecules/cell (2N or 4N) can be analyzed for thousands of cells. Or the amount of modified proteins (e.g. phosphorylation specific fluorescently labelled antibody) will give a fluorescent signal per cell with different intensities. A shift in the intensity shows a decrease or increase of protein modifications compared to the control.

2.6.1 Cell cycle distribution analysis

Cells were collected at different time points after irradiation, kept on ice, washed twice with PBS, fixed with 70% ice cold ethanol and stored until analysis at -20℃. For preparation, cells were rehydrated in PBS and resuspended in 1 ml PBS containing propidium iodide (PI; 3µg/ml) and RNase A (0.3mg/ml;Qiagen). The cell solutions were incubated on a wheel for 1 hour at room temperature (RT). PI is bound stoichiometrically by DNA. Fluorescence intensity was recorded with a BD FACSCalibur flow cytometer (BD Biosciences; excitation at 488 nm and emission at 580 and 650 nm). Cell cycle phases were quantified using FlowJo software (Vers.7.6, Tree Star Inc.), doublets were excluded.

2.6.2 Intensity of H2AX phosphorylation

The protocol was adapted from a publication (*315*). Cells were harvested 30 min after 5 Gy of either type of radiation, washed twice with ice cold PBS, and fixed in ice cold 70% ethanol over night at 4℃. Next day cells were washed in PB S and rehydrated with permeabilization buffer (0.2% Triton X-100, 4% FCS in PBS) for 10 min on ice and stained for 1 h at room temperature with Alexa-488 labelled anti phospho-H2AX (Ser139) or unspecific isotype control at a concentration of 1 µg/mL. After washing with PBS cells were incubated for 30 min at room temperature in PBS containing 3µg/ml propidium iodide and 0.3mg/ml RNase. Fluorescence intensity was measured using a FACSCalibur (BD Biosciences) and analysis was performed using WinMDI 2.9 (free software from facs.scripps.edu in /pub/pc). To compare the levels of intracellular H2AX phosphorylation, the mean fluorescence intensity ratios (MFIR) were calculated by dividing the geometric mean fluorescence intensity of each sample by the geometric mean fluorescence intensity of the control antibody.

2.7 siRNA transfection procedures

For siRNA transfection two different approaches were used. Reverse transfection was used for CHO cells and forward transfection for U2OS cells. The latter protocol was adapted after Sartori *et.al.* (Sartori, 2007). All siRNAs were synthesized by Microsynth (Switzerland).

2.7.1 CHO cells

A day before plating the cells into the flasks for irradiation reverse transfection of AA8 wild type cells was performed after manufactures instructions (Invitrogen). Here the liposome/siRNA mix is directly added to cells during plating, when they are still in suspension. With the Lipofectamine RNAiMAX reagent this procedure is more efficient and less toxic because fewer amount the transfectant is used. Cells were irradiated approximately 48 h after transfection. siRNAs were used at a concentration of 40 nM with 1.7 µL/ml Lipefectamin RNAiMAX.

The siRad51-1 was the same as for human U2OS cells. It was selected, because the siRNA was already available and had only 1 mismatch at position 15 in the hamster mRNA sequence. siRad51-2 was generated with the Microsynth siRNA design tool against gi:1552257 of Rad51 mRNA of *C.griseus*. As the complete *C.griseus* genome is not yet sequenced, a second Blast search was performed against murine sequences to circumvent binding at unspecific sites. The two different siRad51 RNAs were used in every experiment in order to be able to detect unspecific interactions. siRNA against firefly luciferase was used for control transfections as this protein is not expressed in mammalian cells.

Tabelle 2.6 siRNA sequences for treatment of AA8 wild type cells

Name	**Sequence**	**Reference**
siLuc	5’-CGTACGCGGAATACTTCGAdTdT-3’	Sequence adapted from Beta Cell Biology Consortium (Nashville, TN, US)
siRad51-1	5’-GAGCUUGACAAACUACUUCdTdT-3’	(*316*), tested against C.griseus sequence
siRad51-2	5’-GCUGGUUUCCAUACGGUGG-TT-3’	Generated with Microsynth-tool against mRad51 of C.griseus (GI:1552257)

2.7.2 U2OS cells

The human osteosarcoma cells U2OS were plated and transfected 24 hours later, which is called forward transfection. At ~ 50% confluency cells were treated with 33 nM siRNA and 2.9 µl/ml Lipofectamine 2000. Liposome/RNA-bodies were prepared before transfection in OPTIMEM medium. Cell culture medium was changed before transfection to Penicillin/streptomycin free and 5% FCS containing medium. 16 hours later medium was changed to normal growth medium and ~ 8 hours later cells were plated into new flasks for control and different dose points.

Rad51-1, XRCC1 and XRCC4 siRNA sequences were selected out of different publications. These sequences had been validated from other researchers for its specificity and therefore could be used without the need of a second specific siRNA (*316-318*). siXRCC3 was generated with the Microsynth-siRNA tool against GI:153946429, which is the accession number for XRCC3 transcript variant 1. The siRNA sequence covers all three transcript variants of XRCC3. siHSP70B was used as control siRNA as this HSP subtype is not expressed in U2OS cells (*319*).

Tabelle 2.7 siRNA sequences for treatment of U2OS cells

Name	**Sequence**	**Reference**
siHSP70B	5'-GGGAGGACAAGACGUUCUAdTdT-3'	(*319, 320*)
siRad51-1	5'-GAGCUUGACAAACUACUUCdTdT-3'	(*316*)
siXRCC3	5'-UUAAGAAAGCCAAACUGAATT-3'	generated with GI: 153946429
siXRCC1	5'-CUCGACUCACUGUGCAGAAdTdT-3'	(*318*)
siXRCC4	5'-AUAUGUUGGUGAACUGAGAdTdT-3'	(*317*)

2.8 Western Blot

Western blotting was used to check the efficiency of protein down-regulation after siRNA transfection and to follow the kinetics of the DNA damage response induced protein phosphorylations or changes in protein levels.

At indicated times after transfection cells were collected, counted, and lysates were prepared with 10 µL Laemmli-buffer/45 000 cells (2% SDS, 10% glycerol, 0.004% bromphenol blue, 62.5 mM Tris-HCl, pH 6.8).

To follow phosphorylation kinetics after both types of radiation, cells attached to 25 cm² flasks were lysed at the indicated time points by incubation with 100 µl of RIPA buffer (50 mM Tris 7.4, 150 mM NaCl, 1% NP40, 0.25% Sodium deoxycholate, 1mM EDTA; added before use 1 µg/mL Pepstatin, Leupeptine, 1 mM PMSF, 1 mM sodium vanadate and 1 mM sodium fluoride) for 15 min on ice. After scratching and collection of the lysates, they were kept for an additional 15 min on ice and homogenized by pipetting 20 X up and down, before they were frozen on dry ice. All lysates were stored at -20℃ until analysis.

An equal amount of protein was subjected to SDS-PAGE to separate the proteins. Due to different sizes of the proteins different grades of acrylamid polymerization were used (pATM, pDNA-PKcs, Chk2: 8% SDS-gel/ γH2AX: 15% SDS-gel/ all other proteins: 12% SDS-gel). Proteins were blotted from the SDS-gel onto Amersham Hybond-P polyvinylidene difluoride membranes. Depending on the molecular mass of the protein of interest, the time for transfer was different (> 150 kDa = 1.5 h, 100 V at 4℃/< 15 0 kDa = 1 h, 60V at 4℃). Membranes were blocked for 1 h with 5% BSA/TBS solution in case of phospho-protein detection whereas all others were blocked with 5% milk/TBS solution. All listed antibodies in table 2.4 were used at the concentration of manufactures recommendation. Anti-phospho antibodies were diluted in 5% BSA/TBS, all others in 5% milk/TBS. Primary antibody detection was achieved by enhanced chemiluminescence using a corresponding horseradish peroxidase-conjugated second antibody, according to the manufacturer's protocol (Amersham, Freiburg, Germany). To check for loading of equal protein amounts, membranes were washed 3 x 30 min in TBS, reblocked and reprobed with anti-ß-actin antibody.

2.9 Immunofluorescence Microscopy

Immunofluorescence staining was used to quantify initial amounts of γH2AX-foci and to determine kinetics of foci formation/disappearance of different repair proteins/protein modifications (γH2AX, Rad51, 53BP1, pDNA-PKcs). Cells were plated onto plastic slides to prevent the generation of secondary electrons, which occurs when experiments are performed with glass slides and low energetic X-rays. In this way an artificial higher absolute dose could be prevented. Ibidi-µ-slides VI$^{0.4}$ slides were used, which are made of special plastic that is not autofluorescent and exhibits the same physical characteristics as glass but does not interfere with either type of radiation.

24 hrs prior to irradiation cells were plated onto Ibidi-µ-slides VI$^{0.4}$ (Ibidi, 80606, Munich, Germany) at the same cell density as used for the clonogenic survival assay. At the indicated time points after irradiation, cells were fixed and stained with a set of antibodies specific against proteins involved in DNA double strand break repair. Cells were washed twice with PBS, fixed with 4% formaldehyde/PBS for 20 min, washed with PBS (4 x 5 min) and finally

with 0.1 M glycine for storage at 4℃. All samples were stained together. Cells were permeabilised for 5 min with 0.2% ice cold Triton-X-100, blocked for 30 min with 3%BSA/0.1%Tween-20/PBS, followed by 1 h incubation with primary antibodies, diluted 1:100 in 1%BSA/PBS (mouse-γH2AX Ser139-ab/ mouse-Rad51-ab/rabbit-53BP1-ab/ rabbit-pDNA-PKcs-ab). After washing with 1%BSA/PBS (4 x 10min), cells were incubated with the appropriate secondary antibody (1:1000; Alexa-488 or/and Alexa-546). Finally, cells were washed with PBS (4 x 10min), incubated for 15 min with PBS/Dapi (1µg/ml) and washed again twice for 10 min with PBS. The channels were filled with Dako Fluorescence Mounting medium (Dako) and slides were kept at 4℃ until ana lysis. Slides were examined with Leica SP5 confocal microscope or with Zeiss Axiovert 25 microscope. At the Zeiss Axiovert, nuclei were randomly chosen and analyzed real-time during microscopy without any picture generation. With the Leica SP5 z-stacks of at least 50 cells were recorded with a Leica DFC 350 FX camera and merged for analysis in LAS AF Lite software (Leica, free-version). Foci amounts of at least 50 cell nuclei per condition were counted by eye. The experiments were repeated at least three times.

2.10 Metaphase spreads

Another parameter for efficient repair is the quantification of chromosomal aberrations. CHO wild type cells were plated in the same density as for clonogenic survival 24 h before irradiation. 21 hours after irradiation cells were blocked in metaphase by the addition of 0.1 µg/ml Colcemid for 3 h. Thereafter, cells were collected, treated with 5 ml hypotonic KCl-solution (0.075 M, Sigma), and fixed by adding 2 x 5 ml Carnoy's fixative (3:1; Methanol:Acetic acid). Samples were stored at -20℃ until slide preparation. Cell concentration was adjusted (~1x10^6cells/ml) and fixed cells were dropped from ~10 cm height onto pre-cleaned wet slides (Menzel-Gläser, Mattrand, Thermo Scientific, Braunschweig). To gain better chromosome spreading, slides were put top-down above hot water steam and thereafter top-up for 1 min onto a 50℃ heating block. Slides were dried at least over night, stained with 2% Giemsa for 10 min, washed 4 x in cold water and dried again at least over night. Next day they were embedded permanently with Entellan below 24 x 60 mm cover glasses. Slides were coded before picture acquisition and pictures of at least 50 metaphases per condition were acquired with a Leica SP5 (bright field) microscope and a Leica DFC 290 camera. Metaphase spreads were screened for fragments, rings, dicentrics and sister unions. Total amounts and amounts/cell of fragments, rings, dicentrics and sister unions were calculated.

2.11 Statistical Analysis

Data were presented as the mean ± standard error of the mean (SEM) of at least three independent experiments. The results were tested for significance using the two-sided unpaired Student's t test (Excel 2003 or GraphPadPrism Version 5). Results were considered statistically significant when $p < 0.05$ (*) or highly significant $p < 0.001$ (**).

3 Results

In this study we were interested in the differential biological response of wild type/mutant cell pairs of different DNA repair systems with regard to photon vs. proton irradiation. By using the proton spot scanning beam of the Paul Scherrer Institute (PSI) in Villigen, Switzerland, we were automatically the first who used such a beam for a huge radiobiological study. The relative biological effectiveness (RBE) for proton relative to photon irradiation has been studied extensively during the last 60 years, primarily using the traditional proton scattering technique. To our best knowledge one study was performed using the proton scanning beam of the PSI and few studies using the scanning beam at GSI, in Darmstadt. The aim was to determine whether the established RBE for protons also applied to the proton spot scanning technique. Gueuleutte *et al*. measured crypt regeneration in mice, which resulted in a RBE for proton relative to photon irradiation of 1.16 (at the middle of the spread out Bragg peak (SOBP)) (*302*). Thus, this study indicates that a generic RBE of 1.1 used in the clinics is also applicable for proton spot scanning facilities.

However, little is known about the molecular cellular response after proton irradiation. A few molecular studies have been done, which directly compare conventional radiotherapy with proton radiotherapy (mainly scattering technique) using the same experimental settings and studying several different end points such as early apoptotic response, micronucleus formation, γH2AX foci formation, metastatic potential, and mutation frequency in mouse brain (*86, 91, 299, 302*). Different cell systems and experimental set ups have been used in these studies, and therefore it is difficult to draw a clear conclusion.

Our aim was an extensive unbiased study addressing DNA damage induction and DNA repair after proton spot scanning of cells. All experiments were performed in parallel with a 200 keV X-ray reference radiation. The main end points were clonogenic survival, proliferative activity, cell cycle distribution, initial amount of DNA double strand breaks (DSBs), DNA repair kinetics, DNA damage response (DDR) kinetics, and chromosomal aberrations.

One reason for the increased effectiveness of protons could be a different complexity of the generated DNA damage. An exact quantification of DNA damage, especially of very densely packed damage sites, is very difficult or requires very high doses, which might be beyond the physiological range. A setting to study indirectly the quality of the DNA damage was employed. Using DNA DSB repair mutant cell lines, a difference in their survival fractions compared to the wild type cells can indicate problems in the ability to repair certain DNA damages, especially the most toxic DSBs.

Few suitable human cell systems are available to study DNA damage repair systems and their influence on survival after proton compared to photon irradiation, as they often grow

very slowly or are not able to form clones from single cells. Due to the availability of a huge set of characterized DNA repair mutant-/wild type cell pairs and ease in handling, Chinese hamster cells were used. All the molecular details were performed in this hamster cell line setting.

Later on we also performed experiments using more clinically relevant human cell systems. Due to different cellular responses, the Results section is divided into two parts: hamster cell system and human cell systems, however in the end both cell systems will be discussed together.

3.1 Chinese hamster cell line system

All hamster cell lines mentioned in the following chapter are listed in Table 2.1. Two different hamster cell systems were used. Chinese hamster ovary (CHO) cell culture was described in 1958 by Tjio et al. (*321*). In the same year the male Chinese hamster lung fibroblast cell line V79 was introduced (*322*). These hamster cells possess a very low chromosome number (2n=22) compared to other mammalian cells and are an ideal model for genetic studies. The doubling time for both cell lines is 12-16 hours and therefore these cells are easy to use in cell culture (*323*). In the recent years, mechanisms of mammalian DNA repair have been extensively studied in CHO and V79 cells (*135, 211, 266*). Analysis of the *XRCC* genes in hamster cells was important for the understanding of mammalian DNA repair processes, especially of DSB repair. The ability of different *XRCC* genes to correct for DNA damage hypersensitivity led to the identification of proteins involved in several repair pathways (*324*).

However, it is worth mentioning that hamster ovary cells and lung fibroblasts harbour mutated p53. Consequently, *p21* and *Bax* genes are not transcribed and will not lead to ionizing radiation-induced G1 arrest (*325, 326*). Therefore, the overall DDR in p53 mutated cell lines is different compared to p53 wild type cells. On the other hand many tumour cells possess p53 mutations and often display as well a modified DDR, enhanced survival, and growth (*327*). In this regard, CHO cells resemble aggressive tumour cells rather than normal cells.

These two hamster cell systems are well described, easy to use in radiobiological assays and in cytogenetic assays. Furthermore many RBE-related studies have been performed with these cells (*82*). Therefore they were chosen to identify possible differences in radiation sensitivity towards proton versus photon irradiation.

3.1.1 Validation of the experimental set up

For each experiment the cells for proton treatment had to be transported to the PSI from the University Hospital Zurich (USZ) two hours prior to irradiation. After irradiation cells were placed back in an incubator having time to recover. The following day the culture flasks were transported back to the USZ. To mimic the same conditions, cells for reference irradiation with photons were pseudo-transported two times by placing them in the transport container. One day after IR exposure, the photon and proton irradiated cells were processed together for clonogenic survival assays. Three repetitions of a clonogenic assay with a wild type cell line showed no significant variation due to the transport procedures. Survival curves exhibited minor standard deviations (Fig. 3.1B, wild type). Moreover, the plating efficiency of

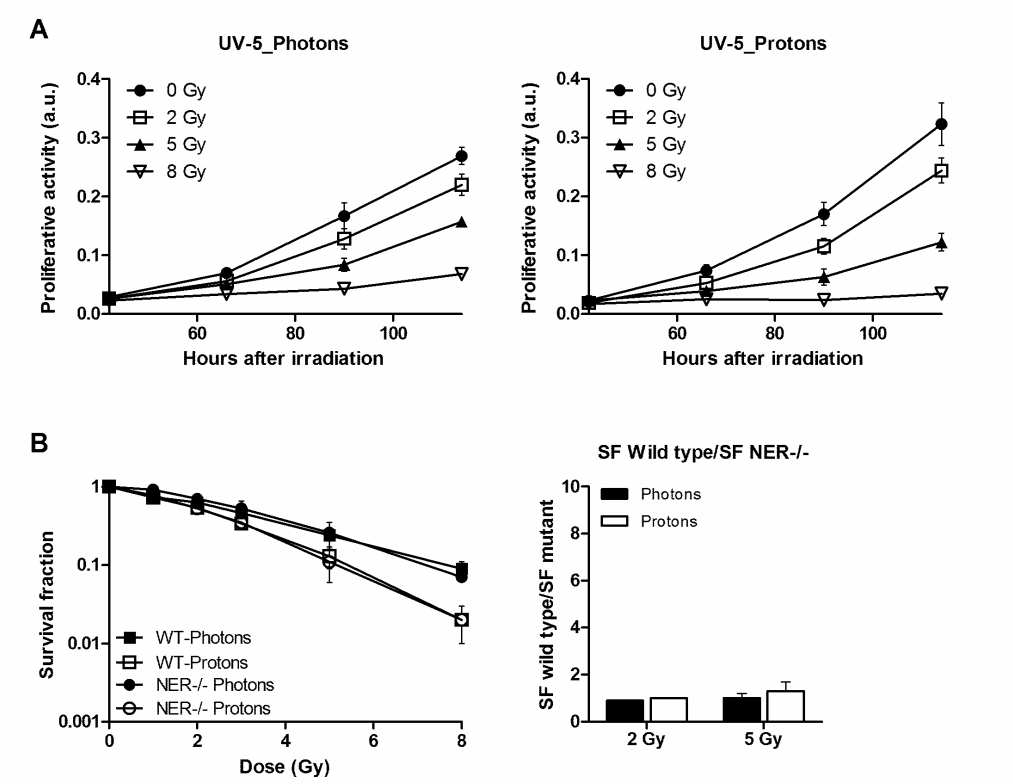

Figure 3.1 Response of NER-deficient cells (ERCC2-/-) to photon and proton irradiation. Cells were irradiated and (A) cell proliferation and (B) clonogenic cell survival (also for AA8 wild type cells) was determined. In (B) survival data and corresponding ratios of SFwild type/SFmutant are plotted. Data points represent mean ± SD or bars represent mean ± SEM; n ≥ 3.

control cells for either treatment was the same (Fig. 3.2). Plating efficiencies show the ability of control/non-irradiated cells to form a colony. To assess proliferative activity a MTT-like assay with AlamarBlue, based on the detection of cellular metabolic activity, was performed. This assay was used as fast initial detection of differences in the sensitivity towards the two different types of radiation. Furthermore, it should assess if the growth rate of the non-irradiated cells was not influenced by either type of treatment (transport, other incubator). Proliferation rates of the non-irradiated control samples followed up to 5 days were equal for

photon and proton experiments (Fig. 3.3). Because of this, we assume that cells were not metabolically stressed and had not activated severe stress responses due to the transport. Initially, the survival of a nucleotide excision repair (NER) mutant (UV-5) was determined. As NER was never found to be involved in the repair of DNA damage induced by ionizing radiation but in the repair of UV-induced DNA damages, no difference compared to the wild type cells was expected (*120*). Determination of the clonogenic survival of UV-5 cells and wild type AA8 cells displayed no differences. Both cell lines are more efficiently killed by proton irradiation, but to the same extent (Fig 3.1B). The decrease in proliferative activity after photon and proton irradiation was in the same range as for wild type cells (Fig. 3.1A+3.3A). Both assays indicate that neither photon-induced DNA damage nor proton-induced DNA damage is repaired via NER.

Since we did use an unbiased approach to uncover molecular differences induced after proton irradiation exposure compared to photon exposure, we did not compare the effects with photon equivalent doses (0.9 Gy protons vs. 1.0 Gy photons) but the same physical doses (1 Gy vs. 1 Gy). The RBE of 1.1 is well known, yet the molecular cause leading to it is far from clear. Therefore it would be incorrect to implement a factor from which we do not even know if it is valid for all genetic backgrounds and conditions. To study molecular parameters after either type of radiation, we did not use equipotent doses, the dose needed to kill the same number of cells, but the same physical doses. This is in contrast to many other studies and will be explained later on. The main focus in the clonogenic survival assays was the differential response comparing wild type versus DNA repair mutant cell lines. For better visualisation, the ratios of the survival fractions for wild type versus mutant cells (SFwild type/SFmutant) were plotted for both types of radiation at 2 dose points (Fig. 3.1B, right bar graph). With the example of NER-/- cells it becomes clear that if the mutant cell line behaves the same way as the wild type cell, the ratio stays close to 1, but if a repair mutant is highly sensitive to one type of radiation, this ratio would increase drastically. In the next chapters different DNA repair mutants were analyzed.

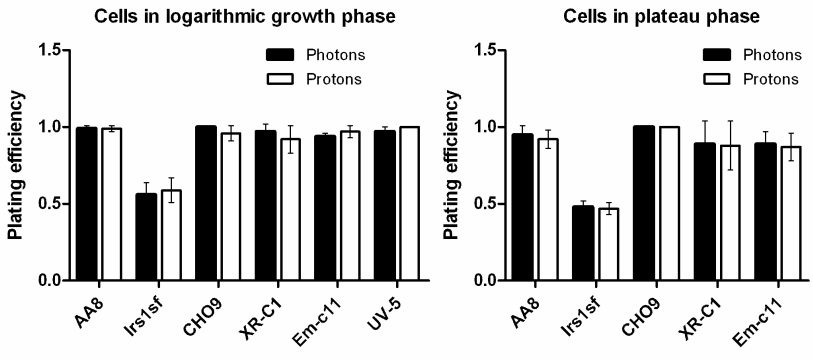

Figure 3.2 Plating efficiencies of not irradiated control cells of the different CHO cell lines seeded as part of the clonogenic survival assay. CHO cells from exponentially growing cell cultures and from plateau phase, growth arrested cell cultures. Data is shown as mean ± SD, n $\geq$ 3.

3.1.2 Proliferative activity of wild type and different DNA double strand break repair mutant cell lines

The following three chapters will focus on DNA double strand break repair. DNA DSBs are the most severe lesions induced by IR, leading directly to cell death if not repaired properly. We investigated the two main repair pathways, homologous recombination (HR) and non-homologous end joining (NHEJ). As fast initial test, if the cells respond differently to the two types of radiation, a proliferation assay was performed as described earlier. The different cell lines were treated with increasing doses of proton or photon radiation (0, 2, 5, 8 Gy).

For all cell lines the non-irradiated controls had the same growth rate irrespective of being in the photon or proton experimental arm (Fig. 3.3) with NHEJ-deficient cells proliferating as fast as wild type cells (Fig. 3.3C+D). The non-irradiated HR-deficient Irs1sf cells showed a one third slower growth rate compared to the corresponding wild type AA8 cell line (Fig. 3.3A+B). 116 hours after 2 Gy of either type of radiation the proliferative activity of both wild type cell lines decreased by only 5-10% (Fig. 3.3A+C). As expected, the proliferative activity of the two DSB repair mutants dropped to 40 – 60% after 2 Gy (Fig. 3.3B+D). HR-/- cells revealed no difference in growth inhibition between the two types of radiation, whereas the NHEJ-/- cells displayed a significant stronger growth inhibition after 2 Gy of proton compared to photon irradiation. With higher doses this difference seen with NHEJ-/- cells was not visible any more, as proliferation dropped under 10% (Fig. 3.3B+D). For wild type cells higher proton radiation exposures (5, 8 Gy) led also to a stronger growth inhibition compared to photon radiation, which was significant at 8 Gy in CHO9 wild type cells (Fig. 3.3A+C).

From these proliferation experiments, we demonstrated greater sensitivity to photon and proton radiation by both HR-/- and NHEJ-/- cells as compared to wild type cells. However, 4.5 days after irradiation exposure with higher doses of protons (5, 8 Gy), fewer wild type cells were metabolically active compared to those irradiated with photons, indicating a stronger efficacy in cell killing by proton irradiation with the PSI spot scanning beam. HR-defective cells were dose-dependently growth-inhibited with no difference regarding the two types of radiation. As expected, NHEJ-deficient cells were the most radiosensitive cells (291). Interestingly, these cells exhibited a differential response to proton versus photon irradiation, with greater growth inhibition after low dose (2 Gy) proton irradiation as compared to photon irradiation.

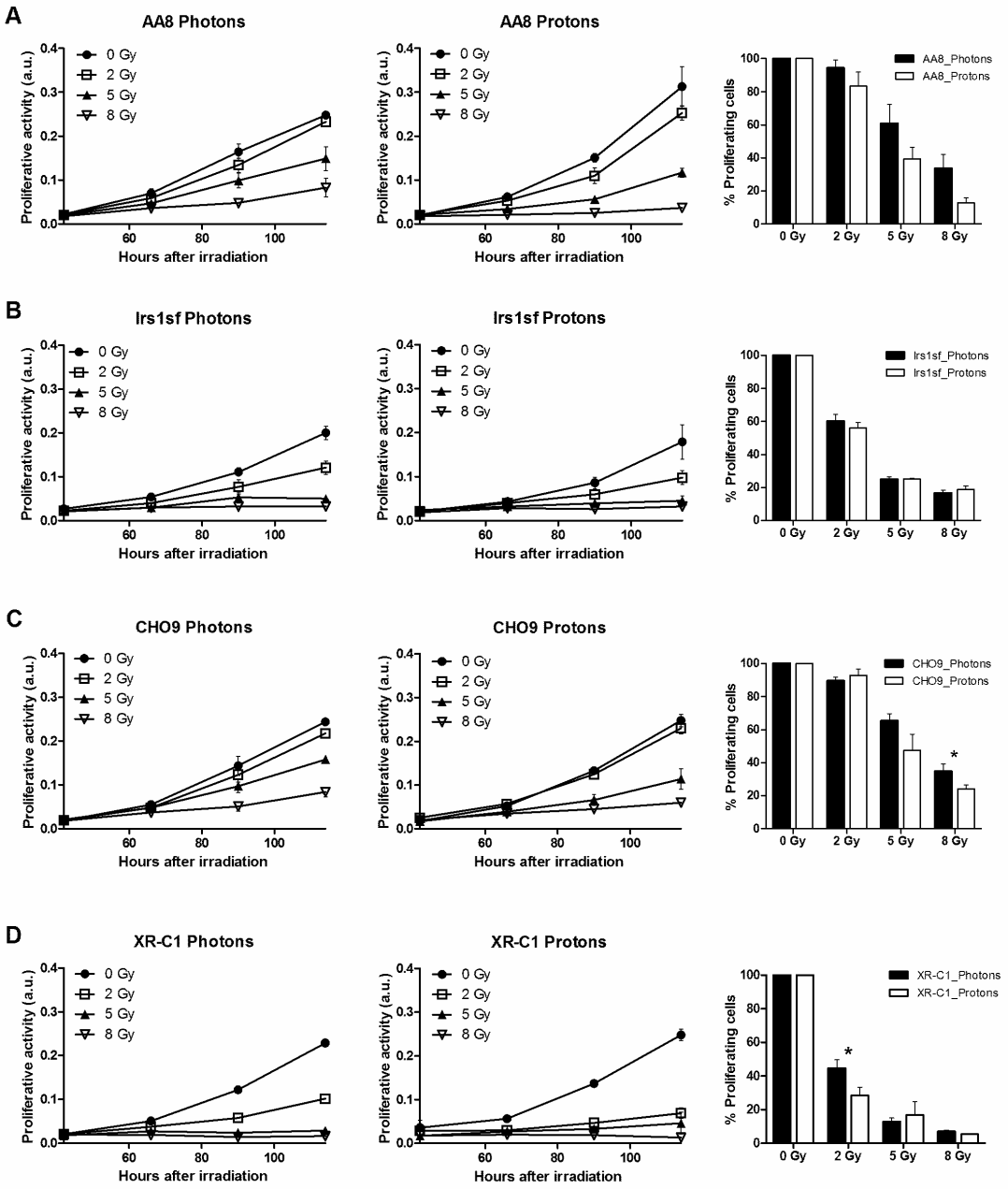

Figure 3.3 Cell proliferation of different CHO cell lines. Cells were irradiated with increasing doses of photons and protons. Proliferative activity at 66, 90, and 116 hours after irradiation and % proliferative activity relative to control after 116 hours are plotted. (A) AA8 wild type cells, (B) HR-deficient Irs1sf (XRCC3-/-) cells (mutant of AA8) (C) CHO9 wild type cells, D) NHEJ-deficient XR-C1 (DNA-PKcs-/-) cells (mutant of CHO9). Data points represent mean ± SD or bars represent mean ± SEM; n ≥ 3; *P<0.05.

3.1.3 Clonogenic survival of logarithmically growing wild type and DSB repair mutant cell lines

Measuring proliferation can mask real cell survival, since a few surviving, well-proliferating cells may give a strong signal. In contrast, a clonogenic survival assay assesses the potential of each single cell to grow into a colony consisting of at least 50 cells. This cell has to repair

all damages before it is able to divide at least for another 5-6 generations. Therefore the colony formation assay (clonogenic assay) is a more accurate measurement of cell survival. In this experiment exponentially growing cells were irradiated, and on the following day cells were harvested, counted, and plated for the clonogenic survival assay. At the time of irradiation, the cell cycle distribution was equal in all samples (Fig. 3.4, logarithmically growing cells). The diverse DSB repair mechanisms show differential activity patterns during the course of the cell cycle. Our interest was to investigate all repair mechanisms. Therefore exponential growth and not G1-arrested conditions were chosen. We assume that aggressively proliferating cancer cells exhibit all cell cycle phases. Fast-proliferating CHO cells resemble such a condition.

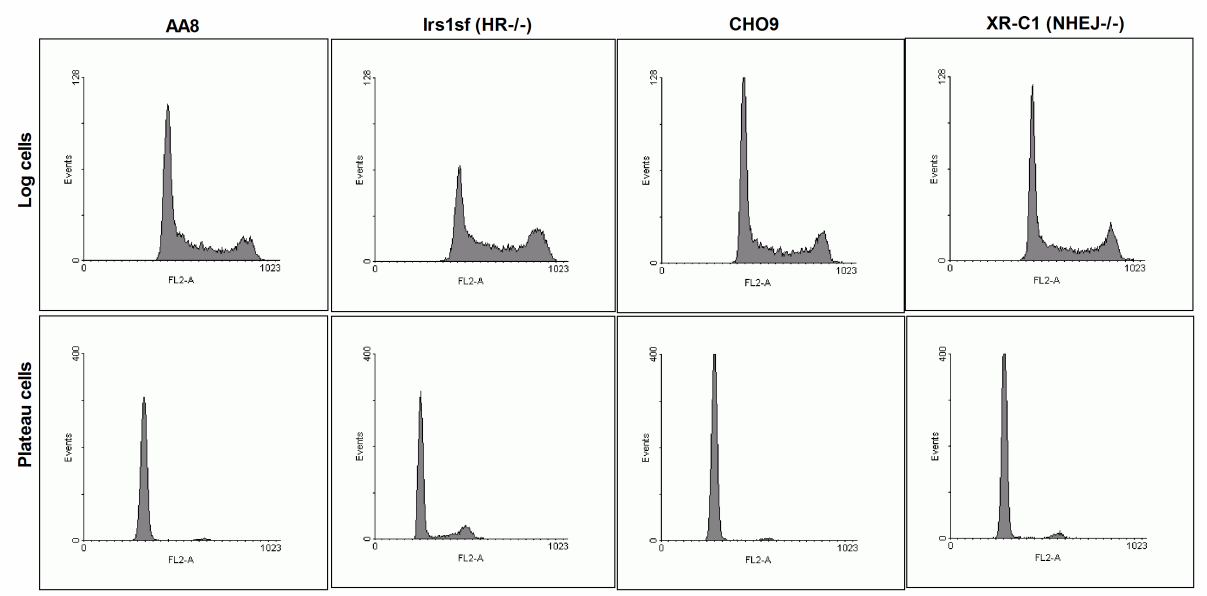

Figure 3.4 Cell cycle distributions at the time point of irradiation in proliferating and plateau phase, growth-arrested AA8 and CHO9-wild type and Irs1sf- and XR-C1-mutated CHO cell lines.

In AA8-CHO wild type cells irradiation with protons decreased cell survival by 1.1 ± 0.1 and 1.8 ± 0.2 fold at 2 and 5 Gy, respectively, when compared to photon irradiated cells (Fig. 3.5A). Similar results were obtained with a second CHO-wild type cell line (CHO9, Fig. 3.5B). The HR-corrupted daughter cell line Irs1sf, which lacks the RecA/Rad51-related protein family XRCC3, was more sensitive to both types of irradiation than the corresponding AA8-wild type cell line (Fig. 3.5A). In contrast to the proliferation results, the HR-deficient cells were also more proton-sensitive, but interestingly to a significantly much stronger extent than the wild type cells, especially at higher dosages (approx. 8 fold and 30 fold more sensitive than wild type in response to proton and photon irradiation, respectively, at 5Gy). The dose-modifying factor at 50% survival for wild type vs. HR-deficient cells after proton irradiation and photon irradiation was 3.44 and 2.66, respectively, which again demonstrated the specifically enhanced sensitivity of HR-deficient cells to proton irradiation.

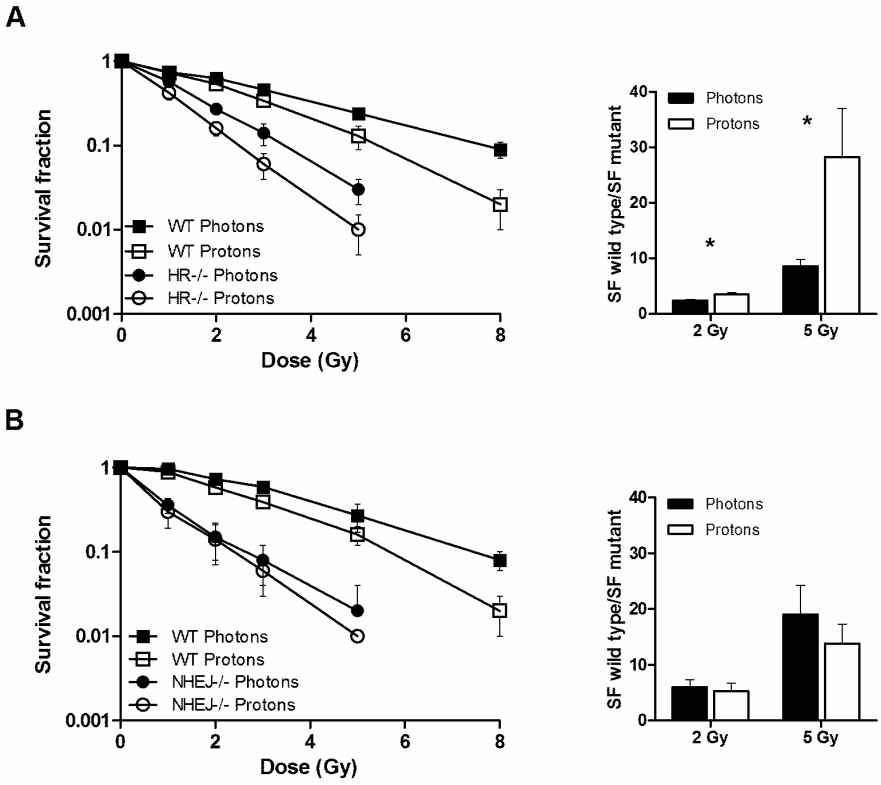

Figure 3.5 Clonogenic cell survival of proton and photon irradiated CHO cell lines. Cells were irradiated in exponential growth phase. Survival data and corresponding ratios of SFwild type/SFmutant are plotted. (A) AA8 wild type cells and corresponding HR-deficient Irs1sf (XRCC3-/-) cells; (B) CHO9 wild type cells and corresponding NHEJ-deficient XR-C1 (DNA-PKcs-/-) cells. Data points represent mean ± SD or bars represent mean ± SEM; n $\geq$ 3; *P<0.05.

The NHEJ-corrupted CHO cells (XR-C1, DNA-PKcs-/-), were even more sensitive than the HR-deficient cells to photon irradiation (CHO9) (Fig. 3.5B), and both the wild type mother cell line (CHO9) and NHEJ-deficient deficient daughter cell line were relatively more sensitive to proton irradiation. However, we could not detect an even further increased sensitivity towards proton irradiation in the NHEJ-deficient cell line compared to wild type cells as observed in the HR-deficient cells ($(SF_{wild\ type}/SF_{mutant})_{photon}$ vs. $(SF_{wild\ type}/SF_{mutant})_{proton}$). This is also shown in representative plates of a clonogenic assay performed with wild type and NHEJ-deficient cells (Fig. 3.6). The more pronounced proton radiosensitivity of HR-deficient cells compared to NHEJ-deficient cells is undermined by RBE-calculations at 10% survival level with a value of 1.44 for HR-deficient cells, whereas NHEJ-deficient cells revealed an even lower value than the wild type cells (1.09 and 1.25, respectively).

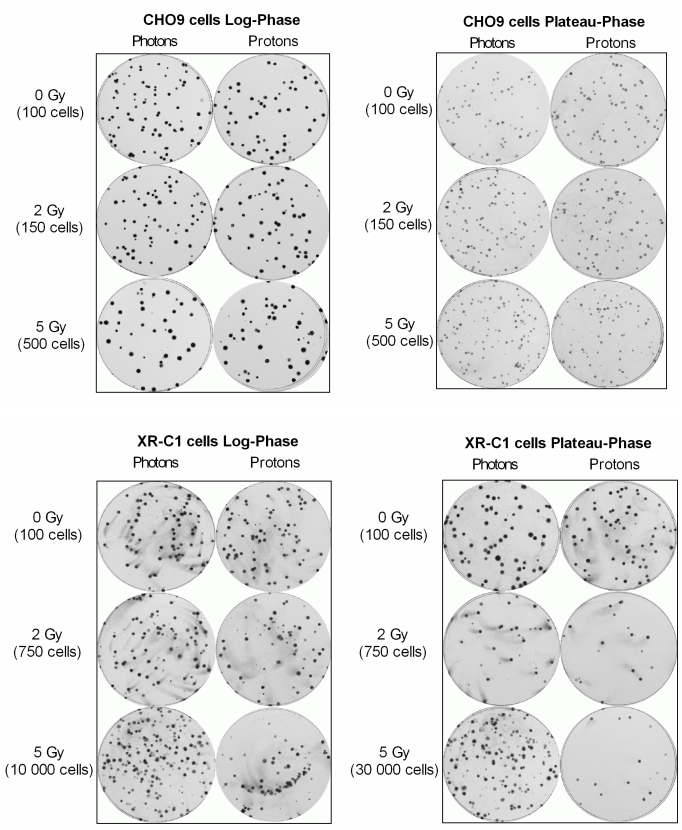

Figure 3.6 Representative pictures of surviving clones from clonogenic assays. Examples from logarithmically growing and growth-arrest survival assays with CHO9 wild type and corresponding NHEJ-deficient XR-C1 (DNA-PKcs-/-) cells, (Log=logarithmic).

3.1.4 Clonogenic survival of wild type and DSB repair mutant cell lines in plateau phase

Homologous recombination requires an intact sister chromatid and is therefore only active during S and G2 phase of the cell cycle (*328*). Thus confluent (plateau) cells, which are arrested in G0/G1-phase of the cell cycle, primarily depend on NHEJ for efficient DNA DSB repair. Wild type, HR-deficient, and NHEJ-deficient CHO cells were grown to confluency and clonogenic survival was determined in response to proton and photon irradiation (Fig. 3.4 cell cycle distribution of plateau-phase cells). Interestingly the differentially enhanced sensitivity of HR-deficient cells to proton irradiation was no longer observed, supporting a critical role of HR for proton irradiation but only in proliferating cells (Fig. 3.7A). Overall HR-deficient cells became more radioresistant. However, they did not reach wild type survival levels. NHEJ and potentially lethal damage repair (PLDR) can cope with more DNA damages in non-proliferating cells, but not all damages can be repaired so that HR-defective cells are still more radiosensitive than wild type cells. In wild type cells parts of the DSBs might be transferred to S phase and repaired with the help of HR.

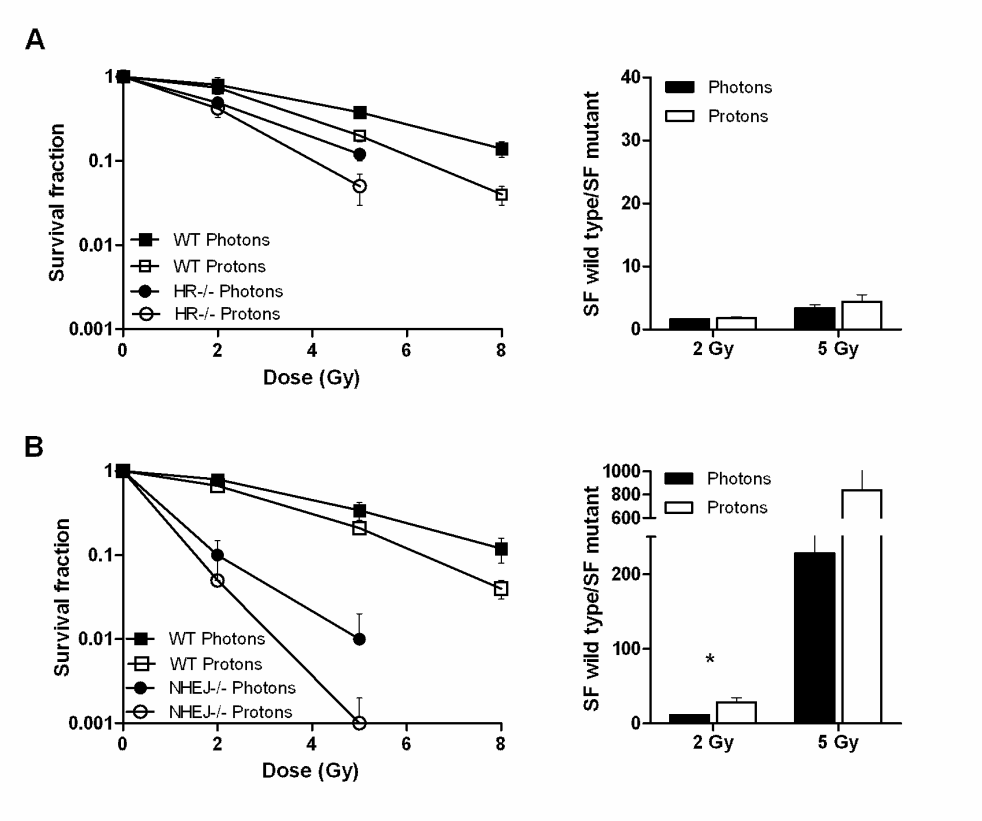

Figure 3.7 Clonogenic cell survival of proton and photon irradiated CHO cell lines. Cells were irradiated in plateau, growth-arrested phase. Survival data and corresponding ratios of SFwild type/SFmutant are plotted. (A) AA8 wild type cells and corresponding HR-deficient Irs1sf (XRCC3-/-) cells; (B) CHO9 wild type cells and corresponding NHEJ-deficient XR-C1 (DNA-PKcs-/-) cells. Data points represent mean ± SD or bars represent mean ± SEM; n $\geq$ 3; *P<0.05.

In contrast, as expected NHEJ-deficient XR-C1 cells were drastically more radiosensitive in plateau phase, as the main repair pathway of G1 phase is missing in those cells. They also became significantly more sensitive to proton irradiation in plateau phase (NHEJ cells showed a 11 fold and 28 fold increased sensitivity towards proton vs. photon irradiation when irradiated in logarithmic or growth arrested phase, respectively at 2 Gy; Fig. 3.5B+3.7B).

These experiments demonstrate increased sensitivity of HR-deficient cells to proton irradiation only when cells are proliferating in S and G2 phase and not in confluent/plateau phase cells. Plateau phase NHEJ-deficient cells were significantly hypersensitive to proton irradiation, indicating a requirement for NHEJ in repairing proton-induced DNA damage in this setting. However, one could also argue that perhaps via alternative repair pathways, part of the photon radiation-induced damage can be repaired in NHEJ-deficient plateau cells. In the case of proton-radiation exposure, the DNA damage might be more severe and alternative pathways cannot repair properly leading to this phenotype.

3.1.5 Single strand break repair and base excision repair mutant cell line

We have limited insight on the role of base excision and single strand break repair (BER and SSBR) after proton radiation exposure. In general it is assumed that 10^5 ionizations, > 1000 base damages, ~ 1000 single-strand breaks, and ~ 20-40 double-strand breaks are generated/cell after exposure to 1 Gy (*4*). Therefore, besides DSB repair, these two repair pathways are important for the survival of a cell after exposure to ionizing radiation (*109*). SSBR uses mainly the same enzyme system as BER. We performed experiments with a cell line that lacks XRCC1, which is involved in both pathways. By using this cell line the importance of both systems was tested together.

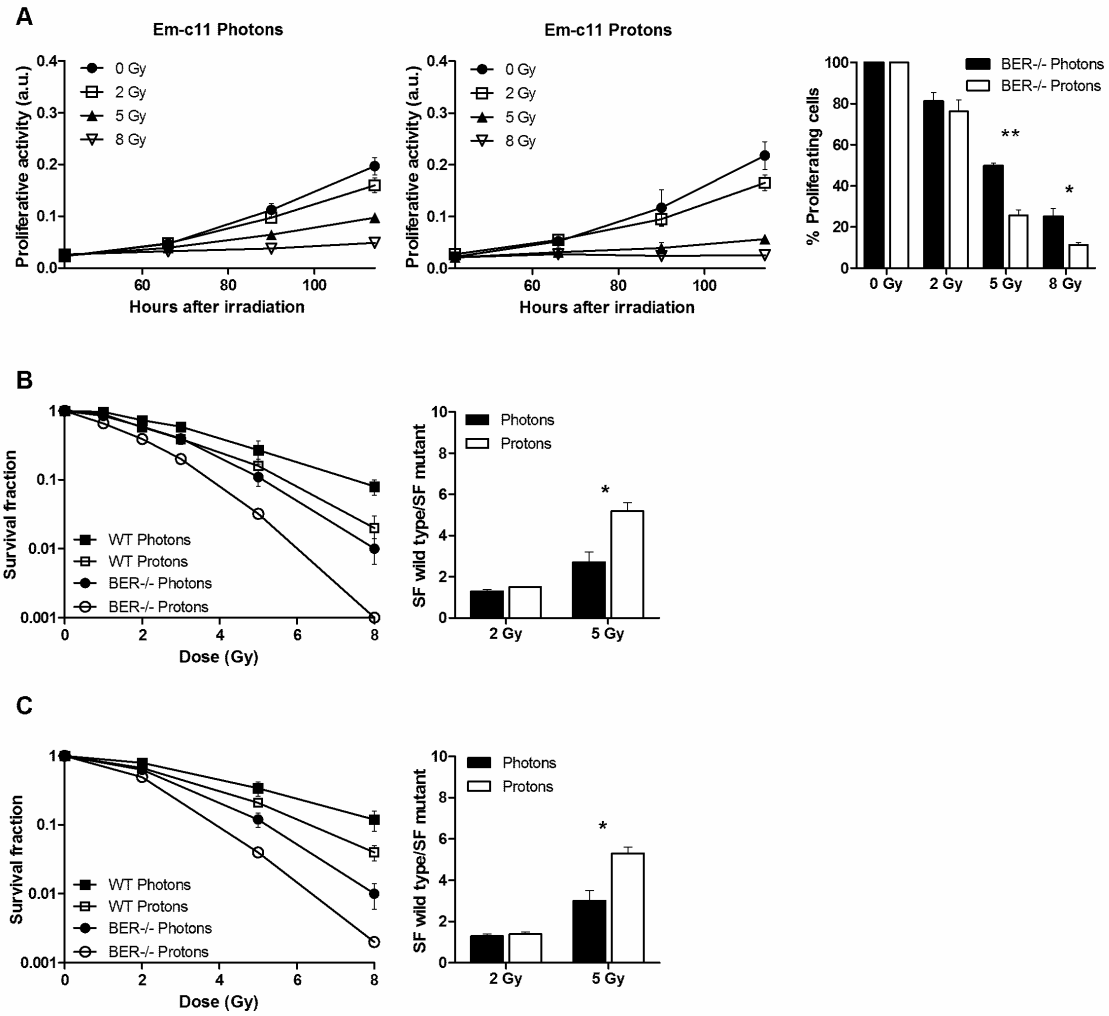

Figure 3.8 Response of BER-deficient Em-c11 cells (XRCC1-/-) to photon and proton irradiation. Cells were irradiated and (A) cell proliferation and (B, C) clonogenic cell survival (also for CHO9 wild type cells) was determined. In (A) proliferative activity at 66, 90, and 116 hours after irradiation and % proliferative activity relative to control after 116 hours are plotted. In (B) for exponentially growing and (C) for plateau, growth-arrested cells survival data and corresponding ratios of SFwild type/SFmutant are plotted. Data points represent mean ± SD or bars represent mean ± SEM; n ≥ 3; *P<0.05, **P<0.01.

Cell proliferation of Em-c11 (XRCC1-/-) was not significantly different between 2 Gy of photon vs. proton irradiation, but 5 and 8 Gy of proton irradiation inhibited cell proliferation significantly stronger in comparison to photon radiation exposure (Fig. 3.8A). On the level of clonogenic survival, XRCC1-mutant cells were 2.7 or 5.2 fold more sensitive compared to wild type cells (CHO9) after 5 Gy of photon or proton radiation, respectively, in logarithmic growth phase (Fig. 3.8B). Proton irradiation more efficiently induced cell death in these cells at higher doses. Upon irradiation in plateau phase the PLDR effect did not occur. XRCC1-deficient cells showed no increased radioresistance like HR-deficient and both wild type cells. Also plateau irradiated mutant cells were significantly more sensitive to proton irradiation than to photon irradiation (Fig. 3.8C). If cells are irradiated in growth-arrested phase, without proliferation stress and with more time to repair damages, does not help to increase cell survival in the case of a XRCC1-mutant cell. The repair of base damages and single strand breaks seems to depend on XRCC1, regardless of the cell cycle or growth stage.

In our hands XRCC1-deficient hamster cells are significantly more sensitive to proton than to photon irradiation at higher doses. Either more initial damages are produced by protons or more damage clusters are generated with increasing doses. If a SSB situated close to a DSB stays un-repaired, then the DSB repair machinery might have severe problems. Even though this experiment demonstrates that single strand breaks/base damages also play a role with regard to a differential sensitivity to proton vs. photon irradiation, we focused on DNA double strand break repair.

3.1.6 Initial amount of DNA double strand breaks

A reason for the better effectiveness of protons could be an increase in initial DNA DSBs after proton irradiation. Another possibility is that not more DSBs are induced but more complex ones. To be able to interpret the differential sensitivity on the level of clonogenic survival, the initial amount of DNA DSBs was determined via γH2AX and 53BP1-foci quantification.

Cells were irradiated with 1 Gy of protons or photons and fixed 12 minutes after irradiation. This time point was chosen, as in preliminary experiments much fewer γH2AX foci were visible in the wild type cells at 30 minutes than at 12 minutes. Partial repair was already completed 30 minutes after irradiation. Furthermore with 1 Gy almost no overlay of foci appeared and it was possible to count foci more accurately. γH2AX foci were quantified in AA8, CHO9, Irs1sf, and XR-C1 cells and showed no difference between the different cell lines and between both types of radiation (Fig. 3.9A). In a later experiment 53BP1 foci were stained. 53BP1 foci can be used as a marker for ongoing DSB repair and have been used by others as a surrogate marker for DSBs, as it is abundant at most of the breaks (*329*). The

maximal foci formation was reported to appear 30 minutes after irradiation (*224*). 30 minutes after 5 Gy the quantification of foci numbers exhibited as well no significant difference for both types of radiation (Fig. 3.9B). A dose of 5 Gy was used because the overall amount of 53BP1 foci was rather sparse in CHO cells. The maximal amount of 53BP1 foci at 30 min after 5 Gy was only about one third of the amount of γH2AX foci (AA8 cells: after 5 Gy 30 γH2AX foci vs. 11 53BP1 foci). γH2AX foci were also quantified 30 minutes after 5 Gy of either radiation type, which revealed no differences in AA8 wild type cells with regard to DSB induction.

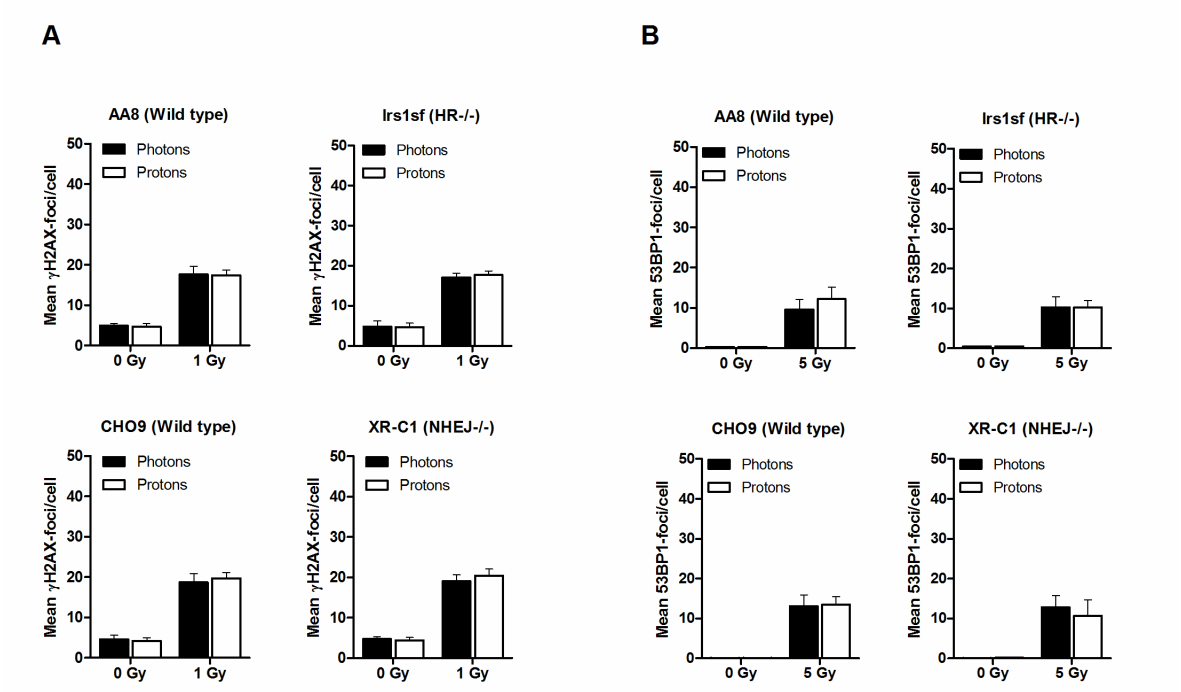

Figure 3.9 Quantification of the initial amount of foci in AA8- and CHO9 wild type and Irs1sf- and XR-C1-mutant cells. (A) γH2AX-foci 12 min after irradiation with 1 Gy (n=5). (B) 53BP1-foci 30 min after irradiation with 5Gy (n=3). Data is shown as mean ± SD.

The initial amount of DNA DSBs is equal, regardless of which type of radiation is used. This suggests that the lower survival rate after proton irradiation is not due an increase in initial DSBs.

3.1.7 Cell cycle distribution after photon and proton irradiation

Carbon and iron ions or low energy protons are densely ionizing particles, inducing a more pronounced G2 arrest (*330*). More severe clustered damage might lead to this prolonged arrest in G2 phase. Depending on the damage complexity and quantity, the duration of the G2 arrest can vary. Therefore we checked the cell cycle distribution at 6, 12, and 24 hours after 5 Gy of each type of radiation.

A G1 phase arrest was not detected in CHO cells. With propidium iodide stainings we solely observed a G2 arrest after low-LET proton irradiation (Fig. 3.10A+B). This was made visible through the relative increase in the amount of G2 phase cells when compared to non-irradiated samples (striped part in Fig.3.10A). The arrest was relatively mild. Only 40-55% of the wild type cells arrested in G2 after 6h after 5 Gy, which indicates further checkpoint defects. Cell cycle distributions of both wild type cell lines were back to control level 24 hours after irradiation, and no significant difference after proton and photon irradiation was

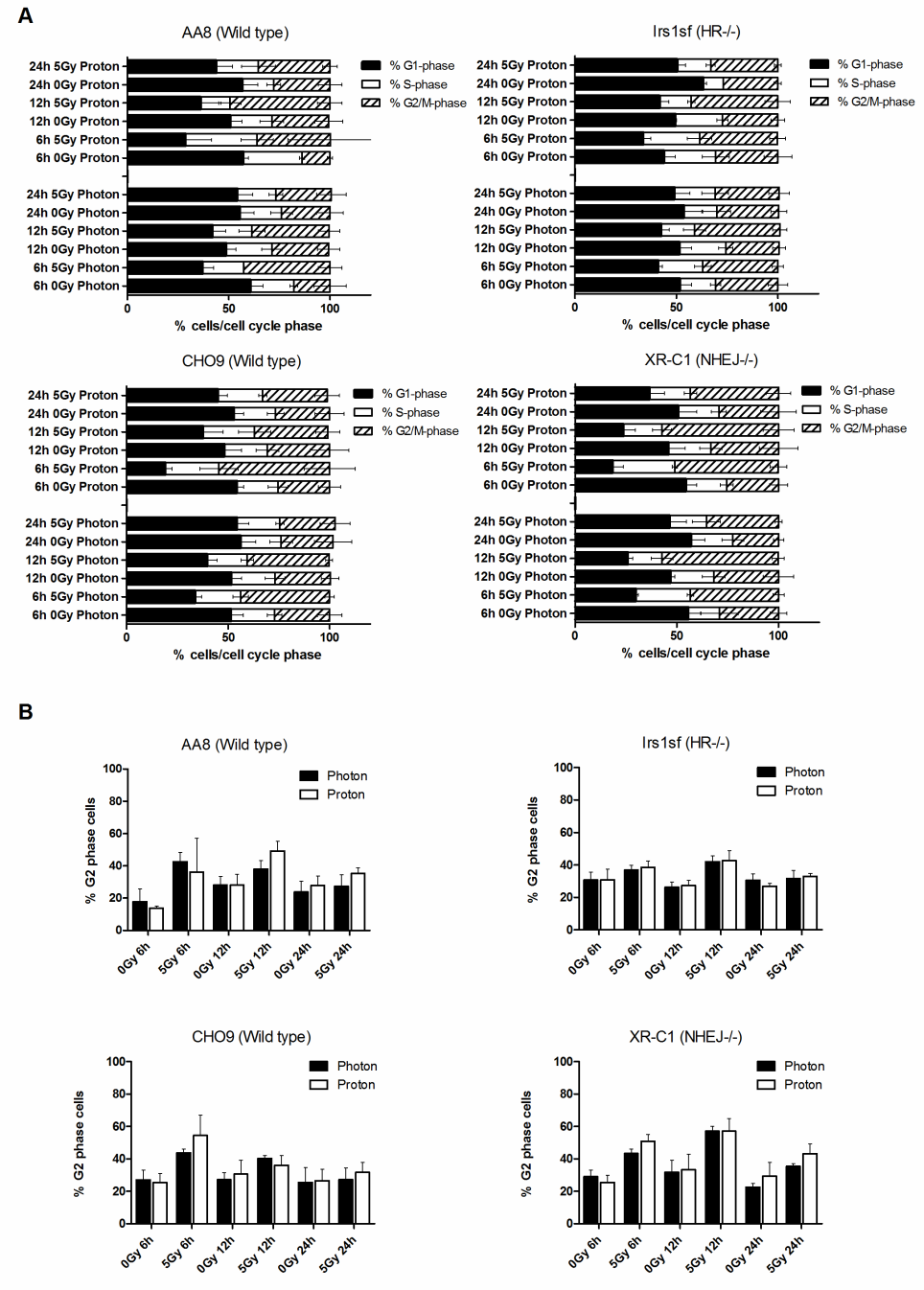

Figure 3.10 Cell cycle distributions of AA8- and CHO9-wild type and Irs1sf- and XR-C1-mutant cells at 6, 12, and 24 hours after irradiation with 5 Gy. (A) Percentage of cells in G1/S/G2-M-phase. (B) Percentage of cells in G2 phase. Data are shown as mean ± SD, n $\geq$ 3.

observed. A defective intra-S phase checkpoint has been reported for Irs1sf (XRCC3-/-) cells (*331*). In this case, cells progress through S phase even if they were irradiated because of the lack of proper checkpoint responses and might produce highly mis-repaired DNA-intermediates. Accordingly, 6 hours after irradiation no increase or decrease in the percentage of S phase cells was observed, which rather indicates a continued progression through S phase (Fig. 3.10A). Sole staining with propidium iodide is not sensitive enough. To differentiate between active or arrested S phase cells one would need to measure additionally the active incorporation of base analogues (e.g. BrdU). The G2 arrest in HR-/- cells was very mild, which indicates as well severe check point defects. We would expect for these cells to show a strong G2 arrest due to their repair defect. NHEJ-deficient cells exhibited the strongest G2 arrest with 60% of the cells in G2 phase at 12 hours after irradiation (Fig. 3.10B), and they still exhibit some arrested cells 24 hours after treatment. However, in the case of both repair defective cell lines and both wild type cell lines no significant difference in cell cycle distributions was detected with regard to which type of radiation was administered.

3.1.8 Clonogenic survival of XRCC3-complemented cells

The initial amount of DSBs is equal after both types of radiation. Therefore the increased radiosensitivity of XRCC3-deficient cells to proton irradiation is rather due to repair problems than to an increased initial DNA damage burden after proton in comparison to photon radiation. To verify our finding that HR-deficiency leads to increased proton radiosensitivity, we used a XRCC3-complemented cell line stably expressing the human wild type XRCC3 gene (*170*). The 1SFK8 transfectant is a clone selected for expression of XRCC3, which revealed substantial complementation to IR (60%) (*170*).

In this experiment AA8 wild type cells from M. Löbrich were used as control cells and the Irs1sf/1SFK8 cell pair from Larry H. Thompson was used to check the relationship of HR-deficiency and proton radiation sensitivity. For this second Irs1sf cell line, the increased sensitivity of XRCC3-deficient cells to protons was also demonstrated (Fig. 3.11A). Due to XRCC3 complementation, 1SFK8 cells showed an increased radioresistance compared to Irs1sf cells. But as shown by Yamada *et al.* they were not fully complemented, as they did not reach the survival level of AA8 wild type cells (Fig. 3.11B). At lower doses, 2 and 3 Gy, the higher sensitivity to proton radiation was no longer seen (1.8 fold and 3.6 fold more sensitive to proton vs. photon irradiation, for 1SFK8 and Irs1sf, respectively at 2 Gy). At 5 Gy the complemented cells were more sensitive to proton than to photon radiation. However, the increased sensitivity to proton radiation was less pronounced than in the case of Irs1sf cells.

Complementation with the human XRCC3 gene renders the Irs1sf cells only 60% more radioresistant. It seems that the accurate activity of XRCC3 requires a fine expression balance where a very high or very low level of XRCC3 did not complement certain sensitivities (*170*). Reasons for incomplete complementation might be a loss of

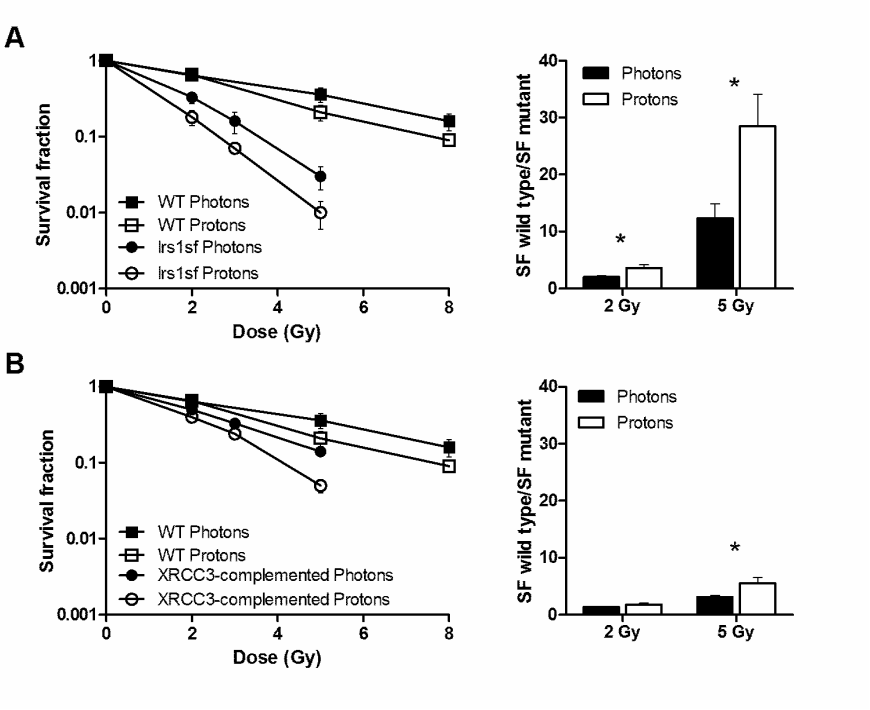

Figure 3.11 Clonogenic cell survival of proton and photon irradiated CHO cell lines. Cells were irradiated in exponential growth phase. Survival data and corresponding ratios of SFwild type/SFmutant are plotted. (A) AA8 wild type cells and corresponding HR-deficient Irs1sf (XRCC3-/-) cells; (B) AA8 wild type cells and corresponding XRCC3-complemented 1SFK8 (XRCC3+/+) cells. Data points represent mean ± SD or bars represent mean ± SEM; n ≥ 3; *P<0.05.

the expression vector in some cells or the unphysiologic XRCC3 expression levels in different cells leading to differential responses. Therefore we might reveal at high doses (5 Gy) for 1SFK8 cells an increased sensitivity towards proton radiation. However, the sensitivity towards proton radiation was lower than in the case of Irs1sf cells. In general we could demonstrate that XRCC3 complementation reduced the increased proton radiosensitivity of Irs1sf cells, which is another proof that the lack of XRCC3 and consequently of HR leads to the superior sensitivity towards proton versus photon irradiation.

3.1.9 Clonogenic survival of Rad51-silenced wild type cells

A third approach to detect the specificity of the HR-defect and increased sensitivity to proton radiation was by down-regulating an important HR-protein in AA8 wild type cells. As the CHO mutants are generated by chemical mutagenesis, they harbour often other mutations beside the described one (*324*). If other mutations beside XRCC3-deficiency were the reason for the increased sensitivity to proton exposure, the effect would not be detected in HR-silenced

AA8 cells or would be mild. Unfortunately the whole genome of the Chinese hamster (*C. griseus*) has not been sequenced so far, and there is no information on the mRNA sequence of *XRCC3*. It was not possible to design a specific siRNA against hamster *XRCC3*. As a substitute Rad51, the major and essential strand transferase for HR, was chosen (*138*). Two different specific siRNAs against *Rad51* were used.

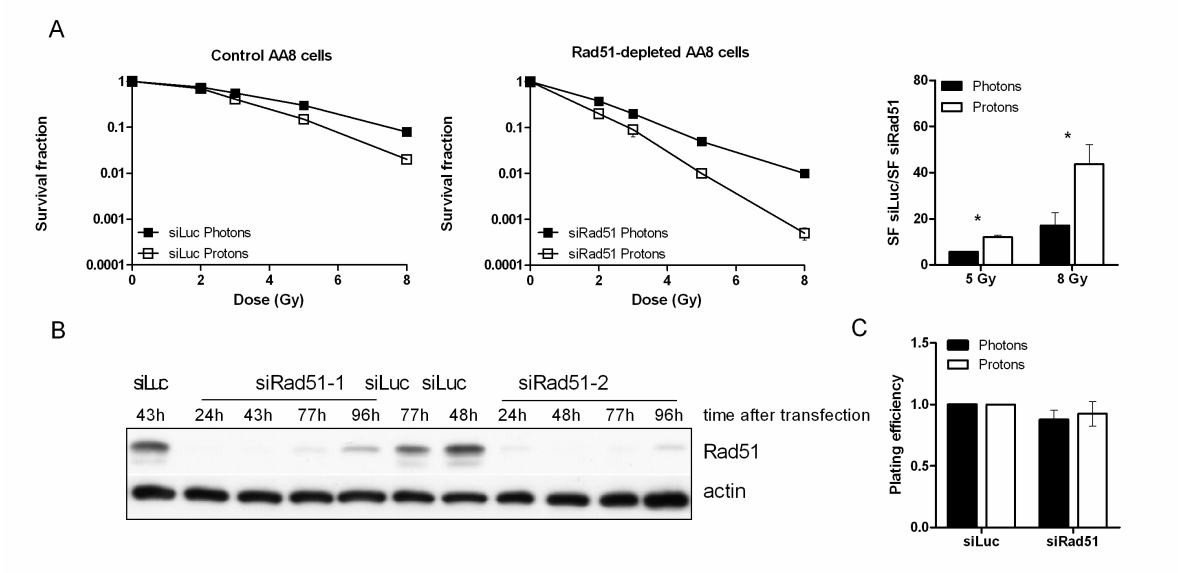

Figure 3.12 Clonogenic survival of AA8 wild type cells. Cells were irradiated in exponential growth phase. Survival data and corresponding ratios of SFwildtype/SFmutant are plotted. (A) Survival of AA8 wild type cells treated with siLuc and siRad51. (B) Down-regulation of the Rad51 protein level validated by western blot. (C) Plating efficiency of siLuc and siRad51-treated control cells. In (A) and (C) siRad51-1 and siRad51-2 data were pooled. Data points represent mean ± SD or bars represent mean ± SEM, n = 2, *P<0.05.

Down-regulation of Rad51 was detectable up to 96 hours after transfection (Fig. 3.12B). Hence Rad51 was silenced for at least another two days after radiation exposure, which was sufficient to result in a strong decrease in clonogenic survival (6 fold at 5 Gy of photons, Fig. 3.12A). Two different siRNAs were used separately during the same experiments, and data were pooled for analysis. Both resulted exactly in the same survival levels. Rad51 depleted cells showed also superior sensitivity towards proton exposure in comparison to siLuciferase treated control cells (Fig. 3.12A). Surprisingly plating efficiency was not strongly reduced (90%; Fig. 3.12C) in siRad51-treated AA8 cells, in contrast to the Irs1sf mutant cells (~55%).
The data demonstrate that Rad51 is highly needed for efficient cell survival during the first 48 hours after radiation exposure in proliferating cells. During this time period HR is essential to repair parts of the DSBs after both photon and proton radiation exposure. In HR-deficient cells, other repair pathways will most probably try to repair the damage, and grossly mis-repaired or non-repaired damage will lead to cell death. This cannot be compensated by the re-expression of Rad51 at later time points. Furthermore, cells lacking Rad51 are significantly more sensitive to proton exposure than to photon exposure, demonstrating another time the importance of HR in proliferating proton exposed cells.

3.1.10 DNA repair kinetics

Irradiation of CHO cells with protons leads to a significantly stronger cell killing compared to photon irradiation at equal doses of each radiation type. Furthermore we observed that HR-deficient cells are much more sensitive to proton irradiation than the corresponding wild type cells or complemented cells. Quantification of the initial amount of γH2AX foci and 53BP1 foci exhibited equal initial amounts of DNA DSBs. Furthermore proton as well as photon irradiated cells revealed equal percentages of cells arrested in G2 phase. These results point to more complex DNA damage generation by proton exposure, which is most probably more difficult to repair. To detect possible repair problems due to a different damage complexity after proton exposure, we followed the induction and removal of DNA repair foci. DNA repair proteins are recruited to the DNA damage site or proteins at the damage site are modified, which appear as discrete foci in immunofluorescence microscopy. Differential repair kinetics can reveal problems of a certain pathway to repair the induced DNA damages. In the following sections, the kinetics of different DNA repair pathways were analyzed. We decided not to compare equipotent doses with regards to cell killing but equal physical doses, which induced the same amount of γH2AX foci and consequently the same amount of DSBs. Our assumption is that with equipotent doses the initial amount of γH2AX foci and thus DSBs would be completely different. Different amounts of DSBs can induce differentially strong stress responses, making it difficult to compare different conditions (*332*).

3.1.10.1 γH2AX repair kinetics

Hundreds to thousands of H2AX molecules become rapidly phosphorylated by the three kinases, ATM, ATR, and pDNA-PKcs at each nascent DNA DSB (*98*). Phosphorylated H2AX, named γH2AX, is used as a marker for DNA damage, especially for DSBs. γH2AX foci disappearance is a marker for general progression of DSB repair (*333*). Long lasting γH2AX foci stand for damage sites that are difficult to repair or that are not repaired at all (*334*). If proton radiation produces a severely more complex DNA damage, the removal of γH2AX foci could be hampered.

Removal of γH2AX foci was determined over 24 hours in the different cell lines in response to 1 Gy of ionizing radiation. Repair kinetics were similar in both wild type cell lines in response to proton and photon irradiation. Over 50% of γH2AX foci were removed in an initial fast repair phase of 3 hours (Fig. 3.13). γH2AX foci removal was delayed in both mutant cell lines, with only 20 – 30% of γH2AX foci reduction during this initial time period. Delayed disappearance of γH2AX foci was only prominent in the HR-deficient cells in response to proton-irradiation (80% vs. 70% residual γH2AX-foci at the 3h time point in response to proton vs. photon irradiation). The amount of residual γH2AX foci 24 hours after

irradiation was also highest in the HR-corrupted cell line in response to proton-irradiation (45% vs. 27% residual γH2AX foci after proton vs. photon irradiation, respectively) (Fig. 3.13). Cell cycle analysis at 6, 12 and 24 h after irradiation displayed no difference in cell cycle distribution for the HR-mutated cells in response to 5 Gy of the two types of radiation (Fig. 3.10). Using a low dose of 1 Gy excludes that cell cycle differences are the cause for this finding.

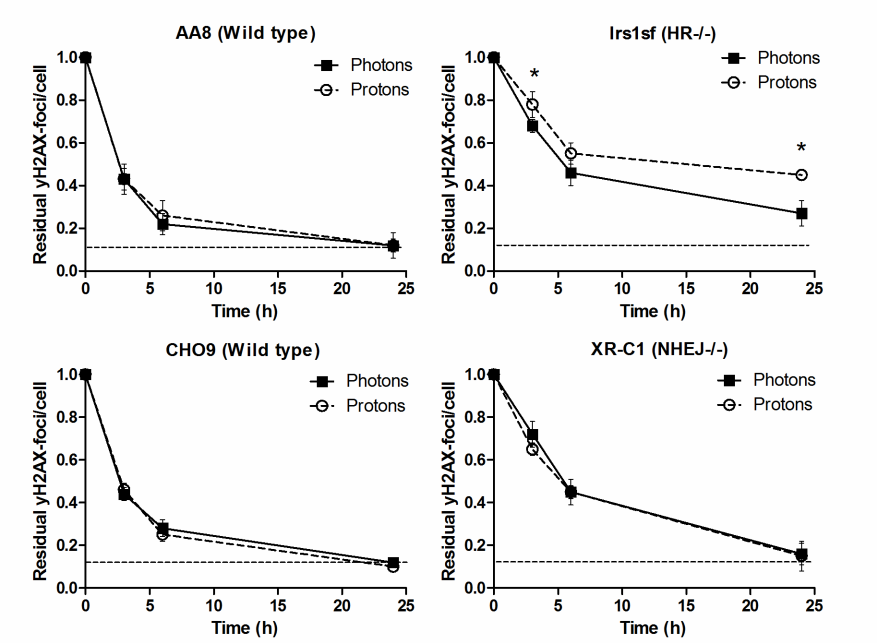

Figure 3.13 Quantification of residual γH2AX foci 3, 6, and 24 hours after proton and photon irradiation with 1 Gy in AA8- and CHO9- wild type and Irs1sf- and XR-C1-mutated cells. Initial amount of foci is set as 1; the dotted line indicates the background level of γH2AX foci in not irradiated cells. Data points represent mean ± SEM; n = 3; *P<0.05.

In a later experiment, HR-deficient cells and wild type cells were irradiated with 5 Gy. Thirty minutes after irradiation of the wild type cells, the initial amount of γH2AX foci was also equal for both types of radiation (Fig 3.14A). Foci disappeared with the same kinetics when compared to the 1 Gy results and were not different between the two types of radiation. XRCC3-deficient cells revealed significantly more residual foci vs. the wild type cells at 3, 6, and 12 hours for both types of IR (Fig. 3.14B), and at this high dose proton-generated residual γH2AX foci became only significantly different 12 hours after irradiation from photon irradiated samples. This can be seen in the microscopy pictures (Fig. 3.14D). These results on the level of residual γH2AX foci correlate with enhanced sensitivity of HR-mutated cells to proton-based irradiation.

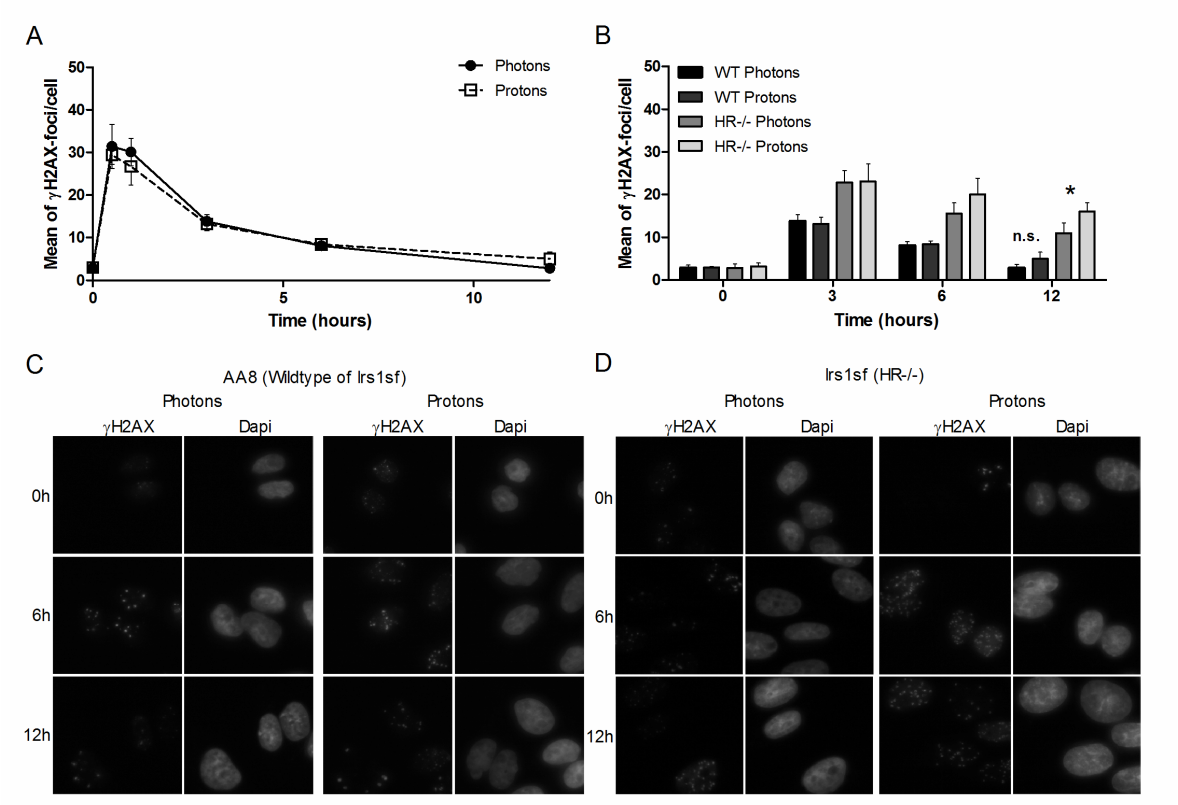

Figure 3.14 Quantification of initial and residual γH2AX foci 0.5, 1, 3, 6, 12, and 24 hours after proton and photon irradiation with 5 Gy. (A) Kinetic of γH2AX foci formation and disappearance in AA8 wild type cells. (B) γH2AX foci amount in AA8 wild type and HR-deficient Irs1sf (XRCC3-/-) cells. Representative immunofluorescence pictures of (C) AA8 wild type and (D) HR-deficient cells with γH2AX-foci and Dapi-stained nuclei 6h and 12h after irradiation (5 Gy). Data points represent mean ± SEM. n=3; *P=0.05.

Comparing the kinetics of γH2AX foci disappearance in NHEJ-mutated and wild type counterpart cells, overall DNA damage repair in NHEJ-mutated cells was also delayed, but no difference in the repair kinetics in response to the two types of irradiation was observed (Fig. 3.13). The low level of residual γH2AX foci at 24 hours in these otherwise highly radiosensitive cells is due to the fact that γH2AX foci could only be counted in cells with intact nuclei, but nuclear cell death-related fragmentation in these cells already started prior to the 24 hour time point.

γH2AX repair kinetics are equal after both types of radiation in wild type cells, indicating that the repair does not seem to be more hampered in the proton-irradiated wild type cells. NHEJ-deficient cells also showed equal but slower repair kinetics after both types of IR. In contrast, HR-deficient cells revealed significantly slower repair kinetics after 1 Gy of proton radiation vs. photon radiation. After 5 Gy photon irradiated samples also showed a longer foci half life, indicating the huge damage burden after higher doses. However, 12 hours after 5 Gy, HR-deficient cells showed more residual foci in the proton vs. photon irradiated samples. This slower γH2AX foci removal or more prominent residual amount of DSBs at 12 hours after

proton irradiation correlates with the enhanced sensitivity of HR-mutated cells to proton-based irradiation.

3.1.10.2 Rad51 foci repair kinetics

So far we demonstrated that HR-defective cells have more problems to repair proton-generated DSBs. In the wild type setting it is not possible to rule out whether certain repair pathways have more problems to repair proton-induced DNA damages. To have a closer look on specific repair pathways, we probed for the following different DNA repair proteins/mediators: Rad51, 53BP1, and pDNA-PKcs. The dose of 5 Gy was chosen due to the strong effect seen in the clonogenic assay. Furthermore the actual amount of Rad51 foci was very low at lower doses like 1 Gy and almost impossible to count.

The Rad51 protein is required for strand invasion during homologous recombination (*335*). The differences in clonogenic survival and γH2AX repair kinetics point to the importance of HR to repair a fraction of proton-induced DSBs. Therefore the kinetics of this repair pathway was followed, which might show more induced Rad51 foci after proton exposure.

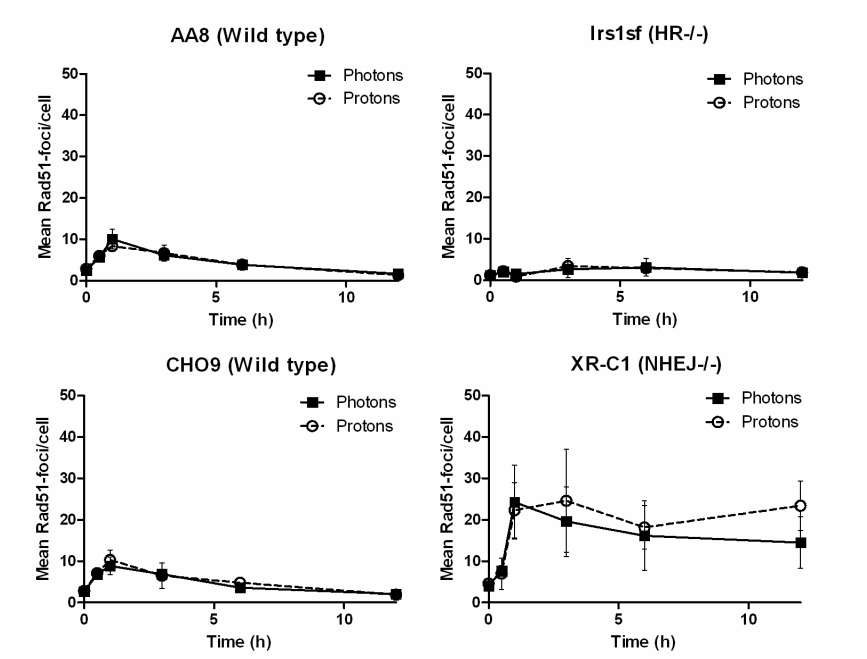

Figure 3.15 Quantification of initial and residual Rad51 foci 0, 0.5, 1, 3, 6, and 12 hours after proton and photon irradiation with 5 Gy in AA8- and CHO9- wild type and Irs1sf- and XR-C1-mutated cells. Data points represent mean ± SEM; n = 3; *P<0.05.

The amount of ionizing radiation-induced Rad51-foci was highest in both wild type cell lines 1 hour following irradiation and returned to basal levels 10 hours following both types of irradiation (Fig. 3.15). In the XRCC3-mutated HR-corrupted Irsf1sf cell line, a slight increase of Rad51-foci at 3 and 6 hours after irradiation was observed in response to both types of

irradiation, indicating that lack of the Rad51-downstream resolvase XRCC3 also affects correct Rad51-foci formation, as also observed by others (*164, 173*). Interestingly the amount of Rad51-foci formed in the NHEJ-corrupted cells in response to both types of irradiation almost tripled in comparison to the amount of Rad51 foci induced in wild type cells, demonstrating compensation for the lack of the competitive NHEJ-DNA-repair machinery in these cells (Fig. 3.15) (*336*). Of note the amount of Rad51 foci remained high for a much longer time period in these cells, indicating a very slow HR-dependent DSB repair capacity in the absence of NHEJ. The amount of cells with over 20 Rad51 foci was significantly higher in the NHEJ-mutant cells compared to the wild type cells at all time points (Fig.3.15). Pictures of nuclei with Rad51 foci illustrate as well the tremendous increase of Rad51 foci in NHEJ-mutant cells compared to wild type cells (Fig. 3.16). The size of early formed Rad51 foci was small at 0.5 and 1 hour after treatment, whereas Rad51 foci at 6 and 12 hours after irradiation increased to 4 times the size of the early ones, indicating extensive resection and therefore foci growth in NHEJ-mutant cells (Fig. 3.16).

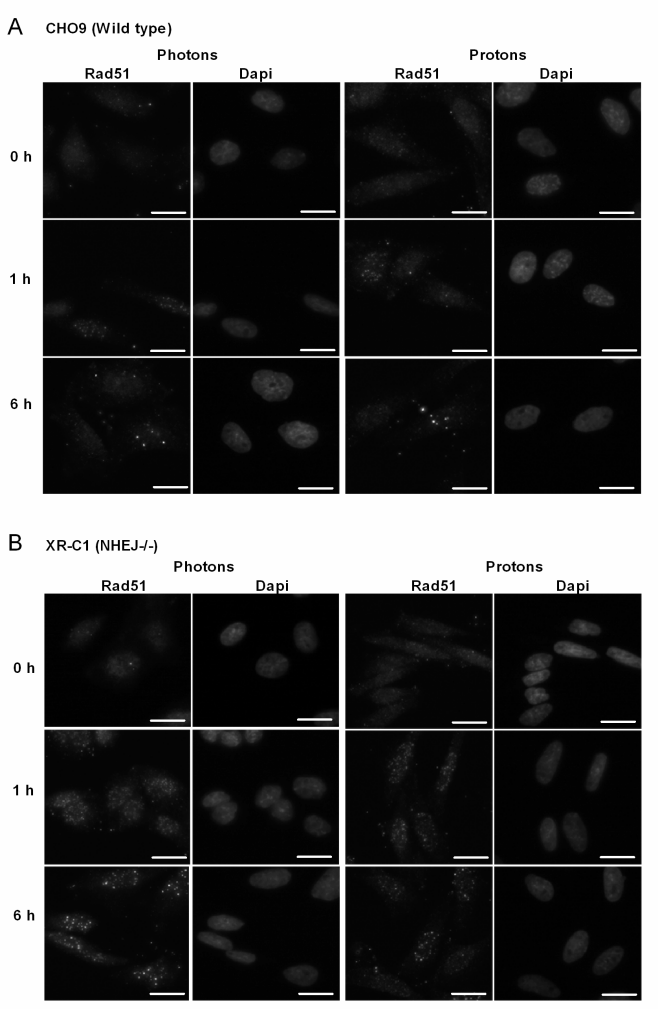

Figure 3.16 Representative immunofluorescence pictures for Rad51 foci formation in (A) CHO9 wild type cells and (B) NHEJ-deficient XR-C1 (DNA-PKcs-/-) cells 0, 1, and 6 hours after photon and proton irradiation with 5 Gy. Cells were stained for Rad51 and Dapi indicates nuclei. Scale bar represents 10 µm.

In the case of wild type cells where all DSB repair pathways are intact, we revealed no difference in Rad51 foci kinetics following either type of radiation. Even though NHEJ-deficient cells displayed overall more Rad51 foci, also no significant difference between the two radiation types could be detected.

3.1.10.3 p53-binding protein 1 foci repair kinetics

53BP1 is involved in DNA DSB repair and promotes ATM-dependent repair of DSBs located in heterochromatic areas (*227*). 53BP1 colocalizes with Mre11/NBS and γH2AX foci, but its foci formation after exposure to IR is not dependent on ATM, NBS or wild type p53 (*224*). Several groups demonstrated that the maximal amount of 53BP1-foci is reached 30 minutes after irradiation (*224*). Furthermore it is in general believed that 53BP1 as a mediator for DSB repair is not involved in HR repair but supports NHEJ by suppressing ATM-dependent processing of broken DNA ends for HR in BRCA1-deficient cells (*230*).

For both wild type cell lines and the HR-mutant cell line, maximal 53BP1-foci formation was detected 30 minutes after exposure. The kinetics of 53BP1 foci disappearance were equal for both types of radiation and back to control levels after 12 hours in the wild type cells (Fig 3.17). This is also the case for the HR-mutant cell line, which shows only a slight delay in foci removal after 6h. 53BP1-dependent repair seems to have no problems with proton-generated DNA damage and proceeds with the same speed in these cell lines. In all three cell lines the amount of 53BP1-positive cells (>1 53BP1-focus/cell) stayed high at ~ 90% until 6 hours after exposure to IR but decreased to 30-40% at 12 hours (Fig. 3.18). NHEJ-mutant cells exhibited a delayed maximal of 53BP1 foci formation appearing at 3h after proton irradiation, which was significantly different from the photon irradiated time course (max at 1h; $p<0.05$) (Fig. 3.17). Overall 53BP1 stayed much longer at damage sites in the NHEJ-mutant cells and showed still >10 foci/cell at 12 hours after irradiation with over 80% 53BP1 foci positive cells (Fig. 3.17 + 3.18). This cell line had a stronger and prolonged G2 arrest than the other three cell lines, which might correlate with this finding. 53BP1 is involved as a mediator for NHEJ in G2 phase DSB repair but not in Rad51-dependent repair (53BP1 and Rad51-foci did not colocalize, data not shown) (*230*).

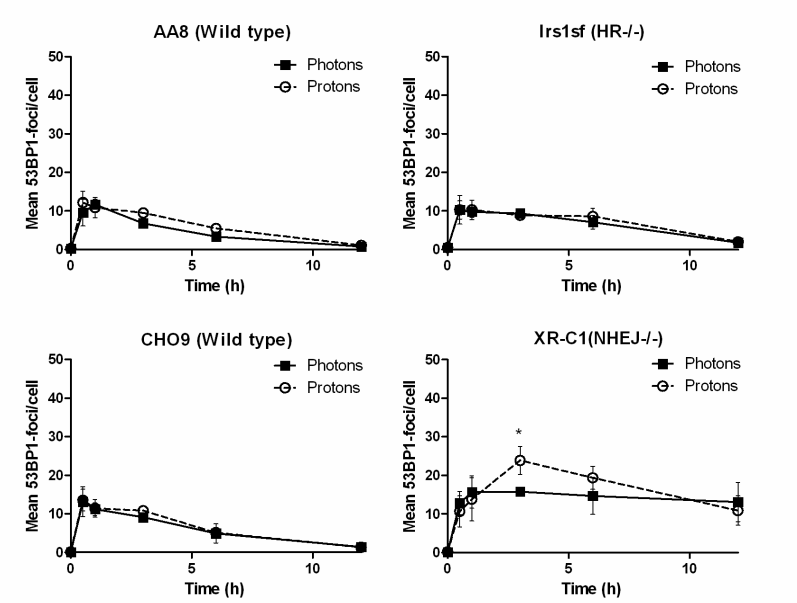

Figure 3.17 Quantification of initial and residual 53BP1 foci 0, 0.5, 1, 3, 6, and 12 hours after proton and photon irradiation with 5 Gy in AA8- and CHO9- wild type and Irs1sf- and XR-C1-mutated cells. Data points represent mean ± SEM; n = 3; *P<0.05.

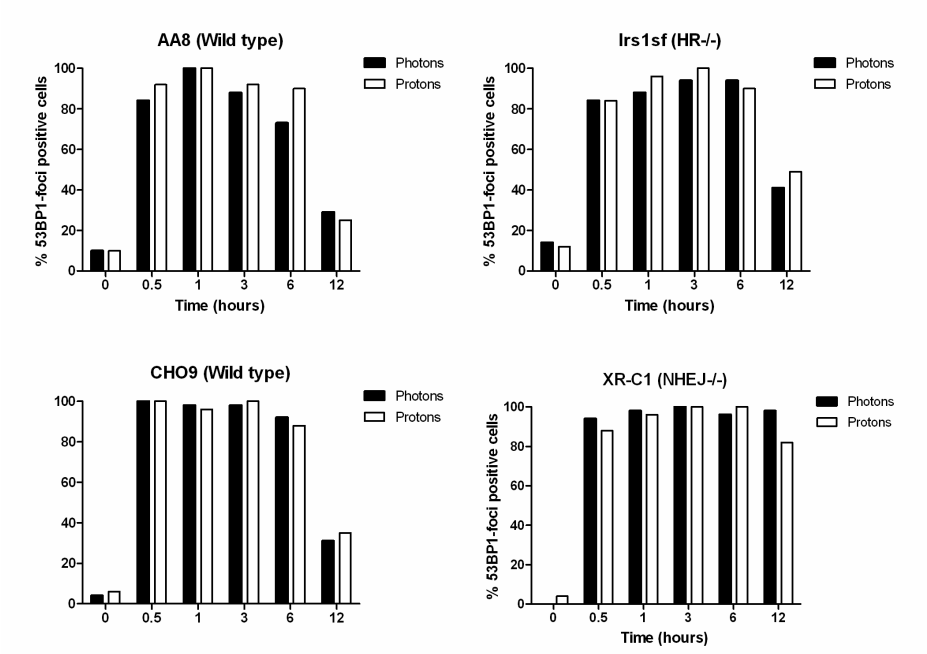

Figure 3.18 Amount of 53BP1 foci positive cells 0, 0.5, 1, 3, 6, and 12 hours after proton and photon irradiation with 5 Gy in AA8- and CHO9-wild type and Irs1sf- and XR-C1-mutant cells. Cells with more than 1 53BP1 focus were counted as positive. Representative values of one experiment.

53BP1 foci formation and disappearance is the same in both wild type cells and HR-deficient cells, regardless which type of radiation is used. But formation is significantly different in NHEJ-deficient cells between the two types of IR, and foci removal is significantly slower when compared to the other 3 cell lines. 53BP1 appears to be an important mediator protein for DSB repair in DNA-PKcs-deficient cells.

3.1.10.4 Phospho-DNA-Pkcs foci repair kinetics

A additional marker to probe NHEJ at the damage site is to follow foci formation of phosphorylated DNA-PKcs (*337*). This analysis could only be performed for 2 cell lines, the HR-deficient and its corresponding wild type cell line. For heavy ion exposure it was reported that the classical NHEJ pathway has difficulties to cope with small fragmented DNA damages (*337*).

In the AA8-wild type cell line a maximum of foci was detected 1 h after irradiation in response to both types of irradiation but to a reduced level in proton-irradiated cells (P=0.04; Fig. 3.19A). Decay of pDNA-PKc foci was similar at the 3 h and 6 h time points and reached again basal levels at the 12 h time point. In the HR-mutated cell line a slight, but statistically not significant, increase in pDNA-PKcs foci was again observed in the photon irradiated cells 1 hour after irradiation. Of note the amount of pDNA-PKc foci remained at a high level for an extended time period in these HR-deficient cells and in response to both types of irradiation, which correlates with the overall delayed kinetics of γH2AX-foci removal in these cells after 5 Gy (see above Fig. 3.13).

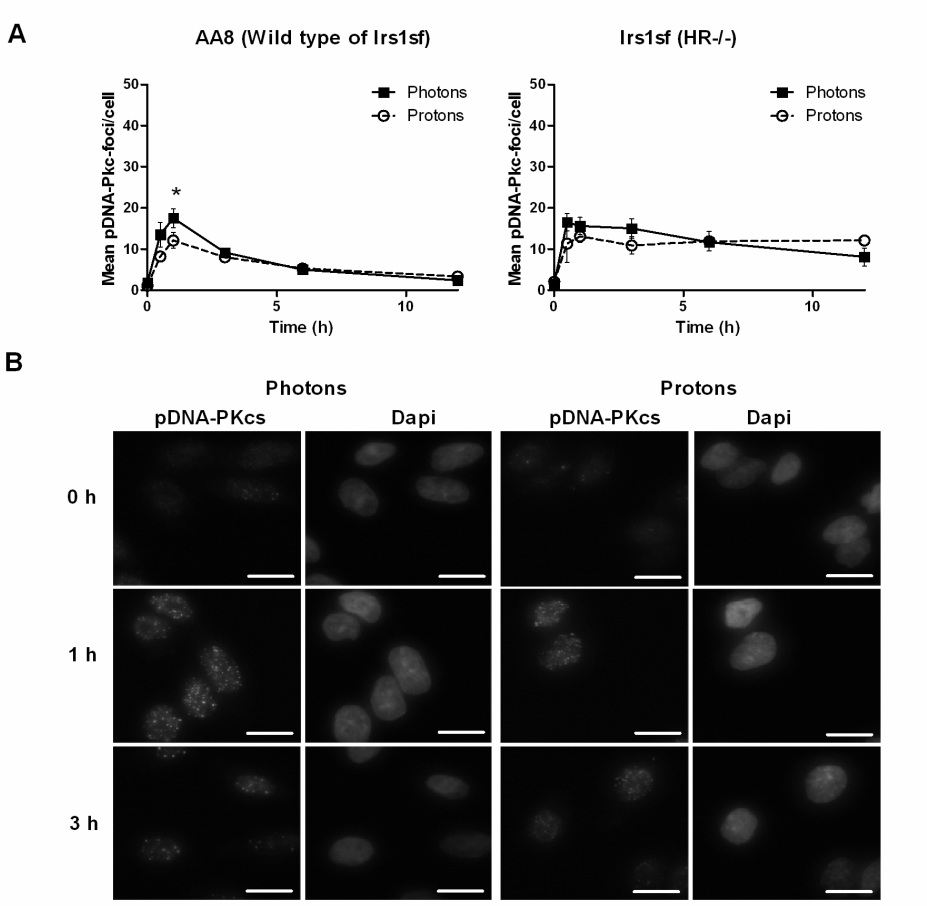

Figure 3.19 (A) Quantification of initial and residual pDNA-PKcs (S2056) foci 0, 0.5, 1, 3, 6, and 12 hours after proton and photon irradiation with 5 Gy in AA8-wild type and Irs1sf-mutated cells. Data points represent mean ± SEM; n = 3; *P<0.05. (B) Representative immunofluorescence pictures for pDNA-PKcs foci formation in AA8- wild type cells 0, 1, and 3 hours after photon and proton irradiation with 5 Gy. Cells were stained for pDNA-PKcs and Dapi indicates nuclei. Scale bar represents 10 µm.

In the wild type cells formation of pDNA-PKcs foci after irradiation with protons appears to be less efficient than after irradiation with photons. Foci removal was equal and back to normal levels after 12 hours. pDNA-PKcs dependent repair appears to have difficulties in the HR-defective cell line, as the amount of foci remains high until 12 hours after exposure.

3.1.11 DNA damage response after both types of radiation

We were interested to explore the overall DNA damage response after exposure to the two types of radiation. ATM is the primary mediator in the response to DSBs. Autophosphorylation of ATM at serine^{1981} occurs within seconds after exposure to ionizing radiation (*338*). Lysates at 15, 30, 60, 180, and 360 minutes after irradiation were analyzed (here we show only 30, 60, 180 min).

Analysis of ATM-phosphorylation in lysates derived from proton and photon irradiated wild type and HR-deficient cells revealed equal kinetics after 5 Gy (Fig. 3.20). ATM was still phosphorylated at 60 minutes after IR exposure. After 180 minutes the signal was already strongly decreased. Phosphorylation of downstream targets such as Chk1 and Chk2 could not be detected with commercially available anti-human antibodies. The appearance of Chk2 double bands was probed, which are due to hyperphosphorylation of the protein. The appearance of these Chk2 double bands was equal in response to both types of radiation with a maximal hyperphosphorylation at 180 min after irradiation (Fig. 3.20). However, in the HR-mutant cells the appearance and duration was less pronounced. Consequently, activation of the DNA damage response is equally fast after 5 Gy of either type of radiation. Unfortunately it was not possible to use an antibody specific for phosphorylation/activation of ATR, another important mediator of the DNA damage response (*96*).

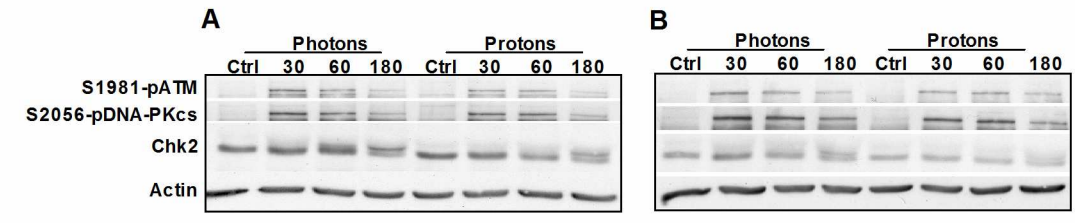

Figure 3.20 DNA damage response after photon and proton irradiation with 5 Gy. Western blot lysates were probed for different markers pATM, pDNA-PKcs, Chk2 and for actin as loading control. Lysates of (A) AA8 wild type and (B) HR-deficient Irs1sf (XRCC3-/-) cells were analyzed. Representative western blot of 3 experiments with each 3 blots.

DNA-PKcs is a PI3K related kinase, which promotes DNA repair by phosphorylation of key proteins. Autophosphorylation at serine^{2056} leads to kinase activation after exposure to ionizing radiation (*196*). The duration and intensity of this phosphorylation was equal after proton and photon irradiation in both cell lines (Fig. 3.20). This is in contrast to pDNA-PKcs-

foci formation, showing differential outcomes of overall phosphorylation status and the actual recruitment to active DNA repair loci (Fig. 3.20 + 3.19). Therefore it cannot be assumed that these two markers directly correlate with each other.

In summary, the overall DNA damage response is equal after exposure to either type of radiation for both wild type and HR-deficient cells.

3.1.12 Chromosomal aberrations

Besides the differential maxima detected for pDNA-PKcs foci formation, the other endpoints probed so far revealed equal repair kinetics after both types of radiation in the wild type cells. Out of these time course studies, it is not possible to conclude if the repair was erroneous or accurate. The proton efficacy on the level of clonogenic survival could be due to a higher percentage of mis-repaired DNA damage after proton irradiation exposure. Therefore both wild type cells were processed for the analysis of chromosomal aberrations. Metaphase spreads of logarithmically growing wild type cells were prepared 24 hours after irradiation with 5 Gy. At this time point, cells irradiated in G1 phase should be the main population in the fixed metaphase cell population. A certain percentage of cells irradiated in G2 phase, which already passed twice through mitosis, can also exist. Or cells irradiated in S phase, which arrested for ~22 hours in the following G2 phase, can be abundant. The abundance of cells with sister unions indicates that part of the cell population was irradiated in S and G2 phase. Sister unions form when both sister chromatids harbour a DSB, which are later mis-repaired. Dicentrics arise during G1 phase from double strand breaks in two different pre-replication chromosomes and are subsequently erroneously connected. Rings arise during G1 from two DSBs in the different arms of a pre-replication chromosome. In both cases, fragments are generated as well. During S phase this fragment is duplicated, showing two equally sized fragments close to each other, and the duplication of the chromosome with the 2 centromeres leads to the typical structure of a dicentric (Fig. 3.21C). Single fragments occur

Tabelle 3.1 Aberration frequency (± SEM)

		0 Gy Photon	5 Gy Photon	0 Gy Proton	5 Gy Proton
AA8	Fragments	0.013±0.008	0.997±0.251	0	1.151±0.713
	Dicentrics	0	0.110±0.056	0	0.357±0.149
	Rings	0	0.037±0.023	0	0.088±0.024
	Sister Unions	0	0.130±0.030	0	0.411±0.067
		0 Gy Photon	5 Gy Photon	0 Gy Proton	5 Gy Proton
CHO9	Fragments	0.007±0.008	0.639±0.202	0.040±0.000	1.270±0.310
	Dicentrics	0.013±0.008	0.113±0.021	0.007±0.008	0.147±0.014
	Rings	0	0.043±0.023	0	0.034±0.022
	Sister Unions	0	0.073±0.028	0	0.136±0.035

when a DSB generated in G2 phase is not repaired at all.

Quantification of fragments, dicentrics, rings and sister unions resulted in a 1.4 – 2.3 fold higher ratio of aberrations/cell after proton versus photon irradiation (Fig. 3.21B and Table 3.1). The increased amount of aberrations and breaks after proton irradiation was not only due to the higher percentage of cells possessing aberrations, as the fold increase determined solely in cells harbouring at least one aberration was still 1.7±0.3 for AA8 cells and 1.2±0.2 for CHO9 cells (data not shown). Tests comparing whole aberration induction result in a significant difference between proton and photon irradiated samples for both wild type cell lines (Mann-Whitney Test; $p<0.05$).

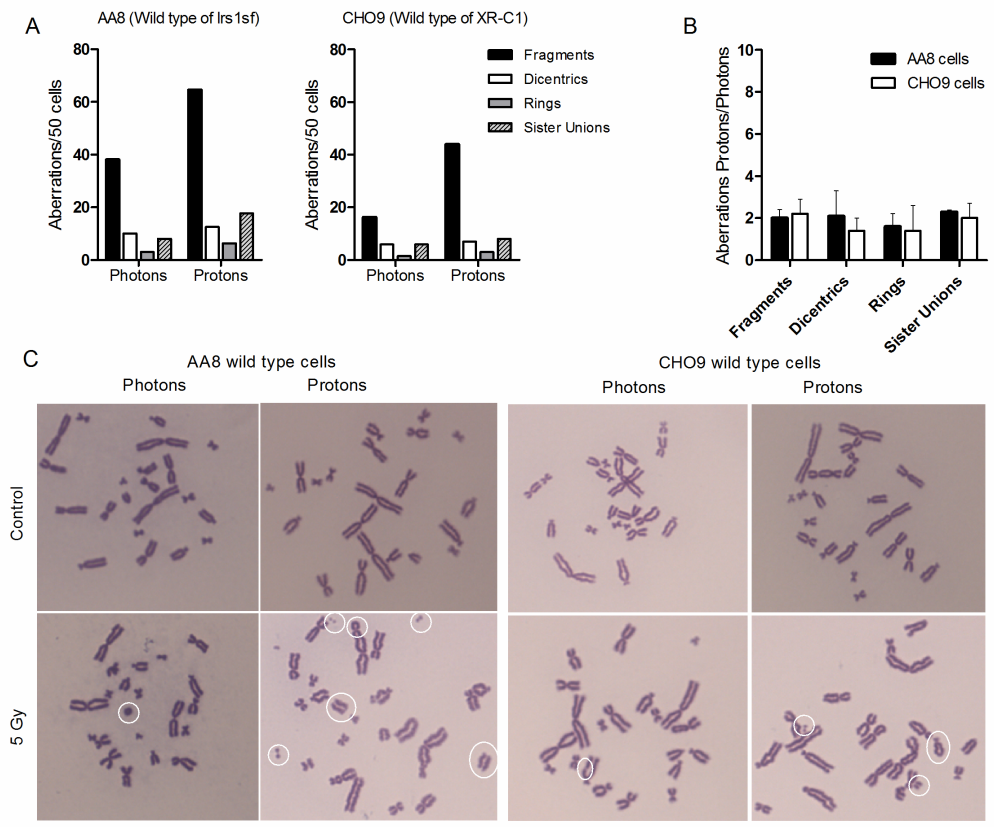

Figure 3.21 Quantification of different chromosome aberrations 24 hours after photon and proton irradiation with 5 Gy in AA8- and CHO9-wild type cells. (A) Total amount of fragments, dicentrics, rings, sister unions detected in 50 cells of a representative experiment. (B) Efficiency of proton-irradiation in aberration induction (ratio amount of aberration protons/amount of aberration photons). Data represent mean ± SD, n = 3. (C) Representative pictures of metaphase spreads for control and irradiated cells (aberrations indicated with white circles).

These results suggest that the accuracy of DNA repair in proton-irradiated cells is lower than in photon irradiated cells most probably due to more complex proton-induced DNA damage. Protons induced significantly more DNA fragments and lethal aberrations such as sister unions, which most probably lead to the better effectiveness (RBE = 1.1) of proton vs. photon irradiation.

3.1.13 Clonogenic survival of additional homologous recombination mutant cell lines

To confirm the significance of HR-deficiency and the increased sensitivity to proton vs. photon irradiation, two additional cell systems, which lack important proteins involved in HR repair, were probed for clonogenic survival in response to both types of irradiation. These two cell systems have been generated from hamster lung fibroblasts.

Rad51c is a Rad51 paralog, which forms complexes with XRCC3 and XRCC2 and is involved in HR repair (*339, 340*). A hamster mutant cell line deficient in Rad51c protein (CL-V4B cells) displayed a significantly higher sensitivity to proton radiation when compared to the corresponding wild type cells (V79B cells), at 3, 5 and 8 Gy (Fig. 3.22A). BRCA2 also plays an important role as mediator protein in homologous recombination. BRCA2 is required for the efficient formation of the Rad51 nucleofilaments (*127*). We therefore also tested a BRCA2-mutant cell pair. For this mutation significant differences were only detected at higher doses, 5 and 8 Gy (Fig. 3.22B). The plating efficiencies were not influenced by the experimental set up. For both wild type cells it was 100%, for Rad51c-mutants ~ 73% and for BRCA2-mutants ~ 50%.

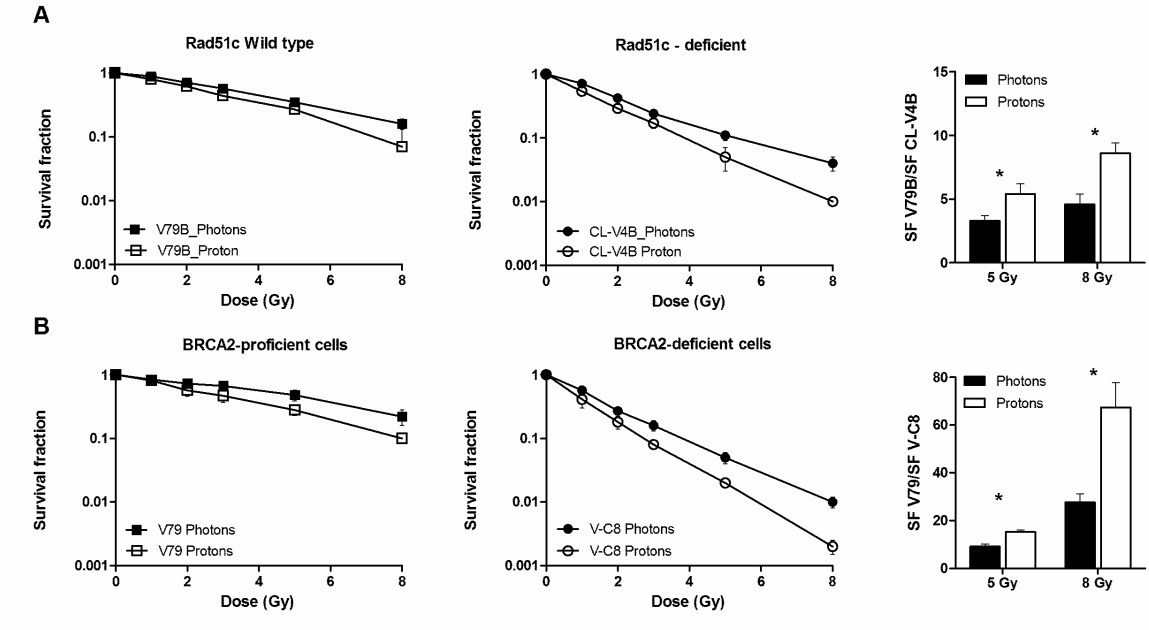

Figure 3.22 Clonogenic cell survival of proton and photon irradiated hamster lung fibroblasts. Cells were irradiated in exponential growth phase. Survival data and corresponding ratios of SFwild type/SFmutant are plotted. (A) V79B wild type cells and corresponding HR-deficient CL-V4B (Rad51c-/-) cells. (B) V79 wild type cells and corresponding HR-deficient V-C8 (BRCA2-/-) cells. Data points represent mean ± SD or bars represent mean ± SEM; n $\geq$ 4; *P<0.05.

As all tested HR-mutant/wild type systems revealed a significant increase in the proton radiosensitivity of HR-deficient cells, HR repair is probably more important for proton-induced DNA damages than for photon-induced ones. Rad51c-deficient and BRCA2-deficient cells

display this effect only at doses starting from 3 or 5 Gy, respectively. Most probably this is due because these two proteins are not essential but promote homologous recombination.

3.2 Human cell systems

For clinical relevance of the data we aimed to verify our finding that HR-deficiency leads to a higher sensitivity towards proton irradiation in a human cell system. Because HR is essential during normal proliferation, very few human cell systems lacking functional HR are available. Those HR-defective cells grow very slowly and have a very low plating efficiency. These points make it difficult to study HR-deficiency in a human system. However, a widely used model cell line for all different kinds of DNA repair studies is a human osteosarcoma cell line (U2OS). The cell line expresses wild type p53 and RB, but is deficient in p16. U2OS-cells are derived from the bone tissue of a fifteen-year-old human female and established in 1964 (by Ponten and Saksela). These cells are very robust, easily treated with different siRNAs, and form colonies within 14 days. Therefore they were used for a siRNA screen in our experiments.

BRCA2 mutations are found in human breast, ovarian, and prostate cancer patients (*176, 341, 342*). In the last decade BRCA2 related studies revealed its mediator function for efficient HR. Isolated patient tumour cells deficient in BRCA2-/- became a nice model to study HR defects. Capan-1 is a human pancreas adenocarcinoma cell line, which harbours loss of heterozygosity (LOH) in one BRCA2 allele and a truncated form of BRCA2 in the second allele. Fortunately these cells are able to grow into clones (*343*). BxPC-3 is often used as a control cell line together with Capan-1 cells. It is a well differentiated pancreatic adenocarcinoma cell line, which matches the mutation status of a number of tumour suppressor genes with Capan-1 cells. Neither of the cell lines contains functional p53, p16, or RB (*186*).

These two cell systems, U2OS and pancreas cells, were used in the second part of this study.

3.2.1 U2OS osteosarcoma cells

3.2.1.1 Clonogenic survival

In order to investigate the relevance of HR, NHEJ, and BER for the treatment response to proton irradiation in a human setting, U2OS cells were treated with different siRNAs against Rad51, XRCC3, XRCC4, and XRCC1. 48 hours after transfection proliferating cells were irradiated and plated for clonogenic survival assays a day later.

HSP70B was used as a target for control siRNA, as the HSP70B isotype is not expressed in these cells (*344*). The sensitivity of U2OS control cells towards proton irradiation (1.49±0.1 and 2.52±0.3 at 2 and 5 Gy; SFphoton/SFproton) was even higher than in CHO wild type cells (1.1±0.1 and 1.8±0.2 at 2 and 5 Gy; SFphoton/SFproton). Plating efficiency (PE) was 60% for all siRNA treatments apart from treatment with siRad51, which resulted in a plating efficiency of 9%, and treatment with siXRCC1 resulted in a PE of 30% (Fig. 3.23). Treatment with Lipofectamine 2000 alone resulted in a reduction of cell proliferation compared to untreated cells, but the radiosensitivity was not affected (data not shown).

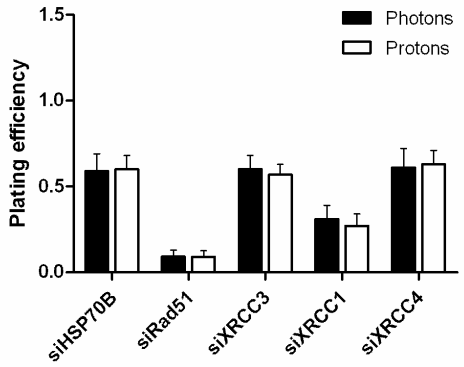

Figure 3.23 Plating efficiencies of control cells from clonogenic survival assays with siRNA-treated U2OS cells. siRNA against HSP70B was used as control; siRad51 and siXRCC3 were used to down-regulate HR, siXRCC1 to down-regulate BER, and siXRCC4 to down-regulate NHEJ. Data points represent mean ± SD, n $\geq$ 3.

Down-regulation of two different proteins involved in HR (Rad51 and XRCC3) revealed no increased sensitivity to proton radiation exposure compared to control cells (Fig. 3.24 A+B). However, silencing of the essential HR recombinase Rad51 resulted in a 6 fold radiosensitization after 5 Gy with photon or proton irradiation whereas siXRCC3 treated cells showed only a 2 fold radiosensitization (Fig. 3.24A+B, bar graphs). This result demonstrates the essential nature of Rad51 and the promoting function of XRCC3 for HR. There was nearly complete down-regulation of both proteins at the time point of irradiation as determined by western blotting (Fig. 3.24, right site, 48h point). We down-regulated as well XRCC1, due to our interesting finding of XRCC1-deficient CHO cells being significantly more sensitive to proton irradiation. Treatment with siXRCC1 resulted in a sensitization of 2.4 and

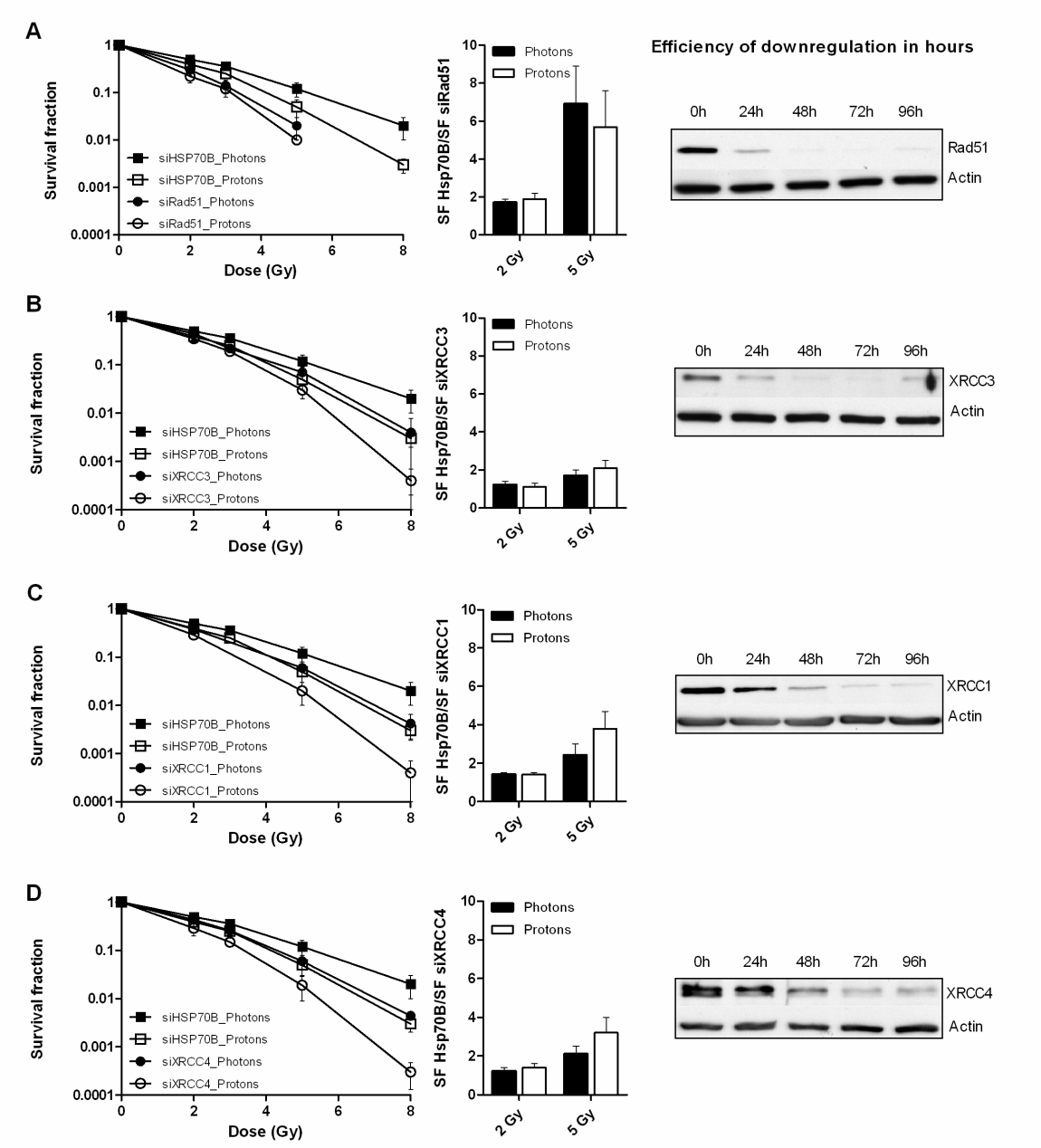

Figure 3.24 Clonogenic cell survival of U2OS cells treated with different siRNAs before exposure to photon and proton irradiation. Cells were irradiated in exponential growth phase. Survival data and corresponding ratios of SFcontrol/SFsilenced are plotted. Efficiency of protein down-regulation is shown by western blots. siHSP70B was used as irrelevant control siRNA in (A, B, C, and D). In (A) siRad51- (HR-/-) treated cells, in (B) siXRCC3- (HR-/-) treated cells, in (C) siXRCC1- (BER-/-) treated cells, and in (D) siXRCC4- (NHEJ-/-) treated cells were analyzed. Data points represent mean ± SD or bars represent mean ± SEM; n ≥ 3.

3.8 fold after 5 Gy of photon and proton irradiation, respectively, but revealed no enhanced sensitivity towards proton irradiation when compared to siHSP70B control (Fig. 3.24C). As a control we targeted as well an important NHEJ protein, XRCC4, which is an adapter protein involved at the NHEJ ligation step together with ligase IV. We achieved a radiosensitization of 2.1 and 3.2 fold at 5 Gy (for photon and proton irradiation respectively) but proton treated cells were not significantly more sensitive than control cells (Fig. 3.24D).

Due to increased complexity of the assay (transfection efficiency, plus several plating steps with the siRNA-transfected cells), the standard deviation in between the different clonogenic assays was elevated. However, all siRNA treatments resulted in the expected radiosensitization in response to photon irradiation. But proton radiation exposure led to the same degree of radiosensitization as photon radiation. Therefore we could not detect the hypersensitivity of HR-/BER-deficient cells towards proton radiation exposure in the U2OS background. With its p53 wild type status U2OS cells might show a different DNA damage response and a different hierarchy of the DNA double strand break repair mechanisms leading to this conflicting result.

3.2.1.2 Initial amount of DNA double strand breaks

The RBE_{10} for proton vs. photon irradiation at 10% survival level is 1.29±0.06 for U2OS cells. We quantified the initial amount of DNA DSBs by counting γH2AX foci and by measuring γH2AX fluorescence intensity with a flow cytometer. The aim was to determine if the enhanced cytotoxicity of proton radiation exposure is due to generation of more initial DNA DSBs by proton irradiation or not.

The initial amount of γH2AX foci is ~ 30 foci/cell in U2OS cells instead of ~ 20 foci/cell in the case of CHO cells. This is due to more nuclear DNA content and the bigger nuclear size of human osteosarcoma cells. Twelve minutes after 1 Gy irradiation the amount of γH2AX foci was equal comparing both types of radiation (Fig. 3.25A). Flow cytometry revealed, for a higher dose (5 Gy), the same fold increase in γH2AX-fluorescence intensity following either type of radiation (Fig. 3.25B). The intensity was measured after 30 minutes, as more time is required to reach maximal phosphorylation of H2AX at higher doses.

With two different approaches it was demonstrated that proton and photon irradiation generate equal amounts of initial DSBs. Therefore we speculate that the enhanced cell toxicity after proton irradiation is not due to an increased DSB induction.

3.2.1.3 γH2AX repair kinetics

Kinetics of DNA repair was only followed in normal non-transfected U2OS cells. As silencing of the different repair pathways did not result in a significant difference in proton radiosensitivity in comparison to control cells, repair kinetics were not expected to be different between the two types of radiation.

The disappearance of γH2AX foci was followed after 1 Gy of either type of radiation. No difference was detected between the two radiation treatments. Similar to the repair kinetics of CHO wild type cells, repair followed a fast kinetic with only 21% of the DNA damage left unrepaired 6 hours after radiation exposure (Fig. 3.25C). It can be speculated whether

exposure to a higher dose would have shown a different γH2AX kinetic at later time points. However, cell lysates at different time points after irradiation with 5 Gy were probed by western blotting for γH2AX and revealed no difference between the two treatment modalities (Fig. 3.25D). Maximal phosphorylation of H2AX appeared after 10 minutes, and the strong γH2AX signal was already decreased after 2.5 hours.

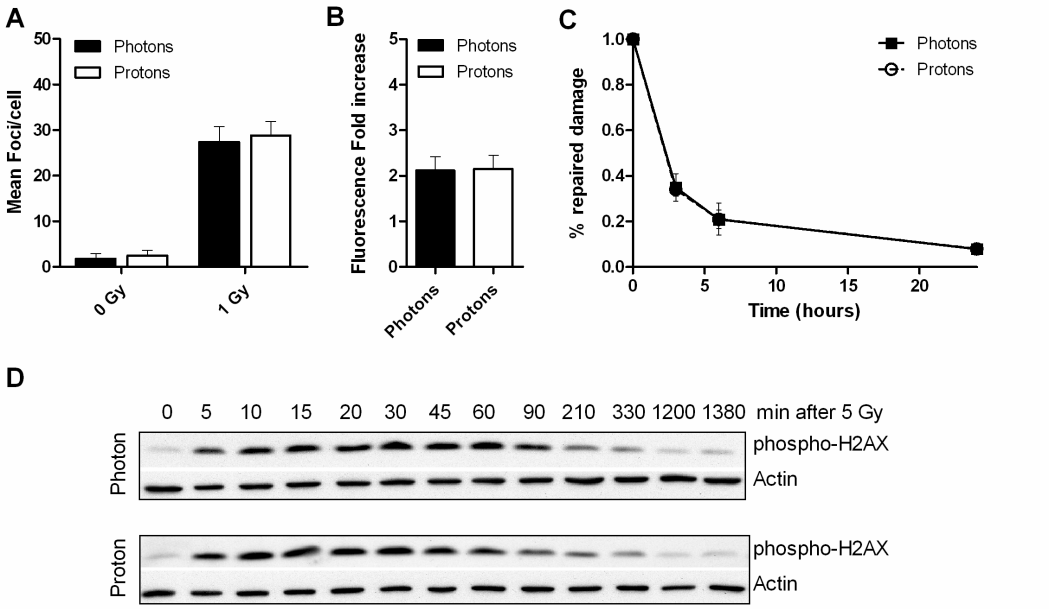

Figure 3.25 Quantification of initial and residual γH2AX foci 0.2, 3, 6, and 24 hours after proton and photon irradiation with 1 Gy in U2OS cells. (A) γH2AX foci amount after 12 min. (B) Quantification of the intensity of H2AX phosphorylation by flow cytometry 30 min after 5 Gy. (C) Kinetics of γH2AX foci after 1 Gy (initial amount of foci is set as 1). (D) Representative kinetic of H2AX phosphorylation from western blots with whole cell lysates after irradiation with 5 Gy. Data points represent mean ± SD; n≥3.

These experiments show that, similar to hamster cells, human cells also followed fast DSB repair kinetics, which was equal regardless of the radiation source. With very similar amounts of induced DSBs, this leads to the speculation that the DNA damage could be less accurately repaired after proton than after photon irradiation.

3.2.1.4 Cell cycle analysis

Cell cycle analysis was performed in non-transfected U2OS cells to determine why these cells respond differently to radiation in comparison to CHO cells.

Twelve hours after irradiation, a dose dependent increase in the G2 cell population was identified for both types of radiation (Fig. 3.26A). Indeed, U2OS cells displayed a very strong G2 arrest, with over 80% of the cells in G2 phase 12 hours after irradiation (Fig. 3.26), whereas in the case of CHO wild type cells, only 40-50 % arrested in G2 phase 12 hours after radiation exposure (Fig. 3.10). Even after 24 hours ~ 60% of the cells stayed in G2 phase, when wild type CHO cells showed already normal, recovered cell cycle distributions. For U2OS cells also no difference was detected with regard to photon and proton irradiation.

In summary, U2OS cells display a very prominent G2 arrest after either type of radiation exposure. Despite its positive p53-status, only a mild or no G1 arrest was detected after

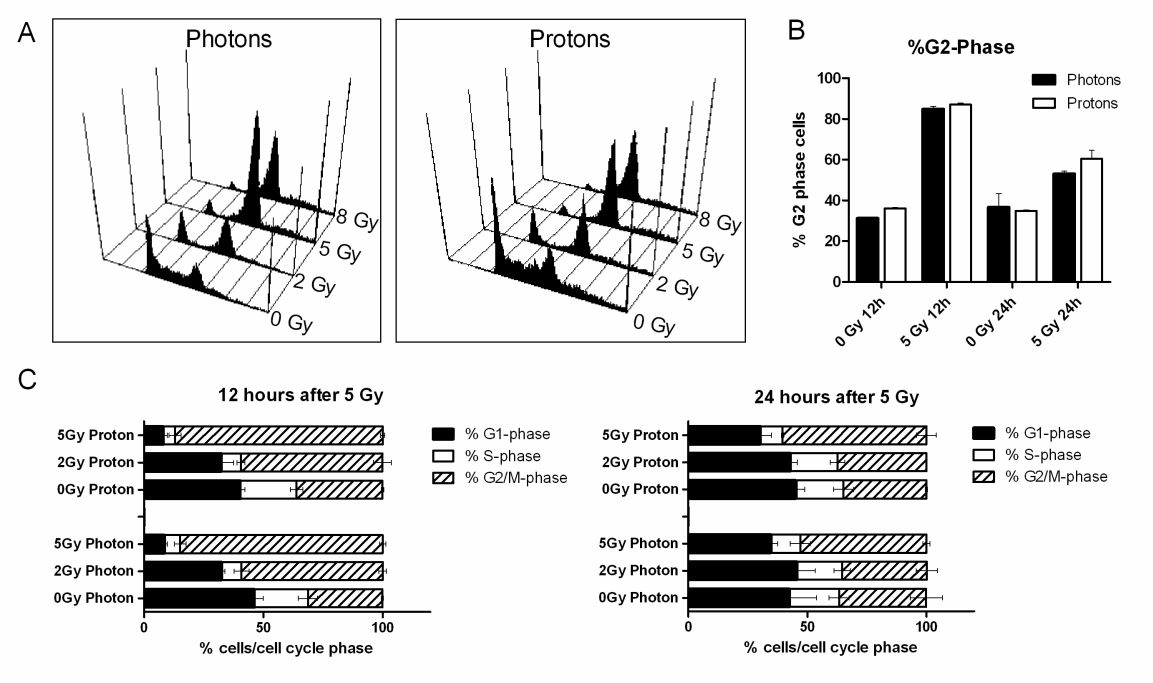

Figure 3.26 Cell cycle distribution of U2OS cells after photon and proton irradiation. (A) Representative histograms of an experiment with dose escalation 12 hours after irradiation. (B) Percentage of cells in G2 phase at 12 and 24 hours. (C) Percentage of cells in G1/S/G2-M phase at 12 and 24 hours. Data points represent mean ± SD, n = 3.

radiation exposure. When U2OS cells were irradiated with higher doses (5, 8 Gy), the G2 arrest lasted in some cases 24 hours and even longer after radiation exposure. In contrast, CHO cells could already progress to mitosis at this time. Too early onset of cell cycle progression as with CHO cells can lead to transfer of improperly repaired or unrepaired DNA damage to mitosis. In that case breaks and other damages will be duplicated and might lead to severe chromosome damages. Due to intact cell cycle checkpoints, U2OS cells will arrest until all DNA damage is properly repaired, which will lead to fewer chromosomal aberrations. This differential checkpoint response might be the main difference between U2OS and CHO cells, leading to the contradictory results.

3.2.2 Human pancreas adenocarcinoma cells

Finally we tested an additional human system with intrinsic HR-deficiency and mutated p53. The pancreatic adenocarcinoma cells, Capan-1 and BxPC-3, are often used for BRCA2-related studies. We performed clonogenic assays to detect the relative sensitivity towards proton versus photon irradiation.

Surprisingly, Capan-1 (BRCA2-/-) cells showed the same survival behaviour after photon irradiation as BRCA2-positive BxPC-3 cells. Meaning BRCA2-defective Capan-1 cells are thus in our hands more radioresistant than shown by others (*345*). The reason for this is not clear. Drastically different plating efficiencies were not the cause for this behaviour. Both cell lines exhibited a plating efficiency ~ 12%, which was similar between photon and proton irradiation experiments. However, we still observed at a high dose (8 Gy) a significantly enhanced sensitivity of Capan-1 (BRCA2-/-) cells towards proton versus photon irradiation, which was not seen in the case of BxPC-3 cells (p=0.02; Fig. 3.27). At lower doses, 2 and 5 Gy, the increased sensitivity of HR-deficient cells was not detectable.

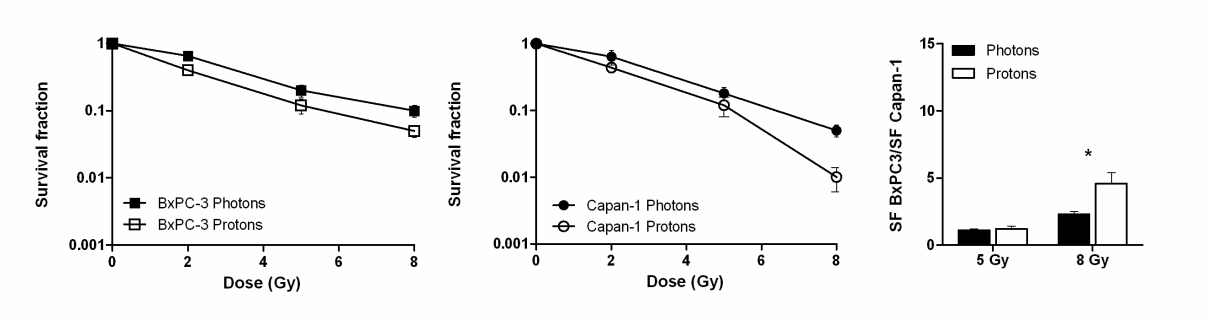

Figure 3.27 Clonogenic cell survival of proton and photon irradiated human pancreas adenocarcinoma cells. Cells were irradiated in exponential growth phase. Survival data and corresponding ratios of SFwild type/SFmutant are plotted. Survival of BxPC3 (BRCA2-proficient) and Capan-1 cells (BRCA2-deficient) is shown. Data points represent mean ± SD or bars represent mean ± SEM; n $\geq$ 3; *P<0.05.

Human pancreatic adenocarcinoma cells with a deleted and a truncated BRCA2 allele (Capan-1 cells) start to show a superior sensitivity towards proton radiation exposure at 8 Gy. In the case of BRCA2-deficient hamster lung fibroblasts (V-C8 cells), we revealed as well only at higher doses (5 and 8 Gy) this enhanced radiosensitivity after proton radiation exposure. A reason might be that BRCA2 is rather a mediator for an efficient HR process than an essential HR protein like Rad51. Furthermore, a Rad52-dependent HR process can overtake repair if the BRCA2 protein is missing and even more mediators like BRCA1, SFR1, SWS1 or XRCC3 could substitute for BRCA2 (*346, 347*). When the DNA damage burden is huge, the BRCA2 protein becomes more important in order to deal with the damage in a faster and more efficient manner.

4 Discussion

4.1 Efficiency of proton irradiation in different cell systems – different parameters

The radiobiological properties of high energy, sparsely ionizing protons have been considered to be close to the properties of 250-keV X-rays. This is also illustrated in a similar oxygen enhancement ratio for proton irradiation as for photon irradiation and a high dependence on an intact DNA repair machinery for cell survival (*52, 53*). Most of the comparative studies have been performed *in vitro* with tumour or untransformed primary normal tissue cells or with laboratory animal systems to define the relative biological effectiveness (RBE) of proton vs. photon irradiation (*82*). These studies let to the clinically used RBE of 1.1, meaning that proton irradiation kills about 10% more of the cells than photon irradiation when the same physical dose is administered. But the cause for the increased efficacy of protons on the molecular level is not clear. Proton irradiation-induced DNA damage might be quantitatively or qualitatively different compared to photon irradiation-induced DNA damage. Furthermore the RBE might be different depending on the genetic background of the tumour or the tumour entity.

In this PhD thesis, I have investigated several molecular and cellular end points in response to photon and proton irradiation using genetically defined biological systems. A special focus has been placed on the involvement of DNA double strand break (DNA DSB) repair after proton vs. photon irradiation. A panel of different cell lines was used to reveal a possible differential sensitivity to proton radiation depending on the repair status or genetic background of the cell. To the best of our knowledge this study is the first to investigate a differential requirement of DNA DSB machineries to counteract cell killing in response to proton irradiation in comparison to photon irradiation.

As has been demonstrated by others, the present work could validate the better efficacy of proton irradiation with regard to cell killing for the proton spot scanning beam. This holds true for several cell types: Chinese hamster ovary cells, Chinese hamster lung fibroblasts, human osteosarcoma cells, and pancreas adenocarcinoma cells. In this study generally the calculated ratios of the survival level of photons divided by the survival level of protons at a certain dose point (SFphotons/SFprotons) are shown. Why we preferred to compare the survival levels at the same physical dose will be explained later on. If this ratios were plotted for increasing dose points, the efficacy of proton irradiation was enhanced, which was specifically prominent in the case of exponentially growing HR-deficient CHO cells. These increasing ratios point towards a more severe DNA damage after proton vs. photon radiation exposure. An explanation might be that with higher doses the amount of the severe DNA

damages increases, leading to the better efficacy of protons. RBE calculations have been performed additionally. The RBE is the ratio of iso-effective doses of photon and proton irradiation. In that case the dose values of the photon and the proton survival plots, which are needed to induce same survival, are divided by each other. We believe that this is the best method regarding survival and clinical applications, but not regarding molecular signalling pathways, as at very different physical doses signalling pathways are most probably differentially strong induced. It was demonstrated by others that the RBE decreases with increasing dose or lower survival levels (*82*). This could be shown as well with our experimental set-up. In our hands, all non-mutated Chinese hamster cell lines and the human U2OS cell line displayed a RBE of 1.2 – 1.3 for proton irradiation. These values are slightly higher than the described one of 1.1. However, *in vitro* experiments were previously documented to result in higher values than 1.1, especially with hamster cells which have a low alpha/beta ratio (*82*). Furthermore spot scanning might lead to a slightly increased RBE (*302*). Crypt regeneration assays in mice intestines using spot scanning resulted in slightly higher RBE-values compared to other proton facilities. One factor might be the movement of the mice intestines from breathing during irradiation, but parameters like the high dose rate during spot scanning could also increase the RBE. For sarcoma cells an intrinsic higher sensitivity to proton radiation was previously reported (*82*), which corresponds to the data we obtained with the human osteosarcoma U2OS cells.

So far the molecular and cellular events and damages leading to this better efficacy of protons have not been identified. Several endpoints are indicative and were already studied by other researchers, which were also checked in this study. In the following sections the initial DNA damage induction, the cell cycle arrest induction, the apoptosis induction, and the possible influence of the dose rate after proton irradiation will be discussed.

A simple reason for the better cell killing efficacy of protons could be that protons induce initially more DNA DSB than photons. To our best knowledge only one other research group has quantified the real amount of initial DNA DSBs after proton irradiation and compared to photon irradiation. Most groups analyzed later time points (0.5 or 1h) but at these time points a fundamental amount of repair has already taken place, and therefore it resembles rather a difference in repair kinetics (*86, 348*). Hada and Sutherland were the sole investigators really analyzing initial DNA damage. T7-DNA was exposed *in vitro* to different types of radiation and with a special technique exact amounts of physical damages could be quantified (*290*). The entities they quantified were DSBs, Fpg-oxypurine non-DSB clusters, and Nfo-abasic non-DSB clusters. Interestingly, the yields of all damages decreased with increasing LET. This is due to the more localized deposition of the energy of heavy particles leading to less but highly complex DNA damages. However, low-LET protons were in the same range of damage induction as X-rays. A difference between both low-LET radiation types was still

detected. Namely, the frequency of DSBs versus abasic and oxybase clusters was higher for high-energy, low-LET protons than for X-rays. This indicates that photon irradiation induces the same amount of complex clusters as proton irradiation but more non-DSB clusters. Thus proton irradiation generates more damage clusters, which include directly generated DSBs (direct DSBs). But DSBs can be also generated indirectly. In the case of photon irradiated cells, abasic and oxybase clusters can be converted to DSBs during early repair processes. Base excision repair can indirectly generate DSBs (indirect DSBs). This is a fast process, finishing usually within 30 minutes after radiation exposure, and generates SSBs as an intermediate. SSBs opposite to another SSB will generate indirectly a DSB. In that case, it would not be possible to differentiate between directly or indirectly induced DSBs or γH2AX foci at 12 or 30 min after 1 Gy or 5 Gy, respectively (*290*). Besides this study working with nucleolytic enzymes to differentiate between the breaks, we were some of the first who checked DNA DSB induction after both types of radiation with the foci quantification technique. Using equal doses of ionizing radiation the amount of initially-induced DNA DSBs were assessed in an RBE-unbiased approach. Based on the results using the two DSB markers, γH2AX and 53BP1 foci, the initial amounts of DNA DSBs induced by both types of IR were equal, which corroborates our approach to investigate the treatment and DNA damage response on the molecular and cellular level using the same doses of ionizing radiation (1 Gy protons and 1 Gy photons), even though they are not equipotent with regard to clonogenic survival. By the means of dosimetry, 1 Gy of photon or proton radiation heat water to the same extent and deposits therefore the same energy amount in water or tissue, regardless which type of radiation is used. As the initial amount of DSB was the same, we assume that the clonogenic survival differences result from a differential severity of the DNA damage. Complex damage is defined to harbour clusters of SSBs, DSBs, and base damages in a region of 2 or more helical turns of the DNA and these cannot be differentiated by foci counting techniques and also not by other techniques beside the one described above. The exact physical-chemical interactions of proton radiation tracks on the molecular level are not clear and are most likely different compared to a photon track. A more localized energy deposition derived from around a proton track might result in more severe damage in the DNA double strand break helix in comparison to the damage induced by the broader track structure of the photon secondary electrons (*49*).

An additional parameter that is usually investigated after radiation exposure is an IR-induced cell cycle distribution. For example if a cell arrests significantly longer or faster in G2 phase this could indicate a more severe DNA damage burden, as the cell requires several attempts to repair the damage and therefore also more time is needed for the repair attempts. We and other research groups were checking a possible differentially strong induction of cell cycle checkpoints. In contrast to other research groups who detected a strong G2 arrest after low

energy proton-radiation exposure (*83, 349*), we did not detect significant differences in cell cycle arrest induction and duration of the arrest between proton (high energy, as used in this study) and photon irradiated CHO cells. Also human U2OS cells exhibited no difference in the growth arrest behaviour after both types of radiation. But compared to CHO cells, U2OS cells displayed a different overall response. 12 hours after 5 or 8 Gy, 80 – 90 % of U2OS cells arrested in G2 phase compared to 40 % of CHO cells (Fig. 3.28). Furthermore the G2 arrest in U2OS cells lasted longer than in CHO cells. Even if U2OS cells harbour an over-amplification of Mdm2 and a lack of $p16^{INKa}$, their wild type p53 appears to work with regard to the induction of a prolonged G2 arrest (*350, 351*). In general the G2 arrest is independent of the p53-status, but especially the prolonged G2 arrest in that phase was shown to depend on p53 (*352*). This means that U2OS cells arrest properly in contrast to CHO cells, which don't arrest properly and erroneous repair due to proliferation stress might not take place in U2OS cells. Other research groups who observed prominent G2 arrests used low energy protons. Due to known differential effects after low vs. high energy proton irradiation, these data might differ from ours. Yet, CHO cells are anyway not very efficient in the induction and duration of cell cycle arrests. They have already a corrupted G1-checkpoint due to the lack of p53, and some CHO cells lack also an intact S-phase checkpoint due to radioresistant DNA synthesis (RDS) (*182, 353*).

The induction of apoptosis is also a parameter often tested in response to irradiation, even if at low doses it is not the primary mode of cell death induced in fibroblasts and other non-lymphocyte cell types. Other research groups detected significant differences in apoptosis induction between proton and photon irradiated cells (*86*). We did not exactly test for apoptotic cells but could check 2 parameters in parallel to other experiments. When the cells were processed for clonogenic survival assays (~20 hours after radiation exposure) we did only observe few dead, floating cells, independent of the types of irradiation. During cell cycle analysis we observed no sub-G1 peaks (12, 24 h after exposure), which could indicate fragmented DNA of apoptotic cells. However, a careful examination should include multiple types of cell lines investigated over increasing doses of IR and at multiple time points. Other studies observed IR-induced apoptosis in CHO cells 2-3 days after IR exposure (*354, 355*). Apoptosis is the most prominent type of cell death in lymphocytes. The reported apoptosis fractions for CHO cells were not higher than 5 % compared to control for CHO wild type cells (*355*). However, a stronger inhibition of the proliferative activity after proton exposure could be observed for the CHO wild type cells in our proliferation assays (at 5 and 8 Gy) almost 5 days after exposure (116 hours, Fig. 3.3). We assume that at this late time point cell death is rather due to mitotic catastrophe or senescence leading probably to secondary apoptosis (*356*).

Another factor that has to be closely discussed and could influence cell survival is the different dose rate between the photon and proton radiation techniques. In this study photon irradiation was administered with 1 Gy/min and proton irradiation with dose rates ranging from 1 to 300 Gy/min. Obviously, this is at maximum a 300 fold difference. At dose rates below 1 Gy/min better cell survival was reported due to sublethal damage repair. However, we assume that sublethal damage repair would not occur in both cases of radiation, as dose-rates were above 1 Gy/min (*357, 358*). On the other hand, investigating biological effects at dose rates above 4 Gy/min was not possible, due to technical limitations of the linear accelerators. Since 2010, with the implementation of the TrueBeam (Varian), dose rates up to 24 Gy/min can be reached (*359*). It can not be excluded that the faster damage deposition by proton spot scanning is one reason for the more severe DNA damage pattern/interaction.
In summary we investigated the better proton efficacy not only on the level of cell survival, but also on the level of DNA damage induction, cell cycle arrest induction, and apoptosis induction. For the three parameters beside cell survival we did not detect a difference in efficacy after both types of radiation. Since we did not observe immediate cell death responses like apoptosis, we assume proton-irradiated cells die through mitotic catastrophe. In the next chapters the kinetics and the accuracy of DNA repair after both types of radiation will be discussed.

4.2 DNA damage induction and repair after proton radiation exposure in different cell lines

The influence of mutated DNA repair machineries on the radiation response towards heavy particle radiation like alpha-particles was tested before (*360*). To our best knowledge this was never tested for low-LET proton radiation. As proton radiation is becoming more and more important in the clinical setting, it is of high interest to study the influence of different genetic settings on the radiation response towards protons.

4.2.1 Nucleotide excision repair and proton irradiation

Overall, clonogenic survival was lower in all proton irradiated than in photon irradiated cell systems, which translates into the well-investigated RBE. NER-deficient cells were not differentially sensitive to proton irradiation in comparison to wild type cells. NER is in general involved in the repair of UV-light induced DNA damages and in interstrand-crosslink (ICL) repair (*120*). Therefore, proton irradiation does not likely generate more ICLs than photon irradiation. NER is not an essential repair pathway for survival after both types of IR. As the

OER was reported to be equal, we also assume that its importance for the repair of proton-induced DNA damage is not increasing in hypoxic situations, where NER is responsible to repair protein crosslink (*122, 237*).

4.2.2 Homologous recombination and proton irradiation

Interestingly, proliferating cells lacking intact homologous recombination were even more sensitive to proton than to photon irradiation, as determined in the homologous recombination-corrupted daughter cell line and the siRad51-treated wild type mother cell line. The increased sensitivity of HR-deficient cells after proton vs. photon irradiation could be reversed in plateau phase XRCC3-deficient cells, where HR is anyway not abundant. This reveals a requirement for HR after proton irradiation in exponentially growing CHO cells, which cannot be compensated by other pathways. The importance of HR was also shown in studies with heavy particles (*361, 362*). Irs2 cells (XRCC2-/-) were more sensitive to α-particles than Xrs-5 cells (Ku70/80-/-) (*360*).

Further evidence is the significantly slower γH2AX foci repair kinetics in the XRCC3-deficient cells after proton irradiation compared to photon radiation exposure. The formation and disappearance of γH2AX foci is a common marker for DSBs and their removal for DSB repair (*266, 333*). To our best knowledge this was never demonstrated before. These results suggest that the residual repair machineries seem to have problems to cope with a certain percentage of proton-generated DSBs.

In contrast to γH2AX foci, the repair kinetics of 53BP1 foci were equal in the HR-mutant cells after both types of IR. 53BP1 foci are also used as DSB markers (*224, 363*). However, disappearance kinetics of 53BP1 foci compared to γH2AX foci have been slightly faster in γ-ray irradiated MCF10A cells and in non-cycling Fe-ion irradiated cells (*329*). In our experiments the initial amount of 53BP1 foci was only one third of the γH2AX foci amount at 30 minutes after 5 Gy. It is possible that the low amount of foci could be due to problems with the used antibody. Furthermore, perhaps due to the rather small 53BP1 foci sizes at 30 minutes after exposure not all foci have been counted. Groesser *et al.* also documented a lower amount of 53BP1 foci compared to γH2AX foci in cycling cells irradiated with higher doses like 2 Gy (*329*). It might be that 53BP1 is more quickly saturated at higher doses and cannot bind to all DSBs any more. In this case 53BP1 foci could not be used as sole DSB markers at high dose levels. Furthermore 53BP1 might not localize to each DSB in certain cell cycle phases. Some research groups showed that 53BP1 is possibly involved in a specific NHEJ-pathway that facilitates ATM dependent repair in heterochromatin independently from DNA-PKcs (*224, 227*). Maybe this specific 53BP1-dependent repair pathway does repair a certain set of damages with the same efficiency in HR-deficient cells

regardless of the type of irradiation exposure. Another possibility is that γH2AX foci could mark other residual damages besides DSBs. But in S/G2 phase cells, 53BP1 foci won't colocalize with Rad51 foci, however γH2AX foci will. Therefore we assume that not all DSBs are marked by 53BP1 colocalization but rather by H2AX phosphorylation. Consequently the specific 53BP1-dependent sub-repair pathway might fix a certain percentage of damages with the same kinetics after both types of radiation in HR-mutant cells.

Foci formation of phosphorylated DNA-PKcs was used as marker for ongoing NHEJ. The kinetic profile showed that this pathway was working much slower in HR-deficient cells than in wild type cells. pDNA-PKcs foci remained at DSBs for a longer time and only started to decline 12 hours after exposure. This pattern was the same in photon and proton irradiated cells. Classical NHEJ might not be able to repair those breaks properly, which are normally processed by HR. The pathway can get blocked for example when NHEJ proteins try to repair breaks at replication forks or when the corresponding second DSB end is too far away (*364*). Also on the western blot level, phosphorylated DNA-PKcs was longer abundant in the HR-deficient cells (Fig. 3.22). After DNA-PKcs is activated at a break, it normally undergoes further conformational changes to be released again (*196*). If this step is blocked, it cannot leave the break and prevents binding of other repair proteins. However, pDNA-PKcs foci might still get resolved at later time points. It was demonstrated that HR can take over repair also at late NHEJ steps (*245*), and perhaps other repair pathways do the same. Unfortunately we did not check later time points where finally pDNA-PKcs foci might become resolved. Our data indicate that pDNA-PKcs foci stay significantly longer at certain DSBs in HR-deficient cells in contrast to the corresponding wild type cells. However, no difference between photon and proton irradiated cells was detected, but we assume that repair still progressed at later time points and was most probably more successful after photon irradiation.

In general we reason that a certain percentage of proton radiation generated complex DSBs can only be repaired by HR. This statement is undermined by three other HR mutant/wild type systems where all mutant cells showed a significant higher sensitivity to proton irradiation than the wild type cells. However, for the BRCA2-deficient cells (hamster and human) we could only demonstrate significant differences at higher doses, 5 and 8 Gy. We argue that the mediator BRCA2 is not as essential as the HR core proteins like Rad51 and XRCC3. Other backup pathways like Rad52-dependent HR might substitute and lead to the smaller effect (*346*).

In contrast, silencing of Rad51 or XRCC3 in U2OS cells did not increase the cellular sensitivity towards proton irradiation. Down-regulation of Rad51 in both cell systems (CHO and U2OS) revealed a differential sensitivity of the cells. CHO cells displayed a 90% plating efficiency even when Rad51 was down-regulated and U2OS cells revealed a 9% plating

efficiency (15% of control). From these findings one could assume that CHO cells do depend to a lower extent on HR. Normally cells are highly sensitive to siRad51 treatment, as the repair of DNA damages generated during replication does highly depend on active HR (*365*). It is not clear why CHO cells are so resistant towards a siRad51 treatment. To explain the differential sensitivities towards proton irradiation we assume the p53 status might have an influence because this status is different in the two cell systems. It was reported that p53 regulates the levels of HR (*144, 150*). Furthermore unrepaired or mis-repaired DNA damage might be better tolerated by CHO cells, which resemble aberrant tumour cells, but not by U2OS cells, which most probably would induce a cell death program.

In the case of high-LET α-particles, which induce complex DNA damage clusters, it has been demonstrated that HR is highly important for the repair in S phase. Even a second pathway SSA, which we did not check in our experiments, was more prominent than NHEJ in CHO S phase cells (*291*). Furthermore classical NHEJ has problems to repair DSBs in damage clusters induced by heavy particles (*366, 367*). Wang *et al.* demonstrated in an elegant assay that Ku proteins cannot bind to overly small DNA fragments. Therefore cellular NHEJ is partially inhibited after heavy ion exposure. Low-energy proton particles deposit a larger energy density within a small radius around the primary track and do cause a different damage pattern than the secondary electron tracks of photon beams (*303*). With increasing depth in the SOBP, the amount of low-energy proton particles increases and therefore some proton tracks in our experiments might show the behaviour described by Friedland inducing the same damage pattern as described by Wang. Based on this concept the treatment outcome after proton irradiation might be differentially affected by various genetic backgrounds.

4.2.3 Non-homologous end joining and proton irradiation

NHEJ-mutant cells are even more sensitive to normal photon irradiation than HR-mutated cells (Fig. 3.5). However, proliferating NHEJ mutant cells showed almost equal survival rates after proton and photon irradiation exposure. Furthermore they repaired photon and proton radiation induced DSBs with the same speed, indicating that the residual repair machinery could deal equally efficiently with photon- and proton-induced DNA damages.

Irradiation in plateau phase causes that only few residual repair pathways (only backup NHEJ) work. NHEJ-deficient cells displayed a low level of survival after photon irradiation, whereas survival dropped down completely after proton irradiation. Under these conditions NHEJ-deficient cells were significantly more sensitive towards proton vs. photon irradiation. This finding suggests that after proton radiation exposure a specific DNA damage cannot be accurately repaired by alternative pathways in G1/G0, whereas for photon radiation induced

DNA damage it is partially possible. If NHEJ-deficient cells proliferate, the proton-radiation specific DNA damage can be repaired by other active repair pathways in S/G2 phase like HR or SSA and G1 phase cells can progress to S/G2 phase where the DSBs get repaired, leading to the equal survival of photon and proton irradiated cells.

On the molecular level we observed that 3-fold more DSBs are occupied by Rad51 and 53BP1 foci in proliferating NHEJ-deficient cells than in wild type cells. Cells lacking NHEJ have unoccupied breaks where other repair proteins can bind to. Significantly more Rad51 foci have been detected by others in NHEJ-deficient cells (*368*). However, not all breaks are suitable for HR, for example if the sister chromatid or homologous chromosome is too distant. When the DNA end is already resected almost no other repair pathway can continue. Only if the resection was not too extensive, MMEJ or SSA could continue with the repair. The Rad51 foci number was high until 12 hours after exposure, indicating that no other pathway could overtake the repair. Another possibility is that Rad51-dependent repair progresses. Foci are resolved, but at the same time still new foci are formed, appearing as no change in foci numbers. What argues against this is that with time Rad51 foci grow in size, meaning that resection most probably still takes place at the same locus. Unusually large Rad51 filaments may present DSBs, which did not yet find a partner for HR or are irreparable and thereby might lead to cell death (*156*). However, this problem for homologous recombination appeared to be similar after both types of radiation. Based on these data we argue that HR cannot cope properly with all abundant DSBs in NHEJ-deficient cells. However, we cannot exclude the possibility that the repair might just take longer. In our experimental set-up we could not detect any differences between photon and proton irradiation induced molecular responses in NHEJ-deficient cells.

With 53BP1 foci, the same result was obtained, foci grew in size and remained significantly longer than in wild type cells. Interestingly, three hours after proton exposure significantly more foci were detected in NHEJ-deficient cells than after photon irradiation. However, 6 and 12 hours after both types of IR the amount of foci was again about the same. Maybe when classical NHEJ is missing, more proton-induced breaks are repaired via 53BP1-dependent repair. Another possibility could be that proton irradiated cells arrest faster than photon exposed ones. Unfortunately at this early time point the cell cycle distribution was not checked. If more cells would be arrested in G2 phase, consequently also more 53BP1 foci might be abundant and counted.

In these experiments, Rad51- and 53BP1-dependent repair pathways are working without the action of DNA-PKcs and try to compensate for the NHEJ-defect. However, both pathways seem to have problems to repair certain breaks or take an extraordinary amount of time. Unfortunately we cannot conclude from these data, which repair pathway leads to the better survival of NHEJ-deficient cells after proton exposure compared to HR-deficient ones.

Later experimental time points (24, 48h) would have been useful to detect the time at which Rad51 and 53BP1 foci become resolved.

In general we identified that lack of NHEJ does not lead to an increased sensitivity towards proton irradiation in proliferating cells. The proton radiosensitivity of proliferating NHEJ-deficient cells was below the level of wild type cells (RBE_{10}=1.09 vs. 1.2), meaning that a certain fraction of proton-induced damage is most probably better repaired by HR. To prove that HR can better repair proton-irradiation induced DNA damages than photon-induced ones, NHEJ-deficient and wild type cells should be irradiated in late-S/G2 phase where HR can properly work. When HR does repair proton-generated DSBs more accurately than other repair pathways, the cell survival should equal photon irradiated ones or might even be better (*291*).

4.2.4 Base excision repair and proton irradiation

Base excision repair mutants were also of interest. Complex DNA double strand breaks harbour several SSBs and base damages around the break. If the repair of these single strand damages is prevented, DSB repair machineries encounter more problems at the break due to the surrounding lesions. Repair might not occur due to docking problems of the repair proteins. Exponentially growing XRCC1-mutant cells were significantly more sensitive to proton irradiation than the wild type cells at doses of 5 and 8 Gy. Unfortunately due to time reasons we could not follow these findings mechanistically. Interestingly XRCC1-deficient cells irradiated in plateau phase did not become more radioresistant like HR-deficient cells. Therefore NHEJ-dependent repair seems to have severe problems when SSBs and base damages are not repaired before it starts working. PLD repair is also not possible in XRCC1-deficient plateau cells. In contrast to the finding in CHO cells, XRCC1 silencing in U2OS cells did not lead to the superior sensitivity towards proton irradiation. A proper cell cycle arrest might lead to the engagement of long patch BER instead of short patch BER, which is not necessarily dependent on XRCC1 (*110*). Overall these data additionally point towards a more complex DNA damage induction after proton irradiation exposure, and inhibition of SSBR could increase the therapeutic window of proton radiotherapy.

4.2.5 Wild type cells and proton irradiation

Since wild type cells also showed a significantly higher sensitivity after proton vs. photon irradiation, we aimed to explain this finding as well on a molecular level. However, the overall smaller differences in comparison to HR-mutants are more difficult to detect with these parameters.

The repair kinetics after proton vs. photon irradiation in CHO wild type cells were not significantly different for γH2AX, Rad51, and 53BP1 foci removal. Neither Rad51-dependent repair nor 53BP1-dependent repair appears to have problems with proton-induced DSBs in the wild type background. On the other hand it is possible that already very small differences might be relevant and translate into the lower survival of wild type cells after proton irradiation. For example 3 hours after 5 Gy of radiation the amount of 53BP1 foci was slightly higher in the proton irradiated samples compared to the photon irradiated ones (Fig. 3.18). Twelve hours after 5 Gy AA8 wild type cells showed more γH2AX foci after proton irradiation, which was not significantly different but still might indicate as well repair problems after proton radiation in the wild type cells. We assume that after application of even higher radiation doses, one would detect most probably a significant difference for residual γH2AX foci between proton and photon irradiated cells in the wild type cells.

The maximal appearance of Rad51 foci was rather early in CHO wild type cells, showing up at 1 hour after radiation exposure whereas in human cells it was described 3-6 hours after exposure to IR (*164, 368*). Most probably this later maximal Rad51 foci formation would also hold true for human U2OS cells, which we did not determine. These differences between CHO and U2OS cells point towards a differential DNA double strand break repair hierarchy. HR is more dominant at early time points after radiation in CHO cells than in human p53-proficient U2OS cells. Possibly Rad51 is kept inactive at earlier time points in human p53-proficient cells and only used at later time points to repair very difficult breaks in U2OS cells. In CHO cells Rad51 is presumably not inhibited and can immediately “go” to the breaks and take part in repair. However, the involvement of Rad51 at repair loci was to the same extent after both types of radiation. From this picture we conclude Rad51-dependent repair is equally important after either type of radiation. Assuming that this pathway is working error-free, other repair pathways must mis-repair or let DSBs go unrepaired after proton irradiation to result in ultimate differences in survival.

A significant difference was detected for pDNA-PKcs-foci formation. In the AA8-wild type cell line a maximum of foci was detected 1 h after both types of radiation but to a reduced level in proton-irradiated cells ($P = 0.04$; Fig. 3.21A). Decay of pDNA-PKc-foci was similar at the 3h and 6h time point and reached again basal levels at the 12h time point, indicating that DNA-PKcs is not as efficiently recruited or phosphorylated at proton induced breaks. The question is what happens with the breaks where no phosphorylation of DNA-PKcs appears. Quantities of 53BP1 and Rad51 foci were not different at this time point. Therefore this percentage of breaks might be repaired via another pathway than 53BP1- or Rad51-dependent repair. SSA could be involved. However, this pathway is known to be mutagenic and might mis-repair an enhanced fraction of proton-generated DSBs (*369*). The breaks could be also left unrepaired and lead to more fragment/break formation. But this is in contrast to the equal γH2AX foci

kinetics after both types of radiation, pointing rather to the involvement and mis-repair through other repair pathways.

Most probably small DNA fragments having a size below 1 Mb cannot be detected equally well by foci-staining techniques as bigger fragments. If more small DNA fragments are generated by proton irradiation, this could make a difference. On the other hand, if γH2AX foci contain few small fragments, repair should follow a slow kinetic, which it does not. Either such breaks are not formed after proton irradiation or they are not marked by our staining techniques.

Furthermore the total amount of pS2056-DNA-PKcs foci was lower than the one of γH2AX-foci. This result is in contrast to the general assumption that almost all breaks are repaired via classical NHEJ. On the other hand DNA repair is divided into a fast and a slow component with classical NHEJ being responsible for the fast part. This very fast initial repair kinetic can already be finished at 1-30 minutes after exposure to IR. Maybe the maximal foci amount at 1 hour after irradiation in wild type cells represents the second wave of repair efforts where classical NHEJ is more pronounced after photon radiation than after proton irradiation.

Tumour cells become more resistant when irradiated in stationary, plateau phase (*370*). This effect is due to repair of potentially lethal damage (PLD). When growth-arrested plateau-phase CHO wild type cells were irradiated, they became also more radioresistant but to the same extent after both types of IR. Therefore the effectiveness of proton irradiation was the same in plateau and proliferating wild type cells. Neither classical NHEJ nor other repair pathways in G1 phase or PLDR could properly repair a certain percentage of DNA damage induced after proton irradiation. In exponentially growing cells the abundant repair pathways do also presumably mis-repair a certain percentage of proton-induced DSBs.

NHEJ proteins show the highest affinity for DSBs and are normally the first ones locating to the breaks. Therefore NHEJ is responsible for the first, fast repair phase and later on in the second slow repair phase other repair pathways join to repair DSBs. Within the first thirty minutes to three hours after exposure to IR a large percentage of breaks is repaired mainly due to classical NHEJ and B-NHEJ. If NHEJ tries to repair breaks with complex damage structures, it seems not to need more time (γH2AX and 53BP1 foci kinetic is equal) but might mis-repair those damages with a higher probability after proton irradiation, translating into the lower survival of proton-irradiated wild type cells. The detection of more dicentrics and rings after proton vs. photon irradiation is pointing to this hypothesis. At later time points the slow repair component becomes important. HR proteins might continue to repair those breaks where NHEJ was blocked. Even during the slow repair phase NHEJ is still involved, but might take more time at complex DSBs. After irradiation with high doses, NHEJ proteins might be all occupied, and free breaks are left for other repair pathways. This saturation

effect could be the reason for the drastically increased sensitivity of HR-deficient cells at 5 and 8 Gy.
In conclusion we detected no differences in the DSB repair kinetics of the wild type cells (γH2AX foci) after low doses (1 Gy) of both types of radiation. At higher doses (5 Gy) we started to see differences. However, they showed only a trend without significance. We assume that at higher doses (8, 10 Gy) proton-irradiated cells would display significantly more residual DSBs correlating with the lower cell survival of CHO wild type cells. Rad51-dependent repair appears to be involved to equal amounts after both types of radiation. Due to the assumption that HR is error-free, we propose parts of the proton-generated DSBs are mis-repaired by another repair pathway, most presumably by NHEJ or SSA.

On the physical-chemical level, the difference between photon and proton irradiation exposure is unclear. If you follow the track of a single proton particle it is not exactly clear why and how the interactions of protons with matter change in the depth of the tissue. Proton irradiation exerts a direct effect, by the proton particle itself and indirect ones, by generating secondary electrons or short range electrons. Due to these short range electrons, protons may induce a more localized damage around its track. Another reason for a different damage complexity could be a minimal enhanced LET. The SOBP consists of a mixture of multiple near-monoenergetic proton beams. Some proton particles reach already the Bragg peak at this certain depth. At the Bragg peak they become so slow that they display low-LET characteristics. These protons might shift the DNA damage profile. This differential DNA damage complexity is most probably leading to the lower cell survival.
Others have determined RBE-values close to 1.0 or even lower ones (*82, 371*), which indicates that certain cell lines can repair the proton damage very well, which is leading to equal survival levels. These cells most probably have an intact DNA damage response (DDR) and a certain set of repair proteins helping them to accurately repair proton-generated DNA damages. Also many *in vivo* experiments show a small RBE. Intact normal tissue should exhibit intact DDRs and intact repair pathways and might therefore repair proton-induced DNA damage more efficiently and accurately than highly mutated tumour cells. In that case, the intact response of normal tissue would improve the therapeutic ratio of proton radiotherapy. In this chapter we have also shown that certain mutations in DNA repair pathways make tumour cells more sensitive to proton irradiation compared to normal cells. Mutations in the HR- or BER-pathway might increase as well the therapeutic ratio for proton radiotherapy. Putting our results together with previous work, we showed that the genetic background of the tumour (maybe also of the patients normal tissue in the case of germline mutations) is influencing the therapeutic ratio of proton radiotherapy.

4.3 Accuracy (and hierarchy) of repair after DNA damage induction by protons

We questioned two possible outcomes after proton vs. photon irradiation: either the DNA damage is more often mis-repaired or even not repaired.

For HR-mutants we could correlate the longer abundance of γH2AX-foci after proton exposure to the significantly reduced survival after proton irradiation. However, in wild type cells we saw equal kinetics for γH2AX, 53BP1, and Rad51 foci after both types of radiation. Only the amount of pDNA-PKcs foci led to the impression that NHEJ has difficulties with proton-induced damages or requires extended periods of time to be activated. Regardless of the superior sensitivity of HR-mutant cells, a clear reason for the classic RBE of 1.1 was not demonstrated. We quantified the amount of chromosomal aberrations in both CHO wild type cell lines (AA8 and CHO9). In this experiment we detected an increased amount of fragments, dicentrics, and rings pointing towards induced and mis-repaired damage in G1 phase. Also many more sister unions could be counted after proton vs. photon irradiation. Rationales for this result could be enhanced mis-repair in S-phase irradiated cells after proton irradiation, or unrepaired DNA damage was transferred to S phase and mis-repaired, or more cells were present in S phase during proton irradiation exposure. The chance for the latter possibility is rather small, as cell cycle data revealed equal distributions and because we see many G1 induced aberrations as well. In conclusion proton-induced DNA damage appears to be more often mis-repaired than the damage after photon exposure, most probably leading to the RBE of CHO cells.

Two fold more sister unions indicate that the damage was erroneously repaired in G2. SSA displays a high activity during this phase (*291*). Therefore this more error-prone repair pathway and NHEJ could lead to mis-repair of the damage, as not all DSBs are substrates for HR.

In the case of heavy particle exposure Ritter *et al.* discussed that the RBE for aberration induction is strongly dependent on the time between radiation exposure and harvest. This is due to more prominent cell cycle delays and loss of heavily damaged cells after heavy particle irradiation (*372*). In that case the RBE for aberration induction with carbon ions was lower than in reality, as the cells were blocked in G2 phase and did not continue progression to M phase. Premature chromosome condensation (PCC) techniques could unmask these discrepancies. But in the case of low-LET proton radiation exposure we did not detect a stronger G2 arrest ~ 24 hours after irradiation. Only at very late time points, growth was significantly inhibited in the proliferation assays. As our samples were prepared 24 hours after irradiation, we exclude this effect for low-LET protons.

What is the rationale for the huge differences regarding chromosomal aberration induction after proton vs. photon radiation exposure? CHO cells are highly proliferative cells and

genetically unstable (*373*). Therefore chromosomal aberrations might manifest faster in these cells due to fast growth behaviour without proper cell cycle arrests. Clonogenic survival and the SFphoton/SFproton ratio at a dose of 5 Gy (1.9±0.4) correlate with the numerical enhanced chromosomal aberrations after proton irradiation.

This mutagenic potential of proton irradiation was already shown in some cell-based and mice-studies (*297, 299*). In peripheral lymphocytes the efficiency of proton irradiation exposure was higher at lower doses and decreased with dose. Interestingly the aberration frequency increased also with greater depth in the SOBP. A variation of aberration induction along the SOBP points towards a differential damage induction within the beam, leading to areas with different probabilities of aberration induction.

In summary, proton irradiation induces more lethal chromosomal aberrations at least at this high dose (5 Gy). This might be the reason for the increased cytotoxicity of proton irradiation. More severe proton-induced DNA damages are repaired erroneously, leading to cell death. Proper mitosis is not possible with dicentrics or sister unions and the cells might not undergo cytokinesis and ending up in a binucleated cell, which dies through mitotic catastrophe or undergoes senescence.

4.4 Translational significance

There is presently a widening gap between the rapid introduction of proton radiotherapy in clinical practice worldwide and the apparent lack of solid radiobiological evidence and data to support the expansion of new clinical indications, particularly when combined with other treatment modalities. The major difference between photon- and particular proton-based radiotherapy is the spatial distribution of energy deposition. Proton particles enter tissue with a low dose, and the maximum dose deposition occurs within the so-called Bragg peak at a depth depending on the controllable beam energy. Behind this Bragg peak region – or Spread-out-Bragg Peak (SOBP) in clinical applications – no significant dose is deposited. For photon irradiation in contrast, the maximum dose is deposited close to the entrance surface of the tissue that is irradiated and also behind the targeted tumour tissue. The physical characteristic of proton radiation provides more localized delivery of the radiation dose to the tumour site than can be achieved with photon-based radiotherapy. The improved dose distribution is exploited either by allowing higher doses to the tumour without increased normal tissue toxicity or by reducing adverse effects at equally effective tumour doses.

Radiobiology experiments conducted several decades ago revealed an approximately 10 % higher biologic effectiveness (RBE) of proton compared to photon irradiation (*82*). In today's clinical practice a generic RBE of 1.1 is employed and seems to be reasonable due to the huge set of experiments that have been performed. However, the RBE can vary heavily

according to the tissue, cell line, or the end point investigated (*82*). There is still a huge black hole with regard to the exact biological events induced along a proton radiation track. It was shown that efficiency can vary along the plateau and SOBP region and is maximal at the distal end of the SOBP and the distal penumbra (*374*).

A few other studies discussed a possible differential DNA damage induction by proton and photon irradiation (*86, 298*). In the present study we elucidated in a clear way that the initial amount of DNA double strand break induction is equal after both types of irradiation with respect to γH2AX and 53BP1 foci induction. The repair kinetic was also the same in most cell lines studied, but we assume the quality of the damage and of the repair products is differentially complex after both types of radiation, leading to the better effectiveness of proton radiation exposure. Repair products with worse quality are highly mis-repaired products consisting of complex chromosomal aberrations. This mis-repaired DNA damage must contribute in large part to the RBE, though we do not exclude other factors contributing to the RBE, e.g. protein damage/stress. An increased part of the proton-induced DNA damage is more severe (more complex) and cannot be properly repaired. Chinese hamster cells lacking intact HR display a drastically stronger decrease in cell survival after proton irradiation than in wild type cells. This reveals that HR is essential to repair parts of these complex breaks.

When proton irradiation induces a more severe damage, this happens most probably also in normal tissue. It cannot be prevented that some parts of healthy tissues are irradiated during proton radiotherapy. Studies with lymphocytes by Manti *et al.* revealed that proton-induced aberrations could be more efficiently transferred to later generations, meaning that mutations might be better propagated after proton-radiation exposure (*298*). This can happen in healthy, co-irradiated tissue and lead to secondary diseases at later time points. Therefore care must be taken when irradiating small children. As little healthy tissue as possible should be co-irradiated during treatment. In older patients, healthy tissue fibroblasts are usually in the G0 phase of the cell cycle. These cells do not divide anymore and could not propagate mutations to later cell generations. However, in the case of children, these tissues are still growing. In this case, mutations can be propagated and can lead to diseases at later time points during life. Even in adolescents secondary cancer can occur. Fibroblasts are stimulated to proliferate during the normal wound healing process (*375*). In response to radiation, a certain percentage of cells dies in the irradiated tissue, leaving free space that stimulates surviving cells to grow, providing an opportunity to forward mutations. On the other side, normal tissue cells possess intact DNA damage response mechanisms. This might prevent the transfer of mutations. Whereas in tumour cells or CHO cells, secondary mutations are most probably very efficiently transferred to later generations due to deregulated DNA damage checkpoints.

If a patient harbours already a heterozygotic mutation in the HR pathway (BRCA1/ BRCA2/ XRCC3) and experiences a complete loss in the tumour compartment it might respond significantly stronger to proton irradiation than with an RBE of 1.1. We showed here that BRCA2 or XRCC3 mutations or Rad51 depletion in a p53-mutated background leads to an increased proton radiosensitivity, which was not observed in p53-proficient cells. This implies that in addition to the HR-mutation the cell has to harbour a deregulated cell cycle checkpoint response in order to be highly sensitive to proton radiation exposure. In this case one could argue normal tissue with BRCA2-/+ has still an intact DDR and would not be more sensitive to proton irradiation, but tumour tissue with acquired BRCA2-/- often has additionally a deregulated DDR (e.g. p53-mutation) and would be highly proton sensitive. Personalized medicine will be more and more important in the future. Determination of the tumour's BRCA1- or 2-status and p53-status could channel patients defective in both markers to proton radiotherapy. Then a lower dose could be prescribed and lead to palliation of the patient's side effects. However, this has to be proven in a tumour model.

In the USA more and more prostate cancer patients are treated with proton radiotherapy. In a recent study 3.1 % of all cases carried a BRCA founder mutation. A BRCA2 founder mutation was associated with a three-fold increase in prostate cancer risk. Mutation carriers had significantly greater risk of recurrence and prostate cancer-specific death than non-carriers (*341, 342, 376*). Due to our findings and the more aggressive phenotype of BRCA2 mutation carriers, those patients should be treated with proton radiotherapy. Maybe a hypofractionated regimen would give good results in the case of very aggressive and relatively radioresistant tumours.

In the recent years enormous knowledge was acquired on the molecular mechanism of DDR and DNA DSB repair. With this knowledge strong efforts were made to establish specific DNA repair inhibitors (*377, 378*). The most specific and promising drugs are Parp-inhibitors (*379*). Unfortunately no specific HR-inhibitor exists yet. But Parp-inhibitors are for example used due to their synthetic lethality characteristics. HR-deficient cells treated with a Parp-inhibitor all die. Parp-1 is involved in repairing single strand breaks, which occur in daily routine due to oxidative stress. If SSBs stay unrepaired until DNA replication, they lead to breaks that must be repaired by HR. HR-deficient cells cannot do this and most probably die. However, in the case of radiotherapy the inhibition of SSB repair is also important, as we showed that cells lacking SSB repair are quite radiosensitive and highly sensitive to protons at higher doses. Combination of those with proton therapy might be very effective. This has to be proven in HR-defective and other cell systems.

Tumours start to become hypoxic already at a size of 1 – 2 mm or when the nearest vessel is 200 µm distant (*380, 381*). Hypoxic cells have down-regulated Rad51-protein levels and consequently reduced HR-activities (*382, 383*). The hypoxic status of the tumour is not

equally distributed. Compartments of the tumour with different oxygen levels could respond differentially to proton irradiation exposure. However, as the OER was reported to be equal for both radiation types, no influence might exist (*52, 53*). On the other hand hypoxic cells do generally not proliferate very fast. When they stay in G1/G0 phase due to unfavourable growth conditions, cells will not propagate chromosomal aberrations and most probably not die.

Our study shows that on the chemical-molecular level, proton irradiation induces a differential DNA damage in comparison to photon irradiation exposure. CHO cells, which resemble p53-deficient, fast proliferating tumour cells, are highly sensitive to proton irradiation and even more sensitive in a situation in which HR is deregulated.

5 Outlook

The following major questions are of interest:

(1) Dissecting the proton radiosensitivity during the cell cycle
(2) Verification of the importance of homologous recombination
(3) *In vivo* normal tissue response
(4) Dose rate effects and RBE differences along the SOBP

5.1 Dissecting the proton radiosensitivity during the cell cycle

A good approach for a more precise analysis of the different involvement of repair pathways is to analyze the behaviour of cell lines in G1 and G2 phase of the cell cycle. Clonogenic assays, repair kinetics, and chromosomal aberration induction analyzed exactly during these phases could elucidate the cell cycle phase, were the main mis-repair after proton irradiation occurs and could elucidate the responsibility of the different repair pathways.

It is not clear if HR could possibly reduce the RBE to 1 or even more due to accurate repair of proton-generated DSBs. Irradiation of late-S/G2 phase synchronized wild type and NHEJ-deficient cells followed by clonogenic survival assays should reveal if the proton survival curve reaches the one of photon irradiated cells or not. During this cell cycle phase the chance exists that all damages, which need HR for proper repair, could be reached by Rad51 as it is expressed in this phase. This experiment might reveal that HR is able to repair proton damage accurately and to increase cell survival. Another group showed after reexpression of the missing HR-protein that these cells survived even better after alpha particle irradiation than after photon irradiation (*291*). If this can be demonstrated one has to be careful with tumours, which show over-activated HR. In that case the RBE might be lower than 1.1 and the therapeutic ratio would be decreased. But it has been reported that an elevated HR status of the tumours did not correlate with the level of radioresistance after photon radiotherapy (*384*).

It will be interesting to probe for γH2AX-foci repair kinetics in G1 arrested (plateau phase) cells where only NHEJ is active and in G2 synchronized cells where mainly NHEJ and HR repair DSBs. This could be performed in wild type cells, detecting more precisely if differential repair kinetics, which could not be visualized in the unsynchronized population, occur in the wild type cells after both types of radiation. Furthermore it could be performed in HR-mutant cells to reveal if in G2 phase cells the described differential repair kinetic will be even more pronounced. In the case NHEJ is working with fast kinetics, regardless of the radiation source administered to G1 phase cells, no difference in the wild type repair kinetics should be observed, and the same should be revealed for HR-mutant cells. But it is possible that after proton exposure of G1 phase cells not all DSBs (γH2AX foci) could be repaired and

might be transferred to S phase to be repaired via HR. In that case more residual γH2AX foci might be detected after proton-radiation exposure. Cells irradiated in G2 phase use mainly NHEJ and HR for repair. In that phase NHEJ starts to become less accurate (*108, 385*). A reason for this might be the different chromatin structure in G1 and G2 phase. Irradiated G2 phase wild type cells might show a repair defect after proton exposure depending on the failure of NHEJ to repair certain damages. In the HR-mutant cells the slower repair kinetic after proton irradiation exposure should then be even more pronounced in G2 phase.

An important missing experiment is the analysis of chromosomal aberration induction in the HR-mutant cells. In the wild type cells a difference in the aberration production after proton versus photon exposure could be detected. However, the repair kinetics had been equal. Therefore we anticipate a more drastic difference in aberration induction in the mutant cells after proton vs. photon irradiation. This experiment would be performed with lower doses of 1 - 2 Gy, as the cells are anyway more sensitive due to their lack of HR.

Irradiation of exponentially growing cells and metaphase preparation 24 hours later generally includes cells, which have been irradiated in G1 phase but could also involve cells, which where irradiated in G2 phase and already finished a cell cycle at the time of fixation. A more precise analysis of the exact types of aberration induction in the different cell cycle phases could give another hint towards the phase, in which main mis-repair takes place. Cell fixation 16 hours after irradiation would exclude cells, which finished another cycle and include only cells, which had been irradiated in G1 phase. Fixation at 3 - 6 hours after irradiation would only include cells, which have been irradiated in G2 phase and which had to repair the damage in that phase. This could show if proton irradiation is more severe for G1 or G2 phase cells with regard to aberration induction and if HR-mutant cells show significantly more aberrations after proton exposure compared to the wild-type cells.

With the chemical premature chromosome condensation (PCC) technique it would be also possible to quantify the initial break induction in G2 phase cells. In that cell cycle phase chromosome condensation with Calyculin A treatment takes only 5 minutes due to the higher levels of cyclin B and allows almost immediate fixation, which could give a second readout about initial break induction. Specific analysis of G1 phase repair would be also of interest. However, chemical chromosome condensation is not possible as no cyclin B is expressed in that cell cycle phase. Another option for the detection of G1 phase repair capacity would be to irradiate plateau phase cells and applying another premature chromosome condensation (PCC). G1 phase cells can be fused with mitotic cells leading to PCC as the right signals are abundant (*386*). Condensation will be finished only 30 minutes after fusion and during analysis one has to differentiate between the mitotic chromosomes of the donor cells and the haploid chromosomes of the cell of interest. In G1 phase cells mainly breaks/gaps can be detected.

5.2 Verification of the importance of homologous recombination

It has never shown before that an HR-defect in human cancer cells does lead to superior sensitivity towards proton irradiation. Therefore it is of high importance to proof our finding in a human cellular setting and later on in an *in vivo* setting.

As we assume that the HR-defect only leads to this increased sensitivity towards proton radiation in a p53-deficient background, Saos-2 osteosarcoma cells would be a good model. These cells are deficient in p53 (*387, 388*). Saos-2 cells, ectopically expressing or not expressing p53, could be treated with siRad51, irradiated, and processed for clonogenic survival. Depletion of Rad51 in the p53-deficient cells should lead to the increased sensitivity towards proton irradiation in contrast to p53-expressing cells. Other cell pairs could be tested as well like BRCA1-deficient breast cancer cells (HCC1937 and HCC1937-wt BRCA1) and another BRCA2-deficient lymphoblast cell line (EUFA423 and EUFA423/wt BRCA2). However, it was shown that BRCA1-deficiency does not lead to a direct HR-defect but to a defect in transcription coupled repair (TCR) (*345*).

Another experiment, which could proof the importance of HR in a human setting, is to treat different p53-deficient tumour cells with HR-inhibitors. Unfortunately no specific inhibitor for HR exists. A possibility would be to use an ATM-inhibitor from KuDOS (Ku55933), which inhibits whole DNA damage signalling and rather both DSB repair pathways (*25*). It might lead to a stronger cytotoxicity in combination with proton than with photon irradiation. Parp-inhibitors like Iniparib, Olaparib, and ABT-888 could be also tested together with proton radiotherapy (*377*). In general Parp-inhibitors reduce the level of BER and they are synthetically lethal in HR-defective tumours (*389*). They might be even beneficial in HR proficient but p53-mutated cells, as inhibition of BER in CHO cells let to an increased proton radiosensitivity (see chapter 3.1.5). If BRCA2-deficient tumours would be treated with a combination of Parp-inhibitors and proton radiotherapy they might display a superior response in comparison to the combination with photon radiotherapy.

In case the experiments proposed in this chapter would reveal superior cell kill in clonogenic survival assays, the ultimate experiment to proof the clinical relevance would be to treat HR-deficient tumour xenografts with proton and photon radiotherapy. When tumours treated with proton radiation regress faster than photon-treated tumours, even if they were treated with photon-equivalent doses, this would show that the effective dose of proton radiation is bigger than anticipated for HR-defective tumours leading to a further reduction in the total dose in proton irradiation plans for BRCA2-deficient tumours. Unfortunately almost no established HR-deficient tumour models exist. A formerly used and possible model is the intramuscularly implantation of V-C8 (BRCA2-/-) or complemented V-C8 cells into the thigh of CD-1 nude mice (*390*). Regarding the limited possibilities to grow BRCA2-deficient tumours, a second option would be to test the combination of proton radiotherapy and the described ATM- or

Parp-inhibitors. Tumours with p53-deficient background would be grown to a certain size and the drug would be administered before exposure to IR. As end point tumour growth delay could be measured, however in this case maybe tumour control might be a more relevant endpoint.

These experiments would change the general assumption that the proton RBE of 1.1 is the same for different tumour types independent of the genetic backgrounds. Further studies would follow analyzing the sensitivity of other tumour types and tumour mutations.

5.3 *In vivo* normal tissue responses

Another important aspect to look at is the normal tissue response after proton radiotherapy treatment. Even with the further reduction of dose given to the healthy tissue with proton intensity modulated therapy (IMPT) it is still important to know the responses of the normal tissue and the frequency of mutations induced. Some research is ongoing with regard to space missions, but the fluences and doses of proton radiation to which astronauts are exposed do not resemble the situation when normal tissue is exposed to proton particles during radiotherapy.

Many studies in mice investigate lymphocyte and intestine crypt regeneration. However, these are acute responding tissues (early responding tissues). Critical other tissue sites are for example the lungs, the brain, and the rectum, which are late responding tissues. In the lungs fibrosis can occur, leading to severe problems for the patient. It is not so easy to define relevant end-points for late-responding normal tissues. Apoptosis will not or very mildly occur as this is a feature of fast regenerating, early responding normal tissue. One could stain for other cell death markers like for senescence markers (SA-ß-Gal, PML, and $p16^{INK4a}$) in thin tissue sections at 4, 8, 12, weeks after exposure (*391, 392*). A lower H&E staining would indicate reduced proliferative activity in the irradiated tissue and could be compared to photon irradiated tissue. Severe prolonged activation of certain signalling pathways could be as well used as a marker to differentiate between photon and proton radiation induced normal tissue responses. Prolonged p53 phosphorylation or p21 activation from 5 days up to 2 weeks after radiation exposure might point to a severe damage response and can lead to the transformation of normal cells (*24*).

Another important endpoint is chromosomal aberration induction. But cells of these tissues do almost not grow and it is nearly not possible to bring them to mitosis. In that case it might be possible to extract cells from the normal tissue that was irradiated and from another place that was not irradiated. After having the cells in medium premature chromosome condensation with the phosphatase inhibitor Calyculin A would help to prepare nuclear spreads with condensed chromosomes in G1 and G2 (*386*). However, the significance of

chromosomal aberrations for normal tissue that is almost not growing might be not that big. Anyhow a study in 2005 with the lacZ reporter transgene assay revealed a significantly increased mutant frequency in brain tissue at 8 weeks after exposure (*299*). Unfortunately, these data were not compared to photon irradiated samples. But it was determined that the same assay performed with spleen tissue showed no induction of mutant frequencies at 16 weeks after exposure indicating that different tissues can clear cells to a better extend or are more prone to aberration induction. A large study in the USA analyzed the risk of a secondary solid tumour formation at any time post-diagnosis of prostate cancer. It was significantly greater after radiotherapy than after surgery (about 6 %). The relative risk increased up to 34 % after 10 years and more. Sites of secondary cancer were the bladder, rectum, and even the lung (*16*). Therefore chromosome aberration analysis of radiation-exposed normal tissue could be a good marker for inter-comparison between the photon- and proton-induced aberration amount and possible secondary cancer risk.

5.4 Dose rate effects and RBE differences along the SOBP

The dose rate can have an effect on cell survival. Dose rates above 1 Gy/min kill cells with the same efficiency. Below 1 Gy/min sublethal damage repair can take place and can lead to better cell survival after radiotherapy. If dose rates above 4 Gy/min can further reduce the cell survival could never be shown before, as this is the maximal dose rate reached with a linear accelerator so far. Only recently a research group demonstrated with the TrueBeam (Varian) that survival of human glioma cell lines could be further decreased at a dose rate of 24 Gy/min compared to 6 Gy/min (*359*). A possible explanation for this might be a higher probability of photon radiation tracks to interact with each other. This finding should be taken with caution as it was only demonstrated once. However, it would be interesting to find out, if the dose rate has an influence on survival in the case of proton radiation. Modulating the dose-rate for different exposures and plating the cells afterwards for clonogenic survival could show if it can influence survival in the case of proton-radiation exposure. For proton radiation this has never been tested before and is of special interest in the case of spot scanning where the dose rate can differ in each spot.

It is clear that the RBE rises at the distal part of the SOBP due lower proton energies, which translate into higher LET-values. However, the RBE in the plateau-region and along the SOBP is not well defined. Petrovic *et al.* showed with a 62 MeV beam that the RBE for radioresistant melanoma cells increases drastically at the distal declining edge (RBE = 7) but is also bigger for centre SOBP proton particles compared to plateau proton particles (RBE = 1.68 vs. 2.08, respectively) (*374*). The RBE varies with the cell line and the beam used. Here melanoma cells were used but the question is, if normal skin cells respond also with this

stronger RBE to protons. If proton radiation is really 1.68 fold more efficient than photon radiation in the plateau region, skin will receive a too high dose. Some radiooncologists performing proton radiotherapy report severe skin reactions, which might essentially be due to a bigger RBE in the plateau region (*393*). But recent studies report only mild skin reactions (*394, 395*). In general skin toxicities appear to be more pronounced in scattered proton radiotherapy. The RBE of skin tissue of different patients also varied between patients (*396*). Here a differential repair status of the normal tissue or other factors could play a role.

The huge RBE in the distal declining part of the SOBP cannot solely be used to treat tumour tissue. Unfortunately due to the safety margins used in radiotherapy planning, mainly healthy tissue receives that huge biological effective dose. This is also the case for carbon ion treatment. The question is, if it is good to sacrifice parts of the healthy tissue for the beneficial saving of the other 95 % of healthy tissue behind the tumour, which will receive no dose. To verify the RBE along the proton beam at PSI, cell culture flasks could be placed in a row in the beam and processed later for clonogenic survival assays. A possible *in vivo* experiment would be the irradiation of spleens of mice, which are placed in a row along the treatment table. That could give more physiological relevant insights. Spleens would be collected and checked for apoptotic cell death and DNA damage induction.

The best would be to compare all those factors in an inter-clinical study as they should be anyway defined for each proton gantry, which is on clinical duty. After that study one could hopefully exclude inter-clinical variations and concentrate on the genetic background of the patients that might influence the relative biological effectiveness of proton radiation.

References

1. P. Kleihues and L. H. Sobin, World Health Organization classification of tumors. *Cancer* **88**, 2887 (2000).

2. H. E. Karim-Kos, E. de Vries, I. Soerjomataram, V. Lemmens, S. Siesling and J. W. Coebergh, Recent trends of cancer in Europe: a combined approach of incidence, survival and mortality for 17 cancer sites since the 1990s. *Eur J Cancer* **44**, 1345-1389 (2008).

3. J. Ferlay, P. Autier, M. Boniol, M. Heanue, M. Colombet and P. Boyle, Estimates of the cancer incidence and mortality in Europe in 2006. *Ann Oncol* **18**, 581-592 (2007).

4. M. a. v. d. K. Joiner, A, Ed., *Basic Clinical Radiobiology*. Hodder Arnold, 2009.

5. E. J. a. A. J. G. Hall, Radiobiology for the Radiologist. *Lippincott Williams and Wilkins Publishing* **6th edition**, 656 (2006).

6. G. Delaney, S. Jacob, C. Featherstone and M. Barton, The role of radiotherapy in cancer treatment: estimating optimal utilization from a review of evidence-based clinical guidelines. *Cancer* **104**, 1129-1137 (2005).

7. J. S. Tobias, The role of radiotherapy in the management of cancer--an overview. *Ann Acad Med Singapore* **25**, 371-379 (1996).

8. M. M. Elkind, H. Sutton-Gilbert, W. B. Moses, T. Alescio and R. W. Swain, Radiation Response of Mammalian Cells Grown in Culture. V. Temperature Dependence of the Repair of X-Ray Damage in Surviving Cells (Aerobic and Hypoxic). *Radiat Res* **25**, 359-376 (1965).

9. J. S. Bedford and J. B. Mitchell, Dose-rate effects in synchronous mammalian cells in culture. *Radiat Res* **54**, 316-327 (1973).

10. J. B. Little, G. M. Hahn, E. Frindel and M. Tubiana, Repair of potentially lethal radiation damage in vitro and in vivo. *Radiology* **106**, 689-694 (1973).

11. J. S. Rasey and N. J. Nelson, Repair of potentially lethal damage following irradiation with X rays or cyclotron neutrons: response of the EMT-6/uw tumor system treated under various growth conditions in vitro and in vivo. *Radiat Res* **85**, 69-84 (1981).

12. H. R. Withers, J. M. Taylor and B. Maciejewski, The hazard of accelerated tumor clonogen repopulation during radiotherapy. *Acta Oncol* **27**, 131-146 (1988).

13. L. M. van Putten, Tumour reoxygenation during fractionated radiotherapy; studies with a transplantable mouse osteosarcoma. *Eur J Cancer* **4**, 172-182 (1968).

14. K. P. Mishra, Fluorescence studies on radiation oxidative damage to membranes with implications to cellular radiosensitivity. *P Indian as-Chem Sci* **114**, 705-711 (2002).

15. E. R. Stadtman, Oxidation of Free Amino-Acids and Amino-Acid-Residues in Proteins by Radiolysis and by Metal-Catalyzed Reactions. *Annu Rev Biochem* **62**, 797-821 (1993).

16. D. J. Brenner, R. E. Curtis, E. J. Hall and E. Ron, Second malignancies in prostate carcinoma patients after radiotherapy compared with surgery. *Cancer* **88**, 398-406 (2000).

17. B. Zhang, Y. Su, G. Ai, Y. Wang, T. Wang and F. Wang, Involvement of peroxiredoxin I in protecting cells from radiation-induced death. *J Radiat Res (Tokyo)* **46**, 305-312 (2005).

18. E. Riklis, I. Emerit and R. B. Setlow, New approaches to biochemical radioprotection: antioxidants and DNA repair enhancement. *Adv Space Res* **18**, 51-54 (1996).

19. T. J. Jenner, C. M. Delara, D. L. Stevens, N. A. Burns and P. Oneill, The Induction of DNA Double-Strand Breaks in V79-4 Cells by Gamma and Alpha Radiations - Complexity of Damage. *Radiat Prot Dosim* **52**, 289-293 (1994).

20. L. Tartier, S. Gilchrist, S. Burdak-Rothkamm, M. Folkard and K. M. Prise, Cytoplasmic irradiation induces mitochondrial-dependent 53BP1 protein relocalization in irradiated and bystander cells. *Cancer Res* **67**, 5872-5879 (2007).

21. L. J. Wu, G. Randers-Pehrson, A. Xu, C. A. Waldren, C. R. Geard, Z. Yu and T. K. Hei, Targeted cytoplasmic irradiation with alpha particles induces mutations in mammalian cells. *Proc Natl Acad Sci U S A* **96**, 4959-4964 (1999).

22. J. K. Leach, S. M. Black, R. K. Schmidt-Ullrich and R. B. Mikkelsen, Activation of constitutive nitric-oxide synthase activity is an early signaling event induced by ionizing radiation. *J Biol Chem* **277**, 15400-15406 (2002).

23. J. K. Leach, G. Van Tuyle, P. S. Lin, R. Schmidt-Ullrich and R. B. Mikkelsen, Ionizing radiation-induced, mitochondria-dependent generation of reactive oxygen/nitrogen. *Cancer Res* **61**, 3894-3901 (2001).
24. R. E. Rugo, M. B. Secretan and R. H. Schiestl, X radiation causes a persistent induction of reactive oxygen species and a delayed reinduction of TP53 in normal human diploid fibroblasts. *Radiat Res* **158**, 210-219 (2002).
25. I. Hickson, Z. Yan, C. J. Richardson, S. J. Green, N. M. B. Martin, A. I. Orr, P. M. Reaper, S. P. Jackson, N. J. Curtin and G. C. M. Smith, Identification and characterization of a novel and specific inhibitor of the ataxia-telangiectasia mutated kinase ATM. *Cancer Research* **64**, 9152-9159 (2004).
26. N. Weizman, Y. Shiloh and A. Barzilai, Contribution of the Atm protein to maintaining cellular homeostasis evidenced by continuous activation of the AP-1 pathway in Atm-deficient brains. *J Biol Chem* **278**, 6741-6747 (2003).
27. S. E. Golding, E. Rosenberg, S. Neill, P. Dent, L. F. Povirk and K. Valerie, Extracellular signal-related kinase positively regulates ataxia telangiectasia mutated, homologous recombination repair, and the DNA damage response. *Cancer Res* **67**, 1046-1053 (2007).
28. A. Khalil, R. N. Morgan, B. R. Adams, S. E. Golding, S. M. Dever, E. Rosenberg, L. F. Povirk and K. Valerie, ATM-dependent ERK signaling via AKT in response to DNA double-strand breaks. *Cell Cycle* **10**, 481-491 (2011).
29. K. Dittmann, C. Mayer, B. Fehrenbacher, M. Schaller, U. Raju, L. Milas, D. J. Chen, R. Kehlbach and H. P. Rodemann, Radiation-induced epidermal growth factor receptor nuclear import is linked to activation of DNA-dependent protein kinase. *J Biol Chem* **280**, 31182-31189 (2005).
30. B. Mukherjee, B. McEllin, C. V. Camacho, N. Tomimatsu, S. Sirasanagandala, S. Nannepaga, K. J. Hatanpaa, B. Mickey, C. Madden, et al., EGFRvIII and DNA double-strand break repair: a molecular mechanism for radioresistance in glioblastoma. *Cancer Res* **69**, 4252-4259 (2009).
31. P. Dent, D. B. Reardon, J. S. Park, G. Bowers, C. Logsdon, K. Valerie and R. Schmidt-Ullrich, Radiation-induced release of transforming growth factor alpha activates the epidermal growth factor receptor and mitogen-activated protein kinase pathway in carcinoma cells, leading to increased proliferation and protection from radiation-induced cell death. *Mol Biol Cell* **10**, 2493-2506 (1999).
32. E. Gulbins and R. Kolesnick, Raft ceramide in molecular medicine. *Oncogene* **22**, 7070-7077 (2003).
33. K. Valerie, A. Yacoub, M. P. Hagan, D. T. Curiel, P. B. Fisher, S. Grant and P. Dent, Radiation-induced cell signaling: inside-out and outside-in. *Mol Cancer Ther* **6**, 789-801 (2007).
34. S. Braunstein, M. L. Badura, Q. Xi, S. C. Formenti and R. J. Schneider, Regulation of protein synthesis by ionizing radiation. *Mol Cell Biol* **29**, 5645-5656 (2009).
35. B. Endlich, I. R. Radford, H. B. Forrester and W. C. Dewey, Computerized video time-lapse microscopy studies of ionizing radiation-induced rapid-interphase and mitosis-related apoptosis in lymphoid cells. *Radiat Res* **153**, 36-48 (2000).
36. M. Garcia-Barros, F. Paris, C. Cordon-Cardo, D. Lyden, S. Rafii, A. Haimovitz-Friedman, Z. Fuks and R. Kolesnick, Tumor response to radiotherapy regulated by endothelial cell apoptosis. *Science* **300**, 1155-1159 (2003).
37. R. Kim, M. Emi, K. Tanabe, Y. Uchida and K. Arihiro, The role of apoptotic or nonapoptotic cell death in determining cellular response to anticancer treatment. *Ejso* **32**, 269-277 (2006).
38. I. B. Roninson, E. V. Broude and B. D. Chang, If not apoptosis, then what? Treatment-induced senescence and mitotic catastrophe in tumor cells. *Drug Resist Updat* **4**, 303-313 (2001).
39. H. B. Forrester, C. A. Vidair, N. Albright, C. C. Ling and W. C. Dewey, Using computerized video time lapse for quantifying cell death of X-irradiated rat embryo cells transfected with c-myc or c-Ha-ras. *Cancer Research* **59**, 931-939 (1999).

40. M. K. Bucci, A. Bevan and M. Roach, 3rd, Advances in radiation therapy: conventional to 3D, to IMRT, to 4D, and beyond. *CA Cancer J Clin* **55**, 117-134 (2005).
41. J. M. Bewes, N. Suchowerska, M. Jackson, M. Zhang and D. R. McKenzie, The radiobiological effect of intra-fraction dose-rate modulation in intensity modulated radiation therapy (IMRT). *Phys Med Biol* **53**, 3567-3578 (2008).
42. N. Tomita, Y. Shibamoto, M. Ito, H. Ogino, C. Sugie, S. Ayakawa and H. Iwata, Biological effect of intermittent radiation exposure in vivo: recovery from sublethal damage versus reoxygenation. *Radiother Oncol* **86**, 369-374 (2008).
43. J. P. Agarwal, B. Nemade, V. Murthy, S. Ghosh-Laskar, A. Budrukkar, T. Gupta, A. D'Cruz, P. Pai, P. Chaturvedi and K. Dinshaw, Hypofractionated, palliative radiotherapy for advanced head and neck cancer. *Radiother Oncol* **89**, 51-56 (2008).
44. A. Al-mamgani, L. Tans, P. H. Van rooij, I. Noever, R. J. Baatenburg de jong and P. C. Levendag, Hypofractionated radiotherapy denoted as the "Christie scheme": an effective means of palliating patients with head and neck cancers not suitable for curative treatment. *Acta Oncol* **48**, 562-570 (2009).
45. M. Guenzi, S. Vagge, N. C. Azinwi, A. D'Alonzo, L. Belgioia, S. Garelli, M. Gusinu and R. Corvo, A biologically competitive 21 days hypofractionation scheme with weekly concomitant boost in breast cancer radiotherapy feasibility acute sub-acute and short term late effects. *Radiat Oncol* **5**, 111 (2010).
46. J. O. Deasy, A. Niemierko, D. Herbert, D. Yan, A. Jackson, R. K. Ten Haken, M. Langer and S. Sapareto, Methodological issues in radiation dose-volume outcome analyses: summary of a joint AAPM/NIH workshop. *Med Phys* **29**, 2109-2127 (2002).
47. R. R. Wilson, Radiological Use of Fast Protons. *Radiology* **47**, 487-491 (1946).
48. C. A. Tobias, J. H. Lawrence, J. L. Born, R. K. Mccombs, J. E. Roberts, H. O. Anger, B. V. A. Lowbeer and C. B. Huggins, Pituitary Irradiation with High-Energy Proton Beams - Preliminary Report. *Cancer Research* **18**, 121-& (1958).
49. M. Goitein, Ed., *Radiation Oncology: A Physicist´s-Eye View*. Springer Science+Business Media, LLC, 2008.
50. A. Ottolenghi, M. Merzagora and H. G. Paretzke, DNA complex lesions induced by protons and alpha-particles: track structure characteristics determining linear energy transfer and particle type dependence. *Radiat Environ Biophys* **36**, 97-103 (1997).
51. G. W. Barendsen, C. J. Koot, G. R. Van Kersen, D. K. Bewley, S. B. Field and C. J. Parnell, The effect of oxygen on impairment of the proliferative capacity of human cells in culture by ionizing radiations of different LET. *Int J Radiat Biol Relat Stud Phys Chem Med* **10**, 317-327 (1966).
52. C. Allen, T. B. Borak, H. Tsujii and J. A. Nickoloff, Heavy charged particle radiobiology: Using enhanced biological effectiveness and improved beam focusing to advance cancer therapy. *Mutat Res* **711**, 150-157 (2011).
53. M. R. Raju, H. I. Amols, E. Bain, S. G. Carpenter, R. A. Cox and J. B. Robertson, A heavy particle comparative study. Part III: OER and RBE. *Br J Radiol* **51**, 712-719 (1978).
54. A. M. Koehler and W. M. Preston, Protons in radiation therapy. Comparative dose distributions for protons, photons, and electrons. *Radiology* **104**, 191-195 (1972).
55. J. K. Ashikawa, C. A. Sondhaus, C. A. Tobias, L. L. Kayfetz, S. O. Stephens and M. Donovan, Acute Effects of High-Energy Protons and Alpha Particles in Mice. *Radiation Research* **S**, 312-& (1967).
56. J. K. Ashikawa, Difference in injury mode, dose-rate dependence and RBE of 730-MeV protons, 100-kVp X-rays, and 200-kVp X-rays. *Biological Effects of Neutron and Proton Irradiation (Vienna, International Atomic Energy Agency)* **1**, 249-260 (1964).
57. G. V. Dalrymple, A series of articles on proton effects. *Radiation Research* **28**, 406-565 (1966).
58. J. Tepper, L. Verhey, M. Goitein and H. D. Suit, In vivo determinations of RBE in a high energy modulated proton beam using normal tissue reactions and fractionated dose schedules. *Int J Radiat Oncol Biol Phys* **2**, 1115-1122 (1977).
59. H. R. Withers and M. M. Elkind, Radiosensitivity and fractionation response of crypt cells of mouse jejunum. *Radiat Res* **38**, 598-613 (1969).

60. M. R. Raju and S. G. Carpenter, A heavy particle comparative study. Part IV: acute and late reactions. *Br J Radiol* **51**, 720-727 (1978).
61. M. R. Raju, Proton radiobiology, radiosurgery and radiotherapy. *Int J Radiat Biol* **67**, 237-259 (1995).
62. M. Urano, L. J. Verhey, M. Goitein, J. E. Tepper, H. D. Suit, O. Mendiondo, E. S. Gragoudas and A. Koehler, Relative biological effectiveness of modulated proton beams in various murine tissues. *Int J Radiat Oncol Biol Phys* **10**, 509-514 (1984).
63. B. Larsson, L. Leksell, B. Rexed, P. Sourander, W. Mair and B. Andersson, The high-energy proton beam as a neurosurgical tool. *Nature* **182**, 1222-1223 (1958).
64. L. Leksell, B. Larsson, B. Andersson, B. Rexed, P. Sourander and W. Mair, Lesions in the depth of the brain produced by a beam of high energy protons. *Acta radiol* **54**, 251-264 (1960).
65. B. Rexed, W. Mair, P. Sourander, B. Larsson and L. Leksell, Effect of High Energy Protons on the Brain of the Rabbit. *Acta Radiologica* **53**, 289-299 (1960).
66. I. J. Constable, M. Goitein, A. M. Koehler and R. A. Schmidt, Small-field irradiation of monkey eyes with protons and photons. *Radiat Res* **65**, 304-314 (1976).
67. T. Bortfeld, H. Paganetti and H. Kooy, Proton beam radiotherapy - The state of the art. *Medical Physics* **32**, 2048-2049 (2005).
68. E. Pedroni, T. Bohringer, A. Coray, E. Egger, M. Grossmann, S. X. Lin, A. Lomax, G. Goitein, W. Roser and B. Schaffner, Initial experience of using an active beam delivery technique at PSI. *Strahlentherapie Und Onkologie* **175**, 18-20 (1999).
69. A. J. Lomax, T. Boehringer, A. Coray, E. Egger, G. Goitein, M. Grossmann, P. Juelke, S. Lin, E. Pedroni, et al., Intensity modulated proton therapy: a clinical example. *Med Phys* **28**, 317-324 (2001).
70. T. F. Delaney, Ed., *Proton and Charged Particle Radiotherapy*. Lippincott Williams & Wilkins, 2007.
71. A. Henig, D. Kiefer, M. Geissler, S. G. Rykovanov, R. Ramis, R. Horlein, J. Osterhoff, Z. Major, L. Veisz, et al., Laser-driven shock acceleration of ion beams from spherical mass-limited targets. *Phys Rev Lett* **102**, 095002 (2009).
72. C. Greubel, W. Assmann, C. Burgdorf, G. Dollinger, G. Du, V. Hable, A. Hapfelmeier, R. Hertenberger, P. Kneschaurek, et al., Scanning irradiation device for mice in vivo with pulsed and continuous proton beams. *Radiat Environ Biophys* (2011).
73. T. E. Schmid, G. Dollinger, V. Hable, C. Greubel, O. Zlobinskaya, D. Michalski, M. Molls and B. Roeper, Relative biological effectiveness of pulsed and continuous 20 MeV protons for micronucleus induction in 3D human reconstructed skin tissue. *Radiotherapy and Oncology* **95**, 66-72 (2010).
74. C. Ares, E. B. Hug, A. J. Lomax, A. Bolsi, B. Timmermann, H. P. Rutz, J. C. Schuller, E. Pedroni and G. Goitein, Effectiveness and safety of spot scanning proton radiation therapy for chordomas and chondrosarcomas of the skull base: first long-term report. *Int J Radiat Oncol Biol Phys* **75**, 1111-1118 (2009).
75. J. E. Munzenrider, Proton therapy for uveal melanomas and other eye lesions. *Strahlenther Onkol* **175 Suppl 2**, 68-73 (1999).
76. A. Staab, H. P. Rutz, C. Ares, B. Timmermann, R. Schneider, A. Bolsi, F. Albertini, A. Lomax, G. Goitein and E. Hug, Spot-Scanning-Based Proton Therapy for Extracranial Chordoma. *Int J Radiat Oncol Biol Phys* (2011).
77. J. D. Slater, C. J. Rossi, Jr., L. T. Yonemoto, D. A. Bush, B. R. Jabola, R. P. Levy, R. I. Grove, W. Preston and J. M. Slater, Proton therapy for prostate cancer: the initial Loma Linda University experience. *Int J Radiat Oncol Biol Phys* **59**, 348-352 (2004).
78. W. H. St Clair, J. A. Adams, M. Bues, B. C. Fullerton, S. La Shell, H. M. Kooy, J. S. Loeffler and N. J. Tarbell, Advantage of protons compared to conventional X-ray or IMRT in the treatment of a pediatric patient with medulloblastoma. *Int J Radiat Oncol Biol Phys* **58**, 727-734 (2004).
79. D. R. Olsen, O. S. Bruland, G. Frykholm and I. N. Norderhaug, Proton therapy - a systematic review of clinical effectiveness. *Radiother Oncol* **83**, 123-132 (2007).

80. M. Lodge, M. Pijls-Johannesma, L. Stirk, A. J. Munro, D. De Ruysscher and T. Jefferson, A systematic literature review of the clinical and cost-effectiveness of hadron therapy in cancer. *Radiother Oncol* **83**, 110-122 (2007).
81. J. J. Coen, A. L. Zietman, C. J. Rossi, J. A. Grocela, J. A. Efstathiou, Y. Yan and W. U. Shipley, Comparison of High-Dose Proton Radiotherapy and Brachytherapy in Localized Prostate Cancer: A Case-Matched Analysis. *Int J Radiat Oncol Biol Phys* (2011).
82. H. Paganetti, A. Niemierko, M. Ancukiewicz, L. E. Gerweck, M. Goitein, J. S. Loeffler and H. D. Suit, Relative biological effectiveness (RBE) values for proton beam therapy. *Int J Radiat Oncol Biol Phys* **53**, 407-421 (2002).
83. C. Di Pietro, S. Piro, G. Tabbi, M. Ragusa, V. Di Pietro, V. Zimmitti, F. Cuda, M. Anello, U. Consoli, et al., Cellular and molecular effects of protons: Apoptosis induction and potential implications for cancer therapy. *Apoptosis* **11**, 57-66 (2006).
84. K. B. Lee, J. S. Lee, J. W. Park, T. L. Huh and Y. M. Lee, Low energy proton beam induces tumor cell apoptosis through reactive oxygen species and activation of caspases. *Exp Mol Med* **40**, 118-129 (2008).
85. A. M. Ristic-Fira, D. V. Todorovic, L. B. Koricanac, I. M. Petrovic, L. M. Valastro, P. G. A. Cirrone, L. Raffaele and G. Cuttone, Response of a human melanoma cell line to low and high ionizing radiation. *Ann Ny Acad Sci* **1095**, 165-174 (2007).
86. L. M. Green, D. K. Murray, A. M. Bant, G. Kazarians, M. F. Moyers, G. A. Nelson and D. T. Tran, Response of thyroid follicular cells to gamma irradiation compared to proton irradiation. I. Initial characterization of DNA damage, micronucleus formation, apoptosis, cell survival, and cell cycle phase redistribution. *Radiat Res* **155**, 32-42 (2001).
87. N. R. Galloway, J. R. Aspe, C. Sellers and N. R. Wall, Enhanced antitumor effect of combined gemcitabine and proton radiation in the treatment of pancreatic cancer. *Pancreas* **38**, 782-790 (2009).
88. E. Giedzinski, R. Rola, J. R. Fike and C. L. Limoli, Efficient production of reactive oxygen species in neural precursor cells after exposure to 250 MeV protons. *Radiat Res* **164**, 540-544 (2005).
89. C. Ziegler, D. Bonnefont-Rousselot, S. Delacroix, J. L. Habrand and A. Mazal, Effectiveness of protons and argon ions in initiating lipid peroxidation in low-density lipoproteins. *Radiat Res* **150**, 483-487 (1998).
90. S. Baluchamy, Y. Zhang, P. Ravichandran, V. Ramesh, A. Sodipe, J. C. Hall, O. Jejelowo, D. S. Gridley, H. Wu and G. T. Ramesh, Differential oxidative stress gene expression profile in mouse brain after proton exposure. *In Vitro Cell Dev Biol Anim* **46**, 718-725 (2010).
91. T. Ogata, T. Teshima, K. Kagawa, Y. Hishikawa, Y. Takahashi, A. Kawaguchi, Y. Suzumoto, K. Nojima, Y. Furusawa and N. Matsuura, Particle irradiation suppresses metastatic potential of cancer cells. *Cancer Res* **65**, 113-120 (2005).
92. V. Stisova, W. H. Abele, K. H. Thompson, P. V. Bennett and B. M. Sutherland, Response of Primary Human Fibroblasts Exposed to Solar Particle Event Protons. *Radiat Res* (2011).
93. J. W. Harper and S. J. Elledge, The DNA damage response: ten years after. *Mol Cell* **28**, 739-745 (2007).
94. S. P. Jackson and J. Bartek, The DNA-damage response in human biology and disease. *Nature* **461**, 1071-1078 (2009).
95. J. Bartek, J. Bartkova and J. Lukas, DNA damage signalling guards against activated oncogenes and tumour progression. *Oncogene* **26**, 7773-7779 (2007).
96. G. D. Wilson, Radiation and the cell cycle, revisited. *Cancer Metastasis Rev* **23**, 209-225 (2004).
97. J. Falck, J. Coates and S. P. Jackson, Conserved modes of recruitment of ATM, ATR and DNA-PKcs to sites of DNA damage. *Nature* **434**, 605-611 (2005).
98. M. Stucki and S. P. Jackson, gammaH2AX and MDC1: anchoring the DNA-damage-response machinery to broken chromosomes. *DNA Repair (Amst)* **5**, 534-543 (2006).
99. M. F. Lavin and S. Kozlov, ATM activation and DNA damage response. *Cell Cycle* **6**, 931-942 (2007).

100. V. Savic, B. Yin, N. L. Maas, A. L. Bredemeyer, A. C. Carpenter, B. A. Helmink, K. S. Yang-Iott, B. P. Sleckman and C. H. Bassing, Formation of dynamic gamma-H2AX domains along broken DNA strands is distinctly regulated by ATM and MDC1 and dependent upon H2AX densities in chromatin. *Mol Cell* **34**, 298-310 (2009).
101. J. An, Y. C. Huang, Q. Z. Xu, L. J. Zhou, Z. F. Shang, B. Huang, Y. Wang, X. D. Liu, D. C. Wu and P. K. Zhou, DNA-PKcs plays a dominant role in the regulation of H2AX phosphorylation in response to DNA damage and cell cycle progression. *BMC Mol Biol* **11**, 18 (2010).
102. S. Matsuoka, B. A. Ballif, A. Smogorzewska, E. R. McDonald, 3rd, K. E. Hurov, J. Luo, C. E. Bakalarski, Z. Zhao, N. Solimini, et al., ATM and ATR substrate analysis reveals extensive protein networks responsive to DNA damage. *Science* **316**, 1160-1166 (2007).
103. P. Hainaut and M. Hollstein, p53 and human cancer: The first ten thousand mutations. *Adv Cancer Res* **77**, 81-137 (2000).
104. B. Vogelstein, D. Lane and A. J. Levine, Surfing the p53 network. *Nature* **408**, 307-310 (2000).
105. J. Bartek, C. Lukas and J. Lukas, Checking on DNA damage in S phase. *Nat Rev Mol Cell Biol* **5**, 792-804 (2004).
106. N. Xu, N. Hegarat, E. J. Black, M. T. Scott, H. Hochegger and D. A. Gillespie, Akt/PKB suppresses DNA damage processing and checkpoint activation in late G2. *J Cell Biol* **190**, 297-305 (2010).
107. J. Huang, L. Zhang, J. Greshock, T. A. Colligon, Y. Wang, R. Ward, D. Katsaros, H. Lassus, R. Butzow, et al., Frequent genetic abnormalities of the PI3K/AKT pathway in primary ovarian cancer predict patient outcome. *Genes Chromosomes Cancer* (2011).
108. P. F. Wilson, J. M. Hinz, S. S. Urbin, P. B. Nham and L. H. Thompson, Influence of homologous recombinational repair on cell survival and chromosomal aberration induction during the cell cycle in gamma-irradiated CHO cells. *DNA Repair (Amst)* **9**, 737-744 (2010).
109. S. Neijenhuis, M. Verwijs-Janssen, U. Kasten-Pisula, G. Rumping, K. Borgmann, E. Dikomey, A. C. Begg and C. Vens, Mechanism of cell killing after ionizing radiation by a dominant negative DNA polymerase beta. *DNA Repair (Amst)* **8**, 336-346 (2009).
110. C. Vens and A. C. Begg, Targeting base excision repair as a sensitization strategy in radiotherapy. *Semin Radiat Oncol* **20**, 241-249 (2010).
111. E. K. Braithwaite, R. Prasad, D. D. Shock, E. W. Hou, W. A. Beard and S. H. Wilson, DNA polymerase lambda mediates a back-up base excision repair activity in extracts of mouse embryonic fibroblasts. *J Biol Chem* **280**, 18469-18475 (2005).
112. W. A. Beard, R. Prasad and S. H. Wilson, Activities and mechanism of DNA polymerase beta. *Method Enzymol* **408**, 91-107 (2006).
113. P. Fortini and E. Dogliotti, Base damage and single-strand break repair: mechanisms and functional significance of short- and long-patch repair subpathways. *DNA Repair (Amst)* **6**, 398-409 (2007).
114. L. Lan, S. Nakajima, Y. Oohata, M. Takao, S. Okano, M. Masutani, S. H. Wilson and A. Yasui, In situ analysis of repair processes for oxidative DNA damage in mammalian cells. *P Natl Acad Sci USA* **101**, 13738-13743 (2004).
115. K. W. Caldecott, XRCC1 and DNA strand break repair. *DNA Repair* **2**, 955-969 (2003).
116. K. W. Caldecott, C. K. Mckeown, J. D. Tucker, S. Ljungquist and L. H. Thompson, An Interaction between the Mammalian DNA-Repair Protein Xrcc1 and DNA Ligase-Iii. *Molecular and Cellular Biology* **14**, 68-76 (1994).
117. R. Fan, T. S. Kumaravel, F. Jalali, P. Marrano, J. A. Squire and R. G. Bristow, Defective DNA strand break repair after DNA damage in prostate cancer cells: Implications for genetic instability and prostate cancer progression. *Cancer Research* **64**, 8526-8533 (2004).
118. E. A. Price, S. L. Bourne, R. Radbourne, P. A. Lawton, J. Lamerdin, L. H. Thompson and J. E. Arrand, Rare microsatellite polymorphisms in the DNA repair genes XRCC1, XRCC3 and XRCC5 associated with cancer in patients of varying radiosensitivity. *Somat Cell Molec Gen* **23**, 237-247 (1997).

119. L. Q. Zhou, J. H. Xia, H. L. Li, J. R. Dai and Y. M. Hu, Association of XRCC1 Variants with Acute Skin Reaction After Radiotherapy in Breast Cancer Patients. *Cancer Biother Radio* **25**, 681-685 (2010).
120. E. C. Friedberg, How nucleotide excision repair protects against cancer. *Nat Rev Cancer* **1**, 22-33 (2001).
121. M. H. Lankinen, L. M. Vilpo and J. A. Vilpo, UV- and gamma-irradiation-induced DNA single-strand breaks and their repair in human blood granulocytes and lymphocytes. *Mutat Res-Fund Mol M* **352**, 31-38 (1996).
122. I. Kuraoka, C. Bender, A. Romieu, J. Cadet, R. D. Wood and T. Lindahl, Removal of oxygen free-radical-induced 5 ',8-purine cyclodeoxynucleosides from DNA by the nucleotide excisicon-repair pathway in human cells. *P Natl Acad Sci USA* **97**, 3832-3837 (2000).
123. D. A. Chistiakov, N. V. Voronova and P. A. Chistiakov, Genetic variations in DNA repair genes, radiosensitivity to cancer and susceptibility to acute tissue reactions in radiotherapy-treated cancer patients. *Acta Oncologica* **47**, 809-824 (2008).
124. K. Hiom, Coping with DNA double strand breaks. *DNA Repair (Amst)* **9**, 1256-1263 (2010).
125. B. Pardo, B. Gomez-Gonzalez and A. Aguilera, DNA repair in mammalian cells: DNA double-strand break repair: how to fix a broken relationship. *Cell Mol Life Sci* **66**, 1039-1056 (2009).
126. P. Huertas, DNA resection in eukaryotes: deciding how to fix the break. *Nat Struct Mol Biol* **17**, 11-16 (2010).
127. S. N. Powell and L. A. Kachnic, Roles of BRCA1 and BRCA2 in homologous recombination, DNA replication fidelity and the cellular response to ionizing radiation. *Oncogene* **22**, 5784-5791 (2003).
128. P. R. Bianco, R. B. Tracy and S. C. Kowalczykowski, DNA strand exchange proteins: a biochemical and physical comparison. *Front Biosci* **3**, D570-603 (1998).
129. I. Amitani, R. J. Baskin and S. C. Kowalczykowski, Visualization of Rad54, a chromatin remodeling protein, translocating on single DNA molecules. *Mol Cell* **23**, 143-148 (2006).
130. K. Valerie and L. F. Povirk, Regulation and mechanisms of mammalian double-strand break repair. *Oncogene* **22**, 5792-5812 (2003).
131. T. Helleday, J. Lo, D. C. van Gent and B. P. Engelward, DNA double-strand break repair: from mechanistic understanding to cancer treatment. *DNA Repair (Amst)* **6**, 923-935 (2007).
132. M. Sebesta, P. Burkovics, L. Haracska and L. Krejci, Reconstitution of DNA repair synthesis in vitro and the role of polymerase and helicase activities. *DNA Repair (Amst)* (2011).
133. N. Bennardo, A. Cheng, N. Huang and J. M. Stark, Alternative-NHEJ is a mechanistically distinct pathway of mammalian chromosome break repair. *PLoS Genet* **4**, e1000110 (2008).
134. D. Murray, R. E. Meyn and S. C. Vanankeren, Variations in the spectrum of lesions produced in the DNA of cells from mouse tissues after exposure to gamma-rays in air-breathing or in artificially anoxic animals. *Int J Radiat Biol Relat Stud Phys Chem Med* **53**, 921-933 (1988).
135. J. M. Hinz, N. A. Yamada, E. P. Salazar, R. S. Tebbs and L. H. Thompson, Influence of double-strand-break repair pathways on radiosensitivity throughout the cell cycle in CHO cells. *DNA Repair* **4**, 782-792 (2005).
136. S. Vispe, C. Cazaux, C. Lesca and M. Defais, Overexpression of Rad51 protein stimulates homologous recombination and increases resistance of mammalian cells to ionizing radiation. *Nucleic Acids Research* **26**, 2859-2864 (1998).
137. E. Sonoda, M. S. Sasaki, J. M. Buerstedde, O. Bezzubova, A. Shinohara, H. Ogawa, M. Takata, Y. Yamaguchi-Iwai and S. Takeda, Rad51-deficient vertebrate cells accumulate chromosomal breaks prior to cell death. *Embo J* **17**, 598-608 (1998).
138. T. Tsuzuki, Y. Fujii, K. Sakumi, Y. Tominaga, K. Nakao, M. Sekiguchi, A. Matsushiro, Y. Yoshimura and T. Morita, Targeted disruption of the Rad51 gene leads to lethality in embryonic mice. *P Natl Acad Sci USA* **93**, 6236-6240 (1996).

139. L. H. Thompson and D. Schild, Homologous recombinational repair of DNA ensures mammalian chromosome stability. *Mutat Res-Fund Mol M* **477**, 131-153 (2001).
140. C. Lengauer, K. W. Kinzler and B. Vogelstein, Genetic instabilities in human cancers. *Nature* **396**, 643-649 (1998).
141. Z. H. Zhou, E. Akgun and M. Jasin, Repeat expansion by homologous recombination in the mouse germ line at palindromic sequences. *P Natl Acad Sci USA* **98**, 8326-8333 (2001).
142. R. S. Maser, K. J. Monsen, B. E. Nelms and J. H. J. Petrini, hMre11 and hRad50 nuclear foci are induced during the normal cellular response to DNA double-strand breaks. *Molecular and Cellular Biology* **17**, 6087-6096 (1997).
143. M. S. Meyn, High Spontaneous Intrachromosomal Recombination Rates in Ataxia-Telangiectasia. *Science* **260**, 1327-1330 (1993).
144. C. Arias-Lopez, I. Lazaro-Trueba, P. Kerr, C. J. Lord, T. Dexter, M. Iravani, A. Ashworth and A. Silva, P53 modulates homologous recombination by transcriptional regulation of the RAD51 gene. *Embo Rep* **7**, 219-224 (2006).
145. C. Dudenhoffer, M. Kurth, F. Janus, W. Deppert and L. Wiesmuller, Dissociation of the recombination control and the sequence-specific transactivation function of P53. *Oncogene* **18**, 5773-5784 (1999).
146. K. L. Mekeel, W. Tang, L. A. Kachnic, C. M. Luo, J. S. DeFrank and S. N. Powell, Inactivation of p53 results in high rates of homologous recombination. *Oncogene* **14**, 1847-1857 (1997).
147. H. W. Sturzbecher, B. Donzelmann, W. Henning, U. Knippschild and S. Buchhop, p53 is linked directly to homologous recombination processes via RAD51/RecA protein interaction. *Embo J* **15**, 1992-2002 (1996).
148. Y. Saintigny, D. Rouillard, B. Chaput, T. Soussi and B. S. Lopez, Mutant p53 proteins stimulate spontaneous and radiation-induced intrachromosomal homologous recombination independently of the alteration of the transactivation activity and of the G1 checkpoint. *Oncogene* **18**, 3553-3563 (1999).
149. H. L. Klein, The consequences of Rad51 overexpression for normal and tumor cells. *DNA Repair* **7**, 686-693 (2008).
150. J. A. F. Hannay, J. H. Liu, Q. S. Zhu, S. V. Bolshakov, L. Li, P. W. T. Pisters, A. J. F. Lazar, D. H. Yu, R. E. Pollock and D. Lev, Rad51 overexpression contributes to chemoresistance in human soft tissue sarcoma cells: a role for p53/activator protein 2 transcriptional regulation. *Molecular Cancer Therapeutics* **6**, 1650-1660 (2007).
151. S. Buchhop, M. K. Gibson, X. W. Wang, P. Wagner, H. W. Sturzbecher and C. C. Harris, Interaction of p53 with the human Rad51 protein. *Nucleic Acids Research* **25**, 3868-3874 (1997).
152. S. P. Linke, S. Sengupta, N. Khabie, B. A. Jeffries, S. Buchhop, S. Miska, W. Henning, R. Pedeux, X. W. Wang, et al., p53 interacts with hRAD51 and hRAD54, and directly modulates homologous recombination. *Cancer Research* **63**, 2596-2605 (2003).
153. A. Slupianek, C. Schmutte, G. Tombline, M. Nieborowska-Skorska, G. Hoser, M. O. Nowicki, A. J. Pierce, R. Fishel and T. Skorski, BCR/ABL regulates mammalian RecA homologs, resulting in drug resistance. *Molecular Cell* **8**, 795-806 (2001).
154. F. Chen, A. Nastasi, Z. Shen, M. Brenneman, H. Crissman and D. J. Chen, Cell cycle-dependent protein expression of mammalian homologs of yeast DNA double-strand break repair genes Rad51 and Rad52. *Mutat Res* **384**, 205-211 (1997).
155. J. Flygare, F. Benson and D. Hellgren, Expression of the human RAD51 gene during the cell cycle in primary human peripheral blood lymphocytes. *Bba-Mol Cell Res* **1312**, 231-236 (1996).
156. W. Henning and H. W. Sturzbecher, Homologous recombination and cell cycle checkpoints: Rad51 in tumour progression and therapy resistance. *Toxicology* **193**, 91-109 (2003).
157. H. Maacke, C. Hundertmark, S. Miska, S. Voss, H. Kalthoff and H. W. Sturzbecher, Autoantibodies in sera of pancreatic cancer patients identify recombination factor Rad51 as a tumour-associated antigen. *J Cancer Res Clin* **128**, 219-222 (2002).

158. G. B. Qiao, Y. L. Wu, X. N. Yang, W. Z. Zhong, D. Xie, X. Y. Guan, D. Fischer, H. C. Kolberg, S. Kruger and H. W. Stuerzbecher, High-level expression of Rad51 is an independent prognostic marker of survival in non-small-cell lung cancer patients. *Brit J Cancer* **93**, 137-143 (2005).
159. S. J. Collis, A. Tighe, S. D. Scott, S. A. Roberts, J. H. Hendry and G. P. Margison, Ribozyme minigene-mediated RAD51 down-regulation increases radiosensitivity of human prostate cancer cells. *Nucleic Acids Research* **29**, 1534-1538 (2001).
160. T. Ohnishi, T. Taki, S. Hiraga, N. Arita and T. Morita, In vitro and in vivo potentiation of radiosensitivity of malignant gliomas by antisense inhibition of the RAD51 gene. *Biochem Bioph Res Co* **245**, 319-324 (1998).
161. N. Liu, J. E. Lamerdin, R. S. Tebbs, D. Schild, J. D. Tucker, M. R. Shen, K. W. Brookman, M. J. Siciliano, C. A. Walter, et al., XRCC2 and XRCC3, new human Rad51-family members, promote chromosome stability and protect against DNA cross-links and other damages. *Mol Cell* **1**, 783-793 (1998).
162. R. S. Tebbs, Y. Zhao, J. D. Tucker, J. B. Scheerer, M. J. Siciliano, M. Hwang, N. Liu, R. J. Legerski and L. H. Thompson, Correction of Chromosomal Instability and Sensitivity to Diverse Mutagens by a Cloned Cdna of the Xrcc3 DNA-Repair Gene. *P Natl Acad Sci USA* **92**, 6354-6358 (1995).
163. M. A. Brenneman, A. E. Weiss, J. A. Nickoloff and D. J. Chen, XRCC3 is required for efficient repair of chromosome breaks by homologous recombination. *Mutat Res-DNA Repair* **459**, 89-97 (2000).
164. D. K. Bishop, U. Ear, A. Bhattacharyya, C. Calderone, M. Beckett, R. R. Weichselbaum and A. Shinohara, Xrcc3 is required for assembly of Rad51 complexes in vivo. *Journal of Biological Chemistry* **273**, 21482-21488 (1998).
165. C. S. Griffin, P. J. Simpson, C. R. Wilson and J. Thacker, Mammalian recombination-repair genes XRCC2 and XRCC3 promote correct chromosome segregation. *Nat Cell Biol* **2**, 757-761 (2000).
166. J. Y. Masson, M. C. Tarsounas, A. Z. Stasiak, A. Stasiak, R. Shah, M. J. McIlwraith, F. E. Benson and S. C. West, Identification and purification of two distinct complexes containing the five RAD51 paralogs. *Gene Dev* **15**, 3296-3307 (2001).
167. J. Henry-Mowatt, D. Jackson, J. Y. Masson, P. A. Johnson, P. M. Clements, F. E. Benson, L. H. Thompson, S. Takeda, S. C. West and K. W. Caldecott, XRCC3 and Rad51 modulate replication fork progression on damaged vertebrate chromosomes. *Molecular Cell* **11**, 1109-1117 (2003).
168. Y. L. Liu, M. Tarsounas, P. O'Regan and S. C. West, Role of RAD51C and XRCC3 in genetic recombination and DNA repair. *Journal of Biological Chemistry* **282**, 1973-1979 (2007).
169. Y. C. Lio, D. Schild, M. A. Brenneman, J. L. Redpath and D. J. Chen, Human Rad51C deficiency destabilizes XRCC3, impairs recombination, and radiosensitizes S/G(2)-phase cells. *Journal of Biological Chemistry* **279**, 42313-42320 (2004).
170. N. A. Yamada, J. M. Hinz, V. L. Kopf, K. D. Segalle and L. H. Thompson, XRCC3 ATPase activity is required for normal XRCC3-Rad51C complex dynamics and homologous recombination. *J Biol Chem* **279**, 23250-23254 (2004).
171. M. A. Brenneman, B. M. Wagener, C. A. Miller, C. Allen and J. A. Nickoloff, XRCC3 controls the fidelity of homologous recombination: roles for XRCC3 in late stages of recombination. *Mol Cell* **10**, 387-395 (2002).
172. G. Nagaraju, A. Hartlerode, A. Kwok, G. Chandramouly and R. Scully, XRCC2 and XRCC3 Regulate the Balance between Short- and Long-Tract Gene Conversions between Sister Chromatids. *Molecular and Cellular Biology* **29**, 4283-4294 (2009).
173. A. L. Forget, B. T. Bennett and K. L. Knight, Xrcc3 is recruited to DNA double strand breaks early and independent of Rad51. *J Cell Biochem* **93**, 429-436 (2004).
174. T. Yoshihara, M. Ishida, A. Kinomura, M. Katsura, T. Tsuruga, S. Tashiro, T. Asahara and K. Miyagawa, XRCC3 deficiency results in a defect in recombination and increased endoreduplication in human cells. *Embo J* **23**, 670-680 (2004).
175. L. Jara, K. Dubois, D. Gaete, T. de Mayo, N. Ratkevicius, T. Bravo, S. Margarit, R. Blanco, F. Gomez, et al., Variants in DNA double-strand break repair genes and risk of

familial breast cancer in a South American population. *Breast Cancer Res Tr* **122**, 813-822 (2010).
176. T. Thorslund and S. C. West, BRCA2: a universal recombinase regulator. *Oncogene* **26**, 7720-7730 (2007).
177. J. J. Chen, D. Silver, S. Cantor, D. M. Livingston and R. Scully, BRCA1, BRCA2, and Rad51 operate in a common DNA damage response pathway. *Cancer Research* **59**, 1752s-1756s (1999).
178. R. Wooster, G. Bignell, J. Lancaster, S. Swift, S. Seal, J. Mangion, N. Collins, S. Gregory, C. Gumbs and G. Micklem, Identification of the breast cancer susceptibility gene BRCA2. *Nature* **378**, 789-792 (1995).
179. M. Tarsounas, A. A. Davies and S. C. West, RAD51 localization and activation following DNA damage. *Philos T Roy Soc B* **359**, 87-93 (2004).
180. S. F. L. Yuan, S-Y.; Chen, G., BRCA2 Is Required for Ionizing Radiation-induced Assembly of Rad51 Complex in Vivo. *Cancer Res* **59**, 3547-3551 (1999).
181. A. R. Venkitaraman, Cancer susceptibility and the functions of BRCA1 and BRCA2. *Cell* **108**, 171-182 (2002).
182. M. Kraakman-van der Zwet, W. J. I. Overkamp, R. E. E. van Lange, J. Essers, A. van Duijn-Goedhart, I. Wiggers, S. Swaminathan, P. P. W. van Buul, A. Errami, et al., Brca2 (XRCC11) deficiency results in radioresistant DNA synthesis and a higher frequency of spontaneous deletions. *Molecular and Cellular Biology* **22**, 669-679 (2002).
183. F. Xia, D. G. Taghian, J. S. DeFrank, Z. C. Zeng, H. Willers, G. Iliakis and S. N. Powell, Deficiency of human BRCA2 leads to impaired homologous recombination but maintains normal nonhomologous end joining. *P Natl Acad Sci USA* **98**, 8644-8649 (2001).
184. A. K. C. Wong, R. Pero, P. A. Ormonde, S. V. Tavtigian and P. L. Bartel, RAD51 interacts with the evolutionarily conserved BRC motifs in the human breast cancer susceptibility gene brca2. *Journal of Biological Chemistry* **272**, 31941-31944 (1997).
185. A. A. Davies, J. Y. Masson, M. J. Mcllwraith, A. Z. Stasiak, A. Stasiak, A. R. Venkitaraman and S. C. West, Role of BRCA2 in control of the RAD51 recombination and DNA repair protein. *Molecular Cell* **7**, 273-282 (2001).
186. M. Bogliolo, R. M. Taylor, K. W. Caldecott and G. Frosina, Reduced ligation during DNA base excision repair supported by BRCA2 mutant cells. *Oncogene* **19**, 5781-5787 (2000).
187. J. H. Wilson, P. B. Berget and J. M. Pipas, Somatic-Cells Efficiently Join Unrelated DNA Segments End-to-End. *Molecular and Cellular Biology* **2**, 1258-1269 (1982).
188. J. A. Downs and S. P. Jackson, A means to a DNA end: The many roles of Ku. *Nat Rev Mol Cell Bio* **5**, 367-378 (2004).
189. T. Mimori and J. A. Hardin, Mechanism of Interaction between Ku Protein and DNA. *Journal of Biological Chemistry* **261**, 375-379 (1986).
190. M. Hammel, Y. P. Yu, B. L. Mahaney, B. Cai, R. Q. Ye, B. M. Phipps, R. P. Rambo, G. L. Hura, M. Pelikan, et al., Ku and DNA-dependent Protein Kinase Dynamic Conformations and Assembly Regulate DNA Binding and the Initial Non-homologous End Joining Complex. *Journal of Biological Chemistry* **285**, 1414-1423 (2010).
191. M. R. Lieber, NHEJ and its backup pathways in chromosomal translocations. *Nature Structural & Molecular Biology* **17**, 393-395 (2010).
192. M. Yaneva, T. Kowalewski and M. R. Lieber, Interaction of DNA-dependent protein kinase with DNA and with Ku: biochemical and atomic-force microscopy studies. *Embo J* **16**, 5098-5112 (1997).
193. C. Wyman and R. Kanaar, DNA double-strand break repair: all's well that ends well. *Annu Rev Genet* **40**, 363-383 (2006).
194. E. Riballo, M. Kuhne, N. Rief, A. Doherty, G. C. M. Smith, M. J. Recio, C. Reis, K. Dahm, A. Fricke, et al., A pathway of double-strand break rejoining dependent upon ATM, artemis, and proteins locating to gamma-H2AX foci. *Molecular Cell* **16**, 715-724 (2004).
195. A. F. Moon, M. Garcia-Diaz, V. K. Batra, W. A. Beard, K. Bebenek, T. A. Kunkel, S. H. Wilson and L. C. Pedersen, The X family portrait: Structural insights into biological functions of X family polymerases. *DNA Repair* **6**, 1709-1725 (2007).

196. T. A. Dobbs, J. A. Tainer and S. P. Lees-Miller, A structural model for regulation of NHEJ by DNA-PKcs autophosphorylation. *DNA Repair* **9**, 1307-1314 (2010).
197. C. Kerzendorfer and M. O'Driscoll, Human DNA damage response and repair deficiency syndromes: Linking genomic instability and cell cycle checkpoint proficiency. *DNA Repair* **8**, 1139-1152 (2009).
198. H. Li, H. Vogel, V. B. Holcomb, Y. S. Gu and P. Hasty, Deletion of Ku70, Ku80, or both causes early aging without substantially increased cancer. *Molecular and Cellular Biology* **27**, 8205-8214 (2007).
199. M. R. Lieber, The Mechanism of Double-Strand DNA Break Repair by the Nonhomologous DNA End-Joining Pathway. *Annual Review of Biochemistry, Vol 79* **79**, 181-211 (2010).
200. L. Spagnolo, A. Rivera-Calzada, L. H. Pearl and O. Llorca, Three-dimensional structure of the human DNA-PKcs/Ku70/Ku80 complex assembled on DNA and its implications for DNA DSB repair. *Molecular Cell* **22**, 511-519 (2006).
201. K. Meek, S. Gupta, D. A. Ramsden and S. P. Lees-Miller, The DNA-dependent protein kinase: the director at the end. *Immunol Rev* **200**, 132-141 (2004).
202. D. Merkle, P. Douglas, G. B. G. Moorhead, Z. Leonenko, Y. P. Yu, D. Cramb, D. P. Bazett-Jones and S. P. Lees-Miller, The DNA-dependent protein kinase interacts with DNA to form a protein-DNA complex that is disrupted by phosphorylation. *Biochemistry-Us* **41**, 12706-12714 (2002).
203. J. Boskovic, A. Rivera-Calzada, J. D. Maman, P. Chacon, K. R. Willison, L. H. Pearl and O. Llorca, Visualization of DNA-induced conformational changes in the DNA repair kinase DNA-PKcs. *Embo J* **22**, 5875-5882 (2003).
204. C. W. Anderson, The DNA-activated protein kinase, DNA-PK. *Faseb J* **10**, D17-D17 (1996).
205. D. W. Chan, R. Q. Ye, C. J. Veillette and S. P. Lees-Miller, DNA-Dependent protein kinase phosphorylation sites in Ku 70/80 heterodimer. *Biochemistry-Us* **38**, 1819-1828 (1999).
206. Y. P. Yu, B. L. Mahaney, K. I. Yano, R. Q. Ye, S. J. Fang, P. Douglas, D. J. Chen and S. P. Lees-Miller, DNA-PK and ATM phosphorylation sites in XLF/Cernunnos are not required for repair of DNA double strand breaks. *DNA Repair* **7**, 1680-1692 (2008).
207. M. van der Burg, J. J. M. van Dongen and D. C. van Gent, DNA-PKcs deficiency in human: long predicted, finally found. *Curr Opin Allergy Cl* **9**, 503-509 (2009).
208. A. Kurimasa, S. Kumano, N. V. Boubnov, M. D. Story, C. S. Tung, S. R. Peterson and D. J. Chen, Requirement for the kinase activity of human DNA-dependent protein kinase catalytic subunit in DNA strand break rejoining. *Molecular and Cellular Biology* **19**, 3877-3884 (1999).
209. Q. Ding, Y. V. R. Reddy, W. Wang, T. Woods, P. Douglas, D. A. Ramsden, S. P. Lees-Miller and K. Meek, Autophosphorylation of the catalytic subunit of the DNA-dependent protein kinase is required for efficient end processing during DNA double-strand break repair. *Molecular and Cellular Biology* **23**, 5836-5848 (2003).
210. P. Douglas, G. P. Sapkota, N. Morrice, Y. P. Yu, A. A. Goodarzi, D. Merkle, K. Meek, D. R. Alessi and S. P. Lees-Miller, Identification of in vitro and in vivo phosphorylation sites in the catalytic subunit of the DNA-dependent protein kinase. *Biochemical Journal* **368**, 243-251 (2002).
211. S. Kuhfittig-Kulle, E. Feldmann, A. Odersky, A. Kuliczkowska, W. Goedecke, A. Eggert and P. Pfeiffer, The mutagenic potential of non-homologous end joining in the absence of the NHEJ core factors Ku70/80, DNA-PKcs and XRCC4-LigIV. *Mutagenesis* **22**, 217-233 (2007).
212. B. L. Ruis, K. R. Fattah and E. A. Hendrickson, The catalytic subunit of DNA-dependent protein kinase regulates proliferation, telomere length, and genomic stability in human somatic cells. *Mol Cell Biol* **28**, 6182-6195 (2008).
213. H. Lucero, D. Gae and G. E. Taccioli, Novel localization of the DNA-PK complex in lipid rafts. A putative role in the signal transduction pathway of the ionizing radiation response (vol 278, pg 22136, 2003). *Journal of Biological Chemistry* **278**, 45040-45040 (2003).

214. K. Iwabuchi, P. L. Bartel, B. Li, R. Marraccino and S. Fields, 2 Cellular Proteins That Bind to Wild-Type but Not Mutant P53. *P Natl Acad Sci USA* **91**, 6098-6102 (1994).
215. K. Iwabuchi, B. Li, H. F. Massa, B. J. Trask, T. Date and S. Fields, Stimulation of p53-mediated transcriptional activation by the p53-binding proteins, 53BP1 and 53BP2. *Journal of Biological Chemistry* **273**, 26061-26068 (1998).
216. J. E. FitzGerald, M. Grenon and N. F. Lowndes, 53BP1: function and mechanisms of focal recruitment. *Biochem Soc T* **37**, 897-904 (2009).
217. Y. Huyen, O. Zgheib, R. A. DiTullio, V. G. Gorgoulis, P. Zacharatos, T. J. Petty, E. A. Sheston, H. S. Mellert, E. S. Stavridi and T. D. Halazonetis, Methylated lysine 79 of histone H3 targets 53BP1 to DNA double-strand breaks. *Nature* **432**, 406-411 (2004).
218. J. Lee, J. R. Thompson, M. V. Botuyan and G. Mer, Distinct binding modes specify the recognition of methylated histones H3K4 and H4K20 by JMJD2A-tudor. *Nature Structural & Molecular Biology* **15**, 109-111 (2008).
219. R. A. DiTullio, T. A. Mochan, M. Venere, J. Bartkova, M. Sehested, J. Bartek and T. D. Halazonetis, 53BP1 functions in an ATM-dependent checkpoint pathway that is constitutively activated in human cancer. *Nat Cell Biol* **4**, 998-1002 (2002).
220. O. Fernandez-Capetillo, H. T. Chen, A. Celeste, I. Ward, P. J. Romanienko, J. C. Morales, K. Naka, Z. F. Xia, R. D. Camerini-Otero, et al., DNA damage-induced G(2)-M checkpoint activation by histone H2AX and 53BP1. *Nat Cell Biol* **4**, 993-997 (2002).
221. B. Wang, S. Matsuoka, P. B. Carpenter and S. J. Elledge, 53BP1, a mediator of the DNA damage checkpoint. *Science* **298**, 1435-1438 (2002).
222. K. Iwabuchi, M. Hashimoto, T. Matsui, T. Kurihara, H. Shimizu, N. Adachi, M. Ishiai, K. I. Yamamoto, H. Tauchi, et al., 53BP1 contributes to survival of cells irradiated with X-ray during G1 without Ku70 or Artemis. *Genes Cells* **11**, 935-948 (2006).
223. K. Nakamura, W. Sakai, T. Kawamoto, R. T. Bree, N. F. Lowndes, S. Takeda and Y. Taniguchi, Genetic dissection of vertebrate 53BP1: A major role in non-homologous end joining of DNA double strand breaks. *DNA Repair* **5**, 741-749 (2006).
224. L. B. Schultz, N. H. Chehab, A. Malikzay and T. D. Halazonetis, p53 Binding protein 1 (53BP1) is an early participant in the cellular response to DNA double-strand breaks. *Journal of Cell Biology* **151**, 1381-1390 (2000).
225. K. A. Wilson and D. F. Stern, NFBD1/MDC1, 53BP1 and BRCA1 have both redundant and unique roles in the ATM pathway. *Cell Cycle* **7**, 3584-3594 (2008).
226. L. Anderson, C. Henderson and Y. Adachi, Phosphorylation and rapid relocalization of 53BP1 to nuclear foci upon DNA damage. *Molecular and Cellular Biology* **21**, 1719-1729 (2001).
227. A. T. Noon, A. Shibata, N. Rief, M. Lobrich, G. S. Stewart, P. A. Jeggo and A. A. Goodarzi, 53BP1-dependent robust localized KAP-1 phosphorylation is essential for heterochromatic DNA double-strand break repair. *Nat Cell Biol* **12**, 177-U191 (2010).
228. M. A. de la Torre-Ruiz and N. F. Lowndes, The Saccharomyces cerevisiae DNA damage checkpoint is required for efficient repair of double strand breaks by non-homologous end joining. *Febs Lett* **467**, 311-315 (2000).
229. K. Iwabuchi, B. P. Basu, B. Kysela, T. Kurihara, M. Shibata, D. Y. Guan, Y. H. Cao, T. Hamada, K. Imamura, et al., Potential role for 53BP1 in DNA end-joining repair through direct interaction with DNA. *Journal of Biological Chemistry* **278**, 36487-36495 (2003).
230. S. F. Bunting, E. Callen, N. Wong, H. T. Chen, F. Polato, A. Gunn, A. Bothmer, N. Feldhahn, O. Fernandez-Capetillo, et al., 53BP1 Inhibits Homologous Recombination in Brca1-Deficient Cells by Blocking Resection of DNA Breaks. *Cell* **141**, 243-254 (2010).
231. Y. Eliezer, L. Argaman, A. Rhie, A. J. Doherty and M. Goldberg, The Direct Interaction between 53BP1 and MDC1 Is Required for the Recruitment of 53BP1 to Sites of Damage. *Journal of Biological Chemistry* **284**, 426-435 (2009).
232. N. K. Kolas, J. R. Chapman, S. Nakada, J. Ylanko, R. Chahwan, F. D. Sweeney, S. Panier, M. Mendez, J. Wildenhain, et al., Orchestration of the DNA-damage response by the RNF8 ubiquitin ligase. *Science* **318**, 1637-1640 (2007).
233. I. M. Ward, K. Minn, K. G. Jorda and J. J. Chen, Accumulation of checkpoint protein 53BP1 at DNA breaks involves its binding to phosphorylated histone H2AX. *Journal of Biological Chemistry* **278**, 19579-19582 (2003).

234. R. Murr, J. I. Loizou, Y. G. Yang, C. Cuenin, H. Li, Z. Q. Wang and Z. Herceg, Histone acetylation by Trrap-Tip60 modulates loading of repair proteins and repair of DNA double-strand breaks. *Nat Cell Biol* **8**, 91-U36 (2006).
235. N. Dimitrova, Y. C. M. Chen, D. L. Spector and T. de Lange, 53BP1 promotes non-homologous end joining of telomeres by increasing chromatin mobility. *Nature* **456**, 524-U551 (2008).
236. K. W. H. Lo, H. M. Kan, L. N. Chan, W. G. Xu, K. P. Wang, Z. G. Wu, M. Sheng and M. J. Zhang, The 8-kDa dynein light chain binds to p53-binding protein 1 and mediates DNA damage-induced p53 nuclear accumulation. *Journal of Biological Chemistry* **280**, 8172-8179 (2005).
237. E. B. Kabotyanski, L. Gomelsky, J. O. Han, T. D. Stamato and D. B. Roth, Double-strand break repair in Ku86- and XRCC4-deficient cells. *Nucleic Acids Research* **26**, 5333-5342 (1998).
238. M. S. Junop, M. Modesti, A. Guarne, R. Ghirlando, M. Gellert and W. Yang, Crystal structure of the Xrcc4 DNA repair protein and implications for end joining. *Embo J* **19**, 5962-5970 (2000).
239. B. L. Sibanda, S. E. Critchlow, J. Begun, X. Y. Pei, S. P. Jackson, T. L. Blundell and L. Pellegrini, Crystal structure of an Xrcc4-DNA ligase IV complex. *Nat Struct Biol* **8**, 1015-1019 (2001).
240. C. N. Wu, S. Y. Liang, C. W. Tsai and D. T. Bau, The Role of XRCC4 in Carcinogenesis and Anticancer Drug Discovery. *Recent Pat Anti-Canc* **3**, 209-219 (2008).
241. H. L. Hsu, S. M. Yannone and D. J. Chen, Defining interactions between DNA-PK and ligase IV/XRCC4. *DNA Repair* **1**, 225-235 (2002).
242. Y. P. Yu, W. Wang, Q. Ding, R. Q. Ye, D. Chen, D. Merkle, D. Schriemer, K. Meek and S. P. Lees-Miller, DNA-PK phosphorylation sites in XRCC4 are not required for survival after radiation or for V(D)J recombination. *DNA Repair* **2**, 1239-1252 (2003).
243. J. Drouet, C. Delteil, J. Lefrancois, P. Concannon, B. Salles and P. Calsou, DNA-dependent protein kinase and XRCC4-DNA ligase IV mobilization in the cell in response to DNA double strand breaks. *Journal of Biological Chemistry* **280**, 7060-7069 (2005).
244. L. Schulte-Uentrop, R. A. El-Awady, L. Schliecker, H. Willers and J. Dahm-Daphi, Distinct roles of XRCC4 and Ku80 in non-homologous end-joining of endonuclease- and ionizing radiation-induced DNA double-strand breaks. *Nucleic Acids Research* **36**, 2561-2569 (2008).
245. F. Delacote, M. G. Han, T. D. Stamato, M. Jasin and B. S. Lopez, An xrcc4 defect or Wortmannin stimulates homologous recombination specifically induced by double-strand breaks in mammalian cells. *Nucleic Acids Research* **30**, 3454-3463 (2002).
246. Y. Saintigny, F. Delacote, D. Boucher, D. Averbeck and B. S. Lopez, XRCC4 in G1 suppresses homologous recombination in S/G2, in G1 checkpoint-defective cells. *Oncogene* **26**, 2769-2780 (2007).
247. K. R. Jones, D. A. Gewirtz, S. M. Yannone, S. M. Zhou, D. G. Schatz, K. Valerie and L. F. Povirk, Radiosensitization of MDA-MB-231 breast tumor cells by adenovirus-mediated overexpression of a fragment of the XRCC4 protein. *Molecular Cancer Therapeutics* **4**, 1541-1547 (2005).
248. C. T. Yan, C. Boboila, E. K. Souza, S. Franco, T. R. Hickernell, M. Murphy, S. Gumaste, M. Geyer, A. A. Zarrin, et al., IgH class switching and translocations use a robust non-classical end-joining pathway. *Nature* **449**, 478-482 (2007).
249. Y. Katsura, S. Sasaki, M. Sato, K. Yamaoka, K. Suzukawa, T. Nagasawa, J. Yokota and T. Kohno, Involvement of Ku80 in microhomology-mediated end joining for DNA double-strand breaks in vivo. *DNA Repair* **6**, 639-648 (2007).
250. E. A. Rahal, L. A. Henricksen, Y. L. Li, R. S. Williams, J. A. Tainer and K. Dixon, ATM regulates Mre11-dependent DNA end-degradation and microhomology-mediated end joining. *Cell Cycle* **9**, 2866-2877 (2010).
251. E. Rass, A. Grabarz, I. Plo, J. Gautier, P. Bertrand and B. S. Lopez, Role of Mre11 in chromosomal nonhomologous end joining in mammalian cells. *Nature Structural & Molecular Biology* **16**, 819-U838 (2009).

252. A. Bothmer, D. F. Robbiani, N. Feldhahn, A. Gazumyan, A. Nussenzweig and M. C. Nussenzweig, 53BP1 regulates DNA resection and the choice between classical and alternative end joining during class switch recombination. *J Exp Med* **207**, 855-865 (2010).
253. H. Wang, Z. C. Zeng, T. A. Bui, S. J. DiBiase, W. Qin, F. Xia, S. N. Powell and G. Iliakis, Nonhomologous end-joining of ionizing radiation-induced DNA double-stranded breaks in human tumor cells deficient in BRCA1 or BRCA2. *Cancer Res* **61**, 270-277 (2001).
254. G. Iliakis, Backup pathways of NHEJ in cells of higher eukaryotes: cell cycle dependence. *Radiother Oncol* **92**, 310-315 (2009).
255. N. Puebla-Osorio, D. B. Lacey, F. W. Alt and C. M. Zhu, Early embryonic lethality due to targeted inactivation of DNA ligase III. *Molecular and Cellular Biology* **26**, 3935-3941 (2006).
256. H. C. Wang, B. Rosidi, R. Perrault, M. L. Wang, L. H. Zhang, F. Windhofer and G. Iliakis, DNA ligase III as a candidate component of backup pathways of nonhomologous end joining. *Cancer Research* **65**, 4020-4030 (2005).
257. M. Wang, W. Wu, B. Rosidi, L. Zhang, H. Wang and G. Iliakis, PARP-1 and Ku compete for repair of DNA double strand breaks by distinct NHEJ pathways. *Nucleic Acids Res* **34**, 6170-6182 (2006).
258. B. Rosidi, M. L. Wang, W. Q. Wu, A. Sharma, H. C. Wang and G. Iliakis, Histone H1 functions as a stimulatory factor in backup pathways of NHEJ. *Nucleic Acids Research* **36**, 1610-1623 (2008).
259. F. Windhofer, W. Q. Wu, M. L. Wang, S. K. Singh, J. Saha, B. Rosidi and G. Iliakis, Marked dependence on growth state of backup pathways of NHEJ. *Int J Radiat Oncol* **68**, 1462-1470 (2007).
260. B. R. Adams, A. J. Hawkins, L. F. Povirk and K. Valerie, ATM-independent, high-fidelity nonhomologous end joining predominates in human embryonic stem cells. *Aging (Albany NY)* **2**, 582-596 (2010).
261. M. Shrivastav, L. P. De Haro and J. A. Nickoloff, Regulation of DNA double-strand break repair pathway choice. *Cell Res* **18**, 134-147 (2008).
262. L. Brugmans, R. Kanaar and J. Essers, Analysis of DNA double-strand break repair pathways in mice. *Mutat Res* **614**, 95-108 (2007).
263. F. Fattah, E. H. Lee, N. Weisensel, Y. Wang, N. Lichter and E. A. Hendrickson, Ku regulates the non-homologous end joining pathway choice of DNA double-strand break repair in human somatic cells. *PLoS Genet* **6**, e1000855 (2010).
264. Z. Mao, M. Bozzella, A. Seluanov and V. Gorbunova, DNA repair by nonhomologous end joining and homologous recombination during cell cycle in human cells. *Cell Cycle* **7**, 2902-2906 (2008).
265. E. Mladenov, P. Kalev and B. Anachkova, The complexity of double-strand break ends is a factor in the repair pathway choice. *Radiat Res* **171**, 397-404 (2009).
266. K. Rothkamm, I. Kruger, L. H. Thompson and M. Lobrich, Pathways of DNA double-strand break repair during the mammalian cell cycle. *Molecular and Cellular Biology* **23**, 5706-5715 (2003).
267. P. Tamulevicius, M. Wang and G. Iliakis, Homology-directed repair is required for the development of radioresistance during S phase: interplay between double-strand break repair and checkpoint response. *Radiat Res* **167**, 1-11 (2007).
268. J. V. Harper, J. A. Anderson and P. O'Neill, Radiation induced DNA DSBs: Contribution from stalled replication forks? *DNA Repair (Amst)* **9**, 907-913 (2010).
269. P. Huertas and S. P. Jackson, Human CtIP mediates cell cycle control of DNA end resection and double strand break repair. *J Biol Chem* **284**, 9558-9565 (2009).
270. M. H. Yun and K. Hiom, CtIP-BRCA1 modulates the choice of DNA double-strand-break repair pathway throughout the cell cycle. *Nature* **459**, 460-463 (2009).
271. F. Esashi, N. Christ, J. Gannon, Y. Liu, T. Hunt, M. Jasin and S. C. West, CDK-dependent phosphorylation of BRCA2 as a regulatory mechanism for recombinational repair. *Nature* **434**, 598-604 (2005).
272. B. P. Chen, D. W. Chan, J. Kobayashi, S. Burma, A. Asaithamby, K. Morotomi-Yano, E. Botvinick, J. Qin and D. J. Chen, Cell cycle dependence of DNA-dependent protein kinase

phosphorylation in response to DNA double strand breaks. *J Biol Chem* **280**, 14709-14715 (2005).
273. S. E. Lee, R. A. Mitchell, A. Cheng and E. A. Hendrickson, Evidence for DNA-PK-dependent and -independent DNA double-strand break repair pathways in mammalian cells as a function of the cell cycle. *Mol Cell Biol* **17**, 1425-1433 (1997).
274. P. Bouwman, A. Aly, J. M. Escandell, M. Pieterse, J. Bartkova, H. van der Gulden, S. Hiddingh, M. Thanasoula, A. Kulkarni, et al., 53BP1 loss rescues BRCA1 deficiency and is associated with triple-negative and BRCA-mutated breast cancers. *Nat Struct Mol Biol* **17**, 688-695 (2010).
275. D. W. Abbott, M. L. Freeman and J. T. Holt, Double-strand break repair deficiency and radiation sensitivity in BRCA2 mutant cancer cells. *J Natl Cancer Inst* **90**, 978-985 (1998).
276. C. Allen, J. Halbrook and J. A. Nickoloff, Interactive competition between homologous recombination and non-homologous end joining. *Mol Cancer Res* **1**, 913-920 (2003).
277. C. Allen, A. Kurimasa, M. A. Brenneman, D. J. Chen and J. A. Nickoloff, DNA-dependent protein kinase suppresses double-strand break-induced and spontaneous homologous recombination. *Proc Natl Acad Sci U S A* **99**, 3758-3763 (2002).
278. E. Convery, E. K. Shin, Q. Ding, W. Wang, P. Douglas, L. S. Davis, J. A. Nickoloff, S. P. Lees-Miller and K. Meek, Inhibition of homologous recombination by variants of the catalytic subunit of the DNA-dependent protein kinase (DNA-PKcs). *Proc Natl Acad Sci U S A* **102**, 1345-1350 (2005).
279. Y. Peng, R. G. Woods, H. Beamish, R. Ye, S. P. Lees-Miller, M. F. Lavin and J. S. Bedford, Deficiency in the catalytic subunit of DNA-dependent protein kinase causes down-regulation of ATM. *Cancer Res* **65**, 1670-1677 (2005).
280. H. Wang, W. Boecker, X. Wang, J. Guan, L. H. Thompson, J. A. Nickoloff and G. Iliakis, Caffeine inhibits homology-directed repair of I-SceI-induced DNA double-strand breaks. *Oncogene* **23**, 824-834 (2004).
281. J. S. Kim, T. B. Krasieva, H. Kurumizaka, D. J. Chen, A. M. Taylor and K. Yokomori, Independent and sequential recruitment of NHEJ and HR factors to DNA damage sites in mammalian cells. *J Cell Biol* **170**, 341-347 (2005).
282. W. Y. Mansour, S. Schumacher, R. Rosskopf, T. Rhein, F. Schmidt-Petersen, F. Gatzemeier, F. Haag, K. Borgmann, H. Willers and J. Dahm-Daphi, Hierarchy of nonhomologous end-joining, single-strand annealing and gene conversion at site-directed DNA double-strand breaks. *Nucleic Acids Res* **36**, 4088-4098 (2008).
283. S. V. Costes, I. Chiolo, J. M. Pluth, M. H. Barcellos-Hoff and B. Jakob, Spatiotemporal characterization of ionizing radiation induced DNA damage foci and their relation to chromatin organization. *Mutat Res* **704**, 78-87 (2010).
284. L. J. Eccles, P. O'Neill and M. E. Lomax, Delayed repair of radiation induced clustered DNA damage: Friend or foe? *Mutat Res* **711**, 134-141 (2011).
285. B. M. Sutherland, P. V. Bennett, J. C. Sutherland and J. Laval, Clustered DNA damages induced by X rays in human cells. *Radiation Research* **157**, 611-616 (2002).
286. S. Malyarchuk, R. Castore and L. Harrison, DNA repair of clustered lesions in mammalian cells: involvement of non-homologous end-joining. *Nucleic Acids Research* **36**, 4872-4882 (2008).
287. P. Pace, G. Mosedale, M. R. Hodskinson, I. V. Rosado, M. Sivasubramaniam and K. J. Patel, Ku70 corrupts DNA repair in the absence of the Fanconi anemia pathway. *Science* **329**, 219-223 (2010).
288. A. G. Georgakilas, P. V. Bennett, D. M. Wilson and B. M. Sutherland, Processing of bistranded abasic DNA clusters in gamma-irradiated human hematopoietic cells. *Nucleic Acids Research* **32**, 5609-5620 (2004).
289. M. Gulston, C. de Lara, T. Jenner, E. Davis and P. O'Neill, Processing of clustered DNA damage generates additional double-strand breaks in mammalian cells post-irradiation. *Nucleic Acids Research* **32**, 1602-1609 (2004).
290. M. Hada and B. M. Sutherland, Spectrum of complex DNA damages depends on the incident radiation. *Radiat Res* **165**, 223-230 (2006).

291. M. Frankenberg-Schwager, A. Gebauer, C. Koppe, H. Wolf, E. Pralle and D. Frankenberg, Single-strand annealing, conservative homologous recombination, nonhomologous DNA end joining, and the cell cycle-dependent repair of DNA double-strand breaks induced by sparsely or densely ionizing radiation. *Radiat Res* **171**, 265-273 (2009).
292. A. Beucher, J. Birraux, L. Tchouandong, O. Barton, A. Shibata, S. Conrad, A. A. Goodarzi, A. Krempler, P. A. Jeggo and M. Lobrich, ATM and Artemis promote homologous recombination of radiation-induced DNA double-strand breaks in G2. *Embo J* **28**, 3413-3427 (2009).
293. S. Covo, J. P. de Villartay, P. A. Jeggo and Z. Livneh, Translesion DNA synthesis-assisted non-homologous end-joining of complex double-strand breaks prevents loss of DNA sequences in mammalian cells. *Nucleic Acids Res* **37**, 6737-6745 (2009).
294. J. M. Brown and L. D. Attardi, The role of apoptosis in cancer development and treatment response. *Nat Rev Cancer* **5**, 231-237 (2005).
295. A. T. Natarajan, A. Berni, K. M. Marimuthu and F. Palitti, The type and yield of ionising radiation induced chromosomal aberrations depend on the efficiency of different DSB repair pathways in mammalian cells. *Mutat Res* **642**, 80-85 (2008).
296. A. Gerelchuluun, Z. Hong, L. Sun, K. Suzuki, T. Terunuma, K. Yasuoka, T. Sakae, T. Moritake and K. Tsuboi, Induction of in situ DNA double-strand breaks and apoptosis by 200 MeV protons and 10 MV X-rays in human tumour cell lines. *Int J Radiat Biol* **87**, 57-70 (2011).
297. S. Matsubara, H. Ohara, T. Hiraoka, S. Koike, K. Ando, H. Yamaguchi, Y. Kuwabara, M. Hoshina and S. Suzuki, Chromosome aberration frequencies produced by a 70-MeV proton beam. *Radiat Res* **123**, 182-191 (1990).
298. L. Manti, M. Durante, G. Grossi, O. Ortenzia, M. Pugliese, P. Scampoli and G. Gialanella, Measurements of metaphase and interphase chromosome aberrations transmitted through early cell replication rounds in human lymphocytes exposed to low-LET protons and high-LET 12C ions. *Mutat Res* **596**, 151-165 (2006).
299. P. Y. Chang, J. Bakke, J. Orduna, S. Lin and R. Doppalaudi, Proton-induced genetic damage in lacZ transgenic mice. *Radiat Res* **164**, 481-486 (2005).
300. S. Baluchamy, Y. Zhang, P. Ravichandran, V. Ramesh, A. Sodipe, J. C. Hall, O. Jejelowo, D. S. Gridley, H. Wu and G. T. Ramesh, Expression profile of DNA damage signaling genes in 2 Gy proton exposed mouse brain. *Mol Cell Biochem* **341**, 207-215 (2010).
301. M. Biaggi, F. Ballarini, W. Burkard, E. Egger, A. Ferrari and A. Ottolenghi, Physical and biophysical characteristics of a fully modulated 72 MeV therapeutic proton beam: model predictions and experimental data. *Nucl Instrum Meth B* **159**, 89-100 (1999).
302. J. Gueulette, H. Blattmann, E. Pedroni, A. Coray, B. M. De Coster, P. Mahy, A. Wambersie and G. Goitein, Relative biologic effectiveness determination in mouse intestine for scanning proton beam at Paul Scherrer Institute, Switzerland. Influence of motion. *Int J Radiat Oncol Biol Phys* **62**, 838-845 (2005).
303. W. Friedland, P. Jacob, P. Bernhardt, H. G. Paretzke and M. Dingfelder, Simulation of DNA damage after proton irradiation. *Radiat Res* **159**, 401-410 (2003).
304. T. D. Griffiths and S. Y. Ling, Effect of ultraviolet light on DNA replication in excision-deficient mammalian cells. *Mutat Res* **132**, 119-127 (1984).
305. A. J. Pierce, R. D. Johnson, L. H. Thompson and M. Jasin, XRCC3 promotes homology-directed repair of DNA damage in mammalian cells. *Genes Dev* **13**, 2633-2638 (1999).
306. A. Errami, D. M. He, A. A. Friedl, W. J. Overkamp, B. Morolli, E. A. Hendrickson, F. Eckardt-Schupp, M. Oshimura, P. H. Lohman, et al., XR-C1, a new CHO cell mutant which is defective in DNA-PKcs, is impaired in both V(D)J coding and signal joint formation. *Nucleic Acids Res* **26**, 3146-3153 (1998).
307. M. Z. Zdzienicka, G. P. van der Schans, A. T. Natarajan, L. H. Thompson, I. Neuteboom and J. W. Simons, A Chinese hamster ovary cell mutant (EM-C11) with sensitivity to simple alkylating agents and a very high level of sister chromatid exchanges. *Mutagenesis* **7**, 265-269 (1992).
308. W. W. Wiegant, R. M. Overmeer, B. C. Godthelp, P. P. van Buul and M. Z. Zdzienicka, Chinese hamster cell mutant, V-C8, a model for analysis of Brca2 function. *Mutat Res* **600**, 79-88 (2006).

309. B. C. Godthelp, W. W. Wiegant, A. van Duijn-Goedhart, O. D. Scharer, P. P. van Buul, R. Kanaar and M. Z. Zdzienicka, Mammalian Rad51C contributes to DNA cross-link resistance, sister chromatid cohesion and genomic stability. *Nucleic Acids Res* **30**, 2172-2182 (2002).
310. J. E. Landers, S. L. Cassel and D. L. George, Translational enhancement of mdm2 oncogene expression in human tumor cells containing a stabilized wild-type p53 protein. *Cancer Res* **57**, 3562-3568 (1997).
311. E. Pedroni, R. Bacher, H. Blattmann, T. Bohringer, A. Coray, A. Lomax, S. X. Lin, G. Munkel, S. Scheib, et al., The 200-Mev Proton Therapy Project at the Paul-Scherrer-Institute - Conceptual Design and Practical Realization. *Medical Physics* **22**, 37-53 (1995).
312. T. Böhringer, http://radmed.web.psi.ch/asm/gantry/scan/n_scan.html.
313. N. A. Franken, H. M. Rodermond, J. Stap, J. Haveman and C. van Bree, Clonogenic assay of cells in vitro. *Nat Protoc* **1**, 2315-2319 (2006).
314. A. Staab, D. Zukowski, S. Walenta, M. Scholz and W. Mueller-Klieser, Response of Chinese hamster v79 multicellular spheroids exposed to high-energy carbon ions. *Radiat Res* **161**, 219-227 (2004).
315. S. H. MacPhail, J. P. Banath, Y. Yu, E. Chu and P. L. Olive, Cell cycle-dependent expression of phosphorylated histone H2AX: reduced expression in unirradiated but not X-irradiated G1-phase cells. *Radiat Res* **159**, 759-767 (2003).
316. M. Ito, S. Yamamoto, K. Nimura, K. Hiraoka, K. Tamai and Y. Kaneda, Rad51 siRNA delivered by HVJ envelope vector enhances the anti-cancer effect of cisplatin. *J Gene Med* **7**, 1044-1052 (2005).
317. P. Ahnesorg, P. Smith and S. P. Jackson, XLF interacts with the XRCC4-DNA ligase IV complex to promote DNA nonhomologous end-joining. *Cell* **124**, 301-313 (2006).
318. H. Luo, D. W. Chan, T. Yang, M. Rodriguez, B. P. Chen, M. Leng, J. J. Mu, D. Chen, Z. Songyang, et al., A new XRCC1-containing complex and its role in cellular survival of methyl methanesulfonate treatment. *Mol Cell Biol* **24**, 8356-8365 (2004).
319. T. K. Leung, M. Y. Rajendran, C. Monfries, C. Hall and L. Lim, The human heat-shock protein family. Expression of a novel heat-inducible HSP70 (HSP70B') and isolation of its cDNA and genomic DNA. *Biochem J* **267**, 125-132 (1990).
320. S. Bekker-Jensen, C. Lukas, R. Kitagawa, F. Melander, M. B. Kastan, J. Bartek and J. Lukas, Spatial organization of the mammalian genome surveillance machinery in response to DNA strand breaks. *J Cell Biol* **173**, 195-206 (2006).
321. J. H. Tjio and T. T. Puck, Genetics of Somatic Mammalian Cells .2. Chromosomal Constitution of Cells in Tissue Culture. *J Exp Med* **108**, 259-& (1958).
322. D. K. Ford and G. Yerganian, Observations on the Chromosomes of Chinese Hamster Cells in Tissue Culture. *J Natl Cancer I* **21**, 393-& (1958).
323. D. F. Krahn, Chinese-Hamster Cell Mutagenesis - a Comparison of the Cho and V79-Systems. *Annals of the New York Academy of Sciences* **407**, 231-238 (1983).
324. J. Thacker and M. Z. Zdzienicka, The mammalian XRCC genes: their roles in DNA repair and genetic stability. *DNA Repair* **2**, 655-672 (2003).
325. W. R. Chaung, L. J. Mi and R. J. Boorstein, The p53 status of Chinese hamster V79 cells frequently used for studies on DNA damage and DNA repair. *Nucleic Acids Research* **25**, 992-994 (1997).
326. H. Lee, J. M. Larner and J. L. Hamlin, Cloning and characterization of Chinese hamster p53 cDNA. *Gene* **184**, 177-183 (1997).
327. D. P. Lane, C. F. Cheok and S. Lain, p53-based cancer therapy. *Cold Spring Harb Perspect Biol* **2**, a001222 (2010).
328. S. C. West, Molecular views of recombination proteins and their control. *Nat Rev Mol Cell Biol* **4**, 435-445 (2003).
329. T. Groesser, H. Chang, G. Fontenay, J. Chen, S. V. Costes, M. Helen Barcellos-Hoff, B. Parvin and B. Rydberg, Persistence of gamma-H2AX and 53BP1 foci in proliferating and non-proliferating human mammary epithelial cells after exposure to gamma-rays or iron ions. *Int J Radiat Biol* (2011).
330. E. Fokas, G. Kraft, H. An and R. Engenhart-Cabillic, Ion beam radiobiology and cancer: time to update ourselves. *Biochim Biophys Acta* **1796**, 216-229 (2009).

331. J. Thacker and M. Z. Zdzienicka, The XRCC genes: expanding roles in DNA double-strand break repair. *DNA Repair (Amst)* **3**, 1081-1090 (2004).
332. T. Uziel, Y. Lerenthal, L. Moyal, Y. Andegeko, L. Mittelman and Y. Shiloh, Requirement of the MRN complex for ATM activation by DNA damage. *Embo J* **22**, 5612-5621 (2003).
333. M. Lobrich, A. Shibata, A. Beucher, A. Fisher, M. Ensminger, A. A. Goodarzi, O. Barton and P. A. Jeggo, gammaH2AX foci analysis for monitoring DNA double-strand break repair: strengths, limitations and optimization. *Cell Cycle* **9**, 662-669 (2010).
334. P. L. Olive, Retention of gammaH2AX foci as an indication of lethal DNA damage. *Radiother Oncol* (2011).
335. M. J. Rossi, O. M. Mazina, D. V. Bugreev and A. V. Mazin, The RecA/RAD51 protein drives migration of Holliday junctions via polymerization on DNA. *Proc Natl Acad Sci U S A* **108**, 6432-6437 (2011).
336. M. Shrivastav, C. A. Miller, L. P. De Haro, S. T. Durant, B. P. Chen, D. J. Chen and J. A. Nickoloff, DNA-PKcs and ATM co-regulate DNA double-strand break repair. *DNA Repair (Amst)* **8**, 920-929 (2009).
337. R. Okayasu, M. Okada, A. Okabe, M. Noguchi, K. Takakura and S. Takahashi, Repair of DNA damage induced by accelerated heavy ions in mammalian cells proficient and deficient in the non-homologous end-joining pathway. *Radiat Res* **165**, 59-67 (2006).
338. C. J. Bakkenist and M. B. Kastan, DNA damage activates ATM through intermolecular autophosphorylation and dimer dissociation. *Nature* **421**, 499-506 (2003).
339. O. S. Gildemeister, J. M. Sage and K. L. Knight, Cellular Redistribution of Rad51 in Response to DNA Damage NOVEL ROLE FOR Rad51C. *Journal of Biological Chemistry* **284**, 31945-31952 (2009).
340. Y. L. Liu, J. Y. Masson, R. Shah, P. O'Regan and S. C. West, RAD51C is required for Holliday junction processing in mammalian cells. *Science* **303**, 243-246 (2004).
341. D. J. Gallagher, M. M. Gaudet, P. Pal, T. Kirchhoff, L. Balistreri, K. Vora, J. Bhatia, Z. Stadler, S. W. Fine, et al., Germline BRCA mutations denote a clinicopathologic subset of prostate cancer. *Clin Cancer Res* **16**, 2115-2121 (2010).
342. T. Kirchhoff, N. D. Kauff, N. Mitra, K. Nafa, H. Huang, C. Palmer, T. Gulati, E. Wadsworth, S. Donat, et al., BRCA mutations and risk of prostate cancer in Ashkenazi Jews. *Clin Cancer Res* **10**, 2918-2921 (2004).
343. H. C. Wang, Z. C. Zeng, T. A. Bui, E. Sonoda, M. Takata, S. Takeda and G. Iliakis, Efficient rejoining of radiation-induced DNA double-strand breaks in vertebrate cells deficient in genes of the RAD52 epistasis group. *Oncogene* **20**, 2212-2224 (2001).
344. A. A. Sartori, C. Lukas, J. Coates, M. Mistrik, S. Fu, J. Bartek, R. Baer, J. Lukas and S. P. Jackson, Human CtIP promotes DNA end resection. *Nature* **450**, 509-514 (2007).
345. D. W. Abbott, M. E. Thompson, C. Robinson-Benion, G. Tomlinson, R. A. Jensen and J. T. Holt, BRCA1 expression restores radiation resistance in BRCA1-defective cancer cells through enhancement of transcription-coupled DNA repair. *J Biol Chem* **274**, 18808-18812 (1999).
346. Z. H. Feng, S. P. Scott, W. Bussen, G. G. Sharma, G. S. Guo, T. K. Pandita and S. N. Powell, Rad52 inactivation is synthetically lethal with BRCA2 deficiency. *P Natl Acad Sci USA* **108**, 686-691 (2011).
347. Y. Qing, M. Yamazoe, K. Hirota, D. Dejsuphong, W. Sakai, K. N. Yamamoto, D. K. Bishop, X. Wu and S. Takeda, The Epistatic Relationship between BRCA2 and the Other RAD51 Mediators in Homologous Recombination. *PLoS Genet* **7**, e1002148 (2011).
348. R. Ugenskiene, K. Prise, M. Folkard, J. Lekki, Z. Stachura, M. Zazula and J. Stachura, Dose response and kinetics of foci disappearance following exposure to high- and low-LET ionizing radiation. *Int J Radiat Biol* **85**, 872-882 (2009).
349. H. Moertel, J. C. Georgi, L. Distel, W. Eyrich, M. Fritsch, G. Grabenbauer and R. Sauer, Effects of low energy protons on clonogenic survival, DSB repair and cell cycle in human glioblastoma cells and B14 fibroblasts. *Radiother Oncol* **73 Suppl 2**, S115-118 (2004).
350. M. A. Al-Mohanna, P. S. Manogaran, Z. Al-Mukhalafi, K. A. Al-Hussein and A. Aboussekhra, The tumor suppressor p16(INK4a) gene is a regulator of apoptosis induced by ultraviolet light and cisplatin. *Oncogene* **23**, 201-212 (2004).

351. V. A. Florenes, G. M. Maelandsmo, A. Forus, A. Andreassen, O. Myklebost and O. Fodstad, Mdm2 Gene Amplification and Transcript Levels in Human Sarcomas - Relationship to Tp53 Gene Status. *J Natl Cancer I* **86**, 1297-1302 (1994).
352. L. A. Allan and M. Fried, p53-dependent apoptosis or growth arrest induced by different forms of radiation in U2OS cells: p21(WAF1/CIP1) repression in UV induced apoptosis. *Oncogene* **18**, 5403-5412 (1999).
353. A. Stepien, A. Grzanka, D. Grzanka, M. Andrzej Szczepanski, A. Helmin-Basa and L. Gackowska, Taxol-induced polyploidy and cell death in CHO AA8 cells. *Acta Histochem* **112**, 62-71 (2010).
354. Z. Somodi, N. A. Zyuzikov, G. Kashino, K. R. Trott and K. M. Prise, Radiation-induced genomic instability in repair deficient mutants of Chinese hamster cells. *International Journal of Radiation Biology* **81**, 929-936 (2005).
355. D. V. Guryev, A. N. Osipov, E. Y. Lizunova, N. Y. Vorobyeva and O. V. Boeva, Ionizing radiation-induced genomic instability in CHO cells is followed by selection of radioresistant cell clones. *Bull Exp Biol Med* **147**, 596-598 (2009).
356. E. Firat, S. Gaedicke, C. Tsurumi, N. Esser, A. Weyerbrock and G. Niedermann, Delayed cell death associated with mitotic catastrophe in gamma-irradiated stem-like glioma cells. *Radiat Oncol* **6**, 71 (2011).
357. J. M. R. Dealmodovar, C. Bush, J. H. Peacock, G. G. Steel, S. J. Whitaker and T. J. Mcmillan, Dose-Rate Effect for DNA-Damage Induced by Ionizing-Radiation in Human Tumor-Cells. *Radiation Research* **138**, S93-S96 (1994).
358. E. Dikomey and I. Brammer, Relationship between cellular radiosensitivity and non-repaired double-strand breaks studied for different growth states, dose rates and plating conditions in a normal human fibroblast line. *International Journal of Radiation Biology* **76**, 773-781 (2000).
359. I. Lohse, S. Lang, J. Hrbacek, S. Scheidegger, S. Bodis, N. S. Macedo, J. Feng, U. M. Lutolf and K. Zaugg, Effect of high dose per pulse flattening filter-free beams on cancer cell survival. *Radiother Oncol* (2011).
360. M. A. Hill, M. T. Herdman, D. L. Stevens, N. J. Jones, J. Thacker and D. T. Goodhead, Relative sensitivities of repair-deficient mammalian cells for clonogenic survival after alpha-particle irradiation. *Radiat Res* **162**, 667-676 (2004).
361. H. Wang, S. Liu, P. Zhang, S. Zhang, M. Naidu and Y. Wang, S-phase cells are more sensitive to high-linear energy transfer radiation. *Int J Radiat Oncol Biol Phys* **74**, 1236-1241 (2009).
362. F. Zafar, S. B. Seidler, A. Kronenberg, D. Schild and C. Wiese, Homologous recombination contributes to the repair of DNA double-strand breaks induced by high-energy iron ions. *Radiat Res* **173**, 27-39 (2010).
363. M. Lassmann, H. Hanscheid, D. Gassen, J. Biko, V. Meineke, C. Reiners and H. Scherthan, In vivo formation of gamma-H2AX and 53BP1 DNA repair foci in blood cells after radioiodine therapy of differentiated thyroid cancer. *J Nucl Med* **51**, 1318-1325 (2010).
364. S. Takeda, E. Sonoda, H. Hochegger, A. Saberi and Y. Taniguchi, Differential usage of non-homologous end-joining and homologous recombination in double strand break repair. *DNA Repair* **5**, 1021-1029 (2006).
365. N. Saleh-Gohari, H. E. Bryant, N. Schultz, K. M. Parker, T. N. Cassel and T. Helleday, Spontaneous homologous recombination is induced by collapsed replication forks that are caused by endogenous DNA single-strand breaks. *Mol Cell Biol* **25**, 7158-7169 (2005).
366. H. Wang, X. Wang, P. Zhang and Y. Wang, The Ku-dependent non-homologous end-joining but not other repair pathway is inhibited by high linear energy transfer ionizing radiation. *DNA Repair (Amst)* **7**, 725-733 (2008).
367. H. Wang, X. Zhang, P. Wang, X. Yu, J. Essers, D. Chen, R. Kanaar, S. Takeda and Y. Wang, Characteristics of DNA-binding proteins determine the biological sensitivity to high-linear energy transfer radiation. *Nucleic Acids Res* **38**, 3245-3251 (2010).
368. J. A. Nickoloff, M. Shrivastav, C. A. Miller, L. P. De Haro, S. T. Durant, B. P. C. Chen and D. J. Chen, DNA-PKcs and ATM co-regulate DNA double-strand break repair. *DNA Repair* **8**, 920-929 (2009).

369. M. S. Fernandes, M. M. Reddy, J. R. Gonneville, S. C. DeRoo, K. Podar, J. D. Griffin, D. M. Weinstock and M. Sattler, BCR-ABL promotes the frequency of mutagenic single-strand annealing DNA repair. *Blood* **114**, 1813-1819 (2009).
370. S. M. J. Afzal, T. S. Tenforde, S. S. Parr and S. B. Curtis, Pld Repair in Rat Rhabdomyosarcoma Tumor-Cells Irradiated Invivo and Invitro with High-Let and Low-Let Radiation. *Radiation Research* **107**, 354-366 (1986).
371. H. J. Baek, T. H. Kim, D. Shin, J. W. Kwak, D. W. Choo, S. B. Lee, Y. Furusawa, K. Ando, S. S. Kim and K. H. Cho, Radiobiological characterization of proton beam at the National Cancer Center in Korea. *J Radiat Res (Tokyo)* **49**, 509-515 (2008).
372. S. Ritter and M. Durante, Heavy-ion induced chromosomal aberrations: a review. *Mutat Res* **701**, 38-46 (2010).
373. L. L. Deaven and D. F. Petersen, The chromosomes of CHO, an aneuploid Chinese hamster cell line: G-band, C-band, and autoradiographic analyses. *Chromosoma* **41**, 129-144 (1973).
374. I. Petrovic, A. Ristic-Fira, D. Todorovic, L. Koricanac, L. Valastro, P. Cirrone and G. Cuttone, Response of a radioresistant human melanoma cell line along the proton spread-out Bragg peak. *International Journal of Radiation Biology* **86**, 742-751 (2010).
375. F. Li, Q. Huang, J. Chen, Y. Peng, D. R. Roop, J. S. Bedford and C. Y. Li, Apoptotic cells activate the "phoenix rising" pathway to promote wound healing and tissue regeneration. *Sci Signal* **3**, ra13 (2010).
376. L. Tryggvadottir, L. Vidarsdottir, T. Thorgeirsson, J. G. Jonasson, E. J. Olafsdottir, G. H. Olafsdottir, T. Rafnar, S. Thorlacius, E. Jonsson, et al., Prostate cancer progression and survival in BRCA2 mutation carriers. *J Natl Cancer Inst* **99**, 929-935 (2007).
377. A. G. Pallis and M. V. Karamouzis, DNA repair pathways and their implication in cancer treatment. *Cancer Metastasis Rev* **29**, 677-685 (2010).
378. J. Thoms and R. G. Bristow, DNA repair targeting and radiotherapy: a focus on the therapeutic ratio. *Semin Radiat Oncol* **20**, 217-222 (2010).
379. A. J. Chalmers, M. Lakshman, N. Chan and R. G. Bristow, Poly(ADP-ribose) polymerase inhibition as a model for synthetic lethality in developing radiation oncology targets. *Semin Radiat Oncol* **20**, 274-281 (2010).
380. M. A. Gimbrone, Jr., S. B. Leapman, R. S. Cotran and J. Folkman, Tumor dormancy in vivo by prevention of neovascularization. *J Exp Med* **136**, 261-276 (1972).
381. G. Helmlinger, F. Yuan, M. Dellian and R. K. Jain, Interstitial pH and pO2 gradients in solid tumors in vivo: high-resolution measurements reveal a lack of correlation. *Nat Med* **3**, 177-182 (1997).
382. R. S. Bindra, P. J. Schaffer, A. Meng, J. Woo, K. Maseide, M. E. Roth, P. Lizardi, D. W. Hedley, R. G. Bristow and P. M. Glazer, Down-regulation of Rad51 and decreased homologous recombination in hypoxic cancer cells. *Mol Cell Biol* **24**, 8504-8518 (2004).
383. N. Chan, M. Koritzinsky, H. Zhao, R. Bindra, P. M. Glazer, S. Powell, A. Belmaaza, B. Wouters and R. G. Bristow, Chronic hypoxia decreases synthesis of homologous recombination proteins to offset chemoresistance and radioresistance. *Cancer Res* **68**, 605-614 (2008).
384. Z. Mao, Y. Jiang, X. Liu, A. Seluanov and V. Gorbunova, DNA repair by homologous recombination, but not by nonhomologous end joining, is elevated in breast cancer cells. *Neoplasia* **11**, 683-691 (2009).
385. J. Guirouilh-Barbat, S. Huck and B. S. Lopez, S-phase progression stimulates both the mutagenic KU-independent pathway and mutagenic processing of KU-dependent intermediates, for nonhomologous end joining. *Oncogene* **27**, 1726-1736 (2008).
386. E. Gotoh and M. Durante, Chromosome condensation outside of mitosis: mechanisms and new tools. *J Cell Physiol* **209**, 297-304 (2006).
387. L. Diller, J. Kassel, C. E. Nelson, M. A. Gryka, G. Litwak, M. Gebhardt, B. Bressac, M. Ozturk, S. J. Baker, et al., P53 Functions as a Cell-Cycle Control Protein in Osteosarcomas. *Molecular and Cellular Biology* **10**, 5772-5781 (1990).
388. K. Okaichi, L. H. Wang, M. Ihara and Y. Okumura, Sensitivity to ionizing radiation in Saos-2 cells transfected with mutant p53 genes depends on the mutation position. *J Radiat Res (Tokyo)* **39**, 111-118 (1998).

389. A. Ashworth, A synthetic lethal therapeutic approach: poly(ADP) ribose polymerase inhibitors for the treatment of cancers deficient in DNA double-strand break repair. *J Clin Oncol* **26**, 3785-3790 (2008).
390. H. E. Bryant, N. Schultz, H. D. Thomas, K. M. Parker, D. Flower, E. Lopez, S. Kyle, M. Meuth, N. J. Curtin and T. Helleday, Specific killing of BRCA2-deficient tumours with inhibitors of poly(ADP-ribose) polymerase. *Nature* **434**, 913-917 (2005).
391. G. P. Dimri, X. H. Lee, G. Basile, M. Acosta, C. Scott, C. Roskelley, E. E. Medrano, M. Linskens, I. Rubelj, et al., A Biomarker That Identifies Senescent Human-Cells in Culture and in Aging Skin in-Vivo. *P Natl Acad Sci USA* **92**, 9363-9367 (1995).
392. W. M. Keyes, Y. Wu, H. Vogel, X. C. Guo, S. W. Lowe and A. A. Mills, p63 deficiency activates a program of cellular senescence and leads to accelerated aging. *Gene Dev* **19**, 1986-1999 (2005).
393. K. R. Kozak, B. L. Smith, J. Adams, E. Kornmehl, A. Katz, M. Gadd, M. Specht, K. Hughes, V. Gioioso, et al., Accelerated partial-breast irradiation using proton beams: initial clinical experience. *Int J Radiat Oncol Biol Phys* **66**, 691-698 (2006).
394. D. A. Bush, J. D. Slater, C. Garberoglio, S. Do, S. Lum and J. M. Slater, Partial Breast Irradiation Delivered With Proton Beam: Results of a Phase II Trial. *Clin Breast Cancer* (2011).
395. S. Rieken, D. Habermehl, A. Nikoghosyan, A. Jensen, T. Haberer, O. Jakel, M. W. Munter, T. Welzel, J. Debus and S. E. Combs, Assessment of Early Toxicity and Response in Patients Treated With Proton and Carbon Ion Therapy at The Heidelberg Ion Therapy Center Using The Raster Scanning Technique. *Int J Radiat Oncol Biol Phys* (2011).
396. M. L. Chua, N. Somaiah, S. Bourne, F. Daley, R. A'Hern, O. Nuta, S. Davies, C. Herskind, A. Pearson, et al., Inter-individual and inter-cell type variation in residual DNA damage after in vivo irradiation of human skin. *Radiother Oncol* **99**, 225-230 (2011).

Curriculum Vitae

Surname	GROSSE (maiden name FRENZEL)
Name	Nicole
Date of birth	18th February, 1983
Nationality	German

EDUCATION

1994-2001	Schiller-Gymnasium (equivalent to high school), Bautzen, Germany
2001-2002	Technical University of Dresden, Germany Bioprocess engineering at the Faculty of Engineering
2002-2004	Technical University of Dresden, Germany Preliminary Diploma in Biology at the Faculty of Science
2004-2007	Private University Witten/Herdecke, Germany Diploma in Biochemistry (equivalent to Master of Science) Diploma thesis: “Molecular Mechanisms of Norepinephrine Inhibiting Spontaneous Fibroblast Migration in a Collagen Matrix”
2007-current	University of Zurich, Switzerland PhD student at the Faculty of Science Participant of the Cancer Biology PhD Program, Cancer Network Zurich

PUBLICATIONS

Grosse N, Hug E, Lomax A, Sartori A, Pruschy M
Differential demands on DNA double strand break repair machineries after proton- and photon-irradiation
In preparation

Rohrer Bley C, Furmanova P, Orlowski K, Grosse N, Broggini-Tenzer A, McSheey PMJ, Pruschy M
Microtubule stabilizing agents and ionizing radiation: Multiple exploitable mechanisms for combined treatment
submitted

ORAL PRESENTATIONS

2nd Students Retreat of Cancer Biology Program Zurich, Bogis-Bossey, Switzerland, 2009
Frenzel N, Hug E, Lomax A, Coray A, Sartori A, Pruschy M
Protons versus Photons – A Molecular Analysis

51st Annual ASTRO Meeting, Chicago, US, 2009
Frenzel N, Hug E, Lomax T, Staab A, Sartori A, Pruschy M
Differential DNA Repair Mechanisms in Response to Proton and Photon Irradiation

9th Day of Clinical Research, University Hospital Zurich, Switzerland, 2010
Grosse-Frenzel N, Hug E, Lomax A, Staab A, Sartori A, Pruschy M
Differential DNA repair in response to proton versus photon irradiation

3rd Students Retreat of Cancer Biology Program Zurich, Wilderswil, Switzerland, 2010
Grosse N, Hug E, Lomax A, Sartori A, Pruschy M
Induction and repair of DNA double strand breaks after proton and photon irradiation

POSTER PRESENTATIONS

3rd Cancer Research Retreat, Cancer Network Zurich, Fiesch, Switzerland, 2008
Frenzel N, Hug E, Pruschy M
Protons vs. Photons – A molecular and cellular analysis

48th PTCOG Meeting, Heidelberg, Germany
Frenzel N, Hug E, Lomax A, Staab A, Sartori A, Pruschy M
Differential DNA repair mechanisms in response to proton and photon irradiation

4th Cancer Research Retreat, Cancer Network Zurich, Monte Verita, Ascona, Switzerland, 2009
Grosse-Frenzel N, Hug E, Lomax A, Staab A, Sartori A, Pruschy M
Differential DNA repair mechanisms in response to proton and photon irradiation

10th Day of Clinical Research, University Hospital Zurich, Switzerland, 2011
Grosse N, Hug E, Lomax A, Sartori AA, Pruschy M
DNA double strand break induction and repair after proton versus photon irradiation

12th International Wolfsberg Meeting on Molecular Radiation Biology/Oncology, Ermatingen, Switzerland, 2011
Grosse N, Hug E, Lomax A, Sartori AA, Pruschy M
DNA double strand break induction and repair after proton versus photon irradiation

Acknowledgements

First of all, I have to highly appreciate Prof. Dr. Eugen B. Hug's and Prof. Dr. Martin Pruschy's initiative and effort to launch this very interesting project. Without it, I would not have started my PhD in the Laboratory for Molecular Radiobiology at the University Hospital Zurich and the centre for proton therapy at the Paul Scherrer Institute (PSI) in Villigen. Especially Prof. Hug believed that more advanced basic biological research is needed to fully understand the advances of proton radiotherapy.

I would like to thank Prof. Eugen B. Hug for introducing me into hadrontherapy, for supporting me at the PSI, and for his useful comments and advices.

I feel much gratitude for Prof. Martin Pruschy, my thesis supervisor, for accepting me as a PhD student and giving me the chance to perform this PhD project in his group. He had quite some proverbs and anecdotes to motivate me. I benefited from his expertise, experience, constant enthusiasm and his encouragement, guidance, support, and criticism.

Furthermore I would like to thank the other members of my PhD thesis committee for their very helpful supervision and support. I thank Prof. Dr. Josef Jiricny for his support at the beginning of my PhD thesis. Prof. Dr. Alessandro A. Sartori who succeeded Prof. Josef Jiricny gave me great input. Due to his expertise, his help was very fruitful, and I am grateful to have him in my committee. I also want to thank my external supervisor Prof. Dr. Ekkehard Dikomey from Hamburg. Although it might have been difficult to supervise me in Zurich, he gave me very good advices and scientific inputs.

I especially want to thank another person from the laboratory for radiation biology and experimental radiooncology at the university hospital Hamburg-Eppendorf. Dr. Kerstin Borgmann introduced me into γH2AX foci analysis and preparation of chromosome spreads. I really profited from it and appreciate highly the warm welcome and guidance in Hamburg.

In addition I would like to thank all current and former members of the Laboratory for Molecular Radiation Biology in Zurich: Dr. Andreas Hollenstein, Andrea Orlando Fontana, Dr. Angela Broggini-Tenzer, Dr. Carla Rohrer Bley, Dr. Colette Shen, Daniel Hug, Katrin Orlowski, Martina Zimmermann, Matthias Eggel, and Van Vuong. Thank you very, very much for the nice atmosphere in the lab and for many more things. I will really miss you!
Many thanks go to Martina Zimmermann for discussing with me my project and my problems.
Special thanks to Colette Shen for proof-reading of this thesis!

Another big thank you is for Carla Rohrer Bley, for listen to my problems, her encouragement and the nice atmosphere in D NUK 14.
I would like to thank as well the Department of Radiation Oncology and especially Prof. Dr. Urs Lütolf and Prof. Dr. Katrin Zaugg for their interest in my project and the support of our research activities. I specially appreciated the constant support and cooperation regarding the radiation facility of all physicists there and the MTRA team.

I specially acknowledge the physicists, MTRAs, and the chief secretary at the centre for proton therapy at PSI. Dr. Adolf Coray, Dr. Terence Böhringer, Dr. Lin Shixiong, Benno Rohrer, and Dr. Stefan König were always very patient helping me with the proton irradiation of cell dishes. Often we had fruitful discussions and time just passed by. A very big thank you goes to Ursula Ludgate for the warm welcome, for introducing me at the centre to all the people, for encouraging me, and for the interesting conversations. I want to thank as well Dr. Adrian Staab who was highly interested in proton radiobiology and motivated me.

Many thanks go to my best friend Dr. Christiane Katja Kleindt. We motivated each other during the time of the PhD and she invested quite some time for proof-reading of my thesis.

The first two and a half years of my PhD I lived in a shared flat with very good friends. Karola and Elisabeth, I want to thank you for the good time while living at Birchstrasse. You supported me also in difficult times and I enjoyed chatting with you, hiking with you, and much more.

Ein ganz liebes Dankeschön geht an meine Familie. Mutti und Vati, Ihr wart immer für mich da und habt an mich geglaubt. Oma Christa und Opa Klaus, Ihr wart immer interessiert und habt meinen Erklärungen gelauscht. Ohne Euch alle wäre ich nie so weit gekommen. Vielen Dank.

Ein ganz besonderes Dankeschön ist für meinen Ehemann Steffen. Ohne Dich wäre ich nie zu dieser interessanten Doktorarbeit gelangt, denn dann wäre ich wahrscheinlich nicht in der Schweiz gelandet. Du warst immer geduldig und hast mir tatkräftig zur Seite gestanden. Du hast mir den Ausgleich beschert, den man braucht, um die Zeit eines PhDs zu bewältigen. Dank Dir habe ich in diesen vier Jahren sehr viel erlebt und die Zeit geniessen können.

Finally, these four years and 4 month were a fantastic time in my life!